Molecular Characterization of Pediatric Brainstem Gliomas (DIPG) and Identification of New Therapeutic Targets

Cláudia Silva Evangelista

NNT : 2018SACLS269

Thèse de doctorat

Molecular characterization of paediatric brainstem gliomas (DIPG) and identification of new therapeutic targets using gene extinction strategies

Thèse de doctorat de l'Université Paris-Saclay
Préparée à Gustave Roussy, UMR8203

École doctorale n°582 Cancérologie, Biologie, Médecine, Santé (CBMS)
Spécialité de doctorat: aspects moléculaires et cellulaires de la biologie

Thèse présentée et soutenue à Villejuif, le 1er octobre 2018 par

Claudia SILVA EVANGELISTA

Composition du Jury :

Dr Olivier AYRAULT Institut Curie (UMR3347 / U102)	**Président**
Dr Eric PASMANT Université Paris-Decartes (EA7331)	**Rapporteur**
Dr Samuel MEIGNAN Centre Oscar Lambret (Inserm U908 UTRT)	**Rapporteur**
Dr Camille LOBRY Gustave Roussy (UMR1009)	**Examinateur**
Dr Marie-Anne DEBILY Université Evry Val-d'Essonne (UMR8203)	**Directrice de thèse**

To my parents,
Claudio and Maria Auxiliadora,
always present although on the other side of the Ocean.

ACKOWLEDGEMENTS

First of all, I would like to thank the members of the jury: Eric PASMANT and Samuel MEIGNEN for having accepted to be thesis reporters and Camille LOBRY and Olivier AYRAULT for evaluating this work.

My sincere thanks to Jacques GRILL who welcome me in his laboratory and with whom in every meeting I learned something new from the most diverse themes. Thanks to my phD supervisor Marie-Anne DEBILY for all the time, patience and guidance over these four years. I also would like to thank David CASTEL for his valuable advices.

I would like to thanks the Brazilian government through the National Council for Scientific and Technological Development (CNPq) and the program "Science without borders" scholarship (process 248943/2013-8) for the financial support from that allowed the development of this project, as well as Canceropole Ile de France, INCa, La Ligue Contre le Cancer and l'Etoile de Martin.

I would like to thanks all the current and former members of the GRILL team: Alexandre PLESSIER, Jane MERLEVEDE, Thomas KERGROHEN, Coralie WERBROUCK, Ludivine LE DRET, Stephanie PICOT, Marco BRUSCHI, Manon LANCIEN, among others. Especially thanks to Emilie BARRET, who has accompanied me since the beginning of the project, Ambre SACCASYN that was extremely helpful during her master internship and last, but not least Virginie MENEZ for her indispensable work and who I'm glad that will give continuity to this project.

Thank you Yann, for the patience, support and love that were essential, especially in the end. To finish I want to thank my friends Jenny, Eliana, Geisa, Stephanie, Matheus and Joana for their support from close and at distance. And finally to my parents, for their support, encouragement and love, which made me become who I am today.

RÉSUMÉ

Les DIPG représentent les tumeurs cérébrales pédiatriques les plus sévères. Aucun progrès dans leur prise en charge n'a été accompli au cours des 50 dernières années et la radiothérapie ne demeure que transitoirement efficace. Récemment, une mutation somatique de l'histone H3 (K27M) spécifique des DIPG a été trouvée chez environ 95% des patients. Elle est aujourd'hui considérée comme l'événement oncogénique initiateur de ces tumeurs. Deux sous-groupes majeurs de patients présentant des programmes oncogéniques et une réponse à la radiothérapie distincte peuvent être définis en fonction du gène dans lequel l'altération survient, codant les variantes protéiques H3.1 ou H3.3. Nous avons réalisé deux cribles de létalité synthétique par ARN interférence ciblant le kinome humain afin d'identifier d'une part les gènes nécessaires à la survie des DIPG et d'autre part les gènes dont l'inhibition sensibilise ces tumeurs à la radiothérapie. Le double objectif de ce projet était de mieux comprendre la biologie sous-jacente à l'oncogenèse des DIPG et de découvrir de nouvelles cibles thérapeutiques.

Nous avons mis en évidence 41 gènes requis pour la survie des DIPG sans effet délétère majeur sur des cellules contrôles normales. Parmi eux, nous avons identifié VRK3 codant une serine thréonine kinase dont les fonctions restent peu décrites à ce jour et qui n'avait jamais été associée préalablement à l'oncogenèse de DIPG. Nous avons pu confirmer par la suite que son inhibition conduit à un arrêt total de la prolifération des cellules de DIPG associé à d'importants changements morphologiques, plus particulièrement dans les tumeurs mutées pour H3.3-K27M. VRK3 constitue par conséquent une nouvelle cible thérapeutique prometteuse dans cette pathologie à l'issue fatale pour la totalité des patients.

En parallèle, un crible de survie similaire a été réalisé en conjonction avec l'irradiation des cellules. Très peu d'ARN interférents ont permis de sensibiliser les cellules H3.3-K27M à la radiothérapie contrairement aux cellules H3.1-K27M. Ce travail nous a permis de mettre en évidence une différence significative de radiosensibilité des modèles vitro de DMG en fonction du sous-groupe de tumeurs considéré, H3.1- ou H3.3-K27M muté, conformément à la survie des patients observée suite à la radiothérapie. Ces résultats inédits laissent entrevoir des perspectives d'amélioration du traitement de référence des patients atteints de DIPG actuellement identique quelle que soit leur génotype.

“The greatest pleasure in life is doing what people say you cannot do”.

Le plus grand plaisir dans la vie est réaliser ce que les autres vous pensent incapables de réaliser.
(Traduction libre)

(Walter BAGEHOT)

SUMMARY

List of abbreviations

List of figures and tables

Introduction

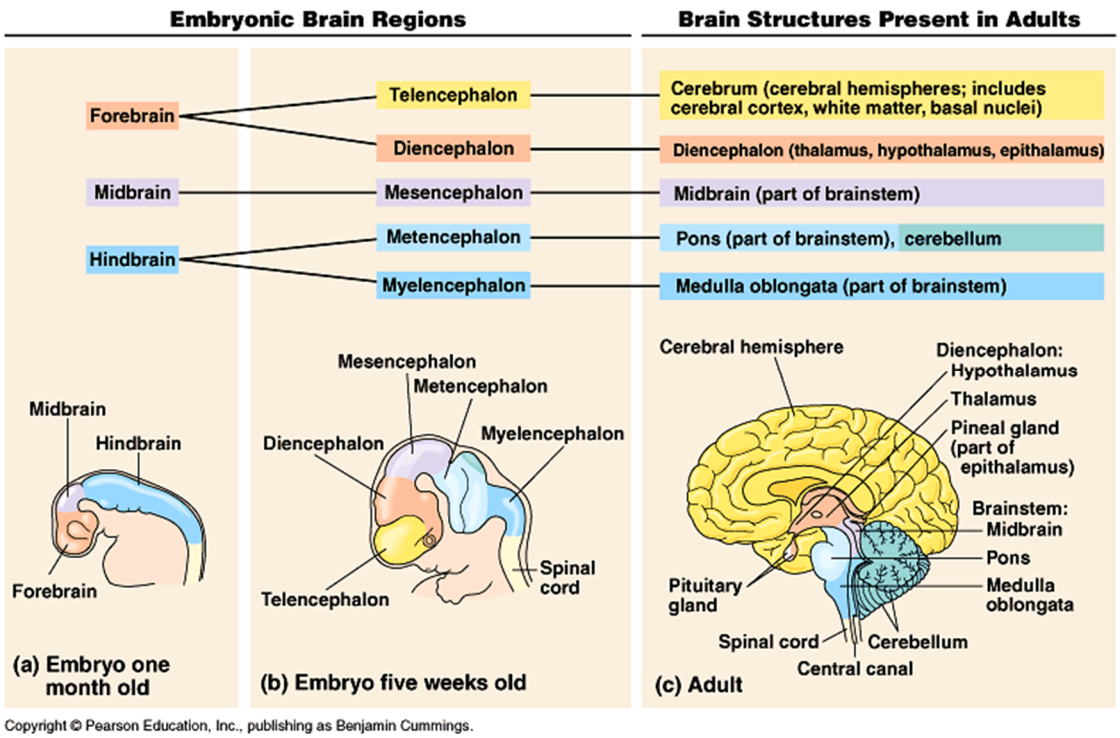

Figure 1. CNS and brain development. The neural tube at the end of the third week of embryogenesis passes through expansions with the formation of the primary brain vesicles: **(a)** forebrain, midbrain and hindbrain. These vesicles are further subdivided forming the **(b)** secondary brain vesicles that will give rise to the complex structure of the brain in adult **(c)**. The forebrain develops into cerebrum and thalamic structures. The brainstem is formed by the midbrain and hindbrain that also gives rise, respectively, to the cerebellum and medulla oblongata (Copyright ® Pearson Education Inc., publishing as Benjamin Cummings).

INTRODUCTION

PART I. BRAIN TUMOURS

1. Early brain development

The brain is a complex structure that plays a vital role in the control of the Central Nervous System (CNS) through an intricate network of molecular, cellular and neuronal processes (Bassett and Gazzaniga 2011). These processes are extremely organized throughout the development and culminates with the formation of the different structures that compose this system (Stiles and Jernigan 2010).

The CNS and brain development starts at the end of the third week of embryogenesis, right after the gastrulation, with the formation of three germinal layers: ectoderm, mesoderm and endoderm. The ectoderm is the external layer in the early embryo that gives rise to the nervous system (S. F. Gilbert 2000). Then, at the end of the fourth week of embryogenesis, the neurulation lead to the formation of the first well-defined neural structure: the neural tube (S. F. Gilbert 2000; Moscoso 2009; Darnell and Gilbert 2017).

At the end of the neurulation, the anterior part of the neural tube expands in three primary brain vesicles: prosencephalon (or forebrain), mesencephalon (or midbrain) and rhombencephalon (or hindbrain) (**Figure 1a**). The prosencephalon is further subdivided into two secondary vesicles (**Figure 1b**): the telencephalon and diencephalon that give rise, respectively, to the cerebral hemispheres and thalamic structures plus retina (**Figure 1c**). The rhombencephalon divides into metencephalon and myelencephalon, with formation of the cerebellum and the medulla oblongata, respectively. Both, mesencephalon and rhombencephalon

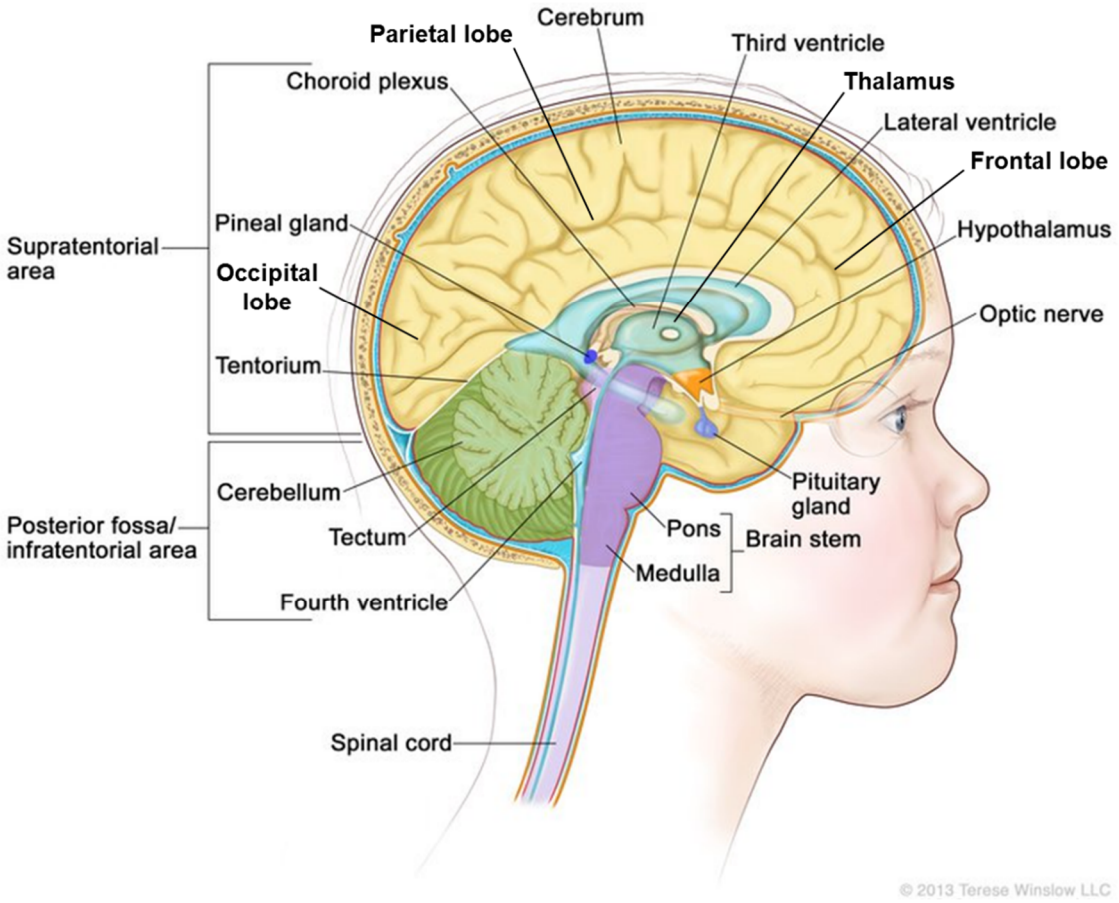

Figure 2. Anatomy of the brain. Mid-sagittal section showing the main structures of the brain at the end of its development. Cerebellum, brain stem and spinal cord are in the infratentorial area, while the other structures belongs to the supratentorial zone (adapted from Winslow 2013).

secondary vesicles contributes in the formation of the brainstem (**Figure 1c**) (Moscoso 2009; Darnell and Gilbert 2017). The posterior part of the neural tube give rise to the spinal cord. The four interconnected cavities derived from the core of the neural tube correspond to the ventricular system of the brain (Moscoso 2009).

Preliminary structures of the brain and CNS are already defined within eight weeks of embryogenesis. The brain development continues during the first years of childhood, reaching almost the total adult volume at the age of 6 (Stiles and Jernigan 2010). During this period, there is a rapid growth and differentiation of the cerebral hemispheres (also named cortex or cerebrum) and subcortical structures (cerebellum and thalamic structures)(**Figure 1c**)(Kostović and Jovanov-Milošević 2006; Moscoso 2009).

2. Anatomy of the brain

The brain is a complex organ (Bassett and Gazzaniga 2011) that can be divided from an anatomical point of view in three main parts: the cerebral cortex, the cerebellum and the brainstem (**Figure 2**).

The largest and most external part of the brain is the cerebral cortex. It is divided into two hemispheres (right and left) and each hemisphere is further subdivided into four lobes: frontal, temporal, parietal and occipital (Keunen, Counsell, and Benders 2017). The frontal lobes are the largest ones. They coordinate reasoning, motor skills, higher level cognition and expressive language. The temporal lobes are localized on the same level of the ears and includes the hippocampus and amygdala. They play roles in sound and language processing, visual and verbal memory, emotion and reaction interpretation. The parietal lobes

are localized behind the frontal lobes. They are responsible for spatial orientation and tactile sensory processing. The occipital lobes are localized near to the back of the skull. Visual processing takes place in these lobes (Bassett and Gazzaniga 2011).

The cerebellum is localized beneath the cortex and below the occipital lobes. It plays a role in motor control, being responsible for body posture, equilibrium and balance by receiving information from the balance system of the inner ear, sensory nerves, auditory and visual systems (McLachlan and Wilson 2017).

The brainstem is localized in front of the cerebellum and is connected to the spinal cord. It includes three parts: midbrain, pons and medulla oblongata. The midbrain controls eye movement, visual and auditory information processing. The pons, localized below the midbrain, is the largest part of the brainstem. It play a crucial role in the transmission of information between the brain and the body. The medulla oblongata is involved in heart control, breathing and consciousness (McLachlan and Wilson 2017).

Between the cortex and the brainstem are localized the structures originated from the diencephalon: the thalamus and the hypothalamus. The thalamus is in charge of sensory and motor signals transmission to the cortex and is involved in consciousness, sleep and memory. The hypothalamus maintains body homeostasis by controlling especially nutrient intake, energy balance, body temperature regulation and serves as the connection of the nervous system to the endocrine system by hormone production and release (Bassett and Gazzaniga 2011).

3. Nervous tissues

Indeed, cellular proliferation, migration and differentiation are the main processes that lead to the formation of the complex brain structure. The macroscopic anatomical modifications in the brain vesicles throughout the embryogenesis reflect the significant important changes occurring at the histological level and the presence of many distinct cell types (Keunen, Counsell, and Benders 2017).

During CNS development, the Neural Stem Cells (NSC) that are widespread in the early neuroepithelium (Qian *et al.* 2000) are uncommitted multipotent cells with self-renewal capacity that undergo differentiation pathways to generate the neural lineages. They are considered as the primary progenitors cells that generate neuronal cells through neurogenesis and glial cells through gliogenesis at different developmental stages (Gage 2000; Temple 2001; Teng *et al.* 2008). Although neurogenesis and gliogenesis have mainly been studied in cerebral cortex in *Drosophila* and *Mus musculus*, knowledge on cortical development can also be applied to other CNS regions and the key developmental stages are remarkably conserved between mammalian species (Jeibmann and Paulus 2009; Lessing and Bonini 2009; Molnár and Clowry 2012; Semple *et al.* 2013).

3.1. Neurogenesis

The neurogenesis starts in the end of gastrulation and remains until postnatal stages in restricted germinal areas of adult brain, *e.g.* subventricular zone and hippocampus (Bystron, Blakemore, and Rakic 2008; Stiles and Jernigan 2010;

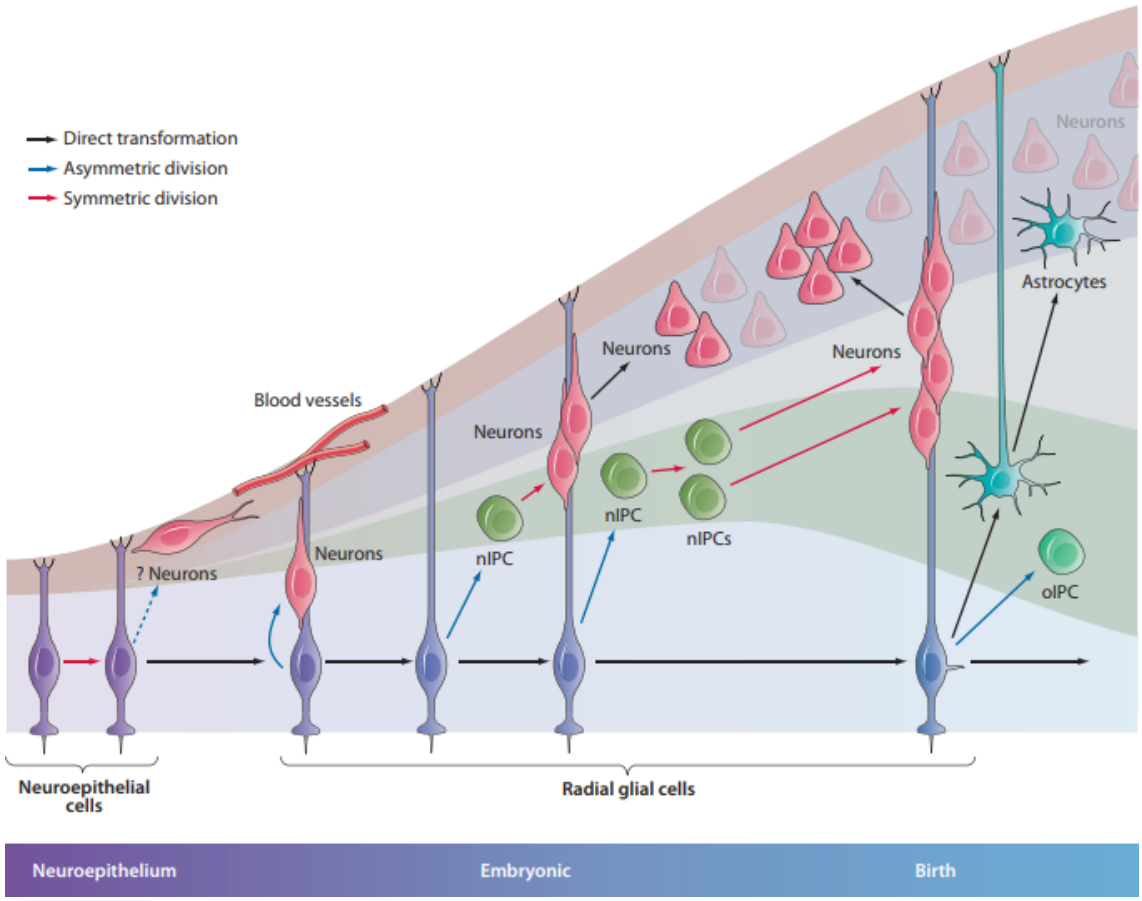

Figure 3. Neurogenesis. Neuroepithelial cells divide symmetrically (red arrow) during early development to maintain its pool of NSCs. Some neuroepithelial cells also seems to generate early neurons. Neuroepithelial cells elongate and convert into radial glial (RG) cells. RG cells can generate neurons directly through asymmetric division (blue arrow) and indirectly by the generation of neuron intermediate progenitor cells (nIPCs). These progenitors undergoes amplification by symmetric division and further differentiate (black arrow) into neurons. The neurogenesis occurs during the embryonic period and post-natal. The RG cells that are responsible for the neuron production will be then committed to the production of glial lineages cells (adapted from Kriegstein and Alvarez-Buylla 2009).

Sacco, Cacci, and Novarino 2018; Sorrells *et al.* 2018). The neuronal cells are essentially generated by two mechanisms (**Figure 3**): (i) the direct division of NSCs, or (ii) through the amplification of the NSCs as intermediate progenitor cells (IPCs). These IPCs are precursors with a more restricted potential of differentiation than NSCs. Both mechanisms allows the amplification and maintenance of the NSCs, before the migration and differentiation in neural lineages (Temple 2001; Kriegstein and Alvarez-Buylla 2009).

Initially, a population of NSCs from the pseudostratified neuroepithelium at the ventricular zone starts to present morphological changes and characteristics of terminally differentiated glial cells, such as apical-basal polarity, apical attachment and expression of astrocyte-specific glutamate aspartate transporter (GLAST), brain lipid-binding protein (BLBP), nestin, vimentin and glial fibrillary acidic protein (GFAP). This population is named Radial Glial (RG) cells and are considered as the neural precursors. They undergo asymmetric cell division that allow self-renewal and the generation of neurons directly or indirectly through neuronal intermediate progenitor cells (nIPCs). The nIPC undergo symmetric division allowing the amplification of these committed precursors that will further differentiate into neurons. The RG cells are also important for neuronal migration along their fibbers to the cortical zone (Temple 2001; Kriegstein and Alvarez-Buylla 2009).

Neurons are responsible by the transmission of information through the generation of action potentials and intercommunication via chemical synapses (Urbán and Guillemot 2014). A typical neuron contain several dendrites which integrate synaptic inputs triggering the axon potential and one unique axon propagating the information (Stiles and Jernigan 2010). Consequently, neurons are

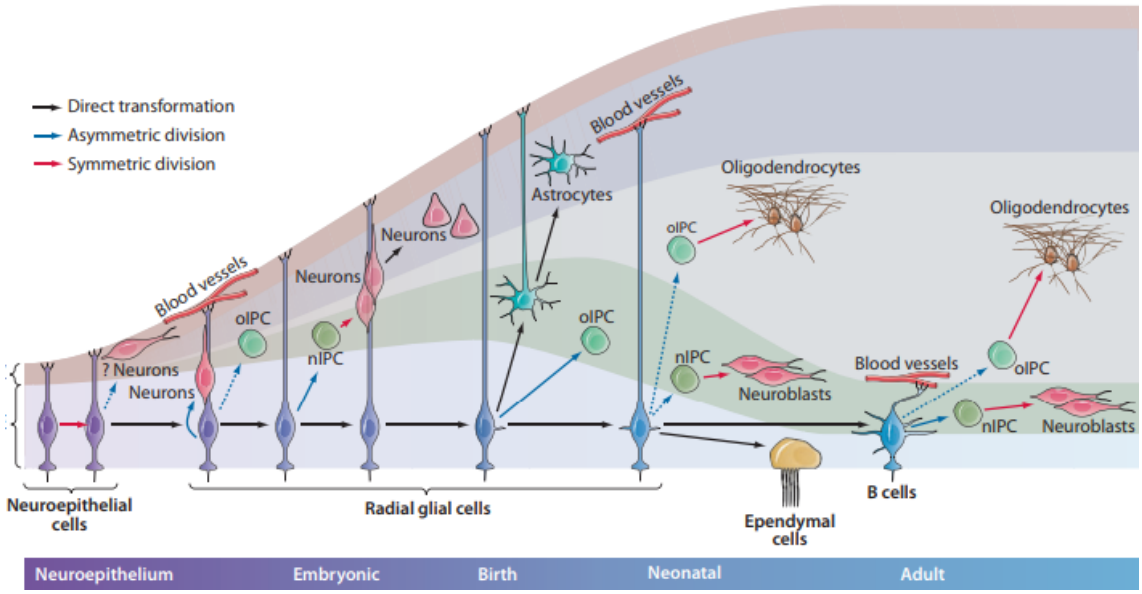

Figure 4. Gliogenesis. Gliogenesis lead to four distinct cell types: oligodendrocytes, astrocytes, ependymal cells and B cells. Similarly to neurons, oligodendrocytes are also derived from RG through intermediate progenitor cells that generate oligodendrocytes (oIPCs). At the end of embryonic development, most RG begin to detach from the apical side and convert into astrocytes while oIPC production continues. A subpopulation of RG retains apical contact and continue functioning as NSCs in the neonate. These neonatal RG continue to generate neurons and oligodendrocytes through nIPCs and oIPCs; some convert into ependymal cells, whereas others convert into type B cells that continue to function as NSCs in the adult (adapted from Kriegstein and Alvarez-Buylla 2009).

among the most highly polarized cell type and this polarization of axon and dendrites underlies their ability to integrate and transmit information (Polleux and Snider 2010). Once established in the cortex, the neurons start to develop its neuronal processes (axons and dendrites) allowing the formation of connections with other neurons. Rudimental neural networks for information processing starts to be organized and by the end of prenatal period the major fiber tracks are already formed (Webb, Monk, and Nelson 2001; Bystron, Blakemore, and Rakic 2008; Stiles and Jernigan 2010).

3.2. Gliogenesis

The glial cells are responsible of several supportive functions of the neurons (Stiles and Jernigan 2010). At the end of the neurogenesis, RG cells passes through a neuronal-to-glial switch, stopping the production of neurons to generate glial cells: astrocytes, oligodendrocytes, B cells and ependymal cells (**Figure 4**). The production and migration of neurons are prenatal events, while proliferation and migration of glial progenitors occurs at the end of embryogenesis and extend throughout childhood, with the differentiation and maturation of the glial cells (Qian *et al.* 2000; Stiles and Jernigan 2010; Urbán and Guillemot 2014).

Astrocytes are the most abundant type of macroglial cells. At the end of development, RG cells migrate to the cortical zone, with a regression of radial process and follow a progressive transformation into multipolar astrocytes. Astrocytes undergo a local amplification through symmetric divisions with formation of astrocytic progenitors cells (aIPCs) before terminal differentiation (Temple 2001; Kriegstein and Alvarez-Buylla 2009). Astrocytes are implicated in the formation of the blood-brain barrier, the regulation of vasoconstriction and vasodilatation and in

the regulation of ion and metabolic brain homeostasis (Rowitch and Kriegstein 2010; Martynoga, Drechsel, and Guillemot 2012; Dimou and Götz 2014).

Oligodendrocyte progenitor cells (oIPCs) are originate throughout development by asymmetric division of RG cells. In the postnatal cortex, oIPCs are distributed all over the brain (Qian *et al.* 2000; Kriegstein and Alvarez-Buylla 2009). While differentiating into oligodendrocytes, oIPCs passes through symmetric divisions. There is an increase of myelin protein expression with the formation of cellular processes that wrap nearby neuronal axons with multi-layered sheaths. These insulating myelin sheath allows a more efficient propagation of electrical signals. The oligodendrocytes are also responsible for the production of tropic factor, axonal integrity and neuronal survival (Stiles and Jernigan 2010; Dimou and Götz 2014).

There are other types of glial cells in the CNS: ependymal cells, B cells and microglia. Ependymal cells seems to originate from the conversion of a subpopulation of RG cells (Kriegstein and Alvarez-Buylla 2009). These cells are localized in the spinal cord and ventricular system and are involved in the production and secretion of cerebrospinal fluid. B cells seems to be quiescent RG cells that maintain the generation of IPCs in the adult brain and acts in the maintenance of epithelial organization (Kriegstein and Alvarez-Buylla 2009; Stiles and Jernigan 2010). The microglia localized throughout the brain and spinal cord, correspond to specialized macrophages being an active immune defence in the CNS (Ginhoux *et al.* 2013).

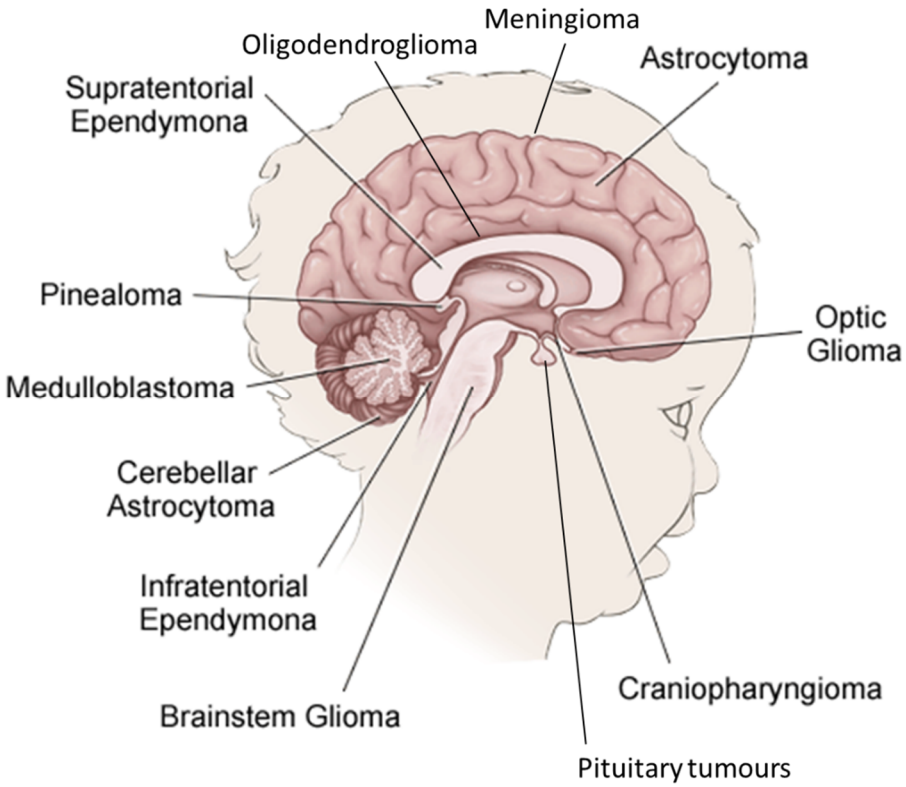

Figure 5. Localization of different types of CNS and brain tumours. The supratentorial tumours develops in the hemispheres and thalamic regions, while infratentorial tumours originate in the cerebellum, brainstem and spinal cord (adapted from Siegfried 2012).

4. Central Nervous System and brain tumours

CNS and brain tumours are a group of neoplasms arising from different neural tissues and in different parts of the brain (**Figure 5**). Several distinct entities can be defined, each one characterized by their own unique biology, treatment and prognosis (Louis *et al.* 2016). Primary CNS tumours are considered a low incident type of neoplasm, representing only 1.4% of all types of diagnosed cancers (Strong *et al.* 2015). Although CNS tumours do not represent a cancer associated with the highest incidence, they are extremely aggressive and the mortality reaches 59.2% of the patients in France (INCa 2018). From a clinical point of view, patients with brain tumours have similar clinical presentations with focal or generalized signs and symptoms, depending on the localization, type and stage of development. The most frequent signs and symptoms are seizure, headache, nausea, vomiting, fatigue, visual problems, balance alterations and cognitive dysfunction (Butowski 2015).

Depending on the type and infiltration level, a full surgical resection of the tumoral tissue can be performed. When it represents risks to neurological functions, in the case of inconclusive diagnostic and/or for treatment decision, a tumour biopsy can takes place. The brain tumour tissue can be accessed during stereotactic, endoscopic or open procedures. In more than 90% of the cases, the biopsy enhances diagnostic yield and the morbidity rate due to the procedure is lower than 2.5% (Patel, Carter, and Chen 2018). Histopathological and molecular analysis of the biopsies allow the confirmation of diagnosis, the definition of specific management strategies, the discovery of biomarkers, as well as the development of preclinical models crucial for research purpose (Puget *et al.* 2015a).

5. Classification of CNS and brain tumours

5.1. Previous classifications

The CNS and brain tumours are rare and extremely heterogeneous, from a biologic and genetic point of view. A standardized classification is an effort in order to integrate and improve the knowledge acquired worldwide of these different entities to a better treatment and prognosis of the patients. It also aims to establish an international consensus of the classification and grading of brain tumours (Louis *et al.* 2007, 2016).

The fourth edition of the World Health Organization (WHO) CNS and brain tumour classification (Louis *et al.* 2007) was the result of a consensus between pathologists, geneticists and oncologists. This edition took into consideration the histological and immunohistochemical features of previous classifications (Zülch 1978; P. Kleihues, Burger, and Scheithauer 1993; Paul Kleihues *et al.* 2002) and integrated evidences of distinct age distribution and localization, differences in clinical behaviour and, most importantly, the advances in genetic profiling. The 4th WHO CNS classification identified seven major categories of brain tumours (**Table 1**)(Louis *et al.* 2007):

1) tumours of neuroepithelial tissue;
2) tumours of cranial and paraspinal nerves;
3) tumours of the meninges;
4) lymphomas and hematopoietic neoplasms;
5) germ cell tumours;
6) tumours of the sellar region;
7) metastatic tumours.

Table 1. 2007 WHO classification and grading of CNS tumours. The seven major categories of tumours and its respective entities and variants are summarized in this table, together with the malignancy grade from I to IV. NOS, not otherwise specified (adapted from Louis *et al.* 2007).

1) TUMOURS OF NEUROEPITHELIAL TISSUE			I	II	III	IV
1.I) gliomas	Astrocytic tumours	Pilocytic strocytoma	x			
		Pilomyxoid astrocytoma		x		
		Subependymal giant cell astrocytoma	x			
		Diffuse astrocytoma				
		Fibrillary astrocytoma		x		
		Gemistocytic astrocytoma				
		Protoplasmic astrocytoma				
		Anaplastic astrocytoma			x	
		Glioblastoma				
		Giant cell glioblastoma				x
		Gliosarcoma				
		Gliomatosis cerebri				
	Oligodendroglial tumours	Oligodendroglioma		x		
		Anaplastic oligodendroglioma			x	
	Oligoastrocytic tumours	Oligoastrocytoma		x		
		Anaplastic oligoastrocytoma			x	
	Ependymal tumours	Subependymoma	x			
		Myxopapillary ependymoma	x			
		Ependymoma				
		Cellular				
		Papillary		x		
		Clear cell				
		Tanycytic				
		Anaplastic ependymoma			x	
1.II) embryonal tumours	Medulloblastoma	Desmoplastic/nodular medulloblastoma				
		Medulloblastoma with extensive nodularity				
		Anaplastic medulloblastoma				x
		Large cell medulloblastoma				
	CNS primitive neuroectodermal tumour	CNS Neuroblastoma				
		CNS Ganglioneuroblastoma				
		Medulloepithelioma				x
		Ependymoblastoma				
	Atypical teratoid/rhabdoid tumour					x
1.III) neuronal and mixed neuronal-glial tumours		Dysplastic gangliocytoma of cerebellum				
		Dermoplastic infantile astrocytoma/ganglioglioma				
		Dysembryoplastic neuroepithelial tumour	x			
		Gangliocytoma	x			
		Ganglioglioma	x			
		Anaplastic ganglioglioma			x	
		Central neurocytoma		x		
		Extraventricular neurocytoma		x		
		Cerebellar liponeurocytoma		x		
		Papillary glioneuronal tumours	x			
		Rosette-forming glioneuronal tumour of the fourth ventricle	x			
		Paraganglioma	x			
1.IV) choroid plexus tumours		Choroid plexus papilloma	x			
		Atypical choroid plexus papilloma		x		
		Choroid plexus carcinoma			x	
1.V) tumours of the pineal region		Pineocytoma	x			
		Pineal parenchymal tumour of intermediate differentiation		x	x	
		Pineoblastoma				x
		Papillary tumours of the pineal region		x	x	
1.VI) other neuroepithelial tumours		Astroblastoma				
		Chordoid glioma of the third ventricle		x		
		Angiocentric glioma	x			

2) TUMOURS OF CRANIAL AND PARASPINAL NERVES		I	II	III	IV
Schwannoma (neurilemoma, neurinoma)	Cellular				
	Plexiform	x			
	Melanotic				
Neurofibroma	Plexiform	x			
Perineurioma	Perineurioma, NOS	x			
	Malignant perineurioma	x	x	x	
Malignant peripheral nerve sheath tumour (MPNST)	Epithelioid MPNST				
	MPNST with mesenchymal differentiation			x	x	x
	Melanotic MPNST				
	MPNST with glandular differentiation				

3) TUMOURS OF THE MENINGES			I	II	III	IV
Tumours of meningothelial cells	Meningioma	Meningothelial	x			
		Fibrous (fibroblastic)	x			
		Transitional (mixed)	x			
		Psammomatous	x			
		Angiomatous	x			
		Microcystic	x			
		Secretory	x			
		Lymphoplasmacyte-rich	x			
		Metaplastic	x			
		Chordoid	x			
		Clear cell	x			
		Atypical		x		
		Papillary	x			
		Rhabdoid	x			
		Anaplastic (malignant)			x	
Mesenchymal tumours		Lipoma				
		Angiolipoma				
		Hibernoma				
		Liposarcoma				
		Solitary fibrous tumour				
		Fibrosarcoma				
		Malignant fibrous histiocytoma				
		Leiomyoma				
		Meiomyosarcoma				
		Rhabdomyoma				
		Rhabdomyosarcoma				
		Chondroma				
		Chondrosarcoma				
		Osteoma				
		Osteosarcoma				
		Osteochondroma				
		Haemangioma				
		Epithelioid haemangioendothelioma				
		Haemangiopericytoma		x		
		Anaplastic haemangiopericytoma			x	
		Angiosarcoma				
		Kaposi sarcoma				
		Ewing sarcoma - PNET				
Primaty melanocytic lesions		Diffuse melanocytosis				
		Melanocytoma				
		Malignant melanoma				
		Meningeal melanomatosis				
Other neoplasms related to mening		Haemangioblastoma	x			

4) LYMPHOMAS AND HEMATOPOIETIC NEOPLASMS	
Malignant lymphomas	
Plasmacytoma	
Granulocytic sarcoma	
5) GERM CELL TUMOURS	
Germinoma	
Embryonal carcinoma	
Yolk sac tumours	
Choriocarcinoma	
Teratoma	Mature
	Immature
	Teratoma with malignant transformation
Mixed germ cell tumour	

6) TUMOURS OF THE SELLAR REGION		I	II	III	IV
Craniopharyngioma	Adamantinomatous				
	Papillary				
Granular cell tumour		x			
Pituicytoma					
Spindle cell oncocytoma of the adenohypophysis					
7) METASTATIC TUMOURS					

A grading system correlating histological diagnosis with malignancy, together with clinical characteristics such as age, neurological performance status, radiological features, tumour localization, cell proliferation indices and genetic alterations was also defined, attempting to establish a prediction of the biological behaviour of these neoplasms (Louis *et al.* 2007):

- *Grade I* tumours are related to neoplasms with low proliferative potential and possibility of cure after surgical resection alone.

- *Grade II* tumours with a low-level of proliferative activity, an infiltrative nature and the possibility of recurrence with increase in malignancy.

- *Grade III* tumours present histological evidence of malignancy, such as nuclear atypia, brisk mitotic activity and increased proliferation.

- *Grade IV* tumours are associated with histological evidence of malignancy, high mitotically activity and, by consequence, rapid disease progression. It typically present necrosis in the site of the tumour, widespread infiltration of surrounding tissue and a tendency for craniospinal dissemination with a fatal outcome in the majority of the cases (Louis et al. 2007; Strong et al. 2015; Louis et al. 2016; Komori 2017).

Among the seven major categories, the tumours arising from neuroepithelial tissue represents more than 80% of the primary CNS and brain tumours (Strong *et al.* 2015). The tumours of neuroepithelial tissue are subdivided, according to the supposed neural tissue of origin:

I) gliomas correspond to tumour cells presenting characteristics of glial lineages;

II) embryonal tumours, from embryonal cells;

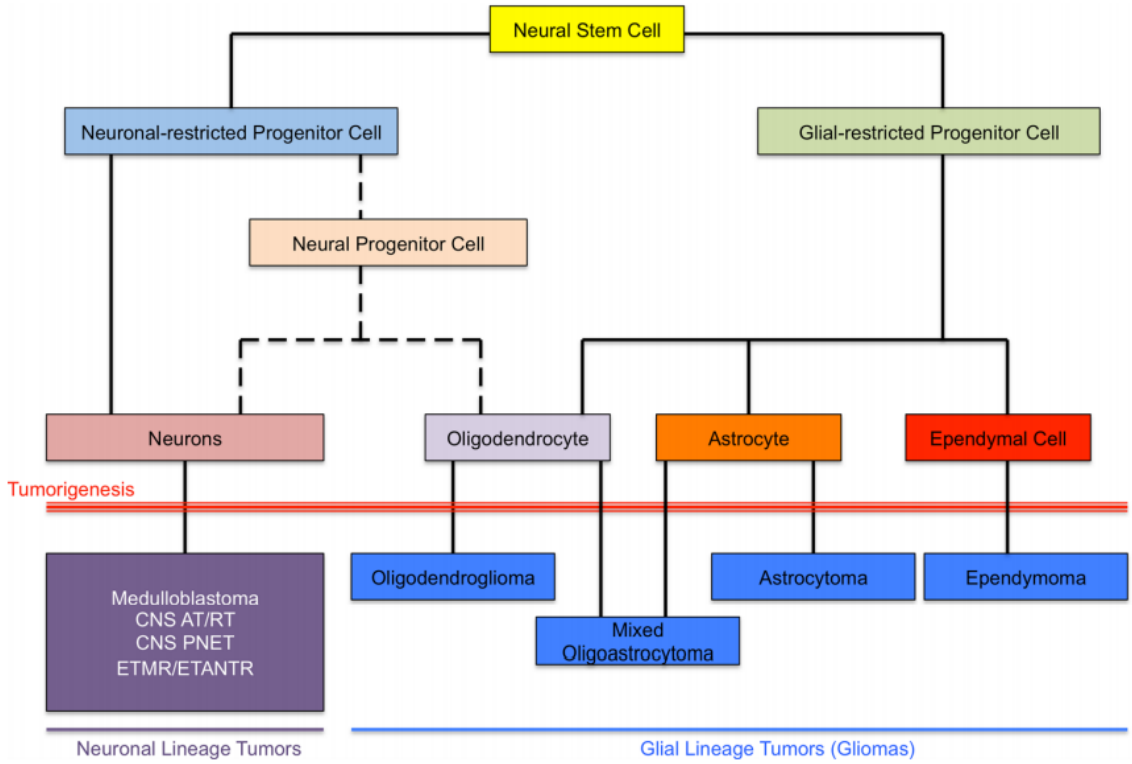

Figure 6. CNS development and tumorigenesis. Schematic representation showing NSC differentiation into neuronal (neurogenesis) and glial cells (gliogenesis), together with tumorigenesis from presumed cell of origin. Medulloblastoma, CNS PNET and ETMR are examples of tumours of presumed neuronal origin (purple). Tumours from presumed glial origin (blue) are collectively called gliomas. CNS Central Nervous System, AT/RT atypical teratoid/rhabdoid tumour, ETMR embryonal tumours with multi-layered rosettes, ETANTR embryonal tumour with abundant neuropil and true rosettes (Fontebasso *et al.* 2014).

III) neuronal and mixed neuronal-glial tumours, from nIPCs and neurons;

IV) choroid plexus tumours, from regionalized ependymal cells;

V) pineocytoma or pineoblastoma for tumours resulting from cells of the pineal region;

VI) other neuroepithelial tumours.

Focusing on the first subgroup (I), malignant gliomas represent 70% of all new diagnosed primary brain tumours (Wen and Kesari 2008; Strong *et al.* 2015). According to histological similarities and presumed cells of origin of the tumour cells, four categories can be defined (**Figure 6**)(Louis *et al.* 2007, 2016):

(i) astrocytomas, in which the tumour cells harbour characteristics of astrocytes. These tumours can present all grades of malignancy.

(ii) oligodendrogliomas, derived from oligodendrocytes. These tumours are usually localized in the cerebrum and are typically grade II;

(iii) ependymomas, develop from ependymal cells in the ventricles and spinal cord (grades I to III). These tumours are frequent in childhood;

(iv) oligoastrocytomas, or mixed gliomas, that conserve both oligodendrocytic and astrocytic characteristics (usually grade III).

5.2. 2016 WHO CNS classification

The WHO CNS classification was updated in 2016 and mainly relied on these histopathological characteristics for the definition into the different entities among these neoplasms. With the advances and the increase accessibility to genomic techniques, such as transcriptomic, whole genome sequencing and methylation

Table 2. 2016 WHO classification of CNS tumours. The advances in genomic techniques have increased the knowledge of molecular basis of tumorigenesis and have allowed to establish subgroups according to genomic alterations. NOS, not otherwise specified (adapted from Louis *et al.* 2016).

TUMOURS OF NEUROEPITHELIAL TISSUE		
Gliomas	Diffuse astrocytic and oligodendroglial tumours	Diffuse astrocytic, IDH-mutant
		Gemistocytic astrocytoma, IDH-mutant
		Diffuse astrocytic, IDH-wildtype
		Diffuse astrocytoma, NOS
		Anaplastic astrocytoma, IDH-mutant
		Anaplastic astrocytoma, IDH-wildtype
		Anaplastic astrocytoma, NOS
		Glioblastoma, IDH-wildtype
		Giant cell glioblastoma
		Gliosarcoma
		Epithelioid glioblastoma
		Glioblastoma, IDH-mutant
		Glioblastoma, NOS
		Diffuse midline glioma, H3 K27M-mutant
		Oligodendroglioma, IDH-mutant and 1p/19q-codeleted
		Oligodendroglioma, NOS
		Anaplastic oligodendroglioma, IDH-mutant and 1p/19q-codeleted
		Anaplastic oligodendroglioma, NOS
		Oligoastrocytoma, NOS
		Anaplastic oligoastrocytoma, NOS
	Other astrocytic tumours	Pilocytic strocytoma
		Pilomyxoid astrocytoma
		Subependymal giant cell astrocytoma
		Pleomorphic xanthoastrocytoma
		Anaplastic pleomorphic xanthoastrocytoma
	Ependymal tumours	Subependymoma
		Myxopapillary ependymoma
		Ependymoma
		Papillary ependymoma
		Clear cell ependymoma
		Tanycytic ependymoma
		Ependymoma *RELA* fusion-positive
		Anaplastic ependymoma
	Other gliomas	Chordoid glioma of the third ventricule
		Angiocentric glioma
		Astroblastoma
Embryonal tumours	Medulloblastomas, genetically defined	Medulloblastoma, WNT-activated
		Medulloblastoma, SHH-activated and *TP53*-mutant
		Medulloblastoma, SHH-activated and *TP53*-wildtype
		Medulloblastoma, non-WNT/non-SHH
		Medulloblastoma, group 3
		Medulloblastoma, group 4
	Medulloblastomas, histologically defined	Medulloblastoma, classic
		Medulloblastoma, desmoplastic/nodular
		Medulloblastoma with extensive nodularity
		Medulloblastoma, large cell/anaplastic
	Medulloblastoma, NOS	
	Embryonal tumour with multilayered rosettes, C19MC-altered	
	Embryonal tumour with multilayered rosettes, NOS	
	Medulloepithelioma	
	CNS Neuroblastoma	
	CNS Ganglioneuroblastoma	
	CNS embryonal tumour, NOS	
	Atypical teratoid/rhabdoid tumour	
	CNS embryonal tumour with rhabdoid features	
Neuronal and mixed neuronal-glial tumours		Dysplastic cerebellar gangliocytoma
		Dermoplastic infantile astrocytoma and ganglioglioma
		Dysembryoplastic neuroepithelial tumour
		Gangliocytoma
		Ganglioglioma
		Central neurocytoma
		Extraventricular neurocytoma
		Cerebellar liponeurocytoma
		Papillary glioneuronal tumours
		Rosette-forming glioneuronal tumour
		Paraganglioma
Choroid plexus tumours		Choroid plexus papilloma
		Atypical choroid plexus papilloma
		Choroid plexus carcinoma
Tumours of the pineal region		Pineocytoma
		Pineal parenchymal tumour of intermediate differentiation
		Pineoblastoma
		Papillary tumours of the pineal region
TUMOURS OF CRANIAL AND PARASPINAL NERVES		
Schwannoma		Cellular schwannoma
		Plexiform schwannoma
		Melanotic schwannoma
Neurofibroma		Atypical neurofibroma
		Plexiform neurofibroma
Perineurioma		
Hybrid nerve sheath tumour		
Malignant peripheral nerve sheath tumour (MPNST)		Epithelioid MPNST
		MPNST with perineural differentiation

TUMOURS OF THE MENINGES	
Menangiomas	Meningioma
	Meningothelial meningioma
	Fibrous meningioma
	Transitional meningioma
	Psammomatous meningioma
	Angiomatous meningioma
	Microcystic meningioma
	Secretory meningioma
	Lymphoplasmacyte-rich meningioma
	Metaplastic meningioma
	Chordoid meningioma
	Clear cell meningioma
	Atypical meningioma
	Papillary meningioma
	Rhabdoid meningioma
	Anaplastic (malignant) meningioma
Mesenchymal, non-meningothelial tumours	Solitary fibrous tumour/haemangiopericytoma
	Haemangioblastoma
	Haemangioma
	Epithelioid haemangioendothelioma
	Angiosarcoma
	Kaposi sarcoma
	Ewing sarcoma - PNET
	Lipoma
	Angiolipoma
	Hibernoma
	Liposarcoma
	Desmoid-type fibromatosis
	Myofibroblastoma
	Inflammatory myofibroblastic tumour
	Benign fibrous histiocytoma
	Fibrosarcoma
	Leiomyoma
	Leiomyosarcoma
	Rhabdomyoma
	Rhabdomyosarcoma
	Chondroma
	Chondrosarcoma
	Osteoma
	Osteochondroma
	Osteosarcoma
Melanocytic tumours	Meningeal melanocytosis
	Meningeal melanocytoma
	Meningeal melanoma
	Meningeal melanomatosis
LYMPHOMAS AND HEMATOPOIETIC NEOPLASMS	
Diffuse large B-cell lymphoma of the CNS	
Immunodeficiency-associate	AIDS-related diffuse large B-cell lymphoma
	EBV-positive diffuse large B-cell lymphoma, NOS
	Lymphomatoid granulomatosis
Intravascular large B-cell lymphoma	
Low-grade B-cell lymphomas of the CNS	
T-cell and NK/T-cell lymphomas of the CNS	
Anaplastic large cell lymphoma, ALK-positive	
Anaplastic large cell lymphoma, ALK-negative	
MALT lymphoma of the dura	
HISTIOCYTIC TUMOURS	
Langerhans cell histiocytosis	
Ercheim-Chester disease	
Rosau-Dorfman disease	
Juvenile xanthogranuloma	
Histiocytic sarcoma	
GERM CELL TUMOURS	
Germinoma	
Embryonal carcinoma	
Yolk sac tumours	
Choriocarcinoma	
Teratoma	Mature teratoma
	Immature teratoma
Teratoma with malignant transformation	
Mixed germ cell tumour	
TUMOURS OF THE SELLAR REGION	
Craniopharyngioma	Adamantinomatous craniopharyngioma
	Papillary craniopharyngioma
Granular cell tumour of the sellar region	
Pituicytoma	
Spindle cell oncocytoma	
METASTATIC TUMOURS	

profiling a massive amount of data were collected. These genomic data have shown that tumours considered originally as the same entity present a broad heterogeneity and consequently led to an improvement of the classification (**Table 2**). Indeed, the 2016 WHO CNS classification (Louis *et al.* 2016) takes into account molecular alterations recently discovered for some entities.

In particular, we can observe a refinement in the classification of the tumours of neuroepithelial tissue, especially in the gliomas. The histological categorization give way to more homogeneous subgroups that takes into account the genetic alterations that have been frequently reported in several studies, such as *IDH*-mutation in diffuse astrocytic and oligodendroglial tumours and 1p/19q-codeletion in oligodendrogliomas (Pollack, Hamilton, et al. 2011, 1; Yang et al. 2012; A. Cohen, Holmen, and Colman 2013; J.-R. Chen et al. 2016; N. Hu, Richards, and Jensen 2016).

Moreover, recent studies have identified K27M mutations in genes encoding the histone H3 in the majority of diffuse gliomas arising in thalamus, brainstem – most frequently into the pons – and spinal cord (Schwartzentruber *et al.* 2012; Sturm *et al.* 2012; Khuong-Quang *et al.* 2012; Puget *et al.* 2012). Based on this alteration, a new entity named Diffuse Midline Gliomas (DMG), H3 K27M-mutant was defined (Louis *et al.* 2016). This entity includes Diffuse Intrinsic Pontine Gliomas (DIPG), a high-grade glioma (HGG) that represent 20% of all paediatric brain tumours, as well as other paediatric HGG (pHGG)(Louis *et al.* 2016). This H3 K27M alteration will be particularly described in more details in further section (PART II.3. H3 recurrent hotspot mutations).

6. Adult *versus* paediatric high-grade gliomas

For the purpose of this thesis, the following sections will focus on HGG. Among the solid tumours, brain tumours are the most common type of paediatric cancers and represents 24.9% of the children diagnosed with cancer before 14 years and 17.2% of adolescents between 15 and 17 years in France (INCa 2018). The brain tumours are the leading cause of childhood cancer mortality, representing 38% of the cases in France (INCa 2018).

The tumours of glial origin are the most frequent type of brain tumours in both adult and paediatric patients. In adults, glioblastoma (GBM) is the most common type of primary malignant high-grade astrocytoma and corresponds to 60% of all patients diagnosed with a brain tumour (Rock *et al.* 2012). Among children's gliomas, the most common type of neoplasm is the low-grade pilocytic astrocytomas, which represent 17% of all paediatric brain tumours. These tumours present a good prognosis with an overall 10-year survival rate superior to 96% (Johnson *et al.* 2014). The second most common type of brain tumours is the Diffuse Intrinsic Pontine Gliomas (DIPG) that represent 10% to 15% of all childhood CNS tumours. However, in contrast to pilocytic astrocytomas, there are almost no survivors in DIPG after two years of diagnosis (Paugh *et al.* 2010; Puget *et al.* 2015b).

Genome-scale profiling of childhood brain tumours have been conducted only quite recently because of the scarcity of the samples. Bax and coll. (2010) performed copy number analysis by comparative genomic hybridization array (aCGH) of 63 HGG from children and young adults. Different levels of genomic alterations were identified (Bax *et al.* 2010): (i) tumours presenting stable genomes with only few focal changes and associated with better prognosis; (ii) aneuploid

profiles characterized by large single copy alteration of whole chromosomes or chromosomal arms; (iii) highly rearranged genomes with numerous intrachromosomal breaks and (iv) genomic profiles with single or multiple high-level amplifications, frequently associated with a worst prognosis.

PDGFRA amplification and *CDKN2A*/B deletion were identified as the most frequent focal events. The most common large alterations were gain of chromosome 1q and loss of chromosome 16q. Additionally, amplifications and deletions affecting *IGF1R*, *PDGFRB*, *PIK3CA*, *CDK6* and *CCND1* were also identified at a lower frequency. Together, *PDFGRA*^{amp}, 1q^{+} and 16q^{-} are the genomic alterations more frequently found in children, even though some of them are also retrieve in adult tumours (Bax *et al.* 2010).

In parallel, Paugh and coll. published a study on a cohort of 78 pHGGs to uncover copy number alterations by single nucleotide polymorphism (SNP) microarray analysis and also identify gene expression signatures underlying pHGG by conducting transcriptomic microarray analysis (Paugh 2010). Likewise, recurrent gain of chromosome 1q was observed in 29% of the cases and *PDGFRA* amplification with consistent overexpression was found in 12% of the cases. Amplified genes at low frequency were identified in 1-4% of the cases in pathways related to cell cycle progression (*CCND2*, *CDK4*, *MYC* and *MYCN*); receptor tyrosine kinases (RTKs) (*EGFR*, *MET*, *PDGFB* and *NRG1*); PI3K (*PIK3C2B*, *PIK3C2G*, *PIK3R5*, *KRAS*, *AKT1* and *S6K1*) and *TP53* regulation (*MDM4*)(**Figure 7**)(Paugh *et al.* 2010).

In adult GBM, copy number, gene expression and mutational analyses identified four subgroups (proneural, proliferative, proliferative/mesenchymal and

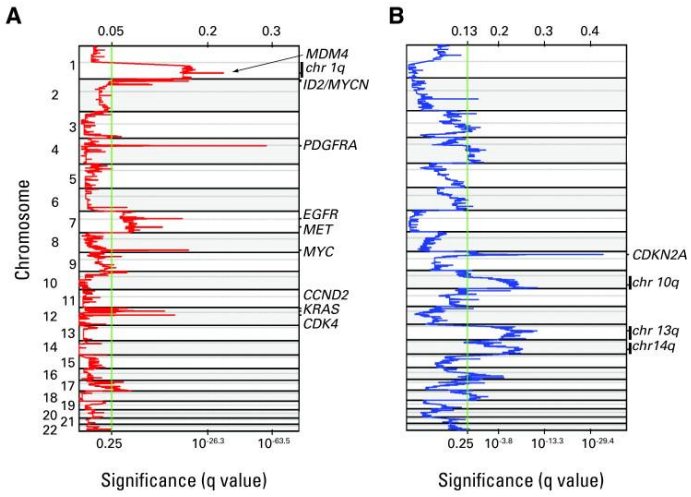

Figure 7. Genomic alterations frequently identified in pHGG. The graphic shows **s**ignificant copy number (A) gains and (B) losses identified in 68 *de novo* pediatric HGGs by Genomic Identification of Significant Targets in Cancer (GISTIC). Chromosome positions at the y-axis, G-score above the x-axis, and false discovery rate are shown along the lower x-axis. The green line indicates the q value threshold of 0.25 (Paugh *et al.* 2010).

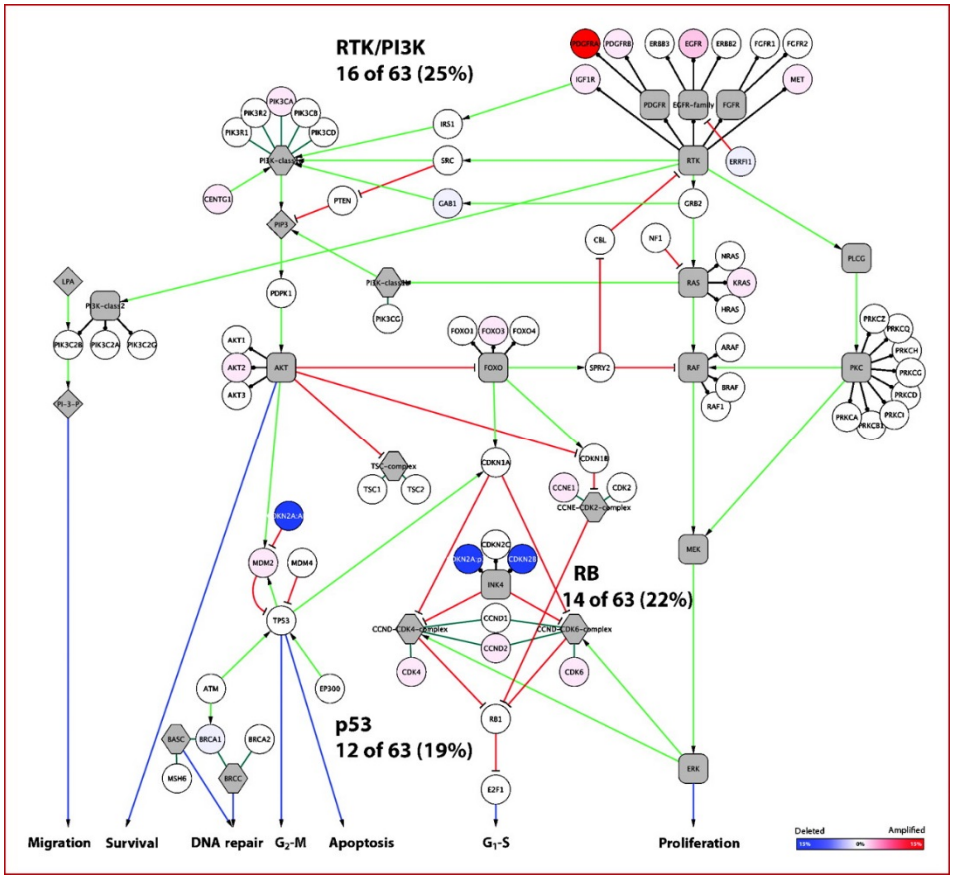

Figure 8. Three core signaling pathways frequently deregulated in adult GBM and copy number changes in pHGG. Heatmap of signaling pathways shown the interactions among the deregulated genes. The frequency of copy number alteration in adult GBM is 59% RTK/PI3K, 70% TP53 and 66 Rb%. In pHGG, these pathways are significantly less deregulated, in respectively 25%, 19% and 22% of the patients. Red cases indicates genes with amplifications and blue cases indicates genes with focal deletion (Bax *et al.* 2010).

mesenchymal) associated with recurrent rearrangements and gene expression signatures (Y. Lee *et al.* 2008). Moreover, three signalling pathways are most frequently affected: alterations in RTK/PI3K pathway (*MET*, *KRAS* and *AKT2*) were detected in 59% of the cases, TP53 signalling pathway (*TP53* and *MDM2*) in 70% and RB (*CCND2*) in 66%. These pathways were less frequently altered in paediatric tumours, respectively in 25%, 19% and 22% of the cases (**Figure 8**)(Bax *et al.* 2010). Additionally recurrent alterations found in adult GBM, such as *PTEN* deletion, *EGFR* amplification (40%) and mutations and *IDH1* hotspot mutations, represent a rare event in childhood gliomas (Pollack *et al.* 2006; Paugh *et al.* 2010; Pollack, Hamilton, *et al.* 2011; Ohgaki and Kleihues 2007).

These studies defined distinct spectrum of molecular alterations revealing key differences between paediatric and adult HGG (Bax *et al.* 2010; Paugh *et al.* 2010). Paediatric HGG can be clearly distinguished from their adult counterpart by the frequent gain of chromosome 1q (30% in children *versus* 9% in GBM), a lower frequency of chromosome 7 gain (13% *vs*. 74%) and 10q loss (35% *vs.* 80%) (Korshunov, Sycheva, and Golanov 2005; Bax *et al.* 2010; Paugh *et al.* 2010). While adults are frequently associated with *PTEN* deletion, *EGFR* amplifications (40%) and *IDH1* hotspot mutations (Pollack *et al.* 2006; Ohgaki and Kleihues 2007; Paugh *et al.* 2010; Pollack, Hamilton, *et al.* 2011), pHGG presents predominantly amplification and overexpression of *PDGFRA* (Bax *et al.* 2010; Paugh *et al.* 2010).

Alongside, our group was able to perform an integrated molecular profiling of large cohort of DIPG samples at diagnosis and non-brainstem pHGG from our closer collaborators at the Neurosurgery Department of Necker Enfants Malades Hospital (Puget *et al.* 2012). Classification method (PCA) based on chromosomal imbalances

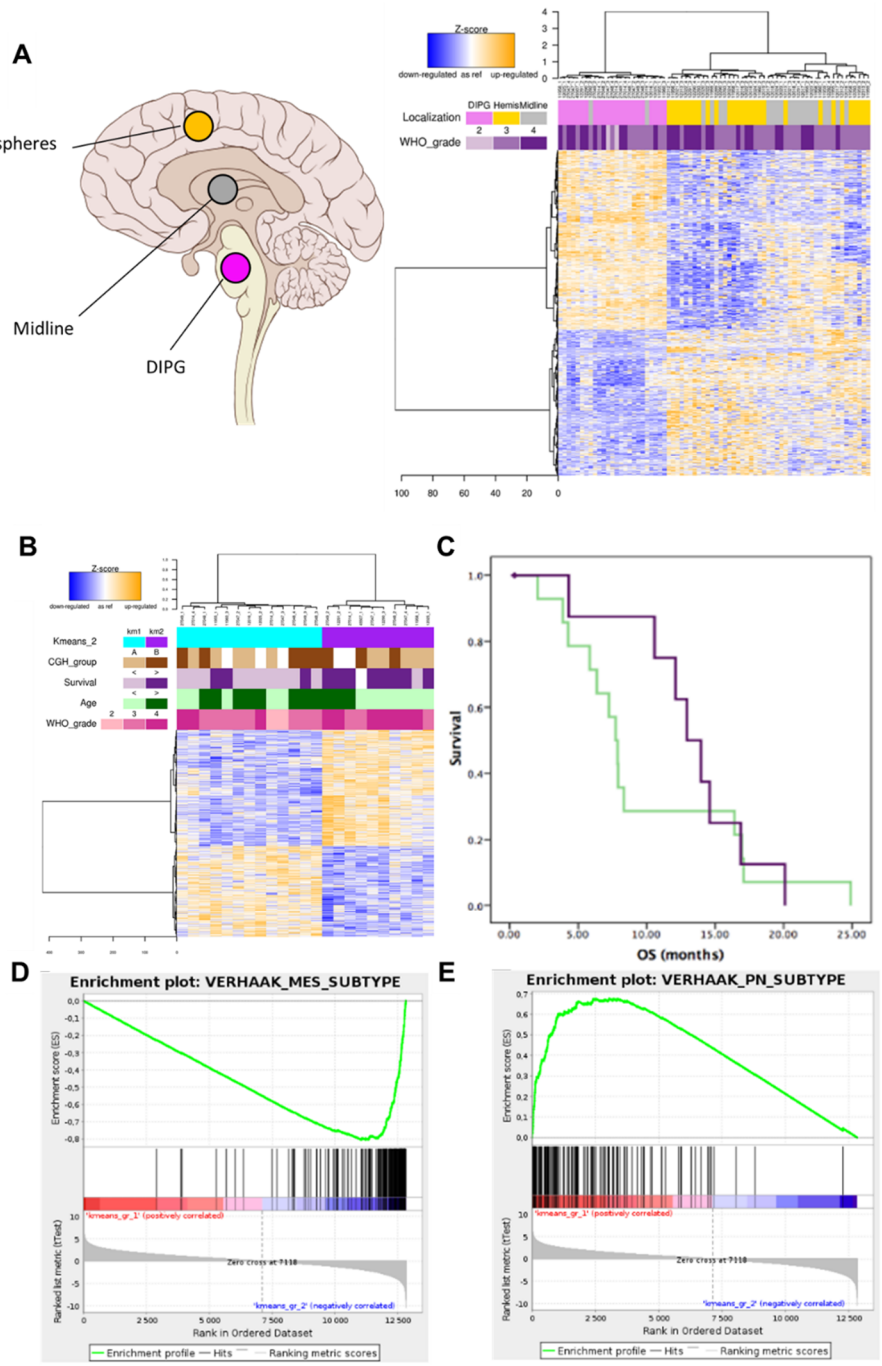

Figure 9. DIPG represents a different group in comparison to supratentorial high-grade gliomas in children. (A) Heatmap of most differentially expressed genes (n=712) between DIPG (n=23), midline and hemispheric (n=49) tumours. Hemispheric, midline/thalamic tumours and DIPG are represented in yellow, grey and purple respectively (Puget *et al.* 2012). (B) Heatmap of most differentially expressed genes (n=643) between the two subgroups of DIPG (n=23). DIPG can clearly be divided into two subgroups considering the different gene expression signatures. (C) Overall survival curves of the two subgroups of DIPG. Gene set enrichment analysis (GSEA) shown that when comparing DIPG subgroups with signatures described for adult GBM, one subgroup (D) is enriched in mesenchymal genes, while the other (E) is enriched in proneural genes (modified from Puget *et al.* 2012).

measured by CGH-array can separate paediatric and adult HGGs, nevertheless they cannot separate non-brainstem pHGG and DIPG. However, gene expression of pHGG clearly separate DIPG as a biologically distinct subgroup of pHGG according to the localization, independent of the malignancy grade (**Figure 9A**). Moreover, DIPG subgroups can be defined by two distinct specific gene expression signatures (**Figure 9B**) (i) a mesenchymal phenotype (**Figure 9D**) in tumours presenting a better outcome (**Figure 9C**): median overall survival (OS) of 12.37 months) and (ii) an oligodendroglial phenotype (**Figure 9E**), which appear largely driven by *PDGFRA* amplification and/or mutation in tumours with a worse outcome (**Figure 9C**) (median OS of 7.73)(Paugh *et al.* 2011; Puget *et al.* 2012).

To explore the alterations in pHGG, Schwartzentruber and coll. performed a comprehensive mutation analysis by whole-exome sequencing (WES) of 48 paediatric GBMs. They identified recurrent mutations in one gene encoding the histone variant H3.3 (*H3F3A)* at two critical positions of the histone tail (K27 and G34), together with mutations in *ATRX* (α-thalassemia/mental retardation syndrome X-linked) and *DAXX* (death-domain associated protein), both part of the chromatin remodelling complex, in 44% of samples. Enlarging the analysis to a cohort of gliomas of different histology and grades (n=784) showed that *H3F3A* mutations are highly frequent in one-third of children brain tumours patients (36%) and occurs rarely in young adults (3%). This is interesting as this is the first human disorder specifically linked to histone mutations (Schwartzentruber *et al.* 2012).

By integration of subsequent genomic data, *i.e.* genome-wide DNA methylation, mutational status, DNA copy-number alterations and gene expression signatures and taking into account clinical variables, such as patient

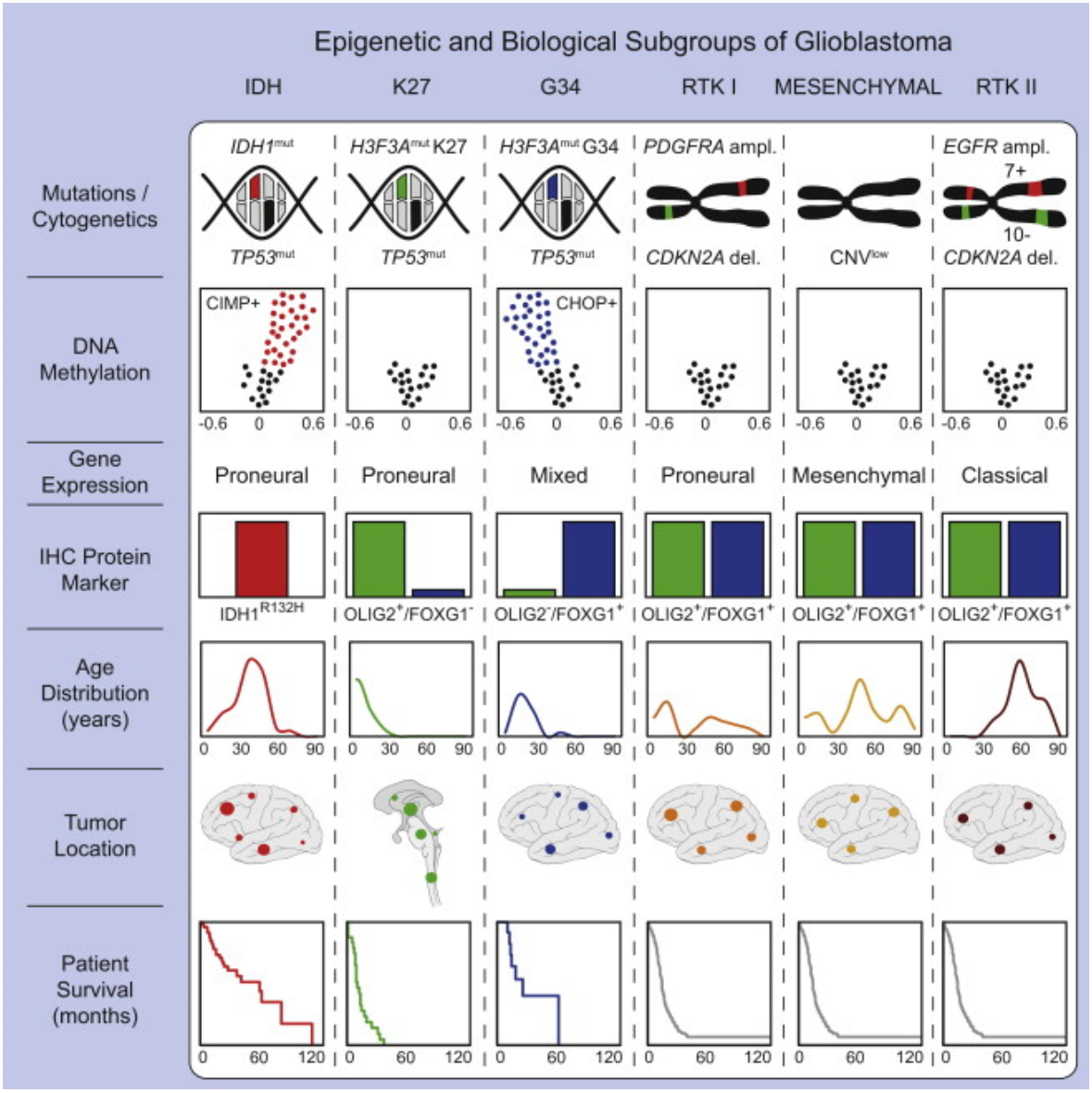

Figure 10. Key Molecular and Biological Characteristics of GBM Subgroups. Six biological subgroups of GBM, indistinguishable by histological appearance, can be defined based on global DNA methylation patterns, which correlate with specific molecular-genetic alterations and key clinical parameters. Three epigenetic GBM subgroups correlate strictly with mutations in *H3F3A* and *IDH1*. H3F3A K27- and G34-mutant GBMs clearly arise in different anatomic compartments, with significant different age of onset. This classification refines the TCGA one (Noushmehr *et al.* 2010; Verhaak *et al.* 2010) by including clinical features to define biologically meaningful subgroups (Sturm *et al.* 2012).

age and tumour localisation the same group was able to identify six distinct GBM subgroups. The six GBM methylation clusters (i) IDH; (ii) K27; (iii) G34; (iv) RTK I (PDGFRA), (v) Mesenchymal; and (vi) RTK II (Classic) and their characteristics are summarized in **Figure 10** (Sturm *et al.* 2012).

Interestingly, both H3.3 mutations identified previously (H3F3A-K27M and G34R/V) have been shown to form different subgroups. Noteworthy for the following section, K27M-mutated tumours are found exclusively in midline structures: thalamus, pons and spinal cord. In supratentorial pHGG, a substitution of a glycine (G) by arginine (A) or valine (V) at the position 34 (G34R or G34V) in the histone H3.3 occurs in 10–19% of the cases and is restricted to cerebral hemispheres (Sturm *et al.* 2012). They also shown differences in gene expression patterns and neuronal lineage markers, that led to hypothesis of distinct cell of origin and embryonic timing for the development of these subgroups (Schwartzentruber *et al.* 2012; Sturm *et al.* 2012). These subgroups will be discussed in more details in the following sections.

PART II. DIFFUSE INTRINSIC PONTINE GLIOMAS

1. General introduction

As mentioned previously, Diffuse Intrinsic Pontine Glioma (DIPG) is the most aggressive form of paediatric brainstem gliomas, representing 10-15% of all the childhood brain tumours (Jansen et al. 2012; Puget et al. 2015b). The delicate localization deep-seated into the pons and the diffuse infiltration of the tumour cells renders these tumours inoperable. In France, 40 to 50 new cases are diagnosed *per* year. DIPG occurs in children and adolescents, with a mean onset between 6 to 9 years. The median OS range from 9 to 12 months after diagnosis and less than 10% of patients survive over 2 years (**Figure 9C**) (Jones and Baker 2014; Buczkowicz and Hawkins 2015; Puget *et al.* 2015b).

The radiotherapy (RT) is the standard treatment. Nevertheless it provides only transient efficiency, delaying tumour progression with a systematically fatal relapse within few months (Zaghloul *et al.* 2014). The median progression-free survival (PFS) is of 5,6 months (Puget *et al.* 2015b). Over the last 50 years, no progress has been made in the treatment, despite the efforts in the use of various chemotherapeutics and radiosensitizing agents in different RT combinatorial protocols (Hummel *et al.* 2016; K. J. Cohen *et al.* 2011; Bailey *et al.* 2013; Zaky *et al.* 2013; Korones *et al.* 2008; Packer *et al.* 2005; Pollack, Stewart, *et al.* 2011; Allen *et al.* 1999; Jennings *et al.* 2002; Porkholm *et al.* 2014) in over 250 clinical trials that have failed to significantly improve the patient survival (Lapin, Tsoli, and Ziegler 2017).

The biopsy of DIPG patients was abandoned until 2002 due to the potential risks of the procedure, the ability to establish diagnosis based on clinical symptoms

and imaging analysis (MR imaging), but also because it did not allow to improve patient's outcome or select a better treatment (Albright *et al.* 1993; Cartmill and Punt 1999; Steck and Friedman 1995). The scarcity of primary material and the previous association of DIPG with both adult and paediatric non-brainstem HGG until 2010 resulted in the absence of significant therapeutic progress and the poor understanding of the underlying molecular mechanisms of this disease (Roujeau *et al.* 2007; Jones and Baker 2014; Puget *et al.* 2015b).

2. Genomic alterations

The reintroduction of biopsies at diagnosis since 2002 by our closer collaborators at the Neurosurgery Department of Necker Enfants Malades Hospital (Roujeau *et al.* 2007; Puget *et al.* 2015b) leaded to several important discoveries especially from our laboratory related to the molecular and histopathological characteristics of DIPG (Puget *et al.* 2012; K. R. Taylor *et al.* 2014; Castel *et al.* 2015). Indeed, as previously mentioned, early molecular profiling studies started to shed light into the different biology underlying adult, paediatric high-grade gliomas and, more specifically, DIPG (Bax *et al.* 2010; Zarghooni *et al.* 2010; Paugh *et al.* 2011; Puget *et al.* 2012; Sturm *et al.* 2012).

Preliminarily WGS analysis in a cohort of DIPG patients (n=24) have allowed to determine that these patients present a low mutation rate, when compared to other tumours. Most frequent mutations were *TP53*, *PI3K/MAPK*, *ACVR1* and *PDGFRA* amplifications respectively in 42%, 46%, 21% and 10% of the cases. The more frequently large scale imbalances identified by copy number and gene expression analysis in DIPG are gains of the chromosome 1q and losses of 11p,

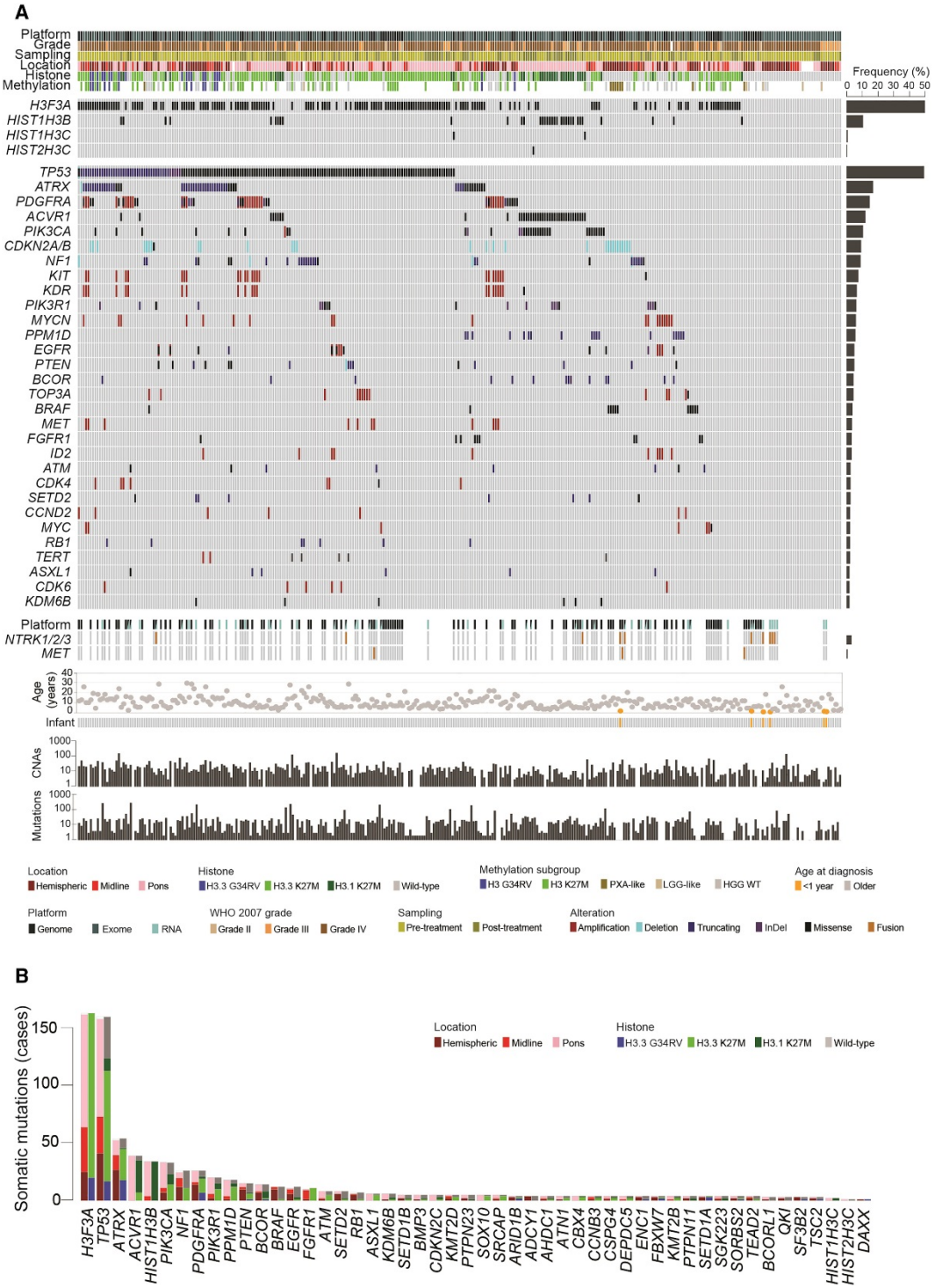

Figure 11. Genomic landscape of pHGG and DIPG. (A) Integrated annotation of genetic alterations (somatic mutations and DNA copy-number changes) for the most frequently altered genes in pHGG/DIPG (n=326). (B) Barplot of all recurrent somatic mutations across the patients, in order of frequency and correlated to anatomical location and histone mutation (Mackay *et al.* 2017).

13q and 14q (Zarghooni *et al.* 2010; Paugh *et al.* 2011; G. Wu *et al.* 2012; Puget *et al.* 2012).

The recent paper of Mackay and coll. integrated molecular genomic, epigenomic and transcriptomic data of 1067 pHGG and DIPG cases from published and unpublished data over the past years (Mackay *et al.* 2017). This study summarized the current knowledge of the genomic mutational landscape of pHGG and DIPG (**Figure 11**). The focal mutations most frequently altered in DIPG are further discussed.

2.1. Tumour suppressor protein 53 (TP53)

TP53 mutations and copy number alterations were identified in 42-71% of DIPG patients (Khuong-Quang *et al.* 2012; Puget *et al.* 2012; Buczkowics *et al.* 2013; Buczkowicz and Hawkins 2015). The TP53 pathway can also be disrupted by alterations in negative regulators, such as *MDM2*, *MDM4* and *ARF*, and alterations in upstream genes of the DNA damage response (DDR) pathway, such as *ATM*, *ATR*, *CHK1* and *CHK2.* Found in 10-12% of the cases, truncating mutations in the TP53-induced phosphatase *PPM1D* have been shown to be functionally equivalent to *TP53* mutations, impairing G1 checkpoint by suppressing the activation of *CHK2* (L. Zhang *et al.* 2014; G. Wu *et al.* 2014).

TP53 gene is one of the most important and well-known tumour suppressor gene. TP53 activation in response to distinct cellular stress signals from different sources (*i.e.* DNA damage, oxidative stress, replicative stress) leads to several cellular responses that include transient cell cycle arrest, DDR, apoptosis and senescence (Joerger and Fersht 2016). The TP53 pathway is frequently altered in

more than 50% types of cancer, leading to genetic instability, invasiveness increase and metastatic potential (Bieging, Mello, and Attardi 2014; Ludwig and Kornblum 2017; Joerger and Fersht 2016, 53).

2.2. Activin receptor type 1 (ACVR1)

Recurrent activating mutations in *ACVR1* gene are found in approximately 20–32% of DIPG patients (Buczkowics *et al.* 2013; G. Wu *et al.* 2014; K. R. Taylor *et al.* 2014). *ACVR1* encode a type I receptor of bone morphogenic proteins (BMP). It has been shown previously to be associated with the congenital autosomic dominant disorder called fibrodysplasia ossificans progressive (FOP) (Katagiri 2012). The consequence of *ACVR1* mutations is an alteration of intermolecular or intramolecular interactions of the mutant receptor that lead to a deregulation of the downstream BMP signalling pathway (Song *et al.* 2010). *ACVR1* mutations cause a constitutive ligand-independent activation of the TGFβ/BMP signalling pathway, resulting in increased levels of SMAD phosphorylation, as well as overexpression of downstream targets *ID1* and *ID2* (Buczkowics *et al.* 2013; G. Wu *et al.* 2014; K. R. Taylor *et al.* 2014).

2.3. Platelet-Derived Growth Factor Receptor α (PDGFRA)

PDGFRA is a Receptor Tyrosine Kinase (RTK) frequently mutated (5-9%) or amplified (28-39%) in DIPG patients (Khuong-Quang *et al.* 2012; Zarghooni *et al.* 2010; Paugh *et al.* 2011; Buczkowics *et al.* 2013; Paugh *et al.* 2013; Puget *et al.* 2012). RTKs are cell surface receptors that act like key regulators of several cellular processes, such as metabolism, proliferation, migration, differentiation and survival

(Lemmon and Schlessinger 2010). Alterations in RTK signalling pathways usually lead to increased activation of cellular processes and tumorigenesis (Regad 2015).

Our group reported that the DIPG subgroup displaying oligodendroglial phenotype is enriched for the genes of the *PDGFRA*-amplified signature described in GBM, associated with increased tyrosine-kinase activity (Puget *et al.* 2012). This alteration is found in older patients and present a most aggressive tumour evolution (Verhaak *et al.* 2010; Puget *et al.* 2012). Additionally, *in vitro* studies using Dasatinib, a multi-tyrosine kinase inhibitor targeting this receptor, have shown a reduction in proliferation, migration and invasion of DIPG cells derived from biopsy at diagnosis (Truffaux *et al.* 2015).

2.4. Phosphatidylinositol-4,5-bisphosphate 3-kinase (PIK3CA)

The PIK3CA signalling pathway is deregulated in DIPG mainly due to *PTEN* focal deletions and mutations in either *PIK3CA* or *PIK3R1*, that are found in 14 and 12-23% of the patients respectively (Buczkowics *et al.* 2013; Grill *et al.* 2012; Buczkowicz *et al.* 2014). These alterations are usually associated with poor prognosis (Pollack *et al.* 2006).

The PI3K pathway regulates diverse cellular processes, including metabolism, survival, proliferation, apoptosis, growth, and cell migration (Chalhoub and Baker 2009). PI3-kinase and PTEN are, respectively, the major positive and negative regulators of this pathway and are frequently altered in cancers. PI3K is responsible for the conversion of phosphatidylinositol-diphosphate (PIP_2) to phosphatidylinositol-3,4,5-trisphosphate (PIP_3) leading to a recruitment and activation of AKT. Activated AKT regulates many substrates by phosphorylation,

thereby activating or inhibiting its targets and inducting cellular growth, survival and proliferation through various mechanisms. PTEN regulates the PI3K signalling by dephosphorylation of the lipid signalling intermediate PIP3, thus acting as a tumour suppressor gene (Chalhoub and Baker 2009; Mantamadiotis 2017; Langhans *et al.* 2017).

2.5. DNA Damage Repair (DDR) pathway

Deletions and loss of heterozygosis (LOH) have been identified at low frequency in several genes related to DDR pathway, such as *RPA1*, *MNAT1* and *GTF2H3* (nucleotide excision repair, NER), *LIG4*, *XRCC4* and *XRCC5* (non-homologous end-joining, NHEJ), *BRCA1*, *BRCA2*, *RAD50* and *RAD51L1* (homologous recombination, HR), *MYH1* (base excision repair, BER), and *PMS1*, *MLH1* and *MSH4* (mismatch repair, MMR)(Zarghooni *et al.* 2010).

Chromosomic gain or overexpression of poly (ADP-ribose) polymerase (*PARP-1*) was found in 54-76% of DIPG patients (Zarghooni *et al.* 2010; Chornenkyy *et al.* 2015). *PARP-1* is involved in DNA damage signalling, recruitment and activation of DNA repair proteins (Rouleau *et al.* 2010). Indeed the overexpression of *PARP-1* associated with other alterations in DDR members, can be considered as one of the mechanisms to escape the DDR and apoptosis, leading to tumorigenesis (Zarghooni *et al.* 2010).

2.6. α-Thalassemia-mental Retardation syndrome X-linked (ATRX)

ATRX frameshift insertions/deletions, premature stop codon or missense single-nucleotide variations (SNVs) have been described in 9-13% of DIPG patients (Khuong-Quang *et al.* 2012; Schwartzentruber *et al.* 2012). The *ATRX* gene encodes a protein involved in telomere maintenance by alternative lengthening of telomeres, depositing histones at heterochromatin and regulating DNA repair mechanisms. Consequently, *ATRX* loss can induce genomic stability (Koschmann *et al.* 2016). Reported in tumours of astrocytic lineage, it is thus used to distinguish them from tumours of oligodendroglial origin (Danussi *et al.* 2018). This alteration is frequently associated with *TP53* modification and older patients (Nandakumar, Mansouri, and Das 2017).

3. H3 recurrent hotspot mutations

The major breakthrough in the elucidation of a DIPG mutational landscape occurred in 2012 with the identification by WGS and WES of specific recurrent hotspot mutation in genes encoding the histone H3 in 95% of DIPG (G. Wu *et al.* 2012; Schwartzentruber *et al.* 2012; Khuong-Quang *et al.* 2012; Castel *et al.* 2015).

This mutation occurs at a highly conserved residue, the lysine (K) at the position 27 and results in its substitution by a methionine (M) (p. Lys27Met or K27M). This substitution occurs at a critical position within the N-terminal histone tail submitted to regulatory post-translational modification (PTM) associated with transcriptional repression (K27). This alteration can be found in different genes encoding histone H3. *HIST1H3B* and *HIST1H3C* genes for the H3.1, *HIST2H3A* gene for H3.2 canonical proteins or *H3F3A* gene for the H3.3 variant protein. H3.1-

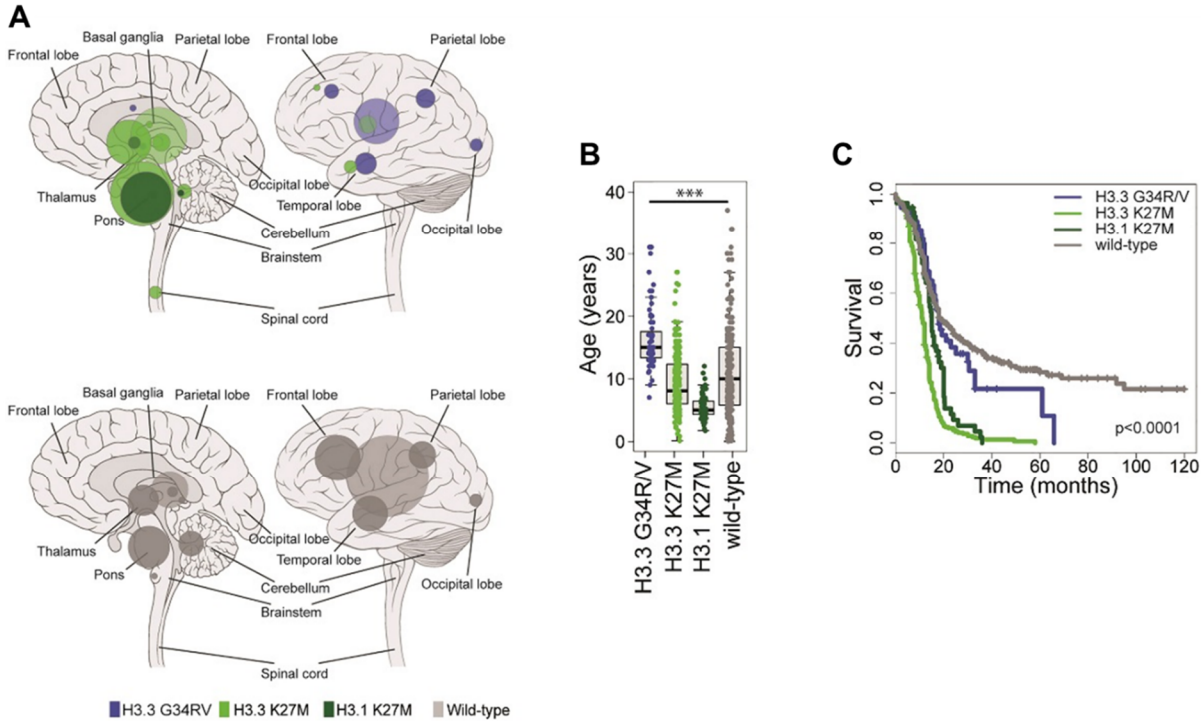

Figure 12. Specific recurrent mutations in histone H3 genes H3.3 (*H3F3A*) and H3.1 (*HIST1H3B* and *HIST1H3C*). (A) H3-K27M mutations are found exclusively into the pons, midline structures and spinal cord. **(B)** Age at diagnosis correlated with histone mutation (n = 753). H3.1 K27M mutations are associated with younger patient age, when compared to H3.3 mutations and WT patients (***Adjusted $p < 0.0001$ for all pairwise comparisons, *t* test). **(C)** Kaplan-Meier plot of overall survival considering histone mutational status (n = 693)(modified from Mackay *et al.* 2017).

K27M mutation are restricted to the pons, whereas H3.3-K27M alteration are found alongside midline structures, *i.e.* pons, thalamus and spinal cord (Castel *et al.* 2015; Mackay *et al.* 2017). H3.1-K27M and H3.3-K27M represent different subgroups with different localization, age of onset and prognosis (**Figure 12**) (Castel *et al.* 2015; Mackay *et al.* 2017).

3.1. Histone proteins and post translational modifications

Histone proteins are involved in DNA packaging. The packaging unit of chromatin is the nucleosome, which is composed by an octamer of four core histone H2A, H2B, H3 and H3, wrapped by 147 base pairs of double-stranded DNA. These units are further tightly coiled and folded into the chromosome structure (**Figure 13A**). The N- or C-terminal tails of the core histones are submitted to several PTMs, such as acetylation (ac), methylation (me), phosphorylation (ph), ubiquitylation (ub), *etc* (**Figure 13B**). These PTM are involves in regulation of chromatin compaction and by this way to chromatin accessibility, thereby regulating gene expression, DNA replication, condensation and DNA repair. The histone H3 is the histone that can be submitted to the greater number of PTM on different amino acid residues (Kouzarides 2007; Xu, Du, and Lau 2014).

Among the different types of histone PTM, acetylation and methylation are the most frequent and strongly linked to regulation of gene expression (Verdone, Caserta, and Di Mauro 2005; Zmarzły *et al.* 2017). The histone acetylation is catalysed by histone acetyltransferases (HAT) that transfer an acetyl group from an acetyl Coenzyme A (acetyl-CoA) donor to the lysine (K) residues. This neutralizes the positive charge of the lysine, weakening DNA-histone interaction and increasing

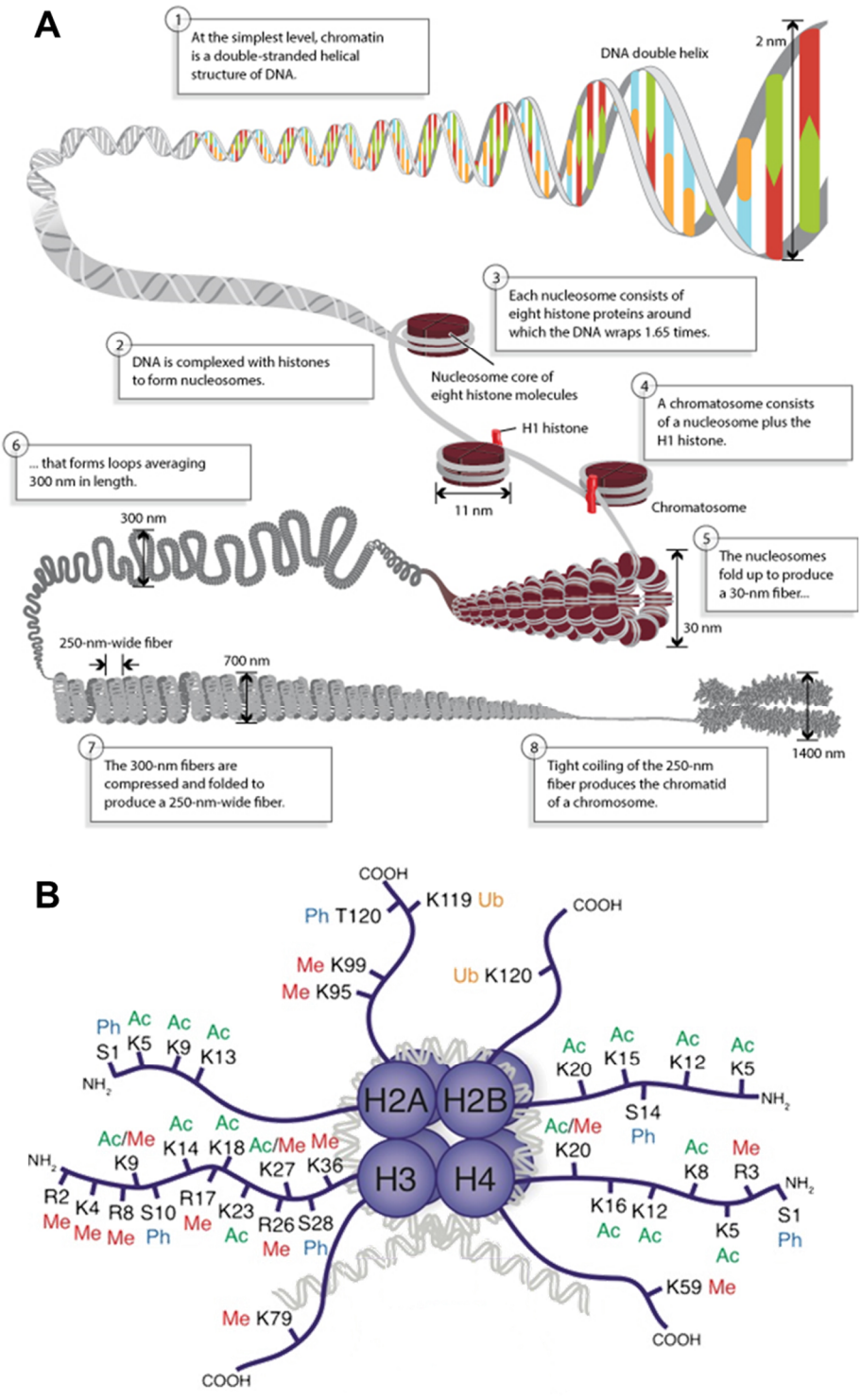

Figure 13. Histones proteins and its functions. (A) DNA packaging. Chromosomal DNA is tightly packaged around histones to form nucleosomes. Each nucleosome is composed by DNA wound around an octamer of four core histones that fold up to form a 30-nanometer chromatin fiber. The chromatin fiber is compressed, folded and tightly coiled into the chromatid of a chromosome (Annunziato 2008). **(B) Histone core post-translational modifications (PTM).** This representation shows the residues of the 4 canonical histones (H2A, H2B, H3, and H4) that can be submitted to different PTM. Me = methylation; Ac = acetylation; Ub = ubiquitination; Ph = phosphorylation (modified from Zhao, Jordan, and Lunyak 2013).

the DNA accessibility to transcriptional activation complexes. On the other hand, histone deacetylases (HDAC) promote chromatin condensation, and consequently repress transcription. Several lysine residues of the histone H3 (K4, K9, K14, K18, K23, K27, K36, K56, K79, K122) can be acetylated or de-acetylated allowing transcriptional activation (Jenuwein and Allis 2001; Johnstone 2002; Garcia *et al.* 2007; Kouzarides 2007; Xu, Du, and Lau 2014).

The histone methylation play a major role in the regulation of active and inactive genomic regions depending on the modified residues and on the number of methyl groups associated. It can occurs on two amino acid residues: lysine that can undergo mono- (me1), di- (me2) and trimethylation (me3); or argine (R) that undergo me1 and me2. The lysine methylation is one of the most abundant PTM and is more frequently observed on residues of histone H3 tails. Histone methyltransferases (HMT) catalyse the transfer of methyl groups from the cofactor S-adenosyl methionine (SAM) to the K or R residues. The active chromatin is associated with H3K4, H3K36, H3K38 and H3K79 methylation, while inactive chromatin is associated with H4K20, H3K9 and H3K27 methylation (Jenuwein and Allis 2001; Garcia *et al.* 2007; Kouzarides 2007; Xu, Du, and Lau 2014).

3.2. Impact of H3-K27M mutation

In order to determine the impact of H3-K27M mutations, Lewis and coll. analysed key regulatory histone modifications in both wild-type (WT) and mutated patients (Lewis *et al.* 2013). They showed that mutated tumours have a significant global loss of the H3-K27me3 repressive mark with a slight increase of H3K27ac compared to WT tumours, without alteration in other regulatory modifications such

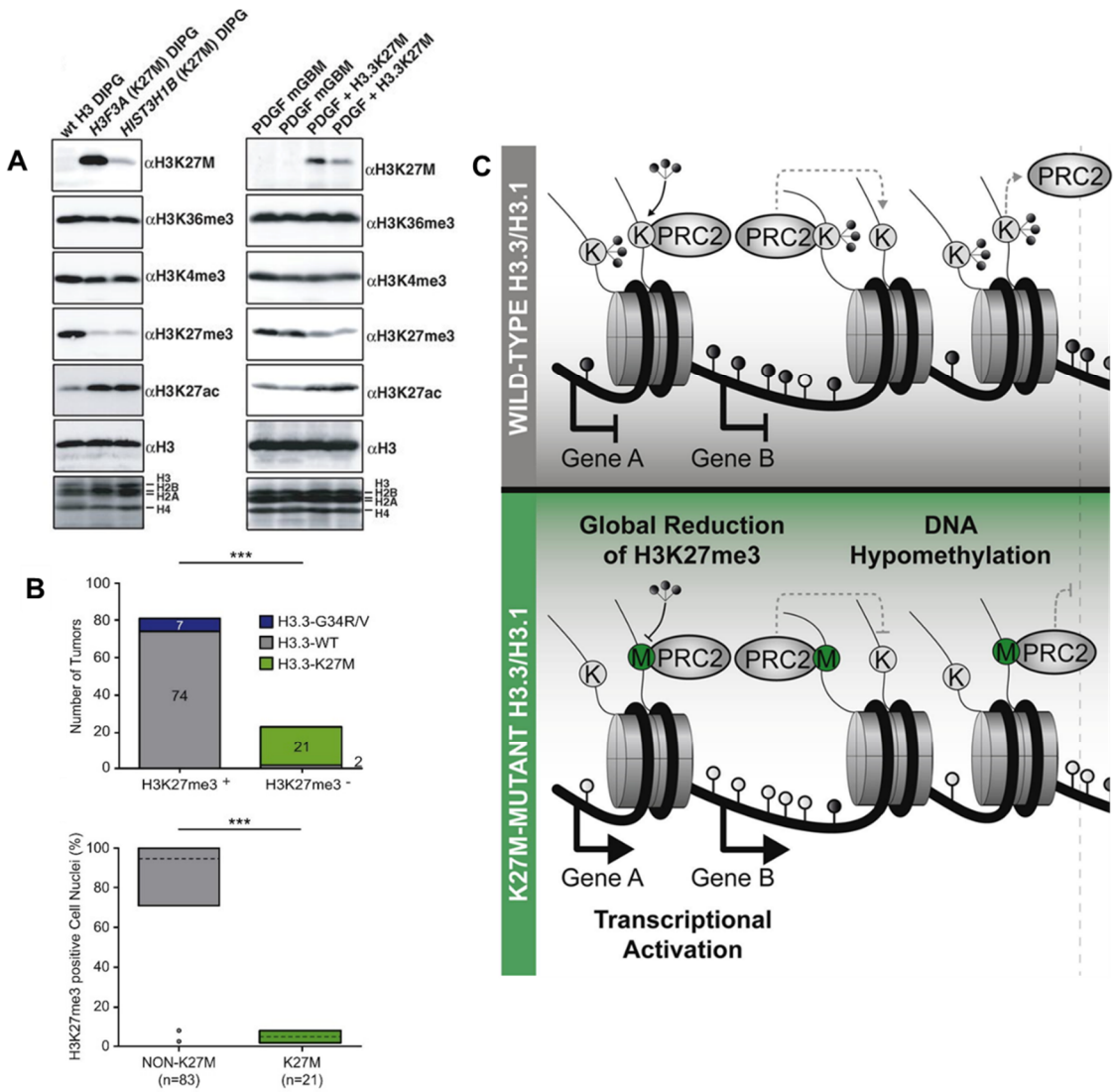

Figure 14. Impact of H3-K27M mutations. Patients carrying histone H3-K27M mutations shown a global reduction of K27 trymethylation on histone H3, without alteration of other epigenetic markers. **(A)** Immunoblots of acid-extracted histones from human DIPG containing *H3F3A* K27M (H3.3) or *HIST3H1B* K27M (H3.1) mutations exhibit a significant decrease in H3K27me3 and a minor increase of H3K27ac (adapted from Lewis *et al.* 2013). **(B)** H3K27me3 immunostaining of wild-type (H3.3-WT), K27M mutant, or G34R/V mutant H3.3 (n=104 pHGGs, ***p < 0.001). IHC of H3K27me3 positive cell nuclei without (non-K27M) or with the K27M mutation (200 cell nuclei/tumor) (***p < 0.001). All K27M mutant pHGGs (n = 21) showed a strong reduction of overall H3K27me3 levels (adapted from Bender *et al.* 2013). **(C)** Impact of H3-K27M mutation on gene expression. Global loss of H3K27me3 is caused by aberrant recruitment of PRC2 to H3-K27M mutant. Histone H3K27M mutant protein sequesters PRC2 histone methyltransferase and functionally inactivates it. Dominant-negative effect of K27M mutant H3.3 results in global loss of H3K27me3. H3K27me3 loss and DNA hypomethylation thereby promoting an open chromatin structure that lead to transcriptional activation in H3-K27M mutated patients (modified from Bender *et al.* 2013).

as, H3-K36me3 and H3-K4me3 (**Figure 14A**). Moreover, Bender confirmed these findings in a larger cohort in which all K27M mutated patients (n=21) presented reduction of H3K27me3 levels (**Figure 14B**)(Bender *et al.* 2013).

In normal cells, the trimethylation on H3K27 is mediated by the Polycomb Repressive Complex 2 (PRC2). This PRC2 multiprotein complex mediates gene silencing by histone di- and/or trimethylation of K27 through its enzymatic subunits EZH1 and EZH2 (Margueron and Reinberg 2011). The H3K27M substitution inhibits the enzymatic activity of EZH2 subunit that no longer can recognize the lysine residue on position 27 of the residual wild-type histone H3, which consequently remain unmethylated. Then the H3-K27M mutation has a dominant-negative effect due to the aberrant recruitment of PRC2 that blocks the methylation of K27 on WT histones. As a result, there is global loss of H3K27me3 level that leads to major gene expression deregulation. Additionally, they have shown that DNA hypomethylation (**Figure 14C**) (Bender *et al.* 2013; Venneti *et al.* 2013; Lewis *et al.* 2013; Chan *et al.* 2013) is also observed in those tumours thus reinforcing the increase of gene expression.

3.3. Differences between histone H3 variants

The same K27M substitution in distinct histone genes *H3F3A* (H3.3) and *HIST1H3B* (H3.1) lead to the same phenotype, a global loss of trimethylation (Bender *et al.* 2013; Castel *et al.* 2015). Despite the same biochemical consequences of the H3K27M alterations, H3.1/2 and H3.3 protein variants differs in several aspects (**Figure 15**). The canonical histones H3.1/2 and the replacement variant H3.3 are the most expressed of the histones H3 and they present 96-99%

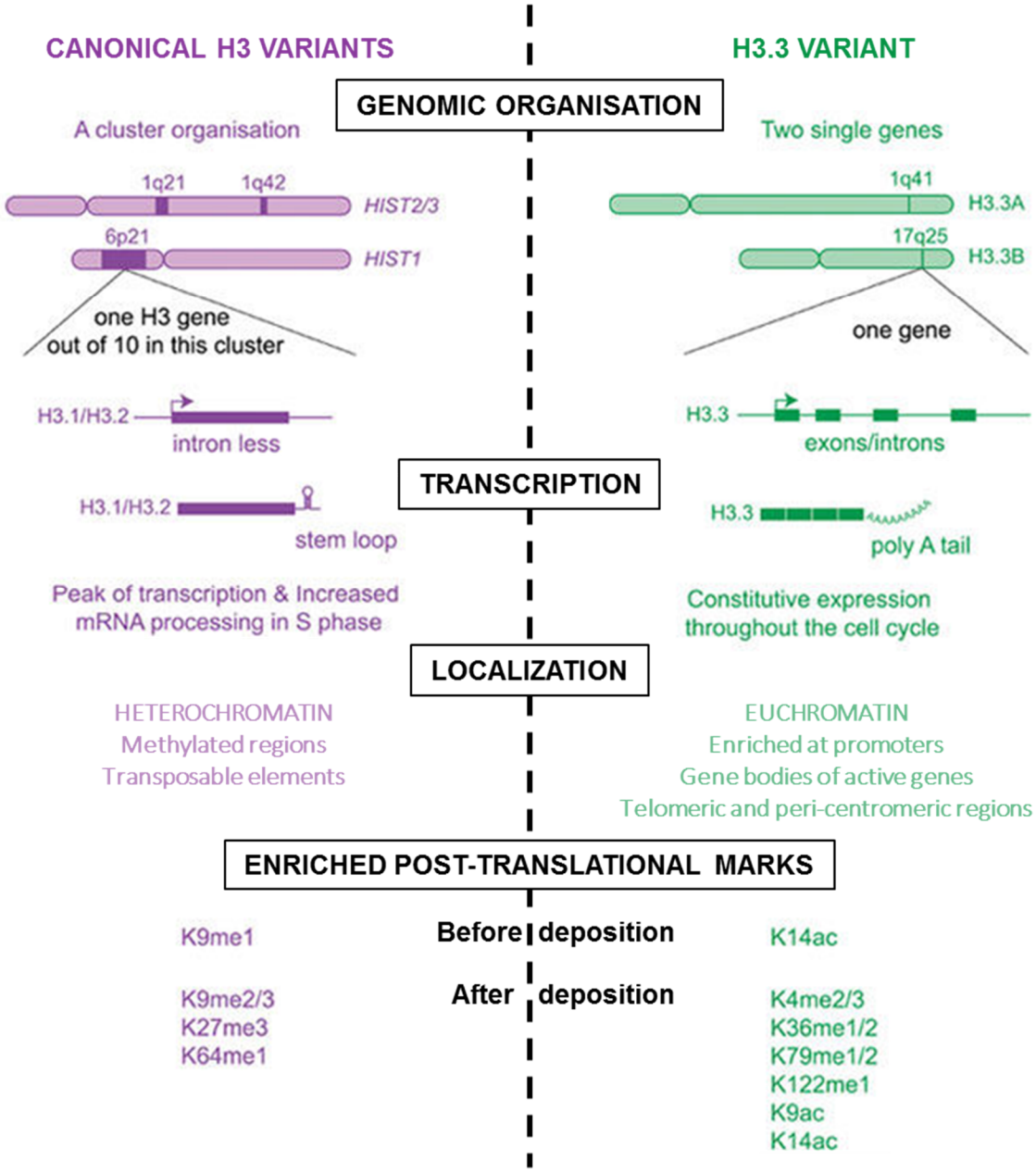

Figure 15. Difference between histone H3 variants. The histone genes have different genomic organization, transcription, localization and post-translational marks. (modified from Szenker, Ray-Gallet, and Almouzni 2011).

amino acid sequence similarity between each other (Xu, Du, and Lau 2014).

The histones H3.1 and H3.2 genes are organized in multicopy cluster of several genes, without introns. The resulting mRNA do not contain a polyA tail but a stem-loop structure at the 3'-end, which contributes to enhance translation efficiency. Since these canonical histones are synthesized during replication (replication-dependent), this allow the rapid packaging of the newly synthesized DNA (Marzluff *et al.* 2002; Szenker, Ray-Gallet, and Almouzni 2011). During replication, H3.1 and H3.2 are deposited by the chaperone chromatin assembly factor 1 (CAF1) right behind the replication fork. These histones are found enriched in inactive DNA methylated regions (Goldberg *et al.* 2010; Szenker, Ray-Gallet, and Almouzni 2011; Jang *et al.* 2015; Talbert and Henikoff 2017).

In contrast, there are two individual genes encoding the H3.3 variants, presenting introns and exons and leading to a polyadenylated mRNA (Marzluff *et al.* 2002; Szenker, Ray-Gallet, and Almouzni 2011). The histone H3.3 variants are replication-independent and are synthesized throughout the cell cycle. They replace the canonical histones through the activity of chaperones, chromatin remodellers and histone-modifying enzymes. This replacement is important to carry out several processes such as transcription, heterochromatin formation and DNA repair (Talbert and Henikoff 2017). The H3.3 variant is deposited by histone regulator A (HIRA) and death domain-associated protein (DAXX) – associated with ATRX (Talbert and Henikoff 2017). During transcription, the nucleosomes are disrupted in order to render the DNA accessible to the transcription machinery. Transcription activates the deposition of histone H3.3 variant replacing the canonical forms at promoters regions and gene bodies of active genes. They are also found accumulated at silent

loci in telomeric and peri-centromeric regions (Goldberg *et al.* 2010; Szenker, Ray-Gallet, and Almouzni 2011; Jang *et al.* 2015; Talbert and Henikoff 2017).

3.4. H3-K27M mutated DIPG subgroups

The analysis of a large cohort of pHGG (n=183) conducted in our laboratory identified 2 new mutations: one patient presenting the K27M mutation in HIST2H3C gene encoding the H3.2 protein variant and one tumour harbouring a mutation in H3F3A gene leading to lysine-to-isoleucine substitution (K27I) (Castel *et al.* 2015). These 2 tumours presented a global loss of H3K27me3. Consequently, the presence H3K27 trimethylation loss in 95% of DIPG biopsies, including WT patients for the H3K27M mutation, is the hallmark of DIPG and is considered the driving event in DIPG oncogenesis (Castel *et al.* 2015).

Considering the differences between the canonical H3.1/2 and the histone variant H3.3, our group aimed to explore the differences and determine the impact of the H3K27M mutations in an extensive cohort of DIPG patients (Castel *et al.* 2015) according to the histone gene affected (K. R. Taylor *et al.* 2014; Castel *et al.* 2015). Sanger sequencing allowed to determine the distribution of H3-K27M in 183 pHGG. H3.1-K27M*,* H3.2-K27M and the new H3.3-K27I tumours appeared to be restricted to the pons so these alterations are considered DIPG specific, while H3.3-K27M tumours are found all along midline, *i.e.* thalamus, pons and spinal cord.

The analysis of the genomic alterations of our cohort, as others groups, shown preferential association of recurrent mutations or/and copy number alterations. Indeed, the recent paper of MacKay and coll. have shown specific events enriched within H3-mutated subgroups (**Figure 11**):

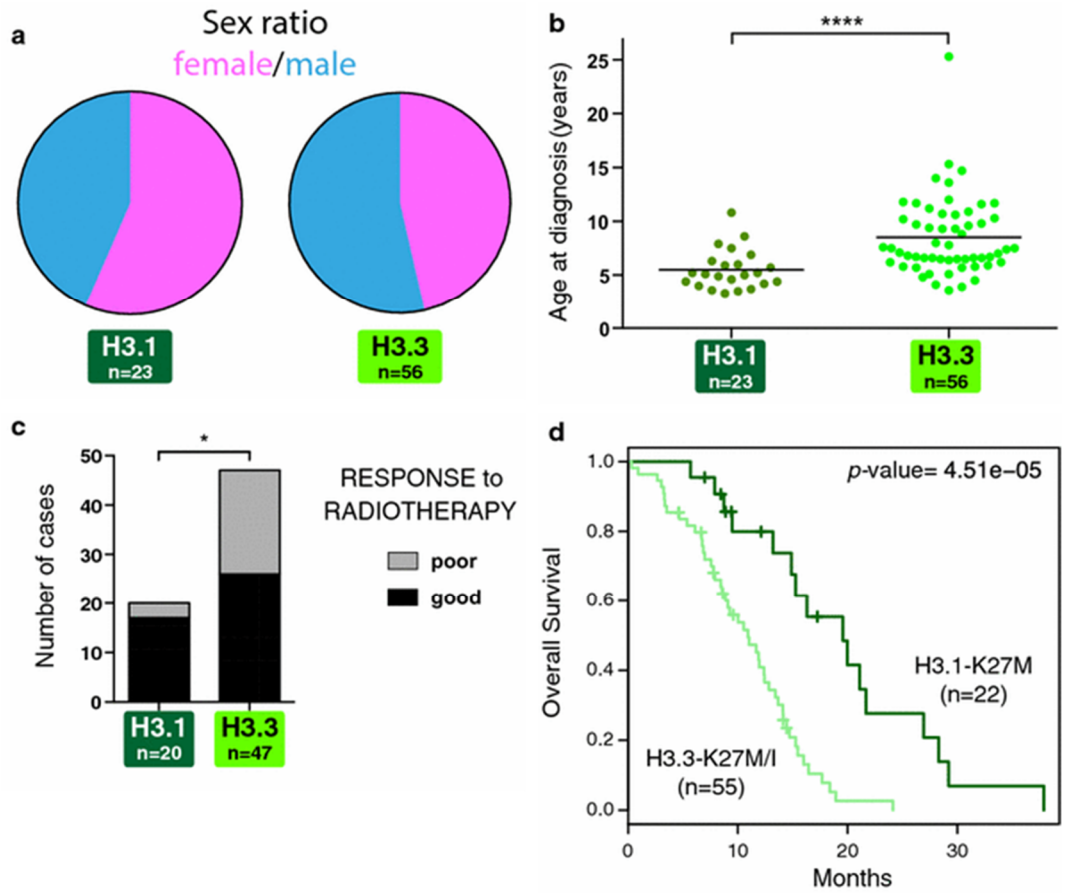

Figure 16. Two clinical DIPG subgroups are defined by histone H3 mutations. (a) There is no significant difference in sex ratio. **(b)** H3.1 age at diagnosis is significantly smaller than H3.3 (in (5.1 *versus* 7.4 years, ****p value <0.0001, n = 79). **(c)** Radiation therapy response in DIPG stratified by H3.1 and H3.3 mutation status. 85% of H3.1-mutated patients were identified as good responders to radiation therapy versus 55.3% in H3.3-mutated cases (p value = 0.0263, two-sided fisher exact test). **(d)** Kaplan-Meier plot of DIPG patients shows that H3.1 tumours are associated with a better overall survival than H3.3 tumours (15.0 *versus* 9.2 months, p value = 4.51e−05; log-rank test)(Castel *et al.* 2015).

- H3.3-K27M tumours are associated with *TP53* mutations (52.9%), frequently co-segregating with *ATRX* deletion/mutation (51.8%). Identified at lower frequency *PDGFRA* and *FGFR1* (20.5%) mutations, *MYC*, *CCND2* and *TOP34* amplifications and several chromatin modifiers are also targeted, such as *BCOR*, *ASXL1, SETD2, KDM6B, SETD1B* and *ARID1B.* Upstream alterations in RTK pathway were found enriched in this group (Puget *et al.* 2012; Castel *et al.* 2015; Mackay *et al.* 2017).
- Amplifications and deletions are rare events in H3.1-K27M. However, they can be associated with a frequent gain of 1q and the whole chromosome 2, loss of 16q, *ACVR1* (84.3%) and *BCOR* (16.2%) mutations. Integrated pathway analysis have shown an enrichment of alterations in the PI3K/mTOR (*PIK3CA* and *PIK3R1*) and BMP signalling pathways (Buczkowics *et al.* 2013; Fontebasso *et al.* 2014; K. R. Taylor *et al.* 2014; Castel *et al.* 2015; Mackay *et al.* 2017).

Regarding clinical characteristics, each subgroup is also associated with distinct features. There is no significant difference in sex ratio (**Figure 16a**). H3.1-mutated patients present a significant earlier onset with the mean age at diagnosis of 5.1 years *versus* 7.4 years for H3.3-K27M patients (**Figure 16b**). However, H3.3-K27M patients present a worst response to radiotherapy than H3.1-K27M patiente, *i.e.* 55.3 *versus* 85% of good responders respectively (**Figure 16c**), relapse significantly earlier (median overall survival 9.2 *vs.* 15 months)(**Figure 16d**) and exhibited more metastatic progression than H3.1-mutated patients (Castel *et al.* 2015).

Analysis of gene expression profiling on our cohort have evidenced that these

subgroups present specific molecular signatures (Puget *et al.* 2012; Castel *et al.* 2015). These signatures have been previously reported by our group without taken into account the H3 mutational status (**Figure 9A**) (Puget *et al.* 2012). Indeed, H3.3-mutated tumours showed oligodendrocytic and proneural gene expression signatures. These H3.3-mutated tumours also presented a downregulation of genes that are usually inhibited in metastasis, which can be related with a metastatic evolution observed in these patients. By contrast, H3.1-mutated tumours present an astrocytic gene expression signature, with an overexpression of genes that have been previously related to the mesenchymal signature of adult GBM. H3.1-mutated tumours also presented up-regulation of genes related in angiogenesis, hypoxia and œdema with can be correlated with clinical and histological analysis (Castel *et al.* 2015).

Moreover, the differences in gene expression profiles, phenotypes and prognosis among H3.1- and H3.3-mutated patients suggest that these histones drives distinct oncogenic programs (Castel *et al.* 2015) or occur in distinct precursor cells. In this context, in order to uncover the oncogenic processes and identify new molecular targets, we conducted an extensive search for genes required for DIPG cell survival, and the genes that sensitize the cells to the radiotherapy by using a high-throughput loss-of function screening, also in order to access the differences and similarities between the H3K27M-mutated subgroups.

PART III. FUNCTIONAL GENOMICS USING RNAi SCREEN

1. RNA interference (RNAi) principle

The first indications of the existence of a RNA-mediated post-translational mechanism repressing gene expression have started in plants (Napoli, Lemieux, and Jorgensen 1990; Metzlaff *et al.* 1997). In animals, RNA silencing was first reported in *Caenorhabditis elegans* (Guo and Kemphues 1995). Then, RNAi have been shown to be a endogenous biological process conserved in eukaryotes (Shabalina and Koonin 2008). Fire and coll. (Fire *et al.* 1998) were the first to elucidated the fundamental mechanism of gene silencing by RNA interference (RNAi) in this model (Fire *et al.* 1998) and were laureates of the Nobel Prize of Physiology or Medicine in 2006 for their discovery.

During the years following the discovery of RNAi, an effort to understand the molecular mechanism identified the main components of the pathway. Small interfering RNAs (siRNAs) and microRNAs (miRNAs) are the two main categories of noncoding RNAs acting in this process. Endogenous miRNAs play a role in the majority of biological processes as for example the control of cell growth, differentiation and proliferation (Chapman and Carrington 2007; Wilson and Doudna 2013). Indeed around 60% of human coding genes were reported to be modulated by miRNA. The siRNAs play a role in defence system against foreign or invasive nucleic acids and against transposon activity maintaining genomic stability. Both molecules have different biogenesis pathways and regulatory mechanisms of action (He and Hannon 2004; Shabalina and Koonin 2008; Wilson and Doudna 2013).

The miRNAs can negatively regulates the expression of multiple messenger RNAs (mRNAs) at once. The canonical biogenesis of miRNAs (**Figure 17**) starts

into the nucleus with the transcription of miRNA genes into a primary miRNA (pri-miRNA) by the RNA polymerase II (Pol II)(Carthew and Sontheimer 2009). The pri-miRNA contains single or clustered double-stranded hairpins with a capped 5' end and 3' polyadenylated end and therefore undergo several steps of maturation (Carthew and Sontheimer 2009; Graves and Zeng 2012). The pri-miRNA structure is important for the recognition and processing by the microprocessor complex. This complex is mainly composed by the nuclear RNase III Drosha and the double-stranded RNA-binding domain (dsRBDs) DGCR8. The pri-miRNA is recognized by Drosha and cleaved into a precursor (pre-) miRNAs of about 65 to 100 nt presenting a hairpin structure. The pre-miRNA is then exported to the cytoplasm by the transport facilitators Exportin-5 and RanGTP (Lund and Dahlberg 2006; Chapman and Carrington 2007; Wilson and Doudna 2013). Once in the cytoplasm, the pre-miRNA is processed by the endonuclease Dicer, containing especially helicase and RNase III activity. The PAZ domain is in charge of Dicer binding at pre-miRNA ends and the RNA III catalytic site cleaves it into a miRNA duplex of 18-25 bp with 2 nt overhang at each end. The miRNA duplex is loaded into the RNA-induced silencing complex (RISC), composed by three proteins: Dicer, Argonaute (AGO) and a double-stranded RNA-binding protein (dsRBP). The AGO protein unwind the duplex and lead to the selection of guide strand and degradation of the passenger strand of the duplex, based on its relative thermodynamic stability (Ha and Kim 2014; Wilson and Doudna 2013). The mature single-stranded miRNA will then guide the miRISC to its mRNA targets. The level of complementarity between the guide and its target define the silencing mechanism that will occur, *i.e.* translation inhibition or mRNA decay. When the miRNA-mRNA present a perfect complementarity, AGO cleaves the duplex mRNA-miRNA and the resulting fragments of mRNA are then

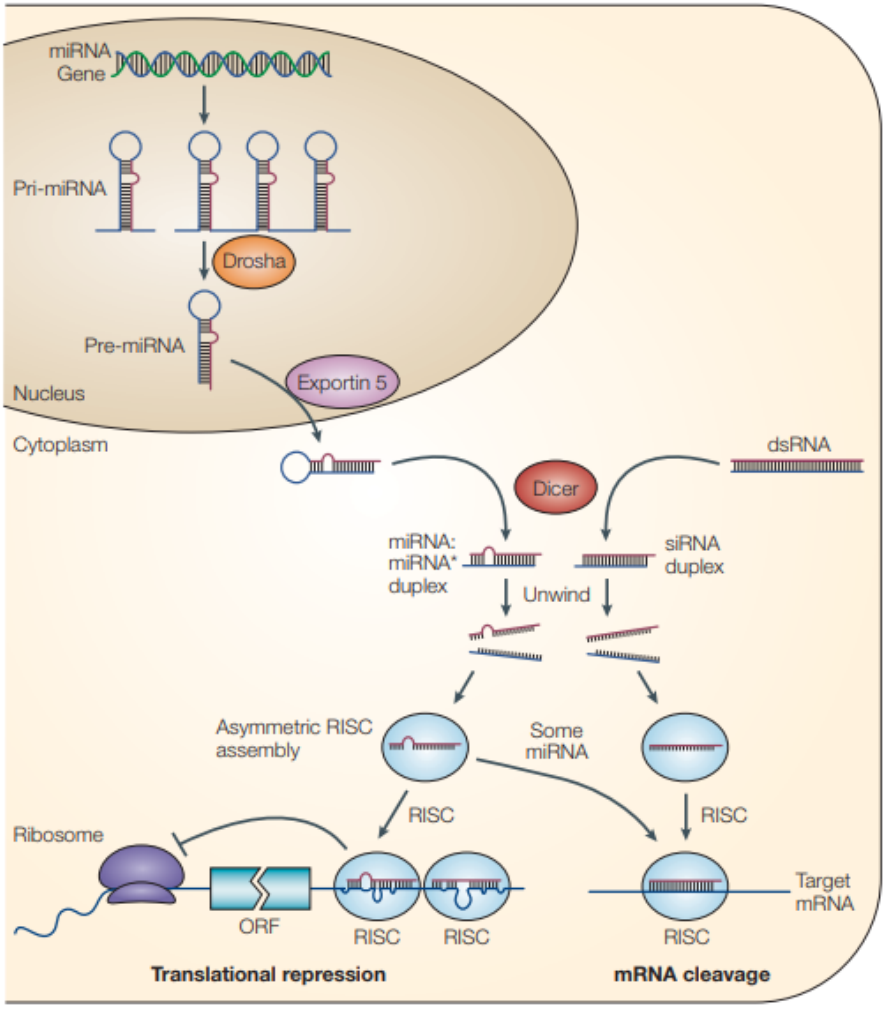

Figure 17. Biogenesis of miRNA and siRNAs. Transcription of miRNA gene is carried out by RNA polymerase II in the nucleus to give pri-miRNA. Inside the nucleus the pri-miRNA transcripts are processed by Drosha into pre-miRNAs of ~70-nucleotide. The pre-miRNAs are transported by Exportin 5 to the cytoplasm where they are processed into miRNA duplexes by Dicer. Dicer is also responsible by processing long dsRNA molecules (either transcribed or artificially introduced) into siRNA duplexes. AGO2, which is a component of RNA-induced silencing complex (RISC), cleaves the passenger strand. The guide strand is then activated and guides RISC to its target mRNA. The partial complementarity leads to translational repression, while full complementary leads to the cleavage of mRNA (He and Hannon 2004).

degraded by exonucleases. Alternatively, if miRNAs present some mismatches when binding to its targets, it can promote gene silencing by mRNA translation. In this case, only 8 nt are required for target recognition by the miRNA, allowing one miRNA to inhibit multiple targets (Carthew and Sontheimer 2009; Graves and Zeng 2012; Wilson and Doudna 2013).

Endogenous siRNAs uses a similar pathway (**Figure 17**). Their transcription gives rise to double-strand RNAs (dsRNAs) (Yu *et al.* 2014). The dsRNAs are exported by Dicer into the cytoplasm where the PAZ and RNase III domains of Dicer generate the duplex of ~21 bp by cleavage – similarly to the pre-miRNA processing (Lam *et al.* 2015). The siRNAs are loaded into AGO and follows the same steps of miRNA biogenesis. By contrast with miRNAs, the siRNA post-transcriptional silencing acts almost exclusively by perfect complementarity with mRNAs. Interestingly, dsRNAs can induce the production of secondary siRNAs though the action of RNA-dependent RNA polymerases (RdRP) which amplify the silencing (Lam *et al.* 2015; Piatek and Werner 2014). Exogenous siRNAs introduced *in vitro* to promote gene extinction enters into the siRNA biogenesis directly into the cytoplasm. In case of mismatches of the synthetic siRNAs with some other mRNAs to their targets, they can lead to gene extinction miRNA-like, promoting inappropriate gene extinction in cells, called off-targets effects (Petri and Meister 2013).

2. RNAi applications

Quickly after its discovery, RNAi appeared as a powerful tool to repress gene expression, easier and faster than knock-out experiment. The application of siRNA-

mediated RNAi in different mammalian cell lines, including human embryonic kidney (HEK293) and HeLa cells was described for the first time in 2001 (Elbashir *et al.* 2001). Followed by the elucidation of its mechanisms, RNAi have become one of the most extensive used approaches of reverse genetics to study gene function (Wilson and Doudna 2013; Boettcher and McManus 2015). This approach have been exploited by researchers *in vitro* and *in vivo* models of several organisms and allowed to decipher gene function, cellular pathways and potential drug targets in several diseases (Boettcher and McManus 2015; Mohr *et al.* 2014).

There are mainly two types of molecules used to promote gene silencing by the endogenous RNAi pathway: siRNA and short hairpin RNA (shRNA)(Mohr *et al.* 2014). Both siRNA and shRNA molecules are designed to target a specific mRNA and minimize off-target effects that could arise from partial complementarity to an unexpected target (Jackson and Linsley 2010). The siRNAs can be chemically synthetized and delivered into the cells by transient transfection (*i.e.* lipotransfection, electroporation, microinjection and nanoparticles). The presence of overhangs at 3' end for the mature siRNA allows its recognition by the proteins of RNAi machinery and directly load into RISC. This strategy allows fast analysis of loss-of-function phenotypes, but is not suitable for long-term studies of RNAi consequences since the constructions are not integrated into the host genome and are lost through cell division and degradation within 72 to 96 hours following their introduction (Brummelkamp *et al.* 2004; Lam *et al.* 2015; Paddison *et al.* 2002, 2004; Vanhecke and Janitz 2005).

For long term studies, a plasmidic vector-based system using integrative lentivirus is used. This system allows the integration of a shRNA expression

cassette into the host genome and its conservation through a constitutive expression of the shRNA constructs. The shRNAs molecules have the same structure that the stem-loop precursors of miRNA/siRNA which are exported into the cytoplasm and cleaved by Dicer producing mature siRNA duplex. Beyond the advantages of the stable cell modification allowing long-term analysis of loss-of-function phenotypes, this strategy: (i) is less expensive than chemical synthesis of siRNAs since the amplification of shRNA plasmids can be performed in bacteria; (ii) with the presence of resistance or fluorescent markers allows the selection of the cells presenting the stable modification; (iii) allows the inductile expression of interfering RNA using inducible promoters, and (iv) is suitable for deconvolution of large-scale RNAi screening by microarray or RNA sequencing

High-throughput RNAi screening allows the massive identification of genes involved in one particular function or phenotype. Preliminarily studies initially took advantage of plate well array-based assays (Moffat and Sabatini 2006; Sharma and Rao 2009; Vanhecke and Janitz 2005). This strategy allows analysis of phenotypes, including subcellular localisation of a protein of interest, protein expression and combination with therapeutic agents. It presents reduced number of false negatives, allows direct identification of active interfering RNAs and can be associated with high content imaging analysis. However, such strategy requires laboratory automatic liquid handling and automatic microscopic evaluation depending of the phenotype used as readout, which is also cost-effective. Thereafter, the generation of lentiviral integrative libraries allowed the development of pooled competitive screening approaches improving both speed and the scale compared to plate-based strategies (Kampmann, Bassik, and Weissman 2014; Mohr *et al.* 2014).

The pooled strategy consists in transducing a large population of cells with a mix of shRNAs targeting several hundreds of genes at once (Kampmann, Bassik, and Weissman 2014; Schaefer *et al.* 2018; Sims *et al.* 2011). Low multiplicity of infection (MOI ~0.3-0.5) is required in order to ensure that at maximum only a single shRNA will be integrated by the host cell. The population can be further subdivided into subgroups that undergo or not selective pressure. There is an amplification of the cellular population and the selection of the cells presenting the phenotype of interest. Several objectives can be achieved from the moment a phenotype can be used as readout, such as cell death, proliferation, differentiation, expression of transmembrane proteins detectable by antibodies, *etc*. After cellular expansion, the cells are harvested from the different subgroups and the genomic DNA is extracted. The entire set of constructions integrated into the host genome are amplified by PCR. The over or under-representation in the control (non-treated) group compared with the group submitted to selective pressure is then accessed by using massive parallel sequencing or microarray-based approaches. This strategy is easily scalable and does not require automation. However there are more expensive costs of deconvolution by genomic approaches and secondary (validation) screen should be performed to validate results.

Among the numerous possibilities of screen objectives, the use of shRNA screens have been reported by several groups (Moffat and Sabatini 2006; Pecot *et al.* 2011; C. Y. Lee *et al.* 2012; Mohr *et al.* 2014; Gao *et al.* 2014) in order to uncover oncogenic processes and identify new molecular targets in these diseases. We will focus on such examples in the following paragraphes.

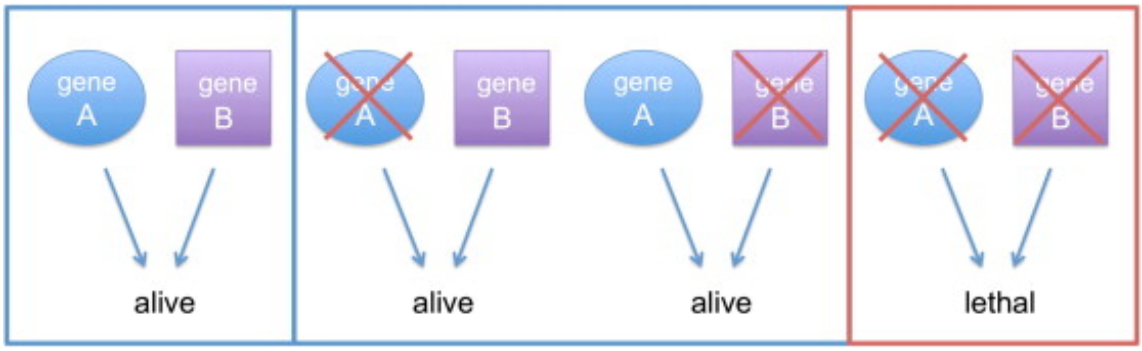

Figure 18. Principle of synthetic lethality. The alteration of one gene individually (either gene A or gene B) do not affect viability, while the simultaneous inactivation of both genes results in cellular death (Nijman 2011).

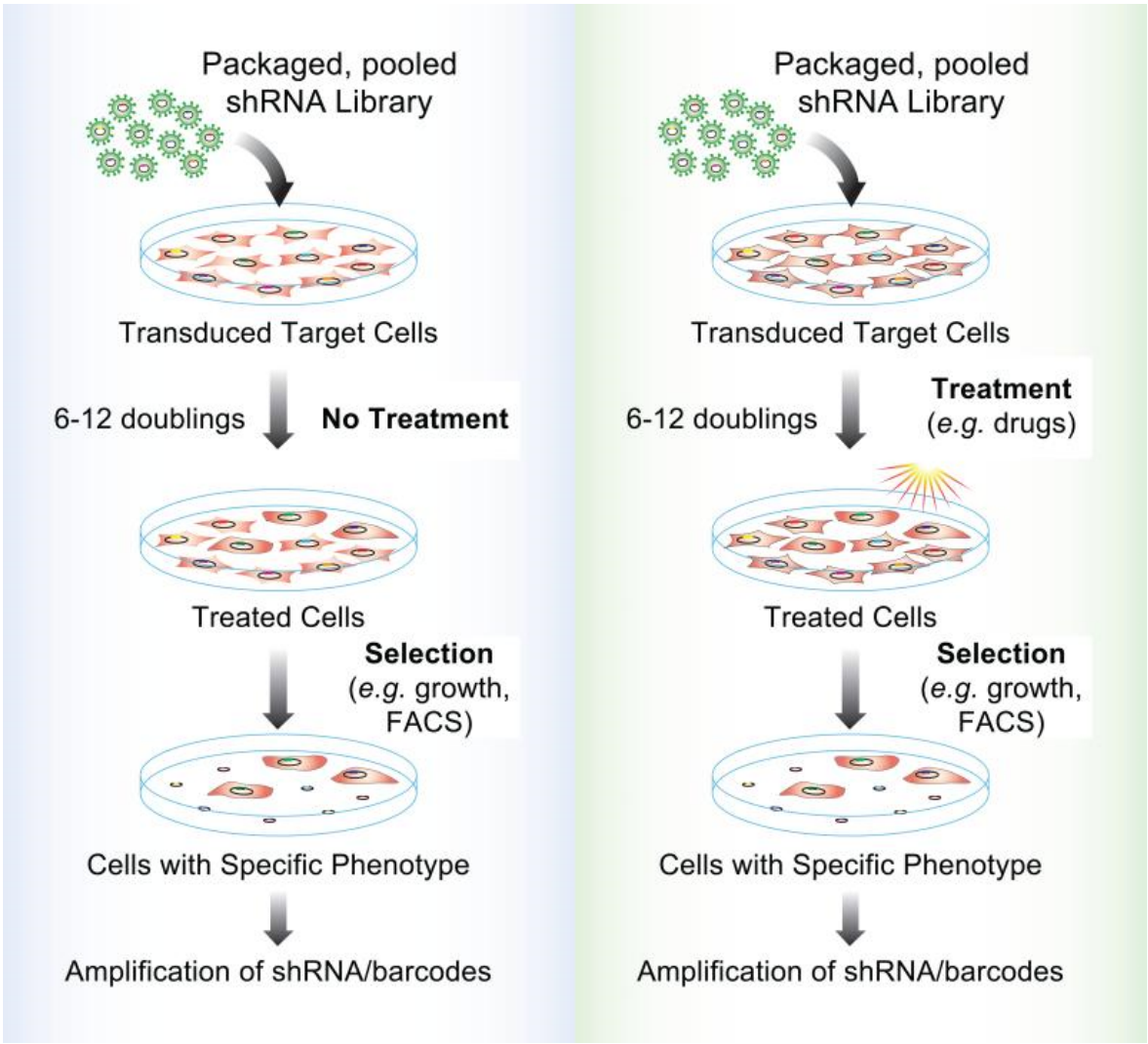

Figure 19. Example of synthetic lethality RNAi screen. Experimental design of a dropout viability screen in order to identify genes required for cell growth (left panel) and that can sensitize the cells to a treatment (right panel). After cellular expansion under selective conditions, the phenotype of the cells is accessed in order to determine potential target genes (Diehl, Tedesco, and Chenchik 2014).

3. Synthetic lethality RNAi screens

Synthetic lethality makes reference to the combinatorial effect of perturbations in two genes leading to a lethal phenotype, while the individual alteration in only one of these genes do not affect viability (**Figure 18**) (O'Neil, Bailey, and Hieter 2017; Thompson *et al.* 2015). These perturbations can refer to either mutations or alterations in gene expression. Over the past years, numerous tumour-specific recurrent mutations and alterations in gene expression have been identified in several cancers. These alterations can be used as the first alterations to conduct synthetic lethal screen (Foiani M., Lucca C., and Ferrari E. 2010; Thompson *et al.* 2015).

The second correspond to the gene extinction by RNAi (**Figure 19**). Consequently, RNAi-based synthetic lethality screens represent a possibility to uncover gene-specific interactions in order to provides new insights into oncogenic mechanistic by identification of biological changes that drive tumour progression (Diehl, Tedesco, and Chenchik 2014) and also vulnerabilities that can be exploited into new drug targets development (O'Neil, Bailey, and Hieter 2017). Moreover, synthetic lethality also allows the identification of genes that have not been previously involved in a given pathology because they are not mutated or differentially expressed, representing non oncogenic addictions.

4. Identification of interfering RNA impairing cell survival

In brain tumours, RNAi screens have been used to uncover molecular properties of these cells and identify new therapeutic targets (Singleton, Earley, and

Heasley 2017). In GBM stem-like cells (GSCs), Cheng and coll. performed a screen using a plate-well based library containing 3.103 shRNAs targeting 668 human kinase genes (Cheng *et al.* 2015). Interestingly, they analysed the two major subgroups of GBM, mesenchymal (MES) and proneural (PN) in order to identify essential genes specific of each subgroup (Cheng *et al.* 2015). GBM MES subgroup is characterized by mutations in *NF1* (37%), *PTEN* and *TP53*, while GBM PN harbours mutations in *TP53* (54%), *IDH1* and *PDGFRA*. They selected the cells presenting cell cycle arrest or committed to cell death by fluorescence-activated cell sorting (FACS). A total of 82 candidate genes were highlighted as essential for proliferation and viability of neurospheres *in vitro.* Among them, 54 genes were identified exclusively in MES GSCs, indicating different dependencies underlying oncogenesis between the GBM subgroups. When comparing gene expression profiling among MES, PN GSCs and NSCs (control derived from human foetal brain), only 2 genes *MET* and *AXL* were found as significantly differentially expressed between MES and PN subgroups. Further analysis have shown that *AXL* knockdown decreases *in vitro* self-renewal and tumorigenicity *in vivo* in GBM MES models, suggesting its potential use as therapeutic target in this subgroup of tumours (Cheng *et al.* 2015).

Also in GBM, Hubert and coll. performed a screen using a shRNA pooled library targeting 1.086 nucleic acid-binding factors in one GSC and one NSC (CB660) as a control (Hubert *et al.* 2013). After 21 days of cellular expansion following transduction, they identified by custom microarrays the shRNAs underrepresented in the GSC compared to the NSC. They identified 27 candidate-genes that were then individually tested using several independent shRNAs. Among the 7 genes that

passed their selection criteria based on shRNA redundancy and growth ratio, *PHF5A* gene was selected as the top hit for the tested GBM GSC (Hubert *et al.* 2013). They further performed a more extensive analysis with a genome-wide library targeting ~19.000 coding genes in 3 cell lines –2 MES GBM and 1 PN GBM – and a control NSC. By contrast with the previous screen, the changes in shRNA representation were accessed by deep-sequencing. The majority of the candidate genes were cell-line specific, reflecting the different genetic backgrounds and the heterogeneity among models (Hubert *et al.* 2013). Only 17 candidate lethal genes were shared by all GSC, including the previously identified *PHF5A*. PHF5A has been reported to be involved in RNA splicing through the recognition of unusual 3' splicing sites (Rzymski *et al.* 2008). Its knockdown results in splicing defects in a subset of genes that are required for cell cycle progression, leading to G2/M cell cycle arrest and impairing GSC viability. Moreover, it also compromises tumour growth and formation in *in vivo* experiments (Hubert *et al.* 2013). A high-throughput drug screen to identify selective *PHF5A* inhibitors *in vitro* is currently ongoing and potentially provide new treatments to GBM patients (Olson 2018).

More recently, Kulkarni and coll. have been interested in the effects of oxygen conditions in adult GBM GSCs (Kulkarni *et al.* 2018). They performed a pooled shRNA screen targeting 10.000 coding genes (including 500 kinases), in 2 primary GBM GSCs under normoxic and hypoxic conditions. They identified by high-throughput sequencing the shRNAs underrepresented in the GSC compared to the NSC and between the two oxygen conditions (Kulkarni *et al.* 2018). Although the initial purpose was a better understanding of genes important for proliferation and survival under different oxygen conditions, they identified genes shared among cell

lines in both conditions. They have identified by this way 81 common hits and ~52% of these genes have previously been described as essential when comparing available data from other RNAi screens (Hart *et al.* 2014). Focussing on kinase targeted genes, 12,8% were identified as underrepresented in a least one condition. Three of them were identified in all conditions: *PLK1*, *SGK1* and *STK36*. *SGK1* already implicated in glioma viability (Talarico *et al.* 2016) have been choose to further validation using either shRNA, CRISPR or pharmacologic inhibitors. The knockdown of *SGK1* impacts proliferation via the activation of apoptotic pathway exclusively in GBM GSCs, when compared to NSC. This gene is also required for *in vivo* tumor growth (Kulkarni *et al.* 2018).

Comparing the results from the different screenings, although they were all interested in uncovering vulnerabilities using GBM GSCs cellular models, there is a small overlapping between the identified targets among the studies. This can result from different characteristics of the different screens. First, the genetic background of a particular *in vitro* model can importantly impact the results. Consequently, as shown by Hubert and coll, the use of several cell lines will limit this risk as it will take into account the disease heterogeneity among patients. Anyway, the majority of the screens uses few cell lines because of the elevated cost of genomic deconvolution especially and the cumbersome of the approach. Additionally, control cells are not always used in parallel because of the cost and the availability. Second, the choice of different RNAi libraries can lead to apparent result discrepancies. Third, the parameters used for hit selection during data deconvolution are not yet standardized. At least, the phenotypic readouts, such as cell viability assays and cell cycle based sorting can also lead to apparent result discrepancies. Still, the major problem is the presence of off-target effect of some invalidated shRNAs, which is counteracted by

the use of libraries highly redundant containing 5 to 10 different shRNAs or siRNAs targeting the same gene. For these reasons, a secondary screen to validate preliminarily hits is fundamental.

5. Identification of interfering RNAs sensitizing cells to radiation

Synthetic lethality screen studies using RNAi in combination with radiation have been used to determine genes whose extinction lead to cellular sensitization to radiotherapy. Such studies can open the door of the identification of combinatorial treatments. As example, Higgins and coll. performed a siRNA screen targeting 200 genes involved in DNA damage repair in human laryngeal carcinoma (Higgins *et al.* 2010). Using a plate-well based strategy, they transiently transfected the cells, submitted to a radiation dose of 4Gy, corresponding to the expected dose leading to 50% of mortality (LD50). The phenotypic readout was the persistence of γH2AX performed 24 hours after irradiation. The formation of DNA double-strand breaks are observed indeed following irradiation, leading to a rapid phosphorylation and recruitment of histone γH2AX at the damaged site. The γH2AX response is maximal in the first minutes following radiation and recruits other proteins involved in the DNA damage repair (Avondoglio *et al.* 2009; Bonner *et al.* 2008). This will be discussed in more details in a further section (PART IV.3.5.1). The majority of the γH2AX foci will be repaired within a few minutes of irradiation and thus disappear. They selected cell with foci persistence over 24h reflecting delayed DNA repair and chromosome breaks which probably subsequently lead to cell death. Epifluorescence microscopic automated analysis allowed the identification of 30 top target genes (Higgins *et al.* 2010). As expected, genes previously implicated in radiosensitivity were

successfully identified, such as *BRCA1, BRCA2* and *RBBP8* (involved in HR) *and LigIV* and *XRCC5* (Ku80) *and PRKDC* (DNA-PKs) (involved in NHEJ). Additionally to the genes already involved in radiosensitivity and essential genes in both irradiated and non-irradiated, as shown in secondary analysis, they identified the DNA polymerase *POLQ*. The knockdown of *POLQ* increases H2AX foci after IR, sensitizes to IR several cell lines (bladder, pancreas and cervix) without effects in normal cells. Recently a small-molecule inhibiting *POLQ* have been identified and would be interesting to be tested as a potential new treatment in these cells (Pomerantz, 2018).

Interestingly, *PLK1* that have been shown to be implicated in GBM cell survival (GS6-22, GS7-2, GS11-1, GS13-1 and MGG 8) (Kulkarni *et al.* 2018), was also associated with radiosensitivity in other GBM cell models (LN18, U87-MG and U251)(Tandle *et al.* 2013). A siRNA-based kinome-wide screen targeting 691 kinases identified *PLK1.* It impair viability by cell cycle arrest during the mitotic phase, inducing mitotic catastrophes and cell death. Moreover, gene knockdown or pharmacological inhibition of *PLK1* before radiation, enhanced radiosensitivity *in vitro* in different GBM cells without effect on normal cells and inhibited *in vivo* tumour growth (Tandle *et al.* 2013). The identification of *PLK1* in different screens with different designs indicates that this gene can be investigated as an important therapeutic target for adult GBM. A phase II clinical trial is currently ongoing in pancreatic neoplasm, lung cancer, lymphoma, ovarian cancer and leukaemia (Harris *et al.* 2012, 1; Lerner *et al.* 2015; Z. Liu, Sun, and Wang 2016).

These screenings examples emphasize the efficiency of functional genomics using RNAi screen to better understand the oncogenesis in different types of cancer

and the possibility of identify new therapeutic targets. So far, no functional genetic high-throughput screen was reported in DIPG, neither for the identification of genes implicated in cell survival, nor for the identification of genes that can sensitize the cells to the standard treatment with radiation.

6. Limitations on the use of RNAi

As discussed above, RNAi is a powerful well-established tool for high-throughput loss-of-function screens and has allowed the identification of cellular pathways and new potential drug targets. The major issue of genome-wide loss-of-function studies using RNAi is an elevated false discovery rate that could reach 20% few years ago (X. D. Zhang 2010; X. D. Zhang *et al.* 2008). These false positive results can be classified in sequence-independent and sequence-specific effects, although they mainly result from sequence-specific off-target effects of RNAi (Mohr and Perrimon 2013). To counteract sequence-independent false positive and false negative results, there is a strong importance on the experimental design (Sharma and Rao 2009; Jackson and Linsley 2010; Sudbery et al. 2010; Schultz et al. 2011; Harrison 2012; Petri and Meister 2013; Schaefer et al. 2018), *i.e*. the choice of the delivery method to avoid immune innate response and toxicity, the choice of the appropriate number of replicates (technical and/or biological) and perform secondary validation (Birmingham *et al.* 2009; Sims *et al.* 2011).

More recently shRNA libraries are designed to overpass sequence-dependent off-target effects. There is a concern in shRNA design to avoid target regions with contiguous nucleotide identity similar to other genes that could likely be

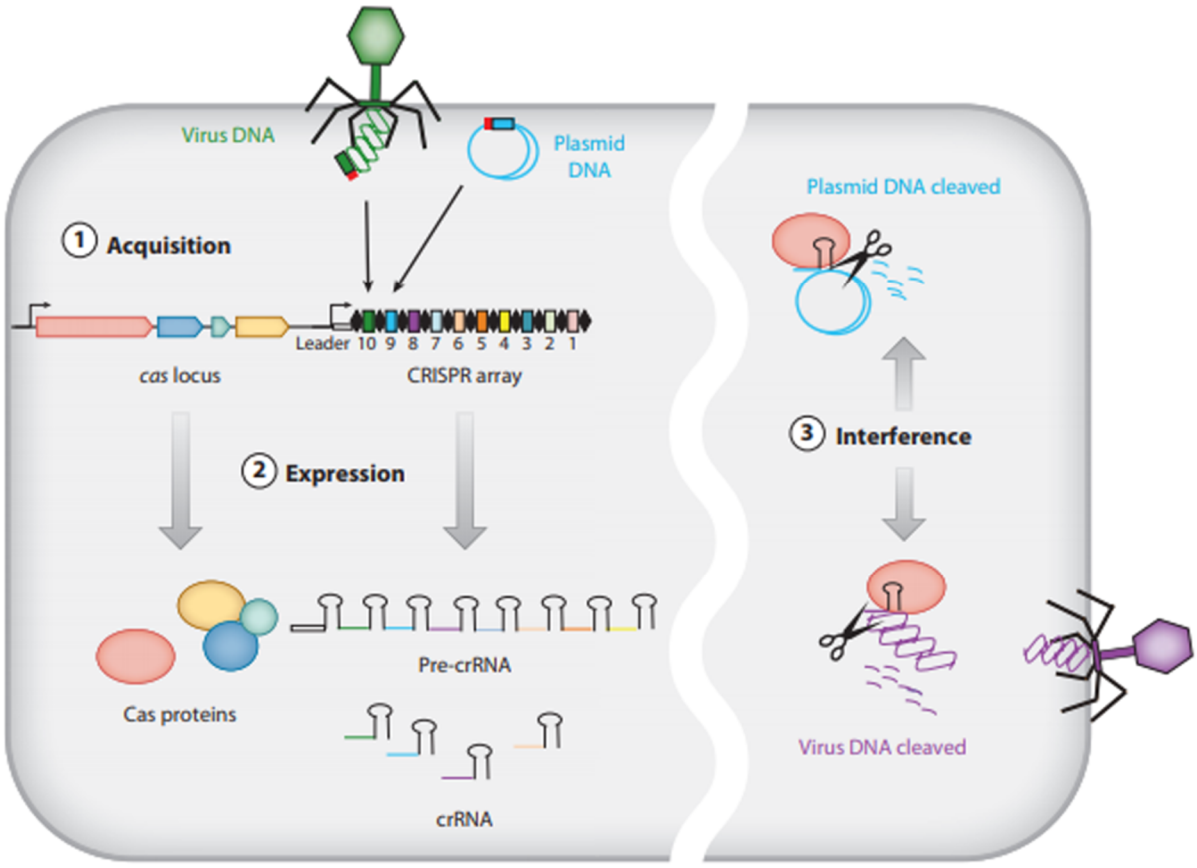

Figure 20. RNA-guided CRISPR-Cas9 immunity system. Bacteria and archaea are able to incorporate foreign nucleic sequences into a specific clustered regularly interspaced short palindromic repeats (CRISPR) locus. These sequences are expressed and acts like an immune system, through degradation of targeted sequences through the action of Cas proteins (Bhaya, Davison, and Barrangou 2011).

targeted by partial complementarity (Petri and Meister 2013). Libraries are currently designed with a high redundancy ranging from 5 to 10 shRNAs by gene, by this way only target genes with multiple shRNAs leading to the same phenotype are selected to increase result robustness. Also, the presence of suitable library internal negative and positive controls allows to confirm the relevance of the screens (Thompson *et al.* 2015; Kampmann *et al.* 2015). When available, comparison with transcriptomic data can support hit selection by selecting only genes expressed in the cells used for the screen. In depth analysis of *in vitro* and *in vivo* effects in a more extensive number of models are also important to fully validate the results (Mohr and Perrimon 2013).

Recently, a new technology of gene extinction based on RNA-guided CRISPR-Cas9 system has emerged. This strategy is based on an RNA-based adaptative immune system discovered in bacteria and archaea in response to viral and mobile genetic elements (**Figure 20**). Bacteria and archaea can integrate short fragments of 20-50 nucleotides of foreign nucleic acids into their genome in a clustered regularly interspaced short palindromic repeats (CRISPR) locus. The CRISPR locus represents a genetic memory and allows rapid response to infections (Barrangou *et al.* 2007; Horvath and Barrangou 2010; Fineran and Charpentier 2012; Wiedenheft, Sternberg, and Doudna 2012).The CRISPR locus is transcribed in a long primary transcript (pre-crRNA) that is processed into a library of short CRISPR-derived RNAs (crRNAs). The mature crRNA is then loaded into CRISPR-associated (Cas) protein and guided to complementary targets. That are several Cas proteins associated, but the *in vitro* CRISPR gene extinction strategies are mainly developed with the Cas9 protein. This RNA-guided DNA-endonuclase participates in CRISPR

RNA processing, recognition and target destruction. The Cas9 protein targets dsDNA sequences containing a PAM and a complementary protospacer sequence and destructs the foreign genetic material by producing double strand breaks (T. Wang *et al.* 2014; Wiedenheft, Sternberg, and Doudna 2012). The system have been adapted to generate targeted double-strand breaks (DSB) into the genome in an efficient way. These DSB are repaired by non-homologous end-joining (NHEJ, discussed in more details in the PART IV.3.5.2), which do not work perfectly and consequently introduces frequent small insertions or deletions thus inducing gene inactivation (Sander and Joung 2014; Housden and Perrimon 2016). It also have been adapted to activate or inhibit the transcriptional activity of a gene of interest (L. A. Gilbert *et al.* 2014; Konermann *et al.* 2015; Rajagopal *et al.* 2016), alter the DNA methylation status (Vojta *et al.* 2016) and induce histone post-translational modifications (Hilton *et al.* 2015; Kwon *et al.* 2017).

RNAi strategies allow the knockdown of a targeted gene, while the CRISPR/Cas9 system introduce double-strand breaks in a specific gene of interest based on a gRNA-defined target sequence, leading to gene inactivation. This strategy was quickly implemented into genetic engineering in order to perform high-throughput genetic screening in mammalian cells (Kampmann, Bassik, and Weissman 2014; Shalem et al. 2014; T. Wang et al. 2014). Several groups have focused on the comparison of RNAi and CRISPR/Cas9 strategies to conduct high-throughput loss-of-function screens (Evers *et al.* 2016; Morgens *et al.* 2016).

Hart and coll. compared the relative performance of these two strategies by targeting standard essential and nonessential genes previously identified in different cell types (Hart *et al.* 2014). Although Morgens and coll. reported a similar

performance of both screens approaches, the overlap between the hits was lower than expected, reaching only 60%. The potential existence of both false positives and false negatives in each approach could explain this result. A combinatorial design using both technologies could limit technological perturbations and allow a robust selection of potential hits (Morgens *et al.* 2016). The pathways involved in CRISPR based gene expression knockdown are totally different from those involved in interference gene extinction by RNAi. Consequently, it is expected to not encounter the same source of bias, even if potential other sources of biases should exist with this strategy. Over the past years, the CRISPR/Cas9 strategy have been extensively studied and the low correlation of the results with those of shRNAs approaches could reflect the different biological pathways that are involved in both techniques.

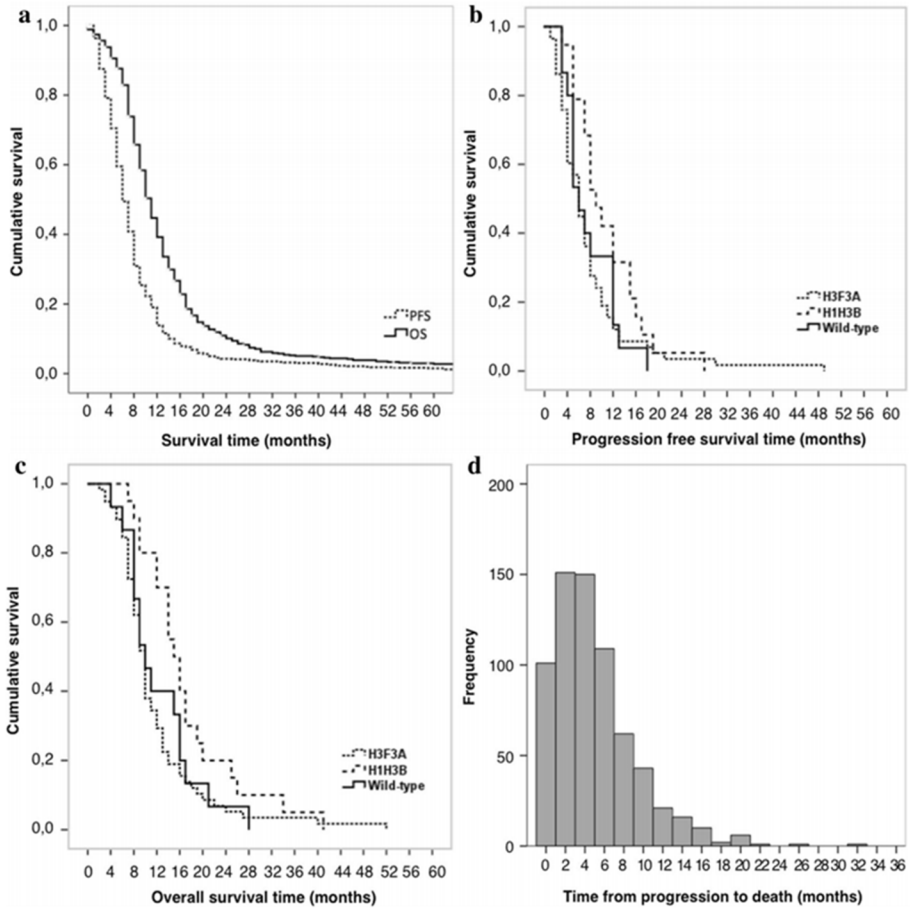

Figure 21. Retrospective survival data from the SIOPE DIPG Network. (a) Kaplan Meier shows PFS (n = 684) and overall survival (OS; n = 691) of DIPG patients. Stratification by mutational status (*H3F3A* n = 59, *H1H3B* n = 20, wild-type n = 15) of **(b)** PFS and **(c)** OS stratified. **(d)** Histogram showing distribution of progression to death (European Society for Paediatric Oncology (SIOPE) Brain Tumour Group: the SIOPE DIPG Network)(Veldhuijzen van Zanten et al. 2017).

PART IV. RADIOBIOLOGY AND RADIOTHERAPY IN DIPG

1. Radiation therapy in DIPG

The benefic effect of the radiation therapy (RT) in DIPG was first reported in 1959 (Coutel 1959). RT remains still the mainstay of treatment although only transiently effective. The treatment protocol consists in fractionated focal intensity modulated radiation therapy (IMRT) or 3D conformal photon-based RT of the tumour along its margins, in a total dose range of 54 to 60 Gy, in 30 to 33 fractions of 1.8–2 Gy, given once daily for 5 days per week over a period of 6 weeks (Vanan and Eisenstat 2015; K. J. Cohen, Jabado, and Grill 2017). RT leads to a temporary improvement of neurological signs (cranial nerve deficit, ataxia and long tract signs) and delay of tumour progression (PFS 5.6-7.6 months) followed by systematically fatal relapse (**Figure 21**) (Hargrave, Bartels, and Bouffet 2006; Janssens *et al.* 2013; Zaghloul *et al.* 2014; Puget *et al.* 2015a; Veldhuijzen van Zanten *et al.* 2017; Lobon-Iglesias *et al.* 2018).

Numerous clinical trials tried unsuccessfully to improve the benefit of its use. Indeed lower doses of RT, inferior to 50 Gy, have shown worse outcomes (F. Lee 1975; Littman *et al.* 1980; T. H. Kim *et al.* 1980). Higher doses ranging from 66 to 78 Gy using hyper-fractionated RT showed no benefit on survival (Allen *et al.* 1999; Mandell *et al.* 1999). Other studies have evaluated RT hypofractionation to improve treatment burden by a reduction of treatment duration but the observed response was similar to standard protocols (Negretti *et al.* 2011; Janssens *et al.* 2013; Zaghloul *et al.* 2014; K. J. Cohen, Jabado, and Grill 2017).

Additionally, the use of RT as neoadjuvant, adjuvant and in combinatorial

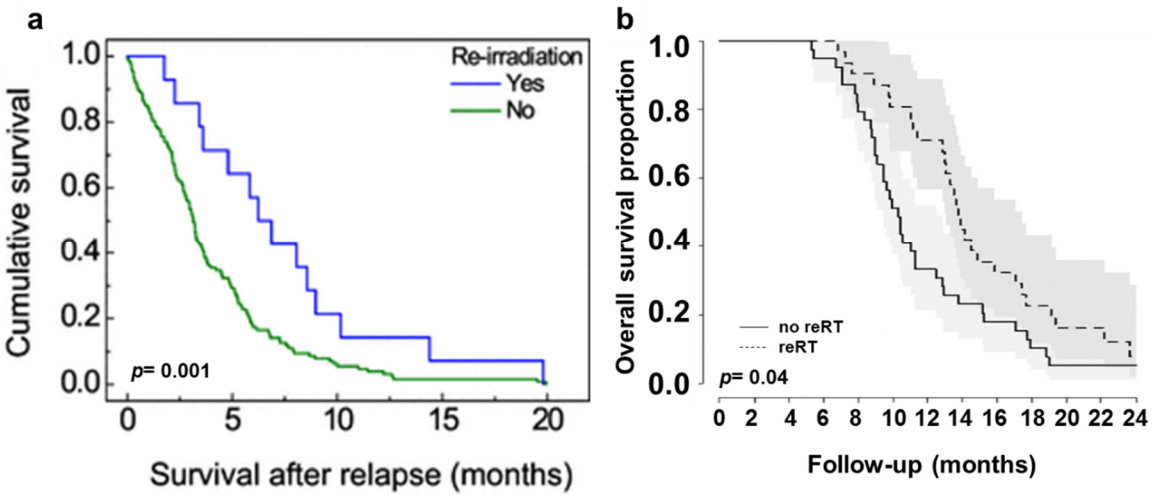

Figure 22. Patient's outcome with and without re-irradiation. Kaplan–Meier with **(a)** PFS (Lobon-Iglesias et al. 2018) and **(b)** OS (modified from Janssens et al. 2017). Re-irradiated patients (blue or dashed line) compared to patients not re-irradiated (green or straight line) had a significant improvement in survival after relapse (p=0.001) and in overall survival (p=0.04).

protocols with different therapeutics, such as radiation sensitizing agents, have shown no improvement in patient's outcome (Hummel *et al.* 2016; K. J. Cohen *et al.* 2011; Bailey *et al.* 2013; Zaky *et al.* 2013; Korones *et al.* 2008; Packer *et al.* 2005; Pollack, Stewart, *et al.* 2011; Allen *et al.* 1999; Truffaux *et al.* 2015; Hennika *et al.* 2017; Grasso *et al.* 2015; I. C. Taylor *et al.* 2015; Jennings *et al.* 2002; Porkholm *et al.* 2014). In summary no progress have been made to improve the radiation therapy efficiency over the last 60 years despite the efforts in over 250 clinical trials (Lapin, Tsoli, and Ziegler 2017).

Recent analysis of the outcome of DIPG patients undergoing re-irradiation at first progression have shown symptom improvement in 80% of patients (Wolff *et al.* 2012; Massimino *et al.* 2014; Janssens *et al.* 2017; Veldhuijzen van Zanten *et al.* 2017; Lobon-Iglesias *et al.* 2018). Furthermore, our laboratory and others have shown a significant increased survival after relapse from 4-6 months to 7.5-8.5 months and an OS from 11-13 to 15-19.8 months (**Figure 22**) (Wolff *et al.* 2012; Massimino *et al.* 2014; Janssens *et al.* 2017; Veldhuijzen van Zanten *et al.* 2017; Lobon-Iglesias *et al.* 2018).

Specifically regarding the histone H3 mutational status, our laboratory reported previously that H3.1-mutated patients are better responders to RT compared to the H3.3-mutated ones (**Figure 16c**)(Castel *et al.* 2015). Indeed, 75% of H3.1-mutated patients survived more than 3 months after relapse *versus* 45% of H3.3 mutated subgroup ($p = 0.023$, Chi square test). The average survival after relapse and OS length was significantly better ($p = 0.007$), 4.9 *versus* 2.7 months (Lobon-Iglesias *et al.* 2018) and 15.0 months compared to 9.2 months respectively for H3.1-K27M and H3.1-K27M patients (**Figure 16d**)(Castel *et al.* 2015).

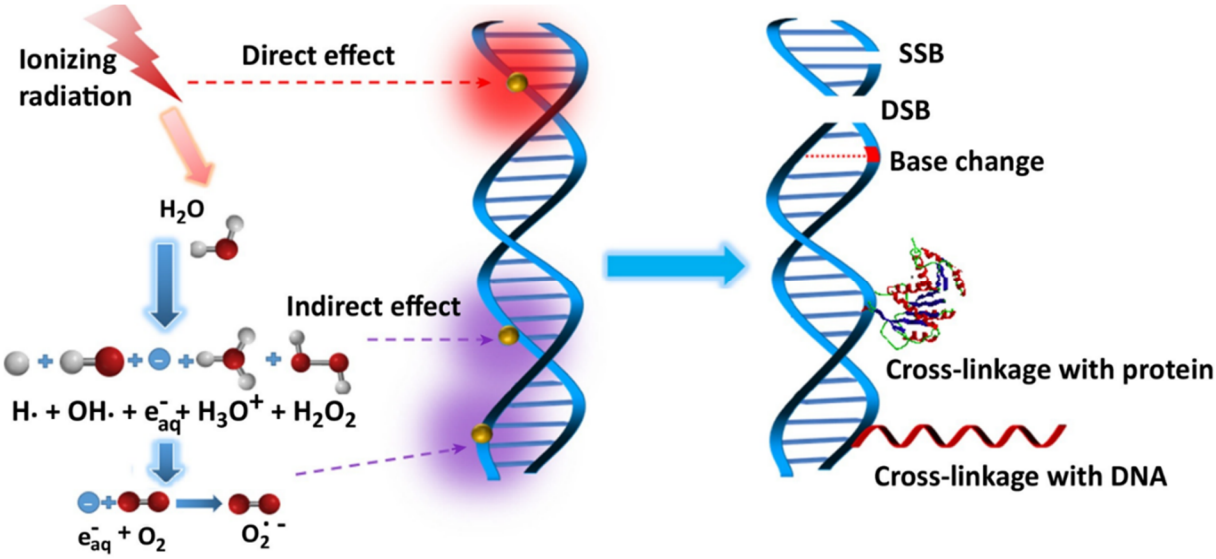

Figure 23. Mechanism of Ionizing Radiation (IR) in Radiation Therapy. IR can damage DNA by direct and indirect effects, through either water radiolysis or the generation of reactive oxygen species (ROS). Among the several types of DNA damages that can be generate by IR there are: single-strand breaks (SSBs), double-stranded breaks (DSBs), base modifications and cross-linking between DNA with a protein or with another DNA molecule (modified from Wang et al. 2018).

2. Mechanisms of ionizing radiation in RT

RT is frequently used as a part of the treatment for several types of cancer and is typically combined to other treatment methods, such as surgery, chemotherapy, or immunotherapy (Baskar *et al.* 2012; Jaffray and Gospodarowicz 2015; H. H. W. Chen *et al.* 2017). In early stages of tumour development, RT can be used in a curative purpose; in other cases, it only can be used as a palliative care, such as *e.g.* relief of neural symptoms and delay of tumour progression for DIPG patients (Puget *et al.* 2015a). RT is also used in combination with surgery, to shrink the tumour before resection when it can be performed (preoperative), allow a more precise radiation delivery (intraoperative) and reduce the risk of recurrence (postoperative)(Baumann *et al.* 2016; H. Wang *et al.* 2018).

RT takes benefit from the direct and indirect effects of ionizing radiation (IR) into the cells (**Figure 23**)(Bolus 2017; H. Wang *et al.* 2018). IR is the term employed to different high-energy photon radiation, such as X-rays and gamma (γ) rays (Negretti *et al.* 2011; Zaghloul *et al.* 2014), and particle radiation, such as alpha (α) or beta (β) particles, carbon ions, electron (e), proton, or neutron beams (Smyth *et al.* 2017; J.-C. Lee *et al.* 2017).

2.1. Direct effects

Direct effects of IR physically damage biomolecules, such as proteins, lipids and especially DNA by direct ionization disruption of molecular structure. Eighty percent of DNA lesions induced by IR are base modifications and 20% are damage to the sugar phosphate backbone. One Gray (Gy, unit of IR dose) induces

approximately 850 pyrimidine lesions, 850 purine lesions, 1000 single-strand breaks (SSB) and 20-40 double-strand breaks (DSB) *per* cell (Cadet, Douki, and Ravanat 2010; Reynolds *et al.* 2013; Yoshihara *et al.* 2014). In the absence of hydroxyl radical (·OH), IR promotes one-electron oxidation with similar efficiency for all nucleotides (Douki *et al.* 2004; L. Zheng and Greenberg 2017; Cadet, Douki, and Ravanat 2010). In the presence of ·OH, IR can promotes nucleotide oxidation:

- Thymine (T): addition across the 5,6-pyrimidine leads to formation of different stereoisomers and H-atom abstraction from the methyl group leads to formation of DNA intrastrand or interstrand crosslinks between the methyl group and the C8 position of guanine or adenine (Pouget *et al.* 2002; Douki *et al.* 2004; Bellon *et al.* 2006; Jiang *et al.* 2007);
- Guanine (G): addition to C8 with formation of 8-oxo-7,8-dihydroguanine (8-oxoG). This radical cation may form DNA–protein crosslinks (Cadet and Wagner 2013; Cadet *et al.* 2014);
- Cytosine (C): formation of •OH adducts, peroxyl radicals, and hydroperoxides. Although detected in the cellular DNA, these products are highly instable and are less characterized (Cadet and Wagner 2013; Madugundu, Cadet, and Wagner 2014);
- Adenine (A): the oxidation of adenine is similar to that of guanine leading to 8-oxoG and DNA–protein crosslinks. Adenine oxidation products are less frequent, which may be explained by a transfer of initial damage from adenine to guanine (Cadet and Wagner 2013).

2.2. Indirect effects

Indirect effects mainly derived from the water radiolysis products that generate free radicals, in particular reactive oxygen species (ROS). ROS are highly reactive molecules containing impaired electrons and can injure biomolecules by chemical reactions, such as hydrogen extraction, addition, disproportionation and electron capture (H. Wang *et al.* 2018). The ionization of the water molecules occurs in three main steps: (i) a *physical* stage, which occurs after the initial matter-ionizing radiation interaction and leads to the formation of ionized water molecules (H_3O^+), excited water molecules (H_2O^*) and sub-excitation electrons (e^-); (ii) a *physico-chemical* stage, in which numerous processes takes place leading to the formation of other ROS and (iii) a *chemical* stage, in which the ROS produced previously will then diffuse and react with each other and with other molecules, such as DNA nucleotides, as mentioned above (Caër and Sophie 2011).

3. DNA Damage Response (DDR)

DNA is constantly submitted to several endogenous sources of damage, such as ROS generation during oxygen metabolism and stalled replication fork during the S phase of cell cycle. A normal cell is submitted to at least 50.000 injuries *per* day due to endogenous agents (Reynolds *et al.* 2013). DNA is also submitted to exogenous injuries by physical and/or chemical agents, such as ultraviolet (UV) light, chemotherapeutics and, as previously mentioned, ionizing radiation (IR). DNA damages can induce genome instability, consequently the DNA damage response (DDR) – a complex network of signalling pathways – counteract these lesions. Together with cell cycle checkpoints, these mechanisms are crucial for the

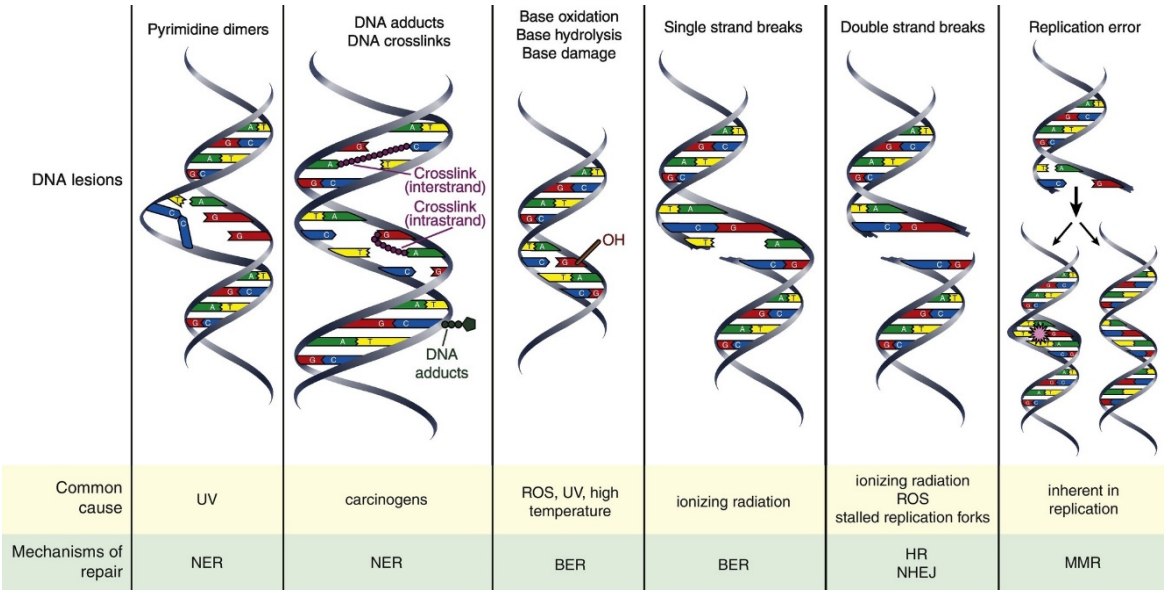

Figure 24. DNA damage response. These are different sources that can cause DNA damage, such as UV, ROS, IR, etc. These sources can cause different types of DNA lesions which requires different mechanisms of repair: base excision repair (BER), nucleotide excision repair (NER), homologous recombination (HR), non-homologous end joining (NHEJ) and mismatch repair (MMR)(modified from Weeden and Asselin-Labat 2018).

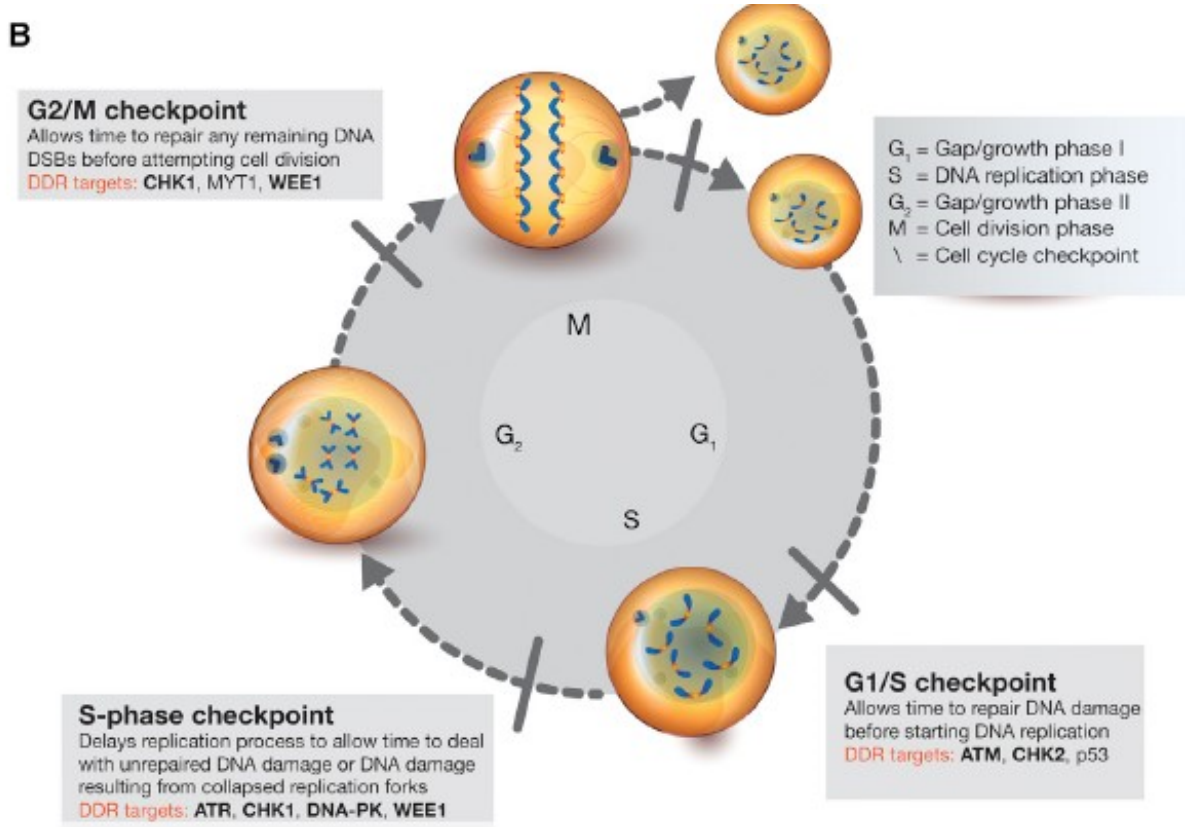

Figure 25. Cell cycle checkpoints. The genomic integrity is maintained by the presence of checkpoints during the cell cycle progression. DNA damage can leads to transient arrest in the G1, S, G2 and M phases represented in red. The major genes acting at each phase are highlighted (O'Connor 2015).

maintenance of the genomic integrity (Branzei and Foiani 2008; Lord and Ashworth 2012).

The DDR mechanisms are tightly dependent of the type of DNA lesion (**Figure 24**), such as bulky adducts, base alkylation, base mismatches, insertions, deletions, single- and double-strand breaks and to the phase of cell cycle (**Figure 25**). The cell cycle is divided in four distinct phases (G1-S-G2-M) and its correct progression is tightly regulated by DNA checkpoints (Kastan and Bartek 2004). Despite these differences, the DDR mechanisms usually comprise five common steps that will be discussed in more detail in the following sections:

(i) recognition of the DNA damage by repair complexes;

(ii) accumulation of DNA repair factors at the damaged site;

(iii) recruitment of cyclin-dependent kinases (CDK);

(iv) activation of downstream targets;

(v) physical repair of the lesion.

3.1. Base Excision Repair (BER)

BER occurs during the G1 phase in order to repair single nucleotide chemical alterations, such as oxidation, alkylation and deamination, and in the S phase, to remove misincorporated uracils, as result of cytosine deamination and incorporation of dUTP instead of dTTP (Branzei and Foiani 2008). These alterations can stall replication or increase other types of damage when not repaired. DNA glycosylases are the enzymes responsible of the initiation of BER pathway by excision of the damaged base, leaving an apurinic/apyrimidinic site (AP-site). AP-endonuclease 1

(APE1) and poly(ADP-ribose) polymerase-1 (PARP-1) are recruited to promote strand incision at the AP-site. The BER complex composed by DNA polymerase β (Polβ) and XRCC1-LIG1/3 repairs the AP-site lesion by excision of the site and replacement with a normal nucleotide via directed gap-filling DNA synthesis (Krokan and Bjørås 2013).

3.2. Nucleotide Excision Repair (NER)

NER is used to repair single-stand lesions that change the primary structure of DNA, *e.g.* DNA adducts and DNA-protein crosslinks. There are two subtypes of NER: transcription-coupled (TC) and global-genome (GG). The TC-NER occurs at the transcribed strand of active genes. The RNA polymerase II is stalled et damaged site and recruits CSA and CSB proteins which initiate TC-NER pathway through NER complex assembly (D'Errico *et al.* 2013). The GG-NER occurs throughout the genome and is consequence of base pairing disruption (Branzei and Foiani 2008; Lord and Ashworth 2012). GG-NER is initiated by the UV-DDB ubiquitin ligase complex and the heterotrimeric XPC/RAD23/CETN2 complex. Following DNA damage recognition, TC-NER and GG-NER converge into the same pathway. The recruitment of the transcription factor II H (TFIIH), the XPA DNA-binding protein and replication protein A (RPA) stabilize and orient the XPF/ERCC1 and XPG endonucleases in the excision of DNA surrounding the lesion follow by the replacement by DNA replication machinery (Lans, Marteijn, and Vermeulen 2012).

3.3. Mismatch Repair (MMR)

DNA mismatch are mostly generated during DNA replication by misincorporation of nucleotides. Mismatch repair (MMR) acts mainly during the S phase for the maintenance of genome stability (Kunkel and Erie 2005). First, the nucleotide miscorporation will be recognized by the MMR proteins MSH6 and MSH2 that will bind to the lesion on newly synthetized DNA. These proteins will then promote MLH1/3, post-meiotic segregation 2 (PMS2), proliferating cell nuclear antigen (PCNA) and exonuclease 1 (EXO1) recruitment to the complex. EXO1 is in charge of excision of the DNA mismatch. Replicative DNA polymerase δ or ε will then add the correct nucleotide thanks to its polymerase activity and the DNA ligase will catalyse the phosphodiester bond to complete the repair (Martin and Scharff 2002; Branzei and Foiani 2008; G.-M. Li 2008; Kunkel and Erie 2005).

3.4. Single-strand break (SSB)

Single strand damages of the double helix frequently occur during replication as a consequence of endogenous or exogenous DNA-damaging agents and as a DDR intermediary of BER. These lesions are usually repaired by BER machinery, as well as homologous recombination (HR) that will be discussed in the following section. Additionally, the DNA damage tolerance (DTT) is another DDR associated mechanism. DTT gives priority to DNA synthesis, preventing fork stalling and potential effects of replication fork collapse, which enable the finalization of DNA replication prior to DDR. DDT includes two pathways:

(i) translesion DNA synthesis (TLS): the replicative DNA polymerase is

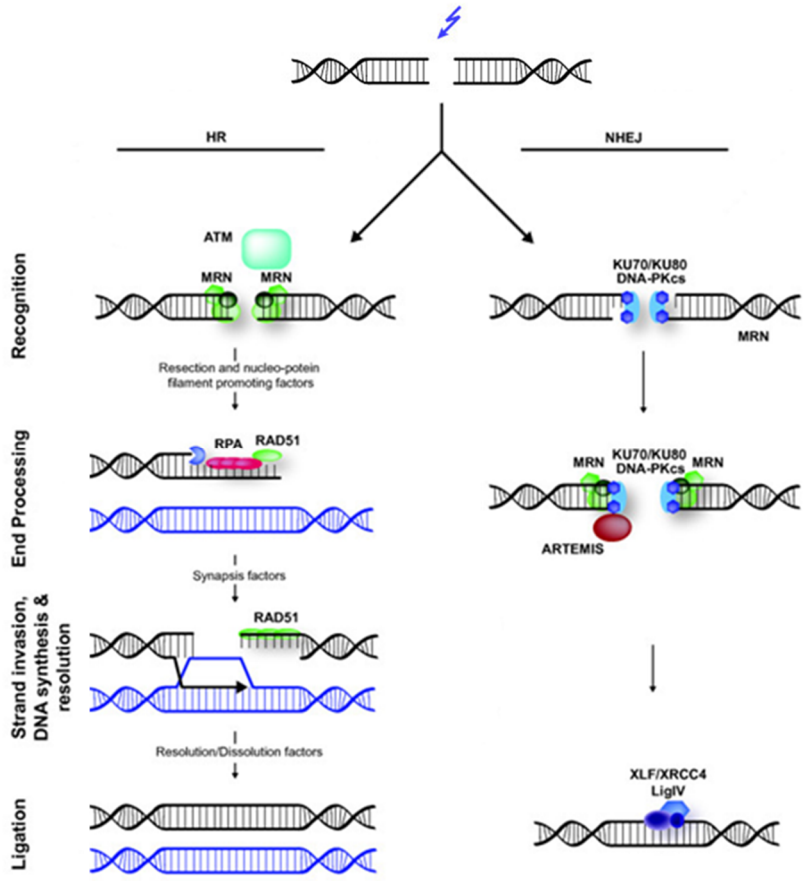

Figure 26. Double-strand break (DSB) repair by homologous recombination (HR) and non-homologous end-joining (NHEJ). HR begins with phosphorylation of the histone H2AX by ATM, which leads to recruitment MRN complex and other proteins involved in repair and checkpoint signalling. DNA end-resection generates single-stranded DNA (ssRNA) that are initially bound by RPA and subsequently replaced by RAD51. RAD51 promotes the invasion of the single-stranded DNA to a homologous double-stranded DNA template, synthesis and repair. In contrast, NHEJ rejoins broken DNA ends, which requires trimming of DNA and can lead to loss of genetic information. The broken DSB are bound by the heterodimer Ku70/80, which recruits DNA-PKs that will phosphorylates and activates repair proteins (modified from Lans, Marteijn, and Vermeulen 2012).

temporarily replaced by an error-prone TLS polymerase that lacks proofreading activity. This polymerase can bypass the SSB though the polymerization of transient DNA strand using a damaged template, or;

(ii) template-switched DNA synthesis (TS): in which the replicative DNA polymerase synthetize a new undamaged strand that is switched with the damaged one at the site of DNA lesion and used as template for replication. TS is considered an error-free process (Zeman and Cimprich 2014; Bi 2015; Abbotts and Wilson 2017; Hashimoto *et al.* 2017).

3.5. Double-strand break (DSB)

Double strands breaks are considered the most lethal form of DNA damage. One of the exogenous factors involved in induction of DSB is ionizing radiation. These lesions are repaired either by homologous recombination (HR) or non-homologous end joining (NHEJ)(**Figure 26**)(Lans, Marteijn, and Vermeulen 2012; Sirbu and Cortez 2013).

3.5.1. Homologous Recombination (HR)

HR is the repair pathway that restore the original DNA sequence at sites of DSB. It acts mainly during the S and G2 phases of cell cycle due to the presence of chromatid sisters that will be used as template to repair the damaged site. The MRE11-RAD50-NBS1 (MRN) protein complex recognizes the DSB, recruits ATM kinase to the damaged site and activates ATM to initiate phosphorylation of its

substrates. Upon lesion, ATM is responsible for the quick phosphorylation of the serine 139 of the histone H2AX giving rise to γ-H2AX at the regions flanking the damage. This response is amplified by other kinases and persists during the first minutes after the damage, leading to the formation of γ-H2AX foci. The number of γ-H2AX foci is directly correlated with the number of DSB into the cells. γ-H2AX is essential for DDR protein recruitment at DSB sites and at replication forks. The MRN-ATM complex is preferentially recruited at the γ-H2AX foci, creating a feedback loop. H2AX is a key regulator of the DDR, though the initialization of HR through the recruitment of downstream effectors, such as, 53BP1, MDC1, RAD51 and BRCA1. Mediator of DNA damage checkpoint protein-1 (MDC1) directly binds to γ-H2AX and is responsible for the recruitment of the recombinase RAD51 to the chromatin. RAD51 is regulated by BRCA1 that activates DNA-end resection through inhibition of 53BP1 dephosphorylation. The DSB damaged site is resected creating a long single-stranded DNA (ssDNA). During replication, staled fork exposed ssDNA is coated with RPA that is required to activate the Ataxia Telangiectasia and Rad3 (ATR) checkpoint activity. RAD51 replaces RPA to search for sequence homology in sister chromatid that is used as a template for the synthesis of new DNA and restoration of the DSB site (Branzei and Foiani 2008; Lord and Ashworth 2012; Lans, Marteijn, and Vermeulen 2012).

3.5.2. Non-homologous end-joining (NHEJ)

NHEJ mediates DSB repair by directly ligating the ends of a DSB together, rather than using homologous DNA. This process can generate deletion or mutation at the DSB site. By contrast with HR, NHEJ occurs throughout the cell cycle and is

the predominant DSB repair during G1, due to the high compaction of chromatin and the absence of sister chromatids. The Ku heterodimer (Ku70/80) binds at the end of a DSB and recruits DNA-PKs that in turn phosphorylates and activates the ligase-XRCC4 complex to join the broken ends (Lord and Ashworth 2012; Lans, Marteijn, and Vermeulen 2012).

3.6. DDR and cell cycle checkpoints

DDR components are tightly coordinated with the cell cycle checkpoints and chromosome segregation machinery in order to maintain genomic stability. The checkpoint kinases mediate cell cycle arrest, while chromatin-remodelling proteins play an important role for the DDR machinery in order to render the DNA accessible at the damage sites (Lord and Ashworth 2012; Hustedt and Durocher 2017).

As previously mentioned, the first step of DDR is the recognition of the DNA damage. The DDR proteins of the MRN complex and RPA have specific co-partners, respectively NBS1 and ATRIP. These partners have important roles in DNA binding and DDR activation (Falck, Coates, and Jackson 2005). Indeed, these proteins are responsible for the recruitment of the core DDR members of the phosphatidyilinositol-3-OH-kinases (PI3K) family: ataxia telangiectasia mutated (ATM) and ataxia telangiectasia and Rad3-related protein (ATR), and DNA-PKs, respectively (Blackford and Jackson 2017).

ATM is activated in response to DSB and is crucial in the activation of G1/S cell cycle checkpoint, preventing entrance in the S phase with damaged DNA. Through its downstream target - the checkpoint protein CHK2, or by direct activation,

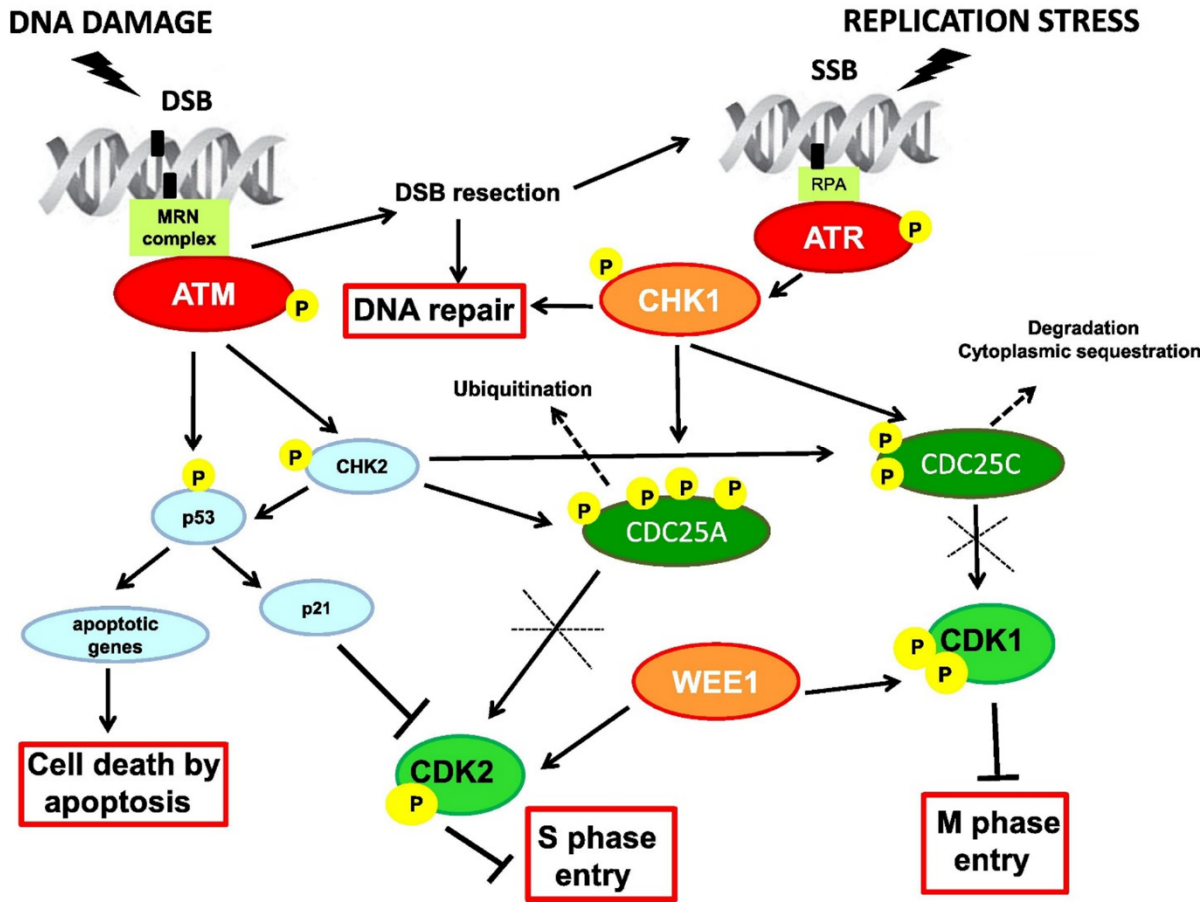

Figure 27. Main cell cycle checkpoints involved in the DDR. ATM, ATR, CHK1 and CHK2 are the major proteins involves in DDR. ATM and ATR are activated in response to DSB and SSB at replication stress or intermediate DSB, respectively. MRN complex is responsible to DSB recognition and ATM activation. This leads to phosphorylation of CHK2 and p53 and consequently to either cell cycle block or cell death by apoptosis. RPA is responsible to SSB recognition and ATR activation. This leads to phosphorylation of CHK1, which once activated leads to phosphorylation and inactivation of the CDC25A and CDC25C respectively involved in dephosphorylation and activation of CDK2 and CDK1. Their inactivation consequently leads to S phase and M phase entry (Carrassa and Damia 2017).

ATM phosphorylates and activates the tumour suppressor TP53. Phosphorylation of cyclin-dependent CDK inhibitor protein p21 (CDKN1A) transactivates p21. The G1 checkpoint cyclin-CDK complexes are inhibited by the accumulated p21, which leads to cell cycle block at G1. ATM is also involved in CHK1 activation by the formation of intermediate ssDNA during DSB repair (**Figure 27**)(Carrassa and Damia 2017; Hustedt and Durocher 2017).

ATR is activated in response to SSB caused by replication stress and during the intermediate response to DSB. RPA binds to single-strand DNA (ssDNA) at SSB sites or at stalled replication forks and recruits Rad17/9-1-1 and ATR/ATRIP complexes, leading to CHK1 phosphorylation. Mediated by CHK1, ATR promotes temporary cell cycle arrest in the late S-phase cell cycle checkpoint. CHK1 subsequently leads to the phosphorylation and inactivation of CDC25A and CDC25C, respectively involved in dephosphorylation and activation of CDK2 and CDK1. CDK activity is also responsible to G2-M transition and its inhibition is important to G2 cell cycle arrest (Carrassa and Damia 2017; Blackford and Jackson 2017).

DNA-PKs are activated by the NHEJ in the response to DSB. This pathway is activated throughout the cell cycle, although it has been shown to be used mainly in G0, G1 and early S phase, in the absence of homologous DNA sequence to HR (Sonoda *et al.* 2006). DNA-PK phosphorylates H2A/H2AX, as well as downstream targets CHK1 and CHK2. It also seems to exhibit an inhibitory phosphorylation effect in ATM (Langerak and Russell 2011; Y. Zhou *et al.* 2017; Blackford and Jackson 2017). PRKDC (X-ray repair cross-complementing group 7, XRCC7) is one example of DNA-PK that acts together with Ku70/80 in DDR. In adult HGG, polymorphisms

in this gene are associated with poor prognosis (M. Hu et al. 2016) and have been associated with cell migration, invasion and metastasis in other types of cancer (Goodwin and Knudsen 2014).

4. Mechanisms of radioresistance in gliomas

As previously mentioned, malignant gliomas are the most incident type of CNS and brain tumours in adults and children (Strong *et al.* 2015). The mainstay treatment is RT, however the therapeutic efficiency is only transitory. Increasing evidences supports that cancer stem-like cells (CSC) are underneath the radioresistance in different types of cancer (Bedard et al. 2013; Kreso and Dick 2014; Han et al. 2017; Goto et al. 2017; Xie et al. 2017; Qi et al. 2017; Cho et al. 2017; Reid et al. 2017; Y. Wang et al. 2018; Zhong et al. 2018). The CSCs are more radioresistant than other glioma cells and are considered a source of poorly differentiated progenitors at the origin of RT resistance (Kelley *et al.* 2016). Three cellular pathways have been reported to be tightly interconnected and associated with CSC radioresistance: DDR, ROS formation and cell cycle checkpoints.

Before mentioned, the activation of CHK1 and CHK2 checkpoint kinases by ATM and ATR in response to DDR, leads to cell cycle arrest and then promote the DNA repair (Smith *et al.* 2010). It has been reported that adult GBM CSCs present a higher activity of ATM, ATR, CHK1 and CHK2, which confers to these cells a stronger G2/M checkpoint activation, increasing DNA repair and, as consequence, promoting radioresistance (Bao *et al.* 2006; Ropolo *et al.* 2009; Bartkova *et al.* 2010). Additionally, ATM activation have been shown to increase radioresistance through

the same mechanism (W. Zhou *et al.* 2013; Enns *et al.* 2015; Paull 2015; Carruthers *et al.* 2015). *In vivo* models of proneural GBM have shown an increased radiosensitivity and survival when treated with ATM kinase-specific inhibitor (Halliday *et al.* 2014). Moreover, CHK1 and CHK2 inhibition have been reported to increase radiosensitivity of GBM CSC (Bao *et al.* 2006; J. Wu *et al.* 2012; Signore *et al.* 2014; Paull 2015).

ATM is also responsible of TP53 activation, a major regulator of genes related to radiation response that is frequently altered in adult GBM (Fei and El-Deiry 2003; C.-L. Lee, Blum, and Kirsch 2013). TP53-altered tumour cells are deficient in G1 checkpoint cell cycle arrest after IR, which leads to radioresistance. Inhibition of upstream regulators of TP53, such as ATM and CHK1, have been shown to efficiently sensitize *TP53*-mutant to IR in orthotropic xenografts models of adult GBM (Biddlestone-Thorpe *et al.* 2013).

The indirect effects of IR through the action of ROS products play critical roles in cell proliferation, differentiation, metabolism, cell death and tumorigenesis (J. A. Cook et al. 2004). CSC have been reported to present low levels of ROS, compared to epithelial cells. These levels are related to increased expression of ROS scavenging systems, such as glutathione (GSH) that confers a protection to CSC (Diehn *et al.* 2009; Malik *et al.* 2016)

The Notch pathway plays a major role in regulating self-renewal and inhibiting differentiation in CSC and neural progenitors (Louvi and Artavanis-Tsakonas 2006; Mizutani *et al.* 2007; J. Wang *et al.* 2010). Notch receptor is activated upon ligand binding, cleavage by γ-secretase, releasing Notch intracellular domain (NICD) into the nucleus, where it regulates the expression of multiple genes. The inhibition of

this pathway with γ-secretase inhibitors (GSIs) and the knockdown of Notch1 and Notch2 have been reported to increase radiation sensitivity of glioma stem cells, reducing cell growth, proliferation and clonogenicity, and promoted apoptosis (Fan *et al.* 2006; J. Wang *et al.* 2010; I. C. Taylor *et al.* 2015). These responses seem to be related to the activation of PI3K/AKT pathway, which is related to growth, migration and invasion in GSC though β-catenin and NF-κB signalling (J. Wang *et al.* 2010; X. Zhang *et al.* 2012). Wnt/β-catenin is another example of signalling pathway crucial for the regulation of stem cell pluripotency, carcinogenesis, tumour invasiveness and radioresistance (Nager *et al.* 2012; Kahn 2015; de Sousa e Melo and Vermeulen 2016; W. Chen *et al.* 2016; Morris and Huang 2016). In glioblastoma, it has been shown *in vitro* and *in vivo* that the degree of malignancy can correlates with β-catenin expression (Rossi *et al.* 2011; J. Zhang *et al.* 2011, 2; K. H. Kim *et al.* 2013). High levels of β-catenin and anti-apoptotic proteins are found implicated in radioresistant gliomas (H. Zheng *et al.* 2010; Y. Kim *et al.* 2012).

Alterations in the PI3K/AKT/mTOR signalling cascade have an important role in malignant transformation, tumour progression, radioresistance and metastatic processes. In GBM, the abnormal AKT signalling due to inactivation of *PTEN* seems to enhance HR and NHEJ DDR promoting the rapid repair of radiation induced DSBs. Radiosensitization though PTEN or AKT inhibition have been observed in glioma cells (Kao *et al.* 2007; H.-F. Li, Kim, and Waldman 2009; Mehta *et al.* 2015). Downstream target of AKT, the inhibition of mTOR kinase activity has been reported to inhibit tumorigenicity, through diminution of cell proliferation and invasion, and enhances radiation-induced autophagy and apoptosis in glioma cells, including DIPG (T.-J. Liu *et al.* 2009; Zhuang, Qin, and Liang 2009; Lomonaco *et al.* 2009;

Cerniglia *et al.* 2012; W. Wang *et al.* 2013; Miyahara *et al.* 2017).

Moreover, several pathways was involved in the radioresistance in adult GBM. In DIPG, characterization of the underlying mechanisms of radioresistance have not been clearly demonstrated. In summary, radioresistance was extensively studied in adult GBM in contrast to DIPG. Despite the important differences between these adult and paediatric GBM, as described in the previous chapters, we can imagine that some of these pathways are maybe also involved in DIPG radioresistance. Some of these aspects will be achieved in this work.

OBJECTIVES

DIPG remains poorly understood, for this reason this PhD project have two main objectives in the identification of DIPG vulnerabilities. In first, (1) systematically identify DIPG cellular oncogenic and non-oncogenic addictions to understand the pathogenic mechanisms and second (2) identify genes that can sensitize the cells to radiation therapy.

Results

RESULTS

ARTICLE I. A kinome-wide shRNA screen uncovers *VRK3* as an essential gene for DIPG survival

Over the last five years, many progresses have been made in the understanding of DIPG, especially with the discovery of a specific somatic mutation in the histone H3 (K27M) present in almost all the patients and that consequently is considered as the driver mutation of this disease. This alteration induces the global loss of the K27me3 epigenetic repressive mark that can have major impact on the cellular transcriptome. Despite this discovery, the knowledge on DIPG biology and oncogenesis remains insufficient. Consequently, we decided to identify genes specifically required for DIPG cell survival without any *a priori*, *i.e.* regarding recurrent and/or oncogenic mutations. To do so, we conducted a synthetic lethality screen using a kinome-wide shRNA pooled library into 4 GSC models harbouring either H3.3-K27M (n=2) or H3.1-K27M (n=2) mutation to cover the heterogeneity of the disease. We successfully identified targets that have already been described as essential genes in other GSC models in adult GBM, such as *PLK1*, *CDK6*, *MTOR*, *BUB1*, *EGFR* and *FGFR*, which confirms the relevance of the screen.

We identified the *VRK3* gene as required for survival in all GSCs tested. VRK3 is a member of the serine threonine kinase family that have never been involved in DIPG oncogenesis previously and for which the functions remain poorly described. We confirmed that its inhibition leads to a complete arrest of DIPG cell proliferation which is additionally associated with important morphological changes, especially in H3.3-K27M mutated tumours, without major deleterious effect in normal cells. VRK3 is therefore a promising new therapeutic target for all patients in this fatal disease.

Title 150 character

A kinome-wide shRNA screen uncovers Vaccinia related kinase 3 (*VRK3)* as an essential gene for Diffuse Intrinsic Pontine Glioma survival

Running title 50 character

RNAi screen identifies *VRK3* as an essential gene in DIPG

Claudia Silva-Evangelista[1], Emilie Barret[1#], Virginie Ménez[1#], Jane Merlevede[1], Thomas Kergrohen[1], Ambre Saccazyn[1], Estelle Oberlin[3,4,5], Stéphanie Puget[6], Kevin Becaria[6], Jacques Grill[1,2], David Castel[1,2] and Marie-Anne Debily[1,7]

1 UMR8203, “Vectorologie & Thérapeutiques Anticancéreuses”, CNRS, Gustave Roussy, Univ. Paris-Sud, Université Paris-Saclay, Villejuif, France
2 Département de Cancérologie de l’Enfant et de l’Adolescent, Gustave Roussy, Univ. Paris-Sud, Université Paris-Saclay, Villejuif, France
3 Inserm UMRS-MD 1197, Villejuif, France
4 Paris-Saclay University, Villejuif, France
5 André Lwoff Institute (IFR89), Villejuif, France
6 Department of Pediatric Neurosurgery, Hôpital Necker-Enfants Malades, Université Paris V Descartes, Sorbonne Paris Cité, Paris, France
7 Université d'Evry-Val d'Essonne, Boulevard François Mitterrand, Evry, France.

[#]These authors contributed equally to this study.

Contact Information of the corresponding author:

Dr Marie-Anne Debily
UMR8203, CNRS "Vectorologie et Thérapeutiques Anticancéreuses"
Institut de Cancérologie Gustave Roussy
114 rue Edouard Vaillant, 94805 Villejuif cedex, France
Et Université d'Evry Val d'Essonne, Département de Biologie
23 boulevard de France, 91037 Evry cedex, France
+33 142 115 100
Email = marie-anne.debily@gustaveroussy.fr

Abstract (250 words, unstructured)

Diffuse intrinsic pontine glioma (or DIPG) are universally fatal pediatric high-grade gliomas associated with a dismal prognosis. They harbor specific substitution in histone H3 at position K27 that induces major epigenetic dysregulations. Most clinical trial failed so far to increase survival, and radiotherapy remain the most efficient treatment, despite only transiently. We conducted the first lentiviral shRNA dropout screen in DIPG to generate a cancer-lethal signature as a basis for the development of specific treatments with increased efficacy and reduced side effects compared to existing anti-cancer therapies. The analysis uncovered 41 DIPG essential genes among the 642 genes of human kinases tested for which several distinct interfering RNAs impaired cell expansion of three different DIPG stem cell cultures without deleterious effect on two control neural stem cells. Among them, *PLK1*, *AURKB*, *CHEK1*, *EGFR*, *GSK3A* especially were previously identified by similar approach in adult GBM indicating common dependencies of these cancer cells and pediatric gliomas. As expected, we observed an enrichment of genes involved in proliferation and cell death processes with a significant number of candidates belonging to PTEN/PI3K and EGFR pathways already under scrutiny in clinical trials in this disease. We highlighted *VRK3,* involved especially in cell cycle regulation, DNA repair and neuronal differentiation as a non-oncogenic addiction in DIPG. Its repression totally blocked DIPG cell growth in the 4 cellular models evaluated, and induced cell death in H3.3-K27M cells specifically but not in H3.1-K27M cells, supporting VRK3 as an interesting and promising target in DIPG.

Keywords : DIPG, RNA interference, synthetic lethality screen, VRK3

Introduction

Diffuse intrinsic pontine gliomas (DIPG) is one of the most difficult therapeutic challenge in pediatric oncology(1). Its location intrinsic to an eloquent brain structure and highly infiltrative behavior precludes any attempt of surgical resection. This tumor is highly resistant to chemotherapy both in the clinic and *in vitro*(2). Radiation therapy is the only validated treatment but it controls tumor progression only transiently. Decades of therapeutic trials blinded to the biology of these neoplasms have not brought any improvement in patient care and median survival remained below one year(3).

The introduction of autopsies and the re-introduction of stereotactic biopsies at diagnosis allowed a better insight in the biology of this disease(4,5) and the establishment of relevant preclinical models(6,7). There are presently no available drugs for clinical use targeting the driver mutation in histone H3 as well as the other most frequent mutated proteins, TP53 and ACVR1 tyrosine kinase receptor, which are mutated only in a subset of tumors. Available targeted therapy can only address secondary, *i.e.* subclonal, alteration such as PI3K/mTOR/AKT pathway activation(4) or *PDGFRA* mutation/amplification(8). It is therefore of paramount importance to discover new vulnerabilities in DIPG cells that could be used to develop new therapies.

Gene extinction strategies are versatile methods to identify the Achille's heel of any tumor cells in an unbiased fashion, *i.e.* not restricted to mutated or altered genes. They have been seldomly used in adult glioblastoma cells using RNA interference (9–16) but not in pediatric high-grade gliomas such as DIPG nor in primary tumor cell cultures. We opted for a kinome-wide shRNA screen as kinases are frequently druggable and this could enable quick validation and transfer in the clinic. In order

to unravel genes required specifically for cell survival of our glioma stem-cell models of DIPG, we filtered the hits to remove the targets, whose extinction impair substantially neural stem cells cultures. This approach identified VRK3, a serine-threonine kinase which interacts with cell cycle and DNA repair especially, as a new vulnerability in DIPG that could be exploited in further therapeutic developments.

Results

A kinome-wide siRNA screen in H3-K27M mutant cells.

We selected four glioma stem cells (GSC) models harboring either H3.3-K27M (n=2, GSC1 and GSC2) or H3.1-K27M (n=2, GSC3 and GSC4) mutations to screen for genes whose inactivation is lethal in H3-K27M tumors. Despite the K27M mutation, DIPG mutational landscape is heterogeneous, consequently we chose the most archetypical GSC models presenting the association of H3.1-K27M and *ACVR1* mutations or H3.3-K27M and *TP53* alteration to reflect the majority of the patients. We conducted a negative selection screen by profiling the depletion of shRNA targeting essential survival genes on GSC. An overview of the procedure is described in fig1A. Briefly, cells were transduced at a MOI of 0.3 with a kinome-wide lentiviral shRNA library targeting the 672 human kinases, grown under puromycin selection for 7 days and genomic samples were collected at 40h and 22 days post-transduction. To enrich for GSC-specific hits, we performed in parallel the screen in two neural stem cell control cells (NSC1 & NSC2) as NSC share molecular and phenotypic features with GSC models including growth in serum-free conditions and similar doubling times.

We estimated by analysis of the sequencing data of the reference timepoint (40h)

that the representativity of the shRNA library (*i.e.* 7 450 distinct shRNAs) was maintained in all the models (average 94% ±0.5). Moreover, high correlation was found between the reference timepoint of the different biological replicates of DIPG and NSC cells (average correlation, r2 = 0.96 ±0.005), thus indicating high reproducibility even between different biological infections.

As expected, deep sequencing revealed that the diversity of shRNAs was reduced over time, the shift between the reference timepoint (40h) and day 22 indicated the specific depletion of a set of shRNAs (Fig1B). Nearly all models gave satisfactory data with the majority of interfering RNAs that remained stable during outgrowth (FigS1A). Fold changes (FCs) were computed as changes in frequency of a particular shRNA between 22 days and the initial control timepoint at 40h. Nonetheless, the distribution of shRNA FCs of GSC2 is less scattered than other cells reflecting that they are less susceptible to shRNA depletion.

DIPG-specific essential genes

To assess the quality of our loss-of-function screen, we took a set of reference essential genes across different human cancer cell lines from Hart *et al.*(17) and examined the distribution of their modulation. As expected, the FC distribution of all shRNAs targeting “essential” genes detected above threshold, was significantly shifted relative to the distribution of interfering RNA targeting non-essential genes for all GSC (FigS1A&B). Interestingly, several genes previously identified as required for adult GBM GSC survival using a similar approach, *i.e. BUB1B*, *PLK1*, *MTOR/FRAP1* were also overall underrepresented at 22 days of outgrowth in our pediatric GSC models (FigS1A, blue dots).

Several criteria were sequentially applied to select shRNAs associated with a

depletion of at least two-fold in the 22-days samples without major deleterious effect in NSC cells (FigS1C). As off-target effect is the major pitfall of RNAi screens leading to false-positive results and because efficiency of the interfering RNAs of the kinase library was not validated previously, we scored a gene as essential for one particular cellular model if at least 3 distinct shRNAs induced a consistent phenotype (*i.e.* a decrease in GSC survival).

The number of common target genes between distinct cellular models indicated that more shRNAs affected survival of H3.1-K27M in comparison with H3.3-K27M corresponding to 47 *versus* 11 genes respectively (Fig2a). However, the pairwise comparisons involving GSC2 led to smaller numbers of shared candidates between 2 GSCs, reflecting that fewer shRNAs are significantly depleted in these cells, as shown previously (Fig1B, FigS1A). By contrast, the H3.1-mutated GSC4 and the H3.3-mutated GSC1 presented the most important overlap with 80 distinct genes. To prioritize the best hits, we filtered out genes for which no expression was detected by RNA-seq profiling (Fig2C). Seven genes were found as impairing cell expansion of all DIPG cells by overlapping the candidate genes of each GSC: *EGFR*, *FGFR1*, *GSK3A*, *MAPK10*, *STK17B*, *TGFBR2*, *TXK.* We could not exclude that the negative impact of *EGFR* and *FGFR1* knockdown (KD) did not result from the use of the corresponding growth factor in the culture medium. Anyway, *EGFR* is overexpressed in approximatively 40% of DIPG(18) and constitutes consequently a potential therapeutic target, currently under clinical trial evaluation (NCT02233049). A phase-2 clinical trial evaluating FGFR1 inhibitor is also open for patient presenting either a gene fusion involving *FGFR1* or an activating mutation in adult glioma (NCT01975701) and it could be of interest in DIPG patients. Interestingly, *GSK3A*, *MAPK10* (also known as *JNK3*), *STK17B* and *TGFBR2* are linked to or directly

involved in PI3K/AKT/mTOR pathway. Activation of the PI3K/AKT/mTOR pathway is a frequent finding known since first paper on DIPG genomics(19), and mutations in this signaling pathway are found in 45% of the cases profiled by WGS (4). All cellular models but GSC1 used in the screen harbor a mutation in this pathway. Again, an inhibitor is currently under evaluation in a DIPG clinical trial (NCT02233049). Surprisingly, TXK, a target of T-cell receptor and associated with AKT signaling was among the best hits, but expressed at a low level in GSC cells (Fig2C).

As GSC2 cellular model appeared quite resistant to shRNA depletion in our experimental conditions, we considered as a potential vulnerability in DIPG a gene fulfilling all the criterion in at least 3 out of 4 of the GSC models used. By this way, we scored 41 genes as essential without major deleterious effect in NSC cells.

Long-term *versus* short-term impact of selected shRNAs

The FCs of the selected hits ranged from 0.19 to 0.47 (median value 0.32) for H3.3-mutated GSC2 which corresponded to smaller changes in frequencies than initially expected when we designed the screen, and also than obtained with the other cells. This observation results potentially from a low doubling time of our GSC models ranging from 1.92 to 2.66 days. Consequently, we performed another screen in H3.3-K27M cells to confirm this hypothesis in the same experimental conditions but by maintaining cells in expansion during 64 days instead of 22 days initially, referred as ‘long-term’ and ‘short-term’ screens, respectively. Moreover, a third H3.3-K27M mutated GSC (GSC5) was added to confirm that GSC2 displays a particular phenotype of resistance to shRNA gene extinction.

The cumulative frequency observed for the initial timepoint replicates in short-term

and long-term screens almost perfectly overlapped for GSC3 and GSC4 reflecting the high reproducibility of the two independent screens (FigS2A). As expected, a significantly more important shift was observed between the 64-days curve and the 40h curve than between the 22-days and 40h curves even for the GSC2 model. The results seemed also globally concordant between the two distinct end points (FigS2B & 2C). All the 41 essential genes identified in the short-term screen were validated in this second long-term screen with lower FCs ranging from 0.02 to 0.15 (median value 0.06) (Fig2C) confirming the relevance of their selection.

Functional analysis of DIPG essential genes

We used pathway annotation sources such as KEGG, Gene Ontology and Reactome to pinpoint key functional gene categories in the list of candidate hits. As expected, a significant enrichment of genes involved in cell cycle regulation and growth arrest as well as cell death pathways was revealed by GO analysis (Fig2C). Among them, *PLK1*, *AURKB* were also identified as required for cell survival in similar dropout screen conducted in adult GBM(12,20). Moreover, in another negative selection screen *ABL1*, *CHEK1*, *EGFR*, *GSK3A*, *IGFR1*, *INSR*, *MAPK10*, *TTK*, *RET* were identified as kinases whose KD alters cell cycle by increasing the number of cells entering in S phase or in SubG1 phase, in either mesenchymal- or proneural- phenotype associated GSC models of adult GBM or both(9). These data revealed a certain similarity in vulnerabilities of adult and pediatric gliomas. Cell motility, and to a lesser extent adherens junctions, also belonged to the biological processes significantly over-represented.

The Forkhead box O (FoxO) signaling pathway, that plays a pivotal role in carcinogenesis of a wide range of cancers by regulating suppression of tumour

growth(21), was found significantly enriched in our analysis with *EGFR*, *INSR*, *IGFR1*, *MAP2K2*, *MAPK10*, *PLK1*, *PLK4*, *SGK3*, *TGFBR2*. The PI3K/AKT pathway promotes cell survival by phosphorylating and thus inhibiting several signaling proteins like FOXO transcription factors, mTORC1 as well as GSK3 that is also part of the core essential genes identified. Surprisingly, we observed that *OBSCN* depletion impaired DIPG survival whereas loss of obscurins was shown to result in enhanced tumor survival and growth by regulating PI3K pathway in breast cancer(22).

PTEN and TP53 appear as key upstream regulators of 34% of the top core essential genes as shown by ingenuity pathway analysis in accordance with our knowledge on DIPG biology. Indeed, PTEN loss is observed in the majority of DIPG patients (23) and at least 40% of DIPG tumor are TP53-deficient (Fig2D)(24).

We decided to focus on new candidates that do not constitute therapeutic target already under evaluation in this disease or do not belong to a well-known altered pathway in DIPG like PI3K/AKT. Moreover, we only considered genes associated with moderate to high expression level in our cellular models as relevant potential therapeutic targets. Among these, Vaccinia-related kinase 3 (VRK3) was selected. VRK3 is poorly studied but has been shown to interact with VRK1 and to be functionally important in cell cycle regulation, mRNA processing, chromatin assembly, and DNA repair(25). Interestingly, another hit, *LMTK3*, interacts with VRK3(25).

VRK3 is a synthetic lethal gene in H3-K27M DIPG cells

The box plot of the FCs of all shRNA targeting *VRK3* (n=15) reflects the important variability among the cells as the spreading of the distribution vary from one model to another (Fig3A & FigS1A, pink dots). Additionally, these data indicated the wide variation in read frequencies for the shRNAs targeting different loci of the same gene, from important depletion to slight enrichment through cell expansion. This observation could result in part from the use of unvalidated shRNA library that should contain interfering RNA unable to lead to target gene extinction or presenting off-target effects. Indeed, 4 distinct shRNAs did not lead to any depletion in any GSC cells and 2 others conduct to a decrease of more than two-fold in only 2 distinct models. Yet, the median of the FCs of all *VRK3* shRNAs was lower in GSC 1, 3 & 4 (from which this target was selected) than in NSC cells.

Then, we evaluated by RT-qPCR the extent of *VRK3* gene extinction after individual transduction of four distinct shRNAs selected in our pipeline, further named shVRK3-1 to 4 (Fig3B, FigS3A & Suppl.Table 1). A significant decrease of more than 2-fold was observed in all the GSCs and NSC cells with all the shRNAs targeting *VRK3* tested (pvalue from 0.0001 to 0.02) except for shVRK3-3 in GSC3 and shVRK3-4 in NSC1 (pvalue 0.12) more probably because of the huge variability among experimental replicates (Fig3B). We did not observe any difference in alternative transcript expression profile between H3.1- and H3.3-mutated tumors (*data not showed*). Interestingly, the shVRK3-3 which led regularly to a lower inhibition of *VRK3,* do not target one of the 3 alternative transcripts of reference that is expressed in our GSCs (FigS3A).

Additionally, the RNAi KD was associated with an important decrease at protein level as shown in GSC3 cells (Fig 3C).

VRK3 expression and prognosis in cancers

To characterize the physiopathological roles of *VRK3* in cancer, we analyzed public transcriptomic data(26) (FigS3B). A significant downregulation of *VRK3* was observed only in pancreatic adenocarcinoma and a significant overexpression in testicular germ cell tumors (ANOVA, q-value<0.01). This gene was not differentially expressed among the 31 remaining tumor types analyzed, indeed a slight downward trend was observed in half of the cases and a mild increase in the other half. In accordance, the overall survival of tumors stratified in 2 subgroups according to *VRK3* expression level is identical (FigS3C). However, in both adult high-grade and low-grade gliomas, *VRK3* is to some extent upregulated in tumors and distinct overall survivals were observed depending on *VRK3* expression level (logrank test, pvalue $1.2e^{-12}$, FigS3B&D). Less difference between tumors associated with a low or high level of *VRK3* was obtained when only considering LGG tumors (logrank test, pvalue 0.00012).

VRK3 inhibition causes cell growth arrest

We next validated that the significant depletion of shVRK3 measured during the primary synthetic lethal screen reflects a deleterious effect of *VRK3* inhibition on DIPG cell growth. A proliferation assay was performed during 12 days following the individual transduction of four distinct shRNAs targeting *VRK3* and 2 negative control shRNAs (Fig4A). First, H3.1-K27M cells appeared more sensitive than H3.3-K27M to both transduction (shCtrl1) and RNA interference (shCtrl2) in comparison

to non-transduced (NT) at the MOI of 3, whereas we did not observe any impact at lower MOI during the screen (Fig4A). *VRK3* KD triggered a complete growth inhibition with the four different interfering RNAs in all cells except for shVRK3-3 in GSC1 (Fig4A&B). Indeed, the cell confluency increased until 144h following transduction with shVRK3-3 as in negative control conditions and then decreased at later time points. Interestingly this interfering RNA was also the less efficient for gene extinction.

VRK3 repression induces distinct morphological changes and cell fate in H3.3-K27M and H3.1-K27M cells

Despite a similar deleterious effect of *VRK3* inhibition on proliferation, we observed distinct outcomes on cell behavior in the two main subgroups of DIPG. Indeed, *VRK3* repression induced important morphological changes in the H3.3-K27M models starting two days after transduction with cell agglutination and loss of cell anchoring to laminin, as shown for GSC2 in Fig4C & FigS4. Analysis of the proportion of positive cells for fluorescent-nucleic acid staining by a cell-impermeant dye showed that these changes were associated with a significant induction of cell death from 96h after transduction. By contrast, H3.1-mutated cells did not neither lose attachment to the flask nor formed cell clusters, and presented longer cellular processes than shCtrl transduced cells. We did not observe any increase in dead cells in H3.1-mutated GSCs. This result indicates that *VRK3* KD leads to cell cycle arrest without cell death enhancement in this subgroup of DIPG.

Discussion

We performed the first negative selection shRNA screen to highlight genes playing a non-redundant role in the oncogenic driver pathways of DIPG and discover oncogene and non-oncogene addictions in DIPG. We used a kinome-wide lentiviral shRNA library as dedicated inhibitors are already available for the vast majority of the kinases, allowing a faster translation in the clinic. We selected candidates presenting a phenotypic consistency across multiple hairpins targeting one gene to limit false positive results. We used GSC models as cancer stem cells are responsible of tumor development and relapse in several tumor types representing therefore important target for drug discovery(27). In addition, we previously demonstrated the ability of GSC cells to induce tumor development in mice(7) and Filbin and coll. confirmed recently that DIPG are mainly composed by cells presenting stem-like properties(28). Thus, it appeared relevant to conduct the screen in these cellular models(7). Seven genes were identified as essential genes specifically in DIPG with no major impact on NSC survival. Clinical trials evaluating specific inhibitors targeting some of these candidates and their pathways (*EGFR*, *FGFR1*, *GSK3A*, *MAPK10*) are currently ongoing, reflecting the heuristic power of systematic perturbation of gene function by RNA interference to discover cancer cell dependencies, and the relevance of our results. Some of these genes were already shown to constitute potential targets in gliomas where their inhibition could induce an anticancer effect: MAPK10/JNK3(29,30), GSK3(31,32), FGFR1 ((33) or AZ4547 in clinical trial) or EGFR that has been targeted in numerous trials. We thus aimed to explore innovative therapeutic strategies in DIPG beyond targeting the PTEN/PI3K and EGFR pathways to provide breakthrough in the management of this fatal disease. We observed heterogeneity among models and interestingly GSC2,

less prone to intrinsic vulnerabilities resulting from gene extinction, derived from a patient presenting a very rapid and metastatic evolution of the disease. To circumvent this issue, we expanded the hit selection to 41 genes depleted in 3 out of 4 GSCs whose extinction led to cell growth arrest or induced cell death. We did not detect important specificity in the oncogenic program of the two main subgroups of DIPG, as the candidates found depleted only in H3.1-mutated cells in the short-term screen was then identified in H3.3-K27M GSC in the long-term screen (*data not showed*). Interestingly, as driver events and gene expression profiles are distinct in adult and pediatric GBM, these tumors shared however some vulnerabilities, like *PLK1* and *AURKB* for example. However, almost all the selected hits do not correspond to genes frequently altered in DIPG, suggesting that the search for therapeutic targets should move beyond targeting genes with recurrent mutations. We subsequently investigated *VRK3* which plays essential roles in synaptic structure and function, neuronal differentiation, potentially modulating a series of cognitive functions(34)(35). This kinase is also involved in cell cycle regulation, DNA repair (25). We proved a major impact of its inhibition on DIPG cell fate as it completely blocked their proliferation. The effect differed between H3.1- and H3.3-mutated cells as the former presented only a cell growth arrest whereas the later also harbored immediate morphological changes and cell death engagement. Indeed, the consequence of *VRK3* KD was more dramatic in the most aggressive DIPG GSCs. The ability of *VRK3* repression to inhibit tumor growth in vivo xenograft model of DIPG should be investigated.

No recurrent alteration of VRK3 have been reported in cancer, indicating that it does not play a major role in tumorigenesis per se. *VRK3* overexpression is linked with a more aggressive phenotype in adult gliomas but its extinction has never been tested

in this setting. Unfortunately, there is no expression data with survival correlation presently available for DIPG in the public databases and also no drug targeting VRK3(36). Targeting VRK3 could be assayed indirectly through the inhibition of its consequences. For example, it has been shown that *VRK3* KD induced a sustained phospho-ERK expression and led to induced cell death in a glutamate-induced neurotoxicity context(35).

VRK3 repression leading to synthetic lethal interaction with H3-K27M mutation, one could speculate that it may be an effective target in DIPG. Indeed, its inhibition seems to be well tolerated in normal stem cells, and ubiquitous germinal *VRK3*-knockout mice were viable, presented normal development and only displayed typical symptoms of autism spectrum disorder(34). This study provides new insights into DIPG intrinsic vulnerabilities and highlights the potential of non-oncogenes as points of intervention for cancer therapeutics in this terrible disease.

Materials and methods

Cell culture

HEK293T cells were grown in DMEM (Thermofisher scientific, Villebon-Sur-Yvette, France) supplemented with 10% fetal bovine serum (Sigma-Aldrich, St. Quentin Fallavier, France) and 1% penicillin/streptomycin (Thermofisher scientific). Stem cells were cultured as previously described(37). The GSCs were derived as described in Plessier *et al* from primary DIPG tumors collected according to the IRB approved protocol (number DC-2009-955) following informed consent for the translational research program obtained from the parents or guardian (7). Normal human NSC derived from hindbrain (NSC1) and mid-forebrain (NSC2) area of the

central nervous system were acquired commercially from Takara Bio Europe (formerly Clontech Laboratories, Inc., Saint-Germain-en-Laye). Human prenatal whole brain crude extract cells (NSC3) were purchased from Applied StemCell (Milpitas, California, USA). NSC4 were derived from human embryo of Carnegie stage 18 obtained following voluntary abortions(38). Tissue collection and use were performed according to the guidelines and with the approval of the French National Ethic Committee (authorization N° PFS10_011). All samples were obtained with the written informed consents of subjects according to Helsinki declaration. Embryonic neural tissues were excised sterilely using microsurgery instruments and a dissecting microscope, in phosphate-buffered saline (PBS) containing 100 U/ml penicillin and 100 mg/ml streptomycin (Thermofisher scientific). Tissue was mechanically dissociated by pipetting into serum-free medium and the single-cell suspension was cultured as neurospheres during one passage, then transferred to an adherent monolayer in laminin-coated flask, as for DIPG cells but without addition of PDGF.

Kinome-wide screen

Fifteen million cells (GSC1-4 and NSC1-2) were transduced with the MISSION® human kinase lentiviral shRNA pooled library containing 7 450 shRNAs targeting 672 genes (Sigma-Aldrich) at a multiplicity of infection (M.O.I.) of 0.3 in order to get an average 600-fold shRNA representation. Forty hours after transduction, half of the cells was harvested for genomic DNA (gDNA) isolation and the other half was selected in puromycin: 0.2 µg/mL (InvivoGen, Toulouse, France) for 4 days then 0.5 µg/mL for 3 days. The cells were then propagated in culture for a total of 22 days after transduction, collected and gDNA extracted with QIAmp DNA Blood Maxi Kit

(QIAGEN, Courtaboeuf, France). To maintain the shRNA fold representation, the entire set of integrated shRNA constructs were PCR amplified from 10.2 ng gDNA in three 100µL reactions as described(39). After amplicon size confirmation, thirty percent of each reaction were pooled and purified using Agencourt AMPure XP (Beckman Coulter, Villepinte, France). The resulting libraries were sequenced to achieve 1,000X coverage over shRNA library in a HiSeq4000 sequencer (Illumina, San-Diego, California, USA). Short reads were mapped to shRNA library with bowtie version 1.1.2 in the R statistical environment. Briefly, read count per shRNA was normalized to the total number of reads per sample to account for the variable read depth using the following equation:

$$\text{Normalized read count } \textit{per} \text{ shRNA} = \frac{\text{read count } \textit{per} \text{ shRNA}}{\text{total number of reads } \textit{per} \text{ sample}} \times 10^6 + 1$$

A multi-step process of filtering was subsequently performed to select the best shRNA candidates (Supplemental figure S1A).

shRNA cloning and lentiviral production

Bacterial glycerol stocks were commercially obtained from Sigma-Aldrich (Supplemental Table 1, shVRK3-1 to -3) or oligonucleotides were purchased from IDT (Leuven, Belgium, shVRK3-4) and cloned by restriction/ligation into a lentiviral pLKO vector modified to express the fluorescent reporter mKate2-NLS following the Broad Institute Protocol(39). The negative control vector containing a non-hairpin insert Ctrl-1 and the MISSION® pLKO.1-puro Non-Mammalian shRNA Control Plasmid DNA (Ctrl-2, SHC002) were purchased from Addgene (Addgene, Cambridge, USA, plasmid #1864) and Sigma-Aldrich, respectively, and modified to express mKate2-NLS. HEK293T cells were transfected with the transgene plasmid,

the packaging plasmids psPax2 (Addgene plasmid #12260) and pMD2.g (Addgene plasmid #12259) using the transfection reagent jetPRIME® (Polyplus transfection, Illkirch, France). Culture medium was collected after 72h and ultracentrifuged. Titration was conducted in HCT116 cells(40). For individual evaluation of shRNA, cells were transduced at M.O.I. of 3.

Proliferation and apoptosis assay

Cells were plated at 10 000-20 000 cells/cm^2 (n=3 for each condition) in 96-well plate and growth monitored daily by videomicroscopy at 10X objective (Incucyte® ZOOM, Essen Bioscience, Welwyn Garden City, UK) during at least 10 days. The percentage of image area occupied by cells was determined by picture segmentation with CellPlayer Analysis software (Essen Bioscience) and used as a measure of the confluence in each condition normalized to the initial point. For YOYO staining assay culture medium was supplemented with 80 nM of the cell impermeant nucleic acid stain YOYO-1 Iodide (491/509) (Thermofisher scientific) and the percentage of image area occupied by green fluorescent cells was determined with CellPlayer Analysis software.

RT-qPCR

Total RNA was extracted at distinct timepoints after transduction using RNeasy Mini kit (QIAGEN) according to manufacturer's instructions. Five hundred ng of RNA were reverse transcribed with Revertaid Polymerase (Thermofisher scientific) and quantitative real-time PCR was conducted with Maxima SYBR Green/ROX qPCR Master Mix (2X) (Thermofisher scientific). Reactions were performed in triplicate (n=3) with primers targeting *VRK3* (VRK3-Forward: 5'-

TGTGGATCCAGAGGACCAGA-3'; VRK3-Reverse: 5'-ACTTGGGCAATAGCGGAAGG-3') and TATA-binding protein (TBP, housekeeping gene; TBP-Forward: 5'-CACGAACCACGGCACTGATT-3'; TBP-Reverse: 5'-TTTTCTTGCTGCCAGTCTGGAC-3') genes. The relative change in gene expression data were analyzed by the $2^{-\Delta\Delta Ct}$ method by comparison with the control sample shCtrl-1(41).

Western blot

One million cells pellets were lysed in Tris HCl 250mM pH 7,5, NaCl 250nM, EDTA 5mM, NP40 1%, heated at 37°C during 45 sec and cooled at -80°C during 45sec, five times. Thirty µg of proteins were separated by electrophoresis in a 4-15% Resolving Gel Electrophoresis (Mini-PROTEAN TGX Stain-Free Precast Gels BIORAD) and transferred to nitrocellulose membrane. Antibodies used are detailed in Supplemental Table 2. Immunoblots were imaged with ChemiDoc MP system with ImageLab 4.1 software (Bio-Rad, Marnes-la-Coquette, France).

Statistics

Statistical comparison and graphs were performed with Prism X (GraphPad Inc, La Jolla, USA). Analysis of variance was used for multiple comparisons and Student test for paired comparisons.

Acknowledgements

DC, JG, MAD acknowledge financial support from Canceropole Ile de France, INCa, La Ligue Contre le Cancer (projet DILESS – DM/CB/003-17) and the charity l'Etoile de Martin.

CSE acknowledges financial support from National Council for Scientific and Technological Development (CNPq)/ Program "Science without borders"

Conflict of Interest

The authors declare no conflict of interest.

References

1. Cohen KJ, Jabado N, Grill J. Diffuse intrinsic pontine gliomas-current management and new biologic insights. Is there a glimmer of hope? Neuro-oncology. 24 mars 2017;

2. Grasso CS, Tang Y, Truffaux N, Berlow NE, Liu L, Debily M-A, et al. Functionally defined therapeutic targets in diffuse intrinsic pontine glioma. Nat Med. juin 2015;21(6):555‑9.

3. Warren KE. Diffuse intrinsic pontine glioma: poised for progress. Front Oncol [Internet]. 28 déc 2012 [cité 17 févr 2016];2. Disponible sur: http://www.ncbi.nlm.nih.gov/pmc/articles/PMC3531714/

4. Taylor KR, Mackay A, Truffaux N, Butterfield YS, Morozova O, Philippe C, et al. Recurrent activating ACVR1 mutations in diffuse intrinsic pontine glioma. Nat Genet. mai 2014;46(5):457‑61.

5. Wu G, Broniscer A, McEachron TA, Lu C, Paugh BS, Becksfort J, et al. Somatic histone H3 alterations in pediatric diffuse intrinsic pontine gliomas and non-brainstem glioblastomas. Nat Genet. mars 2012;44(3):251‑3.

6. Misuraca KL, Hu G, Barton KL, Chung A, Becher OJ. A Novel Mouse Model of Diffuse Intrinsic Pontine Glioma Initiated in Pax3-Expressing Cells. Neoplasia. janv 2016;18(1):60‑70.

7. Plessier A, Le Dret L, Varlet P, Beccaria K, Lacombe J, Mériaux S, et al. New in vivo avatars of diffuse intrinsic pontine gliomas (DIPG) from stereotactic biopsies performed at diagnosis. Oncotarget. 8 août 2017;8(32):52543‑59.

8. Truffaux N, Philippe C, Paulsson J, Andreiuolo F, Guerrini-Rousseau L, Cornilleau G, et al. Preclinical evaluation of dasatinib alone and in combination with cabozantinib for the treatment of diffuse intrinsic pontine glioma. Neuro-oncology. juill 2015;17(7):953‑64.

9. Cheng P, Phillips E, Kim S-H, Taylor D, Hielscher T, Puccio L, et al. Kinome-wide shRNA screen identifies the receptor tyrosine kinase AXL as a key regulator for mesenchymal glioblastoma stem-like cells. Stem Cell Reports. 12 mai 2015;4(5):899‑913.

10. Gargiulo G, Cesaroni M, Serresi M, de Vries N, Hulsman D, Bruggeman SW, et al. In vivo RNAi screen for BMI1 targets identifies TGF-β/BMP-ER stress pathways as key regulators of neural- and malignant glioma-stem cell homeostasis. Cancer Cell. 13 mai 2013;23(5):660‑76.

11. Goidts V, Bageritz J, Puccio L, Nakata S, Zapatka M, Barbus S, et al. RNAi screening in glioma stem-like cells identifies PFKFB4 as a key molecule important for cancer cell survival. Oncogene. 5 juill 2012;31(27):3235‑43.

12. Kulkarni S, Goel-Bhattacharya S, Sengupta S, Cochran BH. A Large-Scale RNAi Screen Identifies SGK1 as a Key Survival Kinase for GBM Stem Cells. Mol Cancer Res. janv 2018;16(1):103‑14.

13. Sa JK, Yoon Y, Kim M, Kim Y, Cho HJ, Lee J-K, et al. In vivo RNAi screen identifies NLK as a negative regulator of mesenchymal activity in glioblastoma. Oncotarget. 21 août 2015;6(24):20145‑59.

14. Tandle AT, Kramp T, Kil WJ, Halthore A, Gehlhaus K, Shankavaram U, et al. Inhibition of polo-like kinase 1 in glioblastoma multiforme induces mitotic catastrophe and enhances radiosensitisation. Eur J Cancer. sept 2013;49(14):3020‑8.

15. Wurdak H, Zhu S, Romero A, Lorger M, Watson J, Chiang C-Y, et al. An RNAi screen identifies TRRAP as a regulator of brain tumor-initiating cell differentiation. Cell Stem Cell. 8 janv 2010;6(1):37‑47.

16. Yang J, Fan J, Li Y, Li F, Chen P, Fan Y, et al. Genome-wide RNAi screening identifies genes inhibiting the migration of glioblastoma cells. PLoS ONE. 2013;8(4):e61915.

17. Hart T, Brown KR, Sircoulomb F, Rottapel R, Moffat J. Measuring error rates in genomic perturbation screens: gold standards for human functional genomics. Mol Syst Biol. 1 juill 2014;10:733.

18. Geoerger B, Hargrave D, Thomas F, Ndiaye A, Frappaz D, Andreiuolo F, et al. Innovative Therapies for Children with Cancer pediatric phase I study of erlotinib in brainstem glioma and relapsing/refractory brain tumors. Neuro Oncol. 1 janv 2011;13(1):109‑18.

19. Zarghooni M, Bartels U, Lee E, Buczkowicz P, Morrison A, Huang A, et al. Whole-Genome Profiling of Pediatric Diffuse Intrinsic Pontine Gliomas Highlights Platelet-Derived Growth Factor Receptor α and Poly (ADP-ribose) Polymerase As Potential Therapeutic Targets. JCO. 3 oct 2010;28(8):1337‑44.

20. Ding Y, Hubert CG, Herman J, Corrin P, Toledo CM, Skutt-Kakaria K, et al. Cancer-Specific Requirement for BUB1B/BUBR1 in Human Brain Tumor Isolates and Genetically Transformed Cells. Cancer Discovery. 2 janv 2013;3(2):198‑211.

21. Farhan M, Wang H, Gaur U, Little PJ, Xu J, Zheng W. FOXO Signaling Pathways as Therapeutic Targets in Cancer. Int J Biol Sci. 2017;13(7):815‑27.

22. Shriver M, Marimuthu S, Paul C, Geist J, Seale T, Konstantopoulos K, et al. Giant obscurins regulate the PI3K cascade in breast epithelial cells via direct binding to the PI3K/p85 regulatory subunit. Oncotarget. 19 juill 2016;7(29):45414‑28.

23. Varlet P, Debily M-A, Teuff GL, Tauziede-Espariat A, Pages M, Andreiuolo F, et al. DIPG-20. PRE-RANDOMISATION CENTRAL REVIEW AND REAL-TIME BIOMARKERS SCREENING IN THE MULTICENTRE BIOLOGICAL MEDICINE FOR DIPG ERADICATION (BIOMEDE) TRIAL: LESSONS

LEARNT FROM THE FIRST 120 BIOPSIES. Neuro Oncol. 22 juin 2018;20(suppl_2):i52‑3.

24. Grill J, Puget S, Andreiuolo F, Philippe C, MacConaill L. Critical oncogenic mutations in newly diagnosed pediatric diffuse intrinsic pontine glioma. Pediatric Blood & Cancer. 1 avr 2012;58(4):489‑91.

25. Lee N, Kim D-K, Han SH, Ryu HG, Park SJ, Kim K-T, et al. Comparative Interactomes of VRK1 and VRK3 with Their Distinct Roles in the Cell Cycle of Liver Cancer. Mol Cells. 30 sept 2017;40(9):621‑31.

26. Tang Z, Li C, Kang B, Gao G, Li C, Zhang Z. GEPIA: a web server for cancer and normal gene expression profiling and interactive analyses. Nucleic Acids Res. 3 juill 2017;45(W1):W98‑102.

27. Chen J, Li Y, Yu T-S, McKay RM, Burns DK, Kernie SG, et al. A restricted cell population propagates glioblastoma growth after chemotherapy. Nature. 23 août 2012;488(7412):522‑6.

28. Filbin MG, Tirosh I, Hovestadt V, Shaw ML, Escalante LE, Mathewson ND, et al. Developmental and oncogenic programs in H3K27M gliomas dissected by single-cell RNA-seq. Science. 20 2018;360(6386):331‑5.

29. Du Z, Song X, Yan F, Wang J, Zhao Y, Liu S. Genome-wide transcriptional analysis of BRD4-regulated genes and pathways in human glioma U251 cells. Int J Oncol. 16 mars 2018;

30. Tang Y, He W, Wei Y, Qu Z, Zeng J, Qin C. Screening key genes and pathways in glioma based on gene set enrichment analysis and meta-analysis. J Mol Neurosci. juin 2013;50(2):324‑32.

31. Korur S, Huber RM, Sivasankaran B, Petrich M, Morin P, Hemmings BA, et al. GSK3beta regulates differentiation and growth arrest in glioblastoma. PLoS ONE. 13 oct 2009;4(10):e7443.

32. Kotliarova S, Pastorino S, Kovell LC, Kotliarov Y, Song H, Zhang W, et al. Glycogen synthase kinase-3 inhibition induces glioma cell death through c-MYC, nuclear factor-kappaB, and glucose regulation. Cancer Res. 15 août 2008;68(16):6643‑51.

33. Di Stefano AL, Fucci A, Frattini V, Labussiere M, Mokhtari K, Zoppoli P, et al. Detection, Characterization, and Inhibition of FGFR-TACC Fusions in IDH Wild-type Glioma. Clin Cancer Res. 15 juill 2015;21(14):3307‑17.

34. Kang M-S, Choi T-Y, Ryu HG, Lee D, Lee S-H, Choi S-Y, et al. Autism-like behavior caused by deletion of vaccinia-related kinase 3 is improved by TrkB stimulation. J Exp Med. 2 oct 2017;214(10):2947‑66.

35. Song H, Kim W, Kim S-H, Kim K-T. VRK3-mediated nuclear localization of HSP70 prevents glutamate excitotoxicity-induced apoptosis and Aβ accumulation via enhancement of ERK phosphatase VHR activity. Scientific Reports [Internet]. déc 2016 [cité 5 janv 2018];6(1). Disponible sur: http://www.nature.com/articles/srep38452

36. Fedorov O, Marsden B, Pogacic V, Rellos P, Müller S, Bullock AN, et al. A systematic interaction map of validated kinase inhibitors with Ser/Thr kinases. Proc Natl Acad Sci USA. 18 déc 2007;104(51):20523‑8.

37. Conti L, Pollard SM, Gorba T, Reitano E, Toselli M, Biella G, et al. Niche-Independent Symmetrical Self-Renewal of a Mammalian Tissue Stem Cell. PLoS Biol [Internet]. sept 2005 [cité 25 mars 2016];3(9). Disponible sur: http://www.ncbi.nlm.nih.gov/pmc/articles/PMC1184591/

38. O'Rahilly R, Müller F, Hutchins GM, Moore GW. Computer ranking of the sequence of appearance of 73 features of the brain and related structures in staged human embryos during the sixth week of development. Am J Anat. sept 1987;180(1):69‑86.

39. GPP Web Portal - Protocols [Internet]. [cité 26 juin 2017]. Disponible sur: http://portals.broadinstitute.org/gpp/public/resources/protocols

40. Barde I, Salmon P, Trono D. Production and Titration of Lentiviral Vectors. In: Current Protocols in Neuroscience [Internet]. John Wiley & Sons, Inc.; 2001 [cité 23 juill 2015]. Disponible sur: http://onlinelibrary.wiley.com.gate1.inist.fr/doi/10.1002/0471142301.ns0421s53/abstract

41. Livak KJ, Schmittgen TD. Analysis of relative gene expression data using real-time quantitative PCR and the 2(-Delta Delta C(T)) Method. Methods. déc 2001;25(4):402‑8.

42. Chang JT, Nevins JR. GATHER: a systems approach to interpreting genomic signatures. Bioinformatics. 1 déc 2006;22(23):2926‑33.

43. Hart T, Tong AHY, Chan K, Van Leeuwen J, Seetharaman A, Aregger M, et al. Evaluation and Design of Genome-Wide CRISPR/SpCas9 Knockout Screens. G3 (Bethesda). 7 août 2017;7(8):2719‑27.

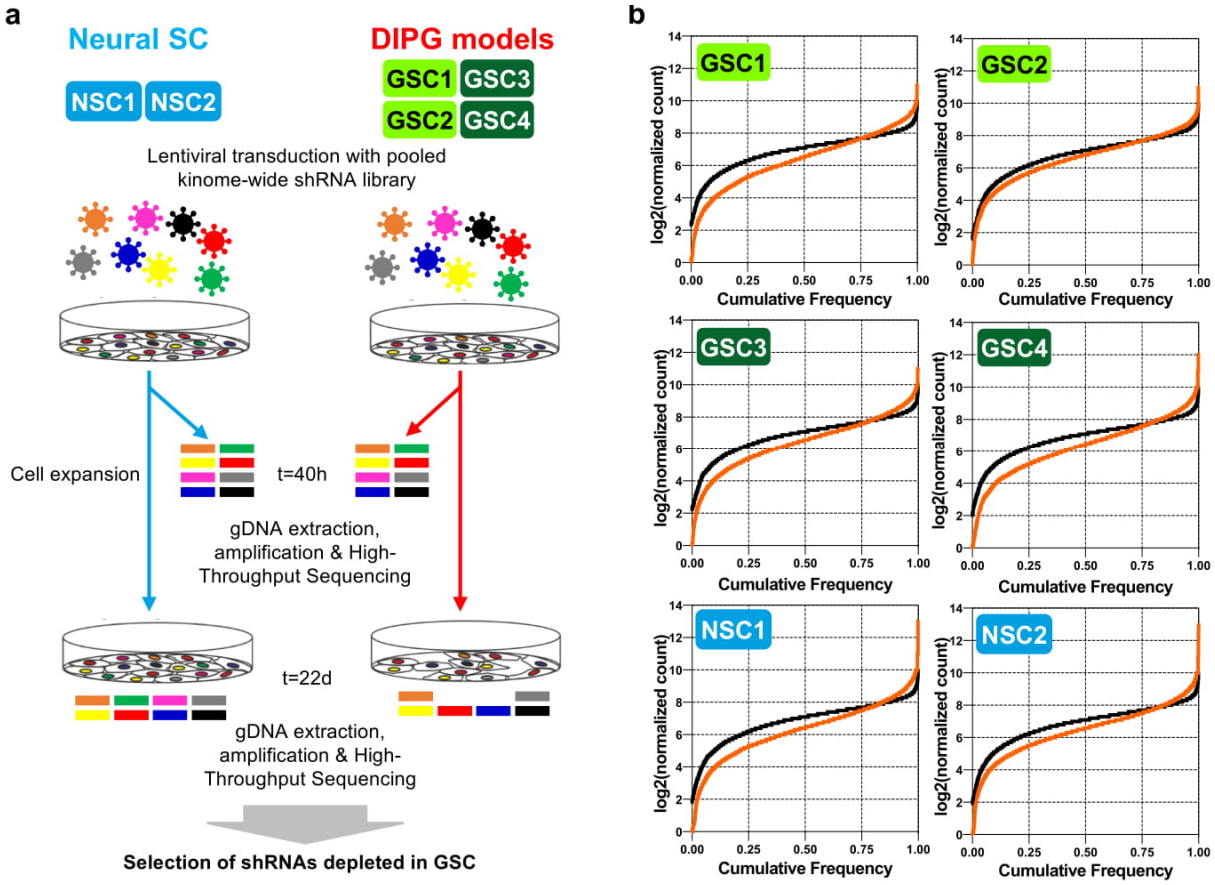
a
Neural SC
NSC1 NSC2
DIPG models
GSC1 GSC3
GSC2 GSC4
Lentiviral transduction with pooled kinome-wide shRNA library
Cell expansion
t=40h
gDNA extraction, amplification & High-Throughput Sequencing
t=22d
gDNA extraction, amplification & High-Throughput Sequencing
Selection of shRNAs depleted in GSC
b
GSC1
GSC2
GSC3
GSC4
NSC1
NSC2
log2(normalized count)
Cumulative Frequency

Figure legends

Figure 1. RNA interference screening of genes required for DIPG survival

a- *In vitro* RNAi screening strategy. Four DIPG cellular models harboring either H3.1-K27M (n=2) or H3.3-K27M mutation (n=2) and two NSC control cells were transduced in parallel with pooled shRNA lentiviruses targeting 672 human kinases (n= 7 450 shRNAs). For each model, genomic DNA was extracted 40h and 22 days after transduction. Genes required for cell expansion over 22 days of outgrowth in comparison to the reference point (40h) were identified by NGS. Candidate genes impairing specifically DIPG cell proliferation without significant deleterious effect on NSC cells were selected.

b- Cumulative frequency of shRNAs 40h and 22 days after transduction. The log2 of normalized read counts were represented for shRNAs with a raw number of reads exceeding 50 at initial time point (40h). GSC1 & GSC2 (light green) and GSC3 & GSC4 (dark green) correspond to H3.3- and H3.1-K27M cells respectively. Shift in the 22-day curve (orange) in comparison with the 40h-curve (black) represents a significant depletion in a subset of essential shRNAs (Wilcoxon matched-pairs signed rank test, *p*-value < 0.0001 for all cell types).

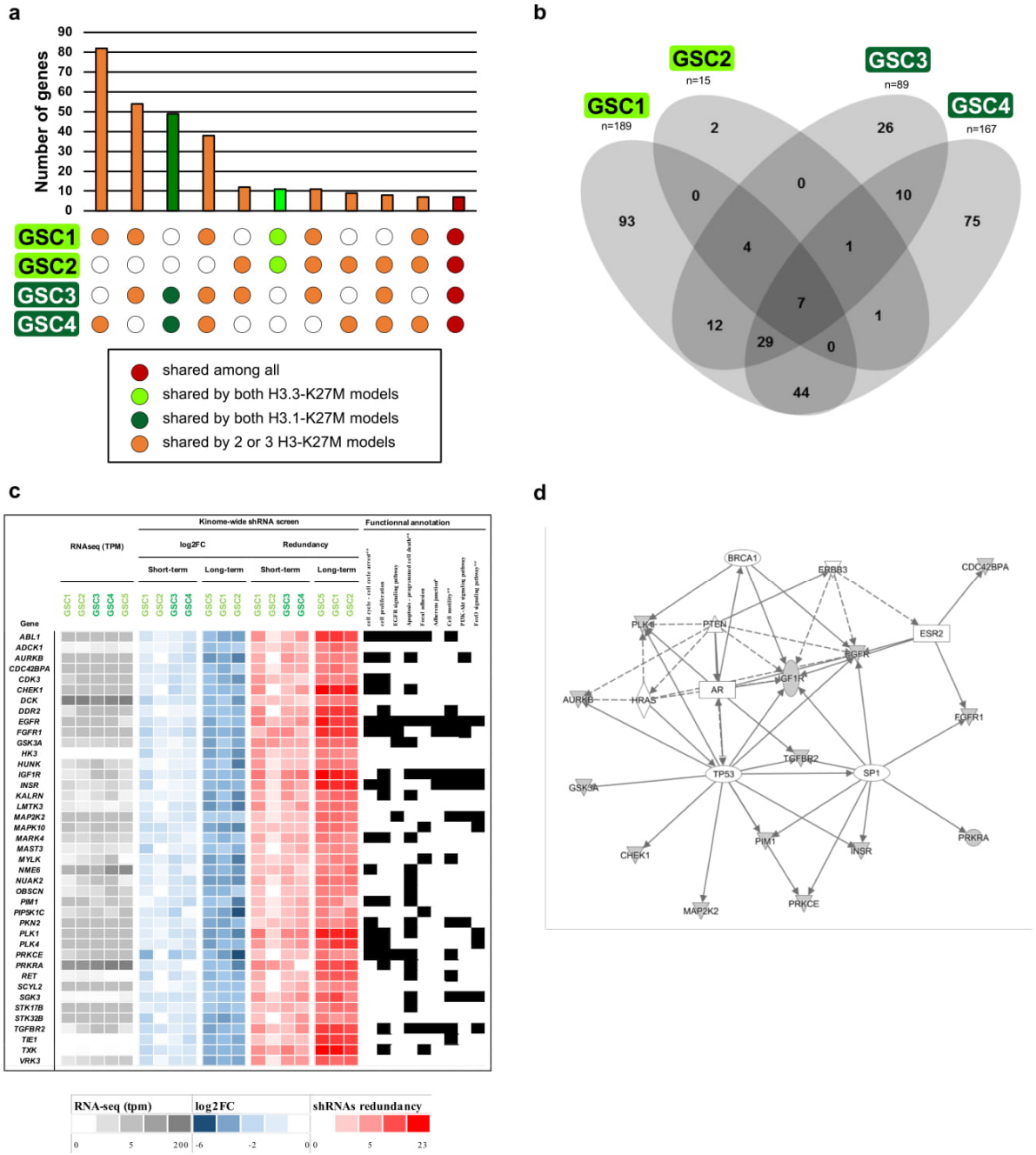
a
Number of genes
90
80
70
60
50
40
30
20
10
0
GSC1
GSC2
GSC3
GSC4
shared among all
shared by both H3.3-K27M models
shared by both H3.1-K27M models
shared by 2 or 3 H3-K27M models
b
GSC1
n=189
GSC2
n=15
GSC3
n=89
GSC4
n=167
93
2
26
75
0
0
10
4
1
7
12
1
29
0
44
c
Kinome-wide shRNA screen
Functionnal annotation
RNAseq (TPM)
log2FC
Redundancy
Short-term
Long-term
Short-term
Long-term
Gene
ABL1
ADCK1
AURKB
CDC42BPA
CDK3
CHEK1
DCK
DDR2
EGFR
FGFR1
GSK3A
HK3
HUNK
IGF1R
INSR
KALRN
LMTK3
MAP2K2
MAPK10
MARK4
MAST3
MYLK
NME6
NUAK2
OBSCN
PIM1
PIP5K1C
PKN2
PLK1
PLK4
PRKCE
PRKRA
RET
SCYL2
SGK3
STK17B
STK32B
TGFBR2
TIE1
TXK
VRK3
RNA-seq (tpm)
log2FC
shRNAs redundancy
0
5
200
-6
-2
0
0
5
23
d
BRCA1
ERBB3
CDC42BPA
PLK4
PTEN
ESR2
EGFR
IGF1R
AR
AURKB
HRAS
FGFR1
TGFBR2
TP53
SP1
GSK3A
PRKRA
PIM1
INSR
CHEK1
PRKCE
MAP2K2

Figure 2. Gene hits selection

a- Gene hits distribution across H3-K27M models. The histograms show the number of genes identified in the screen and shared by at least 2 distinct H3-K27M models. There is a more important number of genes shared by the two H3.1 mutated cellular models (n=38) than by the two H3.3 mutated cellular models (n=11).

b- Overlapping of the gene hits selected as statistically underrepresented at 22 days in comparison with 40 hours after transduction in each H3-K27M cellular model.

c- Functional annotation of target genes. Heatmap representing the RNA-seq gene expression level (tpm), the average modulation of shRNA frequency after 22 days (short-term) or 64 days (long-term) of outgrowth for the shRNA that passed the selection criteria as well as the shRNA redundancy for the 51 genes identified in at least 3 distinct DIPG models. Genes belonging to particular Gene Ontology biological process, KEGG pathway, stringDB and reactome are indicated by a black square. Cell cycle - cell cycle arrest (GO:0045787, GO:0010564, GO:0000278, GO:0007050 & stringDB), cell proliferation (GO0008283, GO:0008284, GO:0008285), EGFR signaling pathway (stringDB), Apoptosis – programmed cell death (GO:0006915, GO:004306, GO:0043065, GO:0012501), Focal adhesion (KEGG pathway hsa04510, gatherDB(42)), Adherens junction (KEGG pathway hsa04520, gatherDB), Cell motility (stringDB & GO:2000145), PI3K-Akt signaling pathway (KEGG pathway hsa04151, reactome), FoxO signaling pathway (KEGG pathway hsa04068). ** enrichment pvalue<0.0065, * enrichment pvalue<0.011, fisher exact test.

d- *PTEN* and *TP53* are identified as key upstream regulators of 14 DIPG essential genes as shown by Ingenuity Pathway Analysis (pvalue=3.24e-06). The nodes reflect the genes or encoded proteins and edges known interactions among

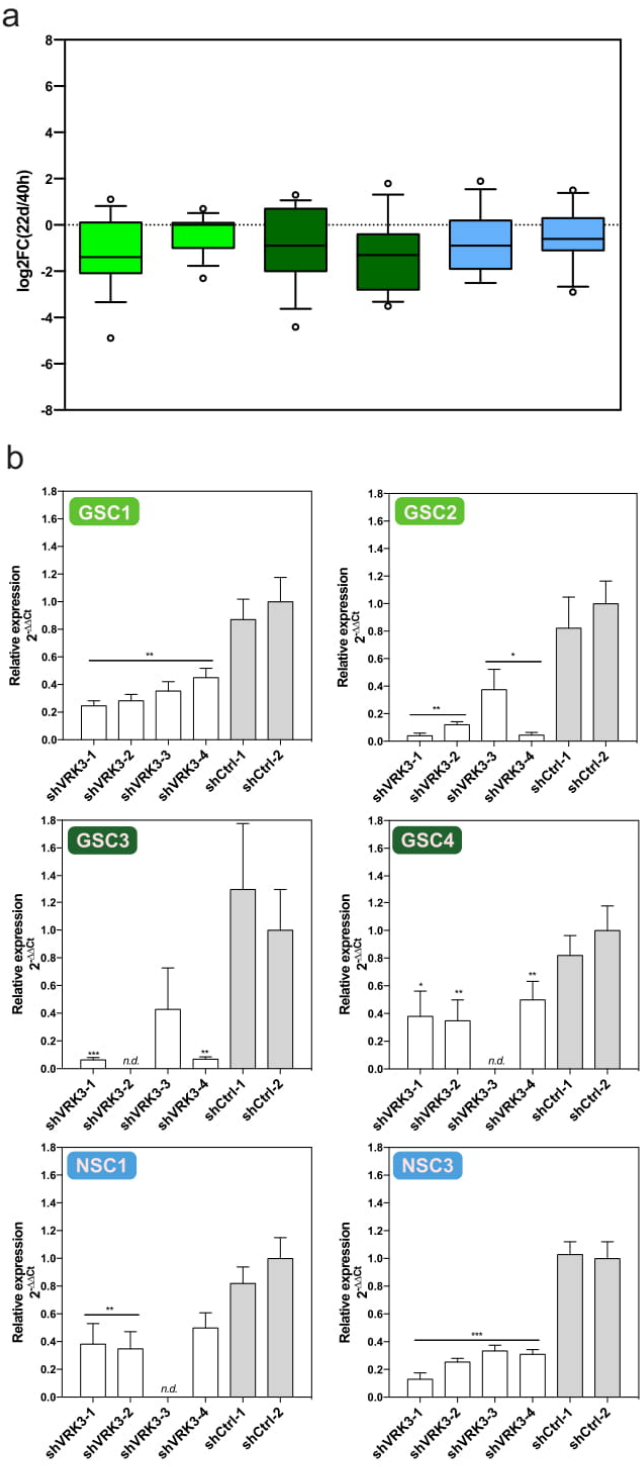
a
log2FC(22d/40h)
b
GSC1
GSC2
GSC3
GSC4
NSC1
NSC3
Relative expression
2-ΔΔCt
shVRK3-1
shVRK3-2
shVRK3-3
shVRK3-4
shCtrl-1
shCtrl-2
n.d.
c
shCtrl-2 120h
shCtrl-2 168h
shVRK3-1 120h
shVRK3-1 168h
VRK3
b-actin

the displayed nodes.

Figure 3. *In vitro* validation of *VRK3* as a DIPG-lethal gene

a- Box-plot representing the modulation of all shRNAs targeting *VRK3* in the primary screen (n= 15). The log2 ratio of shRNA frequency at 22 days *versus* 44h after transduction are represented for all *VRK3*-targeting shRNAs in the 6 cell types analyzed. The whiskers reflect the 10^{th} and 90^{th} percentiles of the distribution.

b- Evaluation of *VRK3* expression inhibition by RT-qPCR after knockdown by four independent shRNAs. Transcript expression levels were measured five days after transduction with 4 independent shRNAs targeting *VRK3* as well as 2 negative controls (shCtrl-1 & shCtrl-2). A significant knockdown was observed for all sh*VRK3* in comparison to the shCtrl2 except for shVRK3-3 in H3.1-K27M GSC3 cells (t-Student test, ***$p \leq 0.001$, **$p \leq 0.01$, * $p \leq 0.05$). Error bars represent the SD from triplicate experiments. *n.d.* not determined.

c- VRK3 quantification by western blot 120 and 168 hours post-transduction with shVRK3-1 and shCtrl-2 in GSC3 cells. ß-actin (45kDa) was used as a loading control. VRK3 (54 kDa).

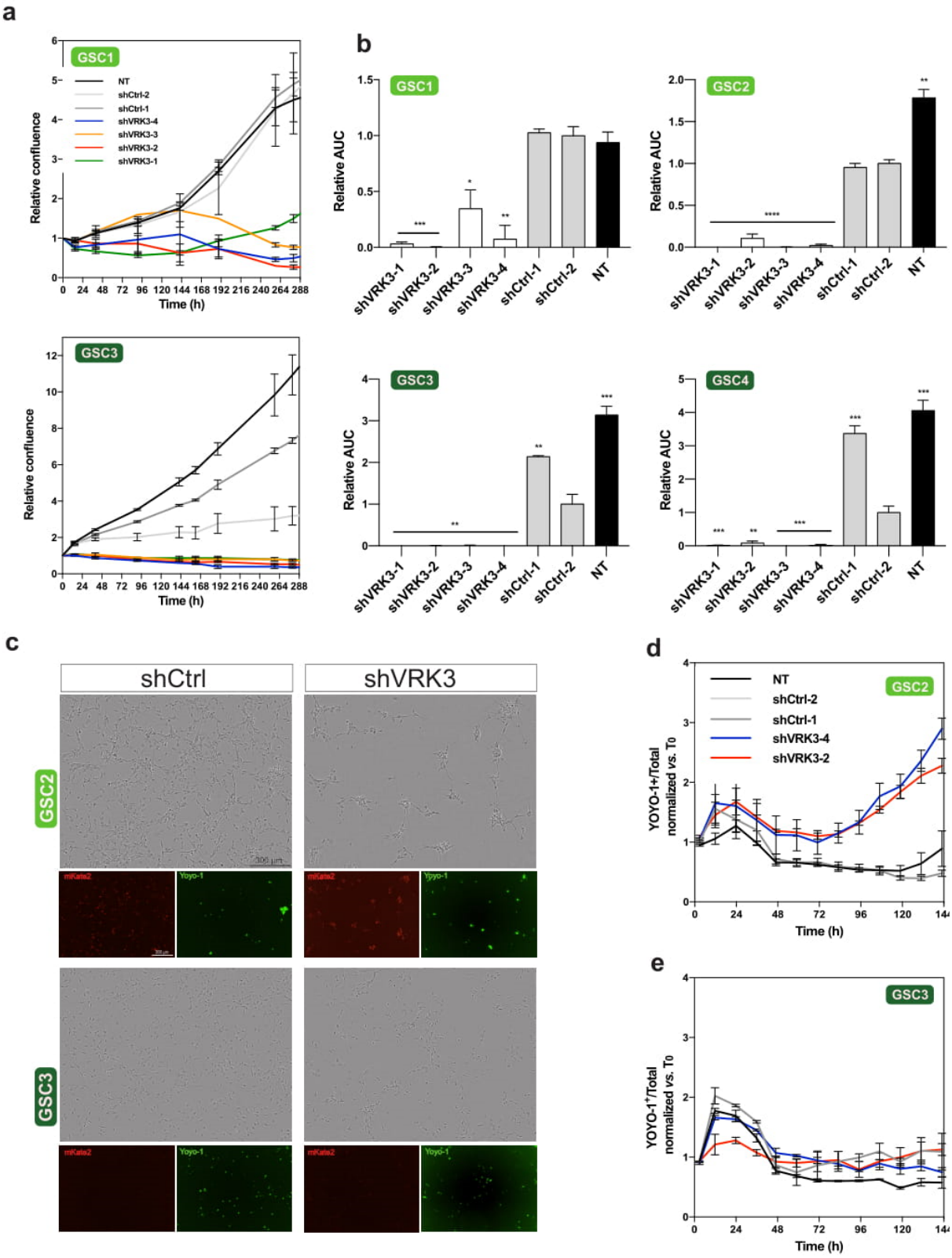
a
GSC1
NT
shCtrl-2
shCtrl-1
shVRK3-4
shVRK3-3
shVRK3-2
shVRK3-1
Relative confluence
Time (h)
GSC3
b
GSC1
GSC2
GSC3
GSC4
Relative AUC
shVRK3-1
shVRK3-2
shVRK3-3
shVRK3-4
shCtrl-1
shCtrl-2
NT
c
shCtrl
shVRK3
GSC2
GSC3
mKate2
Yoyo-1
d
GSC2
YOYO-1+/Total normalized vs. T0
Time (h)
e
GSC3
YOYO-1+/Total normalized vs. T0
Time (h)

Figure 4. *VRK3* inhibition alter DIPG cell growth, morphology and induce cell death

a- *In vitro* proliferation assay in GSC transduced with 4 shRNAs targeting *VRK3* and 2 control vectors. Proliferation was evaluated by videomicroscopy during at least 12 days and the relative confluence was represented according to time. Error bars represent the SD from triplicates.

b- Evaluation of the impact of *VRK3* KD on DIPG proliferation. Area Under the Curve (AUC) value were determined from the time-course as shown in panel a (0-248h) considering y=1 as the baseline, and relative AUC computed using shCtrl-2 as reference. Histograms represent cell expansion 248h after transduction with 4 independent *VRK3* shRNAs (white), 2 negative control vectors (gray) or in non-transduced cells (NT, black) in the 4 DIPG cellular models used in the primary screen. A significant decrease was observed for all shRNA targeting *VRK3* compared to the shCtrl-2 (t-test, ***$p \leq 0.001$, **$p \leq 0.01$, * $p \leq 0.05$). Error bars represent the SD from triplicates.

c- Morphological changes and cell death induction by *VRK3* repression. Phase-contrast images of GSC2 cells (H3.3-K27M) and GSC3 cells (H3.1-K27M) at 120 hours after transduction with either shCtrl-1 or shVRK3-1 are presented. For each condition, fluorescent images of mKate2 expression from the shRNA vector (red) and positive cells for Yoyo-1 intercalant dye (green) are shown below. Scale bars represent 300 µm.

d/e-Evaluation of the proportion of dead cells after *VRK3* inhibition. The Yoyo-1 positive area in the images was determined during 144h after shRNA transduction and normalized to cell confluence (relative to the t0 timepoint) for GSC2 (**d**) and GSC3 (**e**) cells.

a

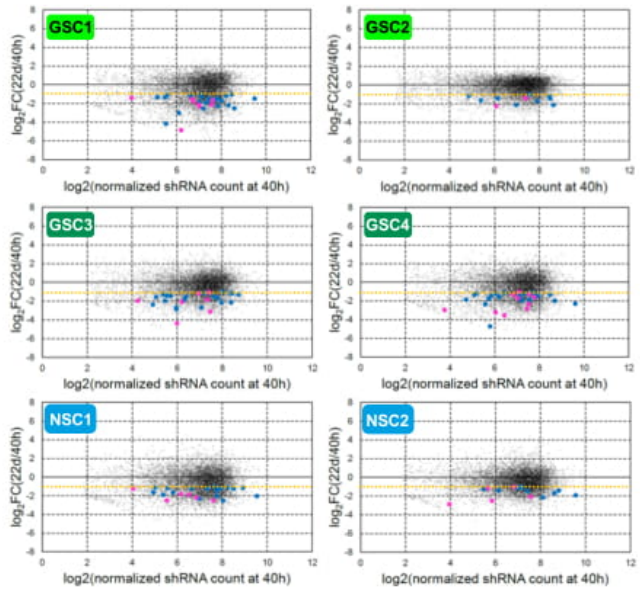
GSC1
GSC2
GSC3
GSC4
NSC1
NSC2
log2FC(22d/40h)
log2(normalized shRNA count at 40h)

b

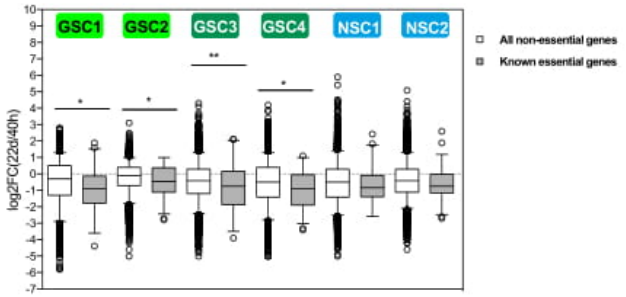
GSC1
GSC2
GSC3
GSC4
NSC1
NSC2
All non-essential genes
Known essential genes
log2FC(22d/40h)

c

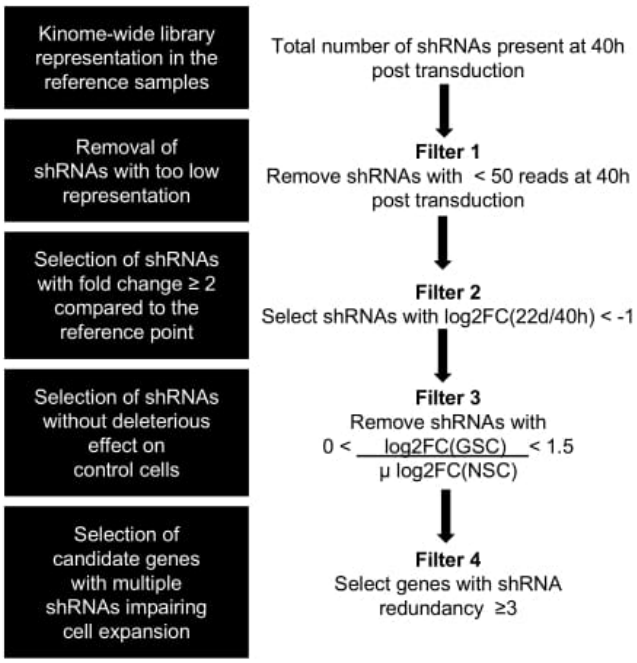
Kinome-wide library representation in the reference samples
Total number of shRNAs present at 40h post transduction
Removal of shRNAs with too low representation
Filter 1
Remove shRNAs with < 50 reads at 40h post transduction
Selection of shRNAs with fold change ≥ 2 compared to the reference point
Filter 2
Select shRNAs with log2FC(22d/40h) < -1
Selection of shRNAs without deleterious effect on control cells
Filter 3
Remove shRNAs with
0 < log2FC(GSC) / μ log2FC(NSC) < 1.5
Selection of candidate genes with multiple shRNAs impairing cell expansion
Filter 4
Select genes with shRNA redundancy ≥3

Supplemental figures

Figure S1.

a- Distribution of shRNA modulation between 40h and 22 days after transduction. Scatter plot presenting the log2 fold change of shRNA normalized read counts at 22 days *vs.* 40h post-transduction as a function of shRNA frequency at 40h. The shRNAs of essential genes for GSC cell expansion identified by Ding *and coll.* (*BUB1B*, *PLK1*, *MTOR*/*FRAP1*(20)) and that have passed the selection criteria detailed in panel c are highlighted in blue. The shRNAs targeting *VRK3* are colored in pink. The yellow dashed line represents the threshold of 'log2FC<-1' used to select interfering RNAs associated with a significant decrease at 22 days.

b- Comparison of the frequency distributions of shRNAs targeting essential and non-essential genes of the kinase library. Box plot of the log2 fold change between 22 days and 40h of all shRNAs targeting non-essential genes among the kinome-wide library (white) or the shRNAs identified as essential genes across different human cancer cell lines by Hart and *coll.*(17,43) and associated with more than 50 reads in the 40 hours samples (*i.e. AURKB*, *CDK11B*, *CDK17*, *DAPK1*, *EPHB4*, *PRKAB2*; grey) are shown. Whiskers represent the 5^{th} and 95^{th} percentiles. **p*-value≤ 0.05, ***p*-value≤ 0.01 for unpaired t-Student test.

c- Flowchart of hit selection criteria. The successive steps applied for candidate gene identification are described.

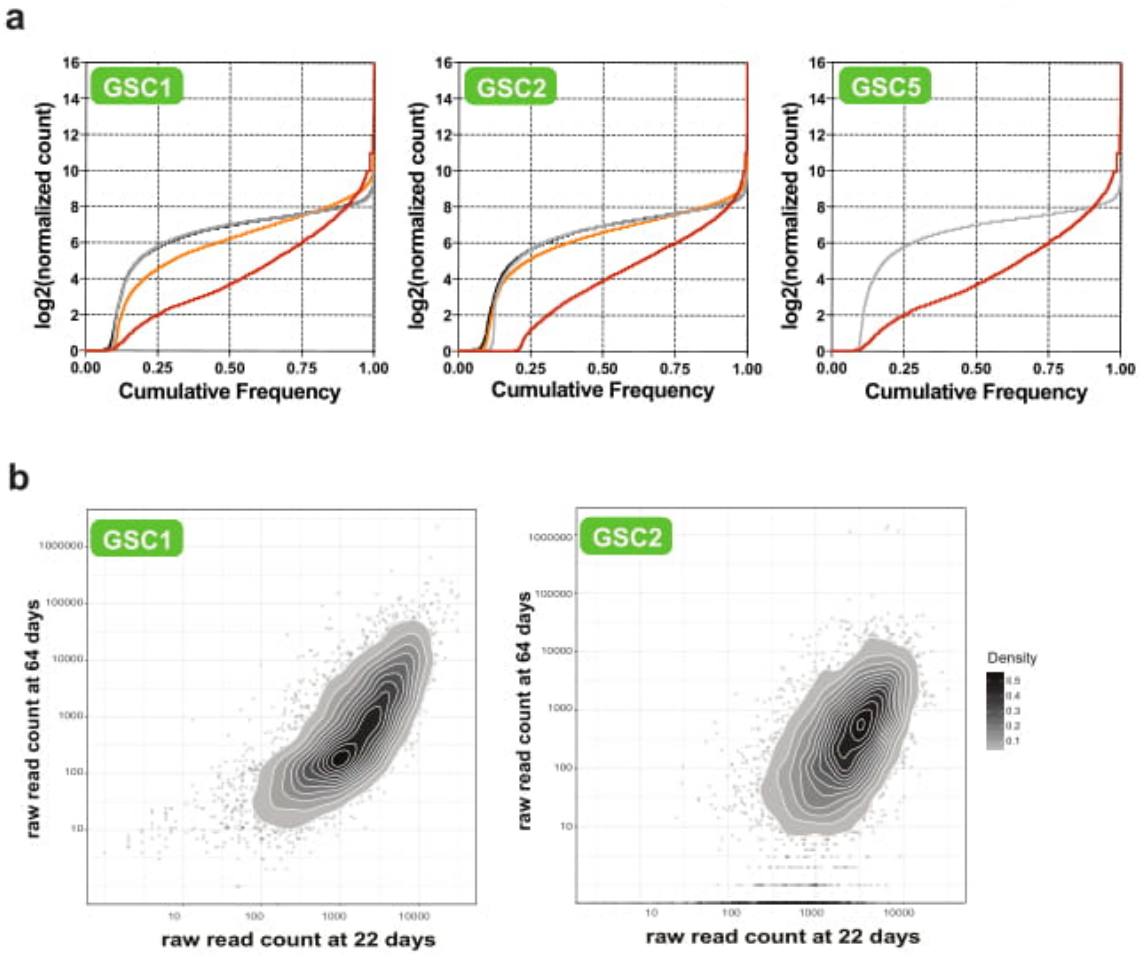
a
GSC1
GSC2
GSC5
log2(normalized count)
Cumulative Frequency
b
GSC1
GSC2
raw read count at 64 days
raw read count at 22 days
Density

Figure S2

a- Comparison of the cumulative frequency of shRNAs in the short-term and long-term RNAi screen in three H3.3-K27M DIPG models. Shift in the 22-days (orange) and 64-days (red) curves represent the significant depletion of essential shRNAs (Wilcoxon matched-pairs signed rank test, ****p*-value < 0.0001 for all cell types) in comparison to the initial time point replicates (black and gray). Statistically significant differences were observed at 22 and 64 days in comparison with initial time point (***p<0.0001 for all tested models). The variation of the frequency is more important at 64 days than 22 days after transduction.

b-Contour plots of the 2D density estimate of the raw read-counts at 64 days *versus* 22 days indicate a correlation between the results of the 2 timepoints for the GSC1 and GSC2 (H3.3-K27M) DIPG models.

a

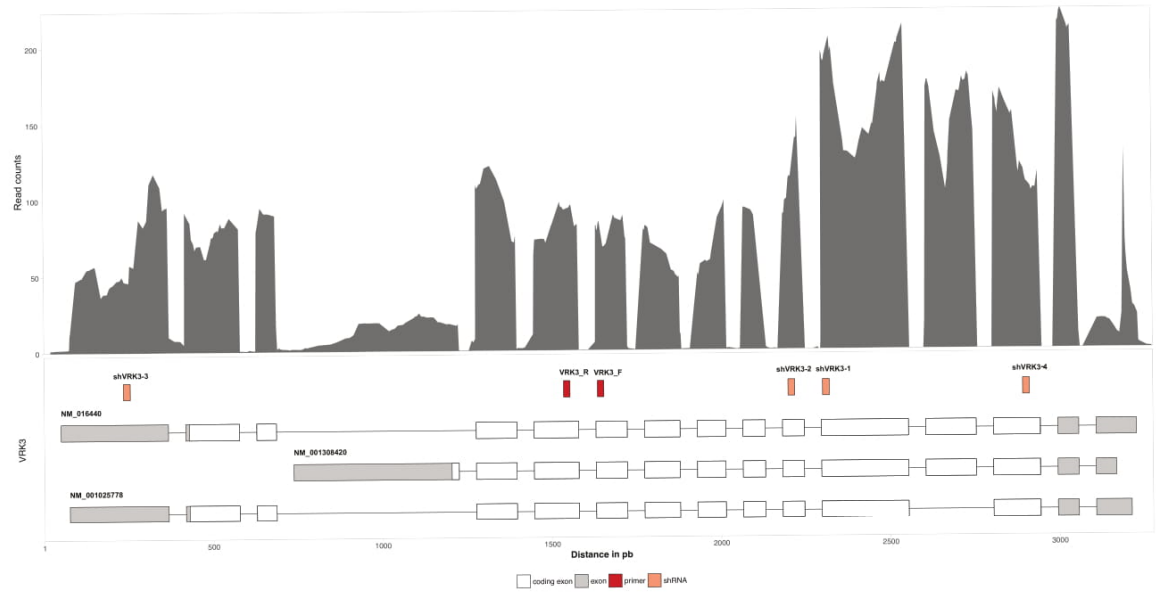
Read counts
shVRK3-3
VRK3_R VRK3_F
shVRK3-2 shVRK3-1
shVRK3-4
NM_016440
NM_001308420
NM_001025778
VRK3
Distance in pb
coding exon exon primer shRNA

b

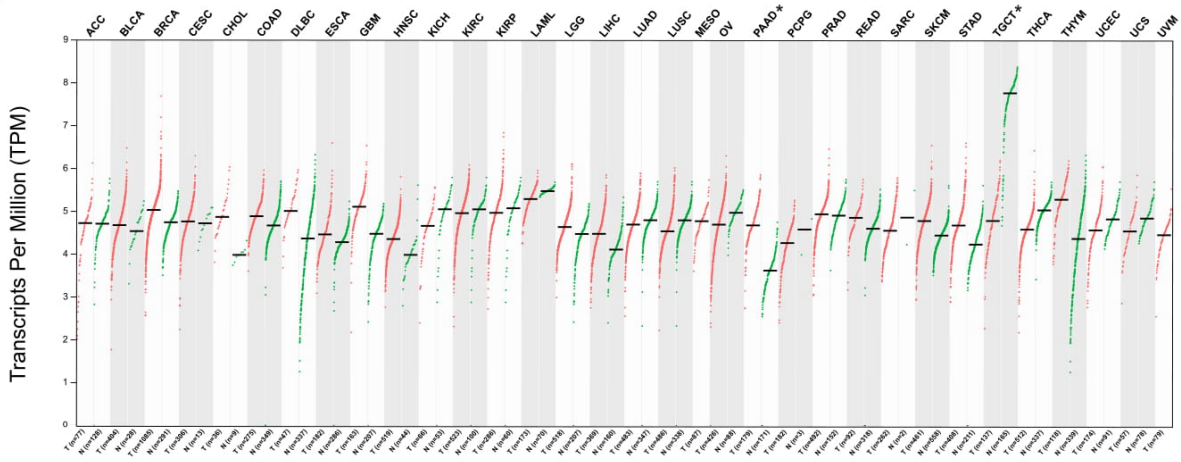
Transcripts Per Million (TPM)
ACC BLCA BRCA CESC CHOL COAD DLBC ESCA GBM HNSC KICH KIRC KIRP LAML LGG LIHC LUAD LUSC MESO OV PAAD* PCPG PRAD READ SARC SKCM STAD TGCT* THCA THYM UCEC UCS UVM

c

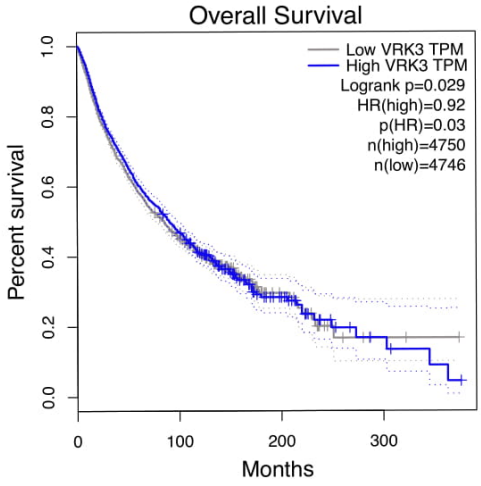
Overall Survival
Low VRK3 TPM
High VRK3 TPM
Logrank p=0.029
HR(high)=0.92
p(HR)=0.03
n(high)=4750
n(low)=4746
Percent survival
Months

d

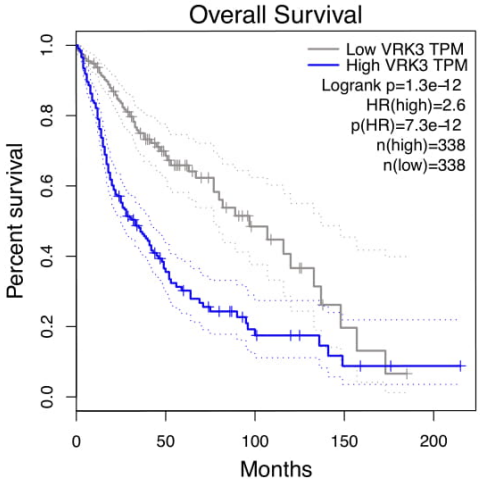
Overall Survival
Low VRK3 TPM
High VRK3 TPM
Logrank p=1.3e-12
HR(high)=2.6
p(HR)=7.3e-12
n(high)=338
n(low)=338
Percent survival
Months

Figure S3

a- Expression level of *VRK3* in DIPG and localization of RNA interfering sequences. RNA-seq coverage according to the genomic location in the *VRK3* locus. The plot reflects the mean of read coverage for a set of 57 DIPG primary tumour samples. The structure of the three Refseq transcripts are represented below. Blocks correspond to exons and lines indicate introns. The coding sequence is indicated in white. The position of the shRNAs targeting *VRK3* (orange) and the RT-qPCR primers (red) are indicated.

b- Expression level of *VRK3* in public RNA-seq data.

The box plot reflects the heterogeneity of *VRK3* expression level among samples from one particular tissue in normal (green) and tumor (red) samples from TCGA and GTEx datasets using Gepia database(26). The $\log_2$(tpm +1) was used for log-scale and q-value threshold from ANOVA analysis set to 0.01 (*). ACC, Adrenocortical carcinoma; BLCA, Bladder Urothelial Carcinoma; BRCA, Breast invasive carcinoma; CESC, Cervical squamous cell carcinoma and endocervical adenocarcinoma; CHOL, Cholangio carcinoma; COAD, Colon adenocarcinoma; DLBC, Lymphoid Neoplasm Diffuse Large B-cell Lymphoma; ESCA, Esophageal carcinoma; GBM, Glioblastoma multiforme; HNSC, Head and Neck squamous cell carcinoma; KICH, Kidney Chromophobe; KIRC, Kidney renal clear cell carcinoma; KIRP, Kidney renal papillary cell carcinoma; LAML, Acute Myeloid Leukemia; LGG, Brain Lower Grade Glioma; LIHC, Liver hepatocellular carcinoma; LUAD, Lung adenocarcinoma; LUSC, Lung squamous cell carcinoma; MESO, Mesothelioma; OV, Ovarian serous cystadenocarcinoma; PAAD, Pancreatic adenocarcinoma; PCPG, Pheochromocytoma and Paraganglioma; PRAD, Prostate adenocarcinoma; READ, Rectum adenocarcinoma; SARC, Sarcoma; SKCM, Skin Cutaneous

Melanoma; STAD, Stomach adenocarcinoma; TGCT, Testicular Germ Cell Tumors; THCA, Thyroid carcinoma; THYM, Thymoma; UCEC, Uterine Corpus Endometrial Carcinoma; UCS, Uterine Carcinosarcoma; UVM, Uveal Melanoma.

c- Overall survival in all tumor types according to *VRK3* expression level.

Kaplan–Meier survival curves of distinct tumor tissue from TCGA and GTEx datasets stratified in two subgroups according to *VRK3* expression level. The samples were divided in high and low *VRK3* by using the median of the distribution of tpm values. No difference in overall survival was shown between the tumors associated with a high expression (n=4 750) and low VRK3 expression (n=4 746) (log rank test, p=0,029). The 95% confidence intervals are shown with dotted line.

d- Overall survival in GBM and LGG tumors according to *VRK3* expression level.

Kaplan–Meier survival curves of patients with a GBM (n=81) or LGG (257) from TCGA and GTEx datasets stratified in two subgroups according to *VRK3* expression level in TCGA and GTEx RNAse datasets(26). The samples were divided in high and low *VRK3* by using the median of the distribution of tpm values. The overall survival is better for tumor associated with a high expression of *VRK3* than those with low expression level (log rank test, p=1.3e-12). The 95% confidence intervals are shown with dotted line.

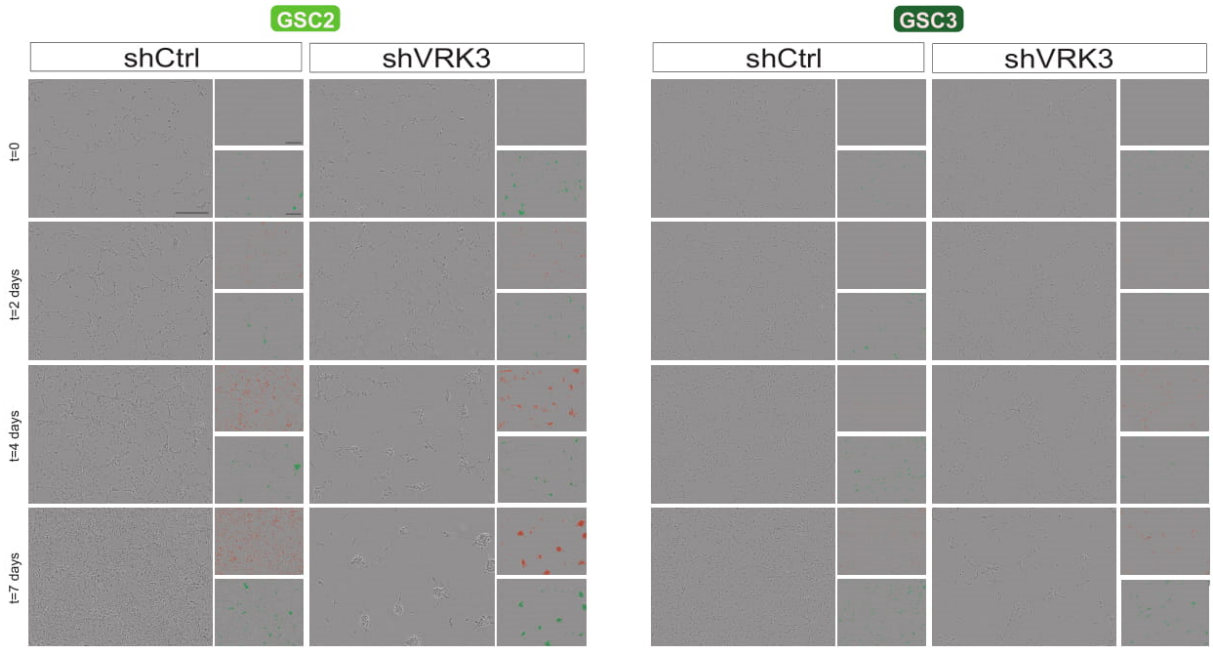
GSC2
shCtrl
shVRK3
t=0
t=2 days
t=4 days
t=7 days
GSC3
shCtrl
shVRK3

Figure S4

Morphological changes and induction of cell death during the 7 days after *VRK3* inhibition

Contrast phase images of H3.3-K27M GSC2 cells and H3.1-K27M GSC3 cells after transduction with either shCtrl-1 or shVRK3-1 are presented at distinct timepoints after transduction. For each condition merged images of phase-contrast and mKate2 fluorescence signal (red) after segmentation by the Incucyte software are presented on the top-right side and merged images of phase-contrast and Yoyo-1 fluorescent signal (green) detected after segmentation are presented on the bottom-right. Scale bars represent 300 µm.

Supplemental information

Supplemental Table I: shRNA sequences shVRK3-1 to 4 & shCtrl-1 and -2

shRNA name	Sigma Aldrich reference	Sequence from 5' to 3'
shVRK3-1	TRCN0000010236	GACAACCAGGGCATTCTCTATCTCGAGATAGAGAATGCCCTGGTTGTCTTTTT
shVRK3-2	TRCN0000010563	ACTCAGGACCACAGAAGCAAACTCGAGTTTGCTTCTGTGGTCCTGAGTTTTTT
shVRK3-3	TRCN0000199854	GCCACTGGTTTCAGGATACTCCTCGAGGAGTATCCTGAAACCAGTGGCTTTTTTG
shVRK3-4	TRCN0000010235	GTATCCAAGCGGCATTCAAATCTCGAGATTTGAATGCCGCTTGGATACTTTTT
shCtrl-1		CCTAAGGTTAAGTCGCCCTCGCTCGAGCGAGGGCGACTTAACCTTAGG
shCtrl-2		CCGGCAACAAGATGAAGAGCACCAACTCGAGTTGGTGCTCTTCATCTTGTTGTTTTT

Supplemental Table II: Antibody list

Antibody	Dilution	Reference	Provider
anti-VRK3	1:1000	#HPA056489	Sigma-Aldrich
Anti-ß-actin	1:5000	#5125	Cell Signaling Technology
goat anti-rabbit IgG, HRP-linked	1:2000	#7074	Cell Signaling Technology
horse anti-mouse IgG, HRP-linked Antibody	1:2000	#7076	Cell Signaling Technology

ARTICLE II. Molecular determinants of response to radiotherapy in DIPG: a clinical and *in vitro* study

As mentioned beforehand, radiation therapy remain the mainstay of treatment of DIPG patients even if it is only transiently effective, delaying tumour progression with a systematically fatal relapse few months after treatment. Our group reported previously a differential response to radiotherapy at diagnosis in DIPG patients depending on the histone H3 mutational status. In this project we decided to better understand H3.1-K27M and H3.3-K27M radioresistance by evaluating the radiosensitivity *in vitro* of our GSC models (n=13) and by assessing the relevance of the identified molecular determinant(s) into the clinics.

We were able to confirm the heterogeneous GSCs response to RT *in vitro* correlating with the duration of the clinical response in the corresponding patients. Contrarily of our initial hypothesis, it appears that the main driver of DIPG radioresistance is the inactivation of TP53, and not the type of mutated histone *per se*. Patients harbouring a TP53 mutation show an earlier relapse and worse prognosis. Moreover, we observe an increase of the *in vitro* radioresistance of TP53-WT GSC after TP53 knock-down. The comparison of tumour molecular data with clinical responses to RT allowed us to consolidate our *in vitro* prediction and propose new possible stratifications in DIPG with respect to response to therapy according to the *TP53* status. Moreover, beyond TP53 alterations, we want to better understand the DIPG radioresistancy and identify new potential target. This can be address without any *a priori* by the use of RNAi and indeed, it was the strategy we chose to access radiosensitivity in our DIPG models.

TP53 pathway alteration is a major driver of radioresistance in Diffuse Intrinsic Pontine Gliomas (DIPG)

Werbrouck, C[1]; Evangelista, CCS[1]; Lobón, MJ[1]; Barret, E[1]; Brusini R[1]; Kergrohen T[1]; Bolle, S[2]; Beccaria, K[3]; Puget, S[3]; Grill, J[1,4]; Debily MA[1,5] & Castel, D[1,4]

1 UMR8203, “Vectorologie & Thérapeutiques Anticancéreuses”, CNRS, Gustave Roussy, Univ. Paris-Sud, Université Paris-Saclay, Villejuif, France

2 Département de Radiothérapie, Gustave Roussy, Univ. Paris-Sud, Université Paris-Saclay, Villejuif, France

3 Department of Pediatric Neurosurgery, Hôpital Necker-Enfants Malades, Université Paris V Descartes, Sorbonne Paris Cité, Paris, France

4 Département de Cancérologie de l’Enfant et de l’Adolescent, Gustave Roussy, Univ. Paris-Sud, Université Paris-Saclay, Villejuif, France

5 Université d'Evry-Val d'Essonne, Boulevard François Mitterrand, Evry, France

Abstract

Purpose:

DIPG are the most severe pediatric brain tumours with a median survival below one year. Radiotherapy is the mainstay of their treatment. When a response is observed, it is only transient. The goal of the study was to identify the underlying molecular determinants of response to radiotherapy in DIPG.

Experimental Design:

We conducted an *in vitro* study to assess the radioresistance of 13 DIPG glioma stem cells (GSCs) cultures. These models derived from stereotactic biopsy performed at diagnosis harbour the different mutations reflecting the variability encountered in patients. Response to radiotherapy of an extended cohort of 78 DIPG was correlated with their genotype.

Results:

The range of lethal dose 50 of the GSCs *in vitro* varied from 0.5 to 7 Gy and was linked to time to progression after radiotherapy in the corresponding patients. *TP53* mutation was identified as the main driver of an increased radioresistance. This finding was further validated by comparing 4 isogenic pairs of $TP53^{WT}$ and $TP53^{KD}$ DIPG cells, confirming the pivotal role of *TP53* inactivation in inducing DIPG radioresistance irrespective of the type of canonical or variant histone H3 mutated. Finally, in an integrated clinical, radiological and molecular study, we show that $TP53^{MUT}$ DIPG patients respond less to radiotherapy, relapse earlier after radiotherapy and have a worse prognosis than their $TP53^{WT}$ counterparts.

Conclusion:

Here we illustrate that *TP53* mutations are driving radioresistance of DIPG in

patients and in their corresponding GSCs. This finding could be important to define more tailored irradiation regimen in these patients.

Translational Relevance

Diffuse intrinsic pontine gliomas are the most severe and common form of malignant brain tumours in children and adolescents. Radiotherapy is the only proven efficient treatment, albeit only bringing a transient response followed by a constant subsequent progression within months. Our study identifies the inactivation of *TP53* as the main driver of resistance to radiation in DIPG glioma stem cells. We also show that patients with *TP53* mutant tumors do not respond to radiotherapy to the same extent than those with *TP53* wild-type tumors both in terms of magnitude and duration, accordingly their survival is worse. These results could be used to tailor radiotherapy schedules (including re-irradiation) in DIPG patients depending on their *TP53* status. Moreover, restoring TP53 functions or downstream pathways could prove to be possible ways to mitigate radioresistance in DIPG.

Introduction

Brain tumours represent the first cause of death from cancer in children, adolescent and young adults. High-grade gliomas are both the most frequent and aggressive malignant brain tumours. DIPG is the most severe form of high-grade glioma and has been recently associated with other diffuse midline gliomas sharing the same driving mutation transforming the Lysine 27 of the regulatory tail of histone H3 into a Methionine (1). DIPG are not operable due to their deep-seated location in a sensible area of the brainstem as well as their infiltrative nature which precludes any surgical attempt.

Since the discovery of the effect of radiation therapy on brainstem tumors(2), this therapeutic modality has remained the only validated treatment for DIPG. It consists of 3D conformal photon-based radiotherapy to a range of 54–59.4Gy given in 30–33 fractions of 1.8Gy daily(3). Changes in fractionation (hyperfractionation or hypofractionation), cumulative dose (up to 72 Gy) as well as the use of various radiosensitizers have failed to improve its effects in patients(4). No progress has been made since then despite the concomitant and adjuvant use of various drugs and radiosensitizing agents in more than 200 trials (5). Prognosis has not significantly changed in the last 50 years and most children affected with this disease will die during the first two years after diagnosis(6). Resistance to standard chemotherapy has been well demonstrated *in vitro* in DIPG cells derived from both diagnosis and autopsy samples(7,8). The K27M somatic mutation described in DIPG occurs in *H3F3A*, encoding the histone variant H3.3, or *HIST1H3B/C* and more rarely *HIST2H3A/C*, encoding canonical histones H3.1 and H3.2, respectively (9–11). Earlier work from our group has suggested that response to radiotherapy,

albeit transient, was not uniform and could be associated with the type of histone H3 harbouring the K27M mutation(11,12) but resistance to radiation has not been explained so far. It seems therefore clinically important to explore resistance to radiotherapy in DIPG and its determinants in order to enable the development of efficient therapeutic combinations with irradiation.

We thus hypothesized the existence of molecular determinants of the response to radiation, including histones H3 mutations in but also alterations in other genes. Indeed, analysis of DIPG mutational landscape by NGS has shown additional recurrent genetic changes such as *PDGFRA* amplification(13), mutations in *ACVR1*, *TP53* and component of the PI3K/mTOR pathway(14–18). Cosegregations of *ACVR1* mutation with H3.1-K27M on one hand and *TP53* alteration with H3.1-K27M on another hand were also reported(15).

First, we used a variety of cellular models of DIPG derived from stereotactic biopsies at diagnosis (*i.e.* treatment naive) to evaluate their radiosensitivity according to their molecular profile. Then we extended our preclinical findings on patient's response by correlating their clinical, radiation response and survival with genomic data.

Material & methods

Clinical samples

Clinical samples were extracted from three retrospective cohort characterized and published previously (11,14,15) provided sufficient material was available to complete genotyping by targeted-sequencing of tumor DNA for the tumors that were not evaluated by NGS. Seventy-eight patients with DIPG were enrolled: 50 H3.3-K27M, 22 H3.1-K27M and 6 wild-type tumors. Only patients presenting histone H3-K27M mutated tumors were included in the analyses.

Genotyping and targeted DNA sequencing

Targeted sequencing was performed by the biology and Medical Pathology platform of Gustave Roussy. Libraries were generated using the Ion AmpliSeq Library kit 2.0, according to the manufacturer's instructions (Life Technologies). The custom designed ampliseq primer pools (Life Technologies) used for library amplification covered 100% of *PPM1D and* 99.8% of *TP53* coding sequences, as well as hotspot loci in *ACVR1, HISTH3A-J, H3F3A, H3F3B, H3F3C and HIS2H3A-D*. The sequencing was performed on an Ion-PGM System (Life technologies) and data were analyzed with the Torrent Suite Variant Caller software and annotated using the reference genome hg19 (GRCh37). All variants were visualized on bam-file using Alamut Visual version 2.9 (Interactive Biosoftware, Rouen, France). An average of 7535× coverage depth was obtained in the different samples.

Cells and culture

GSC (Glioma Stem-like Cells) derived from stereotactic biopsies at diagnosis

performed in Necker-Enfants Malades Hospital (Paris, France) as previously described by Plessier *et al.(19)*. Briefly, after tumour dissociation GSC were cultured as an adherent monolayer on laminin-coated flask (Gibco) in serum-free human neural stem cell culture medium StemPro™ NSC SFM (Thermo) supplemented with PDGF-AA and PDGF-BB (10 ng/ml, Miltenyi Biotec). hNSC1 were cultured from human prenatal whole brain crude extract of commercial origin (Applied Stem Cells, ASE-5001). hNSC2 & hNSC3 were derived from human embryo of Carnegie stage(O'Rahilly et al. 1987) 18 and 22 obtained following voluntary abortions. Tissue collection and use were performed according to the guidelines and with the approval of the French National Ethic Committee (authorization N° PFS10_011). All samples were obtained with the written informed consents of subjects according to Helsinki declaration. Embryonic neural tissues were excised using microsurgery instruments and a dissecting microscope, in PBS containing 100 U/ml penicillin and 100 mg/ml streptomycin (Invitrogen). Tissue was mechanically dissociated by pipetting into serum-free medium. For all three NSC, the single-cell suspension was amplified as neurospheres for one passage, and then transferred in laminin-coated flask to be further cultured as an adherent monolayer in the same medium as for DIPG cells, but without addition of PDGF.

HEK293T and HCT116 cell lines were cultured in DMEM (Gibco) supplemented with 10% fetal bovine serum (Sigma) and 100 U/ml penicillin and 100 µg/ml streptomycin. All cells were maintained in a humidified incubator (37°C, 5% CO_2). Cells were irradiated at indicated doses (320 kV, 4 mA, 1.03Gy/min) with X-ray ionizing radiation in an X-RAD 320 Biological Irradiator (Precision X-Ray Inc.).

Determination of cell survival post-irradiation *in vitro*

GSC or hNSC cells were plated between 10,000 and 30,000 cells/cm^2 in 96-well

plates, irradiated one day after and growth was monitored daily by videomicroscopy at 10X objective (Incucyte® ZOOM, Essen bioscience). Half of the medium was renewed every 3-4 days. Cell survival after irradiation was calculated as described by Buch *et al.*, using growth curves of cells with or without irradiation acquired by videomicroscopy. The surviving fraction for each dose was calculated based on the delay required by irradiated cells to reach a specific confluency compared to non-irradiated cells by taking into account the specific doubling time of each cell lines (Figure 1A)(21). Lethal Dose 50% (LD50) were then computed by analysing replicates experiment that included several radiation doses.

Lentiviral shRNA cloning

Two shRNAs targeting *TP53,* shTP53-1 (TRCN0000003755) and shTP53-2 (TRCN0000003756), were cloned in a pLKO.1 lentiviral vector (Supplementary Table S1). The forward and reverse oligos (Eurofins) were annealed and cloned according to the Broad Institute shRNA cloning protocol (GPP Web Portal N0000003755).

As negative controls, two non-targeting shRNAs were used: shCTL-1, a negative control vector containing a non-hairpin insert (Addgene plasmid #10879) and shCTL-2, a non-mammalian targeting shRNA Control Plasmid DNA (SHC002, Sigma-Aldrich) containing a sequence that should not target any known mammalian genes, but leading to the expression of a small hairpin RNA recognized by the RNA-induced silencing complex (RISC). In the plasmid, the puromycin resistance gene downstream the human PGK promoter was replaced by the NLS-tagged fluorescent protein mTagGFP amplified by PCR with primers flanked by BamHI and KpnI restriction sites.

Lentiviral production and transduction

Lentiviral particles were produced in HEK293T cells using psPax2 and pMD2.g second-generation packaging plasmids (Addgene plasmids #12260 and #12259) transfected using jetPRIME® transfection reagent (Polyplus transfection). Culture medium was collected after 48h and ultracentrifuged, and concentrated virus was aliquoted and store at -80°C. Lentiviral titers (transduction units per mL) were determined by fluorescence tittering assay (22), and GSC were transduced for 4 hours with concentrated virus at a multiplicity of infection of 0.3 and mTagGFP-positive cells were sorted by sorted by FACS several days after.

Protein extraction and immunoblotting

Protein extractions were performed as described previously(23). Protein extracts were separated by electrophoresis on a 4–20% precast polyacrylamide gel (#456-1093, Biorad) and transferred to PVDF membrane (#1704157, Biorad), following the manufacturer's instructions (Trans-Blot Turbo system, Bio-Rad). Membranes were blocked and antibodies were diluted in TBS 1X (#170-6435, Biorad), 5% (w/v) BSA (Euromedex), 0,1% (w/v) Tween20 (Sigma). Protein detection was performed using the following antibodies: TP53 (#sc-126; Santa Cruz, 4°C overnight, 1/500) and Cyclophilin A as loading control (#HCA005, Biorad, 4°C overnight, 1/1000). Primary antibodies were detected by HRP-linked anti-mouse secondary antibody hybridized one hour at room temperature (#7076, Cell Signalling, 1/5000). The signals enhanced by chemiluminescence reagent (#34095, Thermo Scientific) were imaged and analysed with a ChemiDoc MP Imaging System (Bio-Rad) with ImageLab 4.1 software.

Clinical analysis

Retrospective analysis of medical and imaging record of 78 DIPG patients followed at Gustave Roussy with genotyping of *H3F3A*, *HIST1H3B/C*, *TP53* and PPM1D. We have centrally reviewed age, signs, and symptoms at diagnosis, MRI scans, treatment, response and evolution over time.

Clinical response to radiotherapy was defined as improvement in case of disappearance of two or more main diagnostic clinical symptoms leading to a general clinical improvement lasting more than 2 months concurrent with steroids weaning. Clinical response was defined as stabilization in case of lack of positive clinical response and absence of new symptoms. Clinical response was defined as worse in case of the appearance of new symptoms or significant increase of the severity of an existing symptom. Radiological response was evaluated on MRI scans which were performed within 6 weeks after radiotherapy end compared to pre-radiotherapy MRI scans. We considered as positive radiological response when the tumour volume shrinks larger than 30% and as stabilization in case of volume changes inferior to 30% without appearance of new lesions. Progression was defined as tumour growth evidenced on two successive images. Pseudoprogression was set as radiological findings suspicious of tumour progression with a new or enlarging area of contrast agent enhancement which decreased or stabilized without a change in anti-cancer therapy. When these radiological changes were symptomatic, clinical improvement was necessary to take this event into account as pseudoprogression. The time to progression 1 (TTP1) was defined as the time from radiotherapy start to first progression. Overall survival (OS) was determined as the time from diagnosis to death. Finally, OS and TTP1 calculations were based on imaging dates of diagnosis and progression, respectively.

Statistical analysis

Distribution analyses between groups in the case of TTP1 values were performed using the Mann-Whitney non-parametric test. To analyze the correlation between TTP1 & LD50 obtained *in vitro* a ranked based Spearman nonparametric correlation was used. Proportions comparisons were performed using a Chi-squared proportion test except for analysis presenting head-counts below 5 were a Fisher exact test was used. All statistical analyses were performed using PRISM software v7 (GraphPad), and minimum threshold for significance was considered for p-value<0.05.

Survival curves comparisons (univariate analysis)

Survival functions were estimated with the Kaplan-Meier method and all survival function estimate comparisons were performed using a log-rank test in PRISM software v7.

Multivariate survival analysis

The multivariate survival analysis was conducted on 78 patients. First a set of covariates corresponding to the age at diagnosis, sex, Histone H3, *TP53, ACVR1* and *PPM1D* mutational status), was tested using a univariate Cox model. Only significant variables were kept for the multivariate Cox model analysis. All calculations were performed using the R ‘survival’ package.

Results

Distribution of DIPG stem cells radiosensitivity *in vitro*

In order to decipher the underlying molecular basis of the variable clinical response of DIPG patients to RT, we assessed the cellular consequences of radiation *in vitro* using DIPG cellular models deriving from primary tumors at diagnosis (19). However, these glioma stem-like cells (GSCs) did not allow for classical clonogenic assays commonly used to evaluate radiosensitivity. Indeed, GSCs presented a high motility when cultured in adherent condition on laminin coated flask, or presented highly heterogeneous and most often poor survival in semi-solid culture as single cells in collagen gels, matrigel or methylcellulose (*data not showed*). We thus decided to follow the proliferation of GSCs treated or not with radiation over 3 weeks by videomicroscopy, in order to mathematically infer the surviving fractions of irradiated cells from the growth curves (Supplemental FigS1). Indeed, this alternative assay was previously shown to provide comparable information to clonogenic studies in several cell lines(21) (Fig.1A). Irradiation of a H3.1-K27M GSC culture (GSC5) with doses ranging from 0.25 to 4 Gy induced a dose-dependent latency in cell growth kinetics (Fig.1B). In contrast, H3.3-K27M GSC8 showed very mild alteration of its growth for such doses, requiring 6-8 Gy to observe a significant decrease of the relative confluence (Fig.1C). These experiments were repeated 4 times and led to similar results allowing to calculate surviving fractions at each dose for the all cellular models, two representative GSCs being represented in Fig.1D. The lethal-dose 50 (LD50) was then defined on these survival fraction curves, *i.e.* 0.7 and 5.95 Gy for GSC5 and GSC8, respectively.

The heterogeneous radioresistance of *in vitro* avatars correlates with the duration of patient clinical response to initial RT

We extended our analysis to a total of 13 GSCs with K27M mutations in either H3.1 and H3.2 canonical histone H3 or in the H3.3 variant, and confirmed the wide spectrum of response to radiation in the cells with LD50 ranging from 0.5 to 7.4 Gy. We then compared the cellular response to IR *in vitro* to the duration of the clinical response after the first RT observed in the patients of origin of these models. We plotted GSCs LD50 *in vitro* v*ersus* the time to first progression post-RT (TTP1) in patients and evidenced a significant negative correlation between these two parameters. DIPG patients presenting a longer clinical response led to GSCs models with lower LD50, confirming the relevance of our *in vitro* results of radiosensitivity (Fig. 1E; Spearman correlation coefficient -0.71, p-value=0.0086). Strikingly, in this extended dataset we could not define two groups of radiosensitive H3.1/2-mutated GSCs *vs.* more radioresistant H3.3-mutated GSCs. Eighty-five percent of the models had LD50 below 2 or above 6, with only two GSCs presenting an intermediate radiosensitivity, the H3.2-K27M cellular model and one H3.3-K27M (GSC12). Indeed, even if 4 of the 5 H3.1-mutated cells were associated with LD50 around or below 2 Gy, the last one presented the highest LD50 (7.4 Gy)(Fig2A). Similarly, H3.3-mutated cells spanned highly variable LD50. Consequently, the radiosensitivity could not be explained by their histone H3 genotype.

Analysis of secondary driver mutations in GSCs identifies *TP53* alteration as a molecular determinant of radioresistance in DIPG

In order to identify the molecular origin to the difference of radioresistance in these patient-derived cellular models, we profiled the most common recurrent mutations

found in DIPG: *AVCR1*, *TP53*, *PPM1D* or in the *PI3K/AKT/MTOR* pathway. Our selected panel of DIPG cellular models contained the canonical H3.1-K27M & *ACVR1* or H3.3-K27M & *TP53* mutated samples (n=3 and n=4, respectively; Fig. 2A). It was also enriched for less frequent genotypes with H3.3-K27M & $TP53^{WT}$ samples or GSCs mutated in *PPM1D,* and even rarer genotypes such as H3.1/2-K27M & $TP53^{MUT}$ (Fig. 2A). Alterations in the *PI3K/AKT/MTOR* pathway were found in 4/5 H3.1-K27M and 3/7 H3.3-K27M mutated samples and included mutations of *PIK3CA*, *PIK3R1* and *AKT3*.

As GSCs appeared to separate mainly into two main groups according to their LD50, we confronted the sensitivity to radiation with their mutational landscape. All DIPG cells with a low LD50 were $TP53^{WT}$, and conversely all *TP53*-mutated belonged to the radioresistant subgroup, with significantly different LD50 of 1.1 Gy ±0.5 and 5.5 Gy ±1.7, respectively (Fig. 2B; *p*-value=0.0012, Mann-Whitney test). Despite some heterogeneity in the LD50, no other genetic alteration aside from *TP53*-mutation seemed to correlate with LD50 values or to drive an increase in radioresistance.

Three human neural stem cells (hNSC) control cultures were also included in analysis. Their average LD50, *i.e.* 0.58 Gy ±0.22, was close to $TP53^{WT}$ GSCs ones , whereas *TP53*-mutant cells proved to be more resistant to radiations (p-value=0.024, Mann-Whitney test) (Fig.2B). With respect to *PPM1D* mutant GSCs, their radiosensitivity was slightly higher than the ones of NSCs and $TP53^{WT}$ GSCs (Fig.2A)

In vitro radioresistance is increased in $TP53^{WT}$ DIPG cells following *TP53* knock-down

In order to specifically evaluate the influence of the TP53-pathway inactivation on DIPG cellular response to radiation, we next though of measuring LD50 in isogenic

cells with induced inactivation of *TP53*. For this, we transduced 2 H3.1-K27M and 2 H3.3-K27M GSCs associated with low LD50 with lentiviral constructs encoding two independent shRNAs targeting *TP53* transcripts, or negative control shRNAs. As expected, TP53 protein level increased following a 4 Gy irradiation in both non-transduced and cells transduced with control shRNA even if some heterogeneity existed among the cellular models (Fig. 3A-B). Cells irradiated or not both showed decreased TP53 levels following *TP53*-shRNAs introduction and this was even more sticking post-IR. Next, the response to IR of these cells was analysed as previously, and all 4 GSCs tested exhibited a significantly increased LD50 after *TP53*-KD (Fig. 3C). Interestingly, this increase was overall higher in all shTP53-2 transduced cells in accordance with the more efficient repression of TP53, excepted for GSC6 which also displayed the most important variation among replicates in LD50 evaluation (Fig. 3B-C).Similar results were after TP53 inhibition in either $TP53^{WT}$ & $PPM1D^{WT}$ (GSC4&5) and $TP53^{WT}$ & $PPM1D^{MUT}$ models (GSC6). The comparison of LD50 in isogenic $TP53^{WT}$ and *TP53*-KD cells thus confirmed the pivotal role of *TP53* in inducing DIPG radioresistance whichever the histone H3 mutated.

Patients with a $TP53^{MUT}$ DIPG show earlier relapse post-RT and overall worse prognosis

Given the central role identified for *TP53* mutation in DIPG *in vitro*, we analysed clinical response to RT in a well annotated retrospective cohort of DIPG patients. We sequenced histone *H3*, *TP53*, *ACVR1* and *PPM1D* genes in 79 patients with full clinical record. Depending on the genes probed, we obtained successful genotyping results ranging from 68 (86%) for *ACVR1* to 78 (99%) cases for *HIST1H3B*.

As measure of RT efficiency, and thus response to radiation, we first analysed the

time to first progression after treatment (TTP1) in patients and found significant differences according to the *TP53* status, 9.1 months versus 5.8 months for $TP53^{WT}$ and $TP53^{MUT}$ (Fig. 4A; *p*-value=0.0003, Mann-Whitney test). Accordingly, $TP53^{MUT}$ patients showed a worse prognosis with a median OS of 9 months *vs.* 14 months for $TP53^{WT}$ (Fig. 4B, *p*-value=0.0003, log-rank test). We next performed univariate analyses with the following variables: histone H3, *TP53*, *ACVR1* and *PPM1D* mutation status, as well as the age and sex of patients. Both the histone H3, *ACVR1* and *TP53* alterations were significant predictor of the survival, of which only *TP53* mutational status remained significant in a multivariate analysis (Table 1; p-value=0.0139).

Discussion

Response to radiotherapy in DIPG is not uniform albeit unequivocally only transient (9). In this work, we demonstrate that it can be associated with the heterogenous mutational landscape of human disease and specifically to the presence of *TP53* mutations. Despite their high frequency in DIPG, around 42%, mutations in *TP53* are not initiating the disease in DIPG(15). Patients harboring germ-line *TP53* mutations (Li-Fraumeni Syndrome) rather develop H3-K27 WT tumors and rarely in the brainstem(24). The panel of 13 GSCs was selected to cover most combinations of the principal alterations encountered in DIPG at diagnosis including rare $TP53^{MUT}$ H3.1/2-K27M associations, without reflecting their relative frequencies in the DIPG population. This allowed us to assess *in vitro* DIPG radioresistance and screen for the contribution of the distinct genomic alterations. As a pre-requisite to our explanatory approach, we correlated LD50 in GSCs to TTP1 in patients and showed that the heterogeneous response to RT observed in DIPG patients seems mostly defined by a cell-autonomous response to radiation that can be evaluated *in vitro*. We demonstrated through a molecular analysis that the main driver of resistance to radiation in DIPG cells seems to be the inactivation of *TP53* function in H3.3- and H3.1-mutated cells as well. Additionally, our *in vitro* data are corroborated by a clinical retrospective analysis showing that *TP53*-mutated DIPG patients present a shorter response post-RT and a worse prognosis. Conversely, the histone H3.3-K27M mutation was associated with a worse prognosis in a previous study(11), but it seemed to impact neither radioresistance *in vitro*, nor overall survival in our multivariate analysis when *TP53* mutations are taken into account. The discrepancy between these two studies likely results from a confounding effect as the majority of

H3.3-K27M samples are also *TP53*^{MUT} whereas H3.1-K27M samples rarely are(25). Anyway, only a slight difference in term of radiosensitivity was observed between NSC and H3-K27M/*TP53*^{WT} tumors suggesting that most of the causes of radioresistance in DIPG could be caused by TP53 dysfunction. Our study confirms that mutations in TP53 identify DIPG patients with worse prognosis. This is in line with our previous report which showed that patients with LOH at *TP53* locus identified by CGH-Array of the tumor had a worse outcome with a median survival of 7 months *versus* 12 months (13), recently confirmed by a meta-analysis of K27M-mutated gliomas(26). This worse prognosis can now be linked to the poor response to radiotherapy.

PPM1D truncating mutations causing the loss of its regulatory domain were reported to negatively regulate TP53 activity through increased phosphatase activity at Ser15 of p53(27,28). Unexpectedly, the two *PPM1D*^{MUT} GSCs we tested did not show elevated LD50 for irradiation *in vitro*. Accordingly, mutations in this gene were not predictive of a bad prognosis in the univariate survival analysis of the patients. Moreover, the increase in LD50 following *TP53* inhibition was similar in *PPM1D*^{MUT}/*TP53*^{WT} and *PPM1D*^{WT}/*TP53*^{WT} GSCs. Phosphorylation at Ser15 by PPM1D is stimulating transactivation of TP53 responsive promoters(29) but since the transactivating role of T53 is not its only mechanism of action, it cannot be expected to phenocopy the consequences of TP53 mutations or loss.

Similarly, GSC activation mutations in the *PI3K/AKT/MTOR* pathway did not overtly impact radioresistance *in vitro* whereas mTOR inhibitors were shown to radiosensitize DIPG cells(30). In a recent study, *PI3K/AKT/MTOR* activation assessed through *PTEN* loss of expression however appeared as a common feature in DIPG, not restricted to tumors with mutations in components in the pathway(31).

One can therefore consider that the benefic effect of mTOR inhibitors could be independent of genomic alteration of component of *PI3K/AKT/MTOR* pathway.

The correlation of *in vitro* evaluation of radioresistance and clinical response to IR indicated that *in vitro* GSC mirror the bulk of tumor cells *in vivo*. It confirmed the relevance of using stem-like model of DIPG to study the disease *in vitro*, in accordance with recent results from Filbin *and coll.* showing that most DIPG cells *in vivo* display a stem-like profile(32).

In conclusion, we showed that *TP53* mutations status is a biomarker to predict radioresistance in DIPG patients and that TP53 mutations explain most of the differences in radiosensitivity between DIPG GSCs and NSCs. We suggest that these mutations should be taken into account when radiotherapy plans, especially with re-irradiation, are considered. Downstream and eventually beyond TP53 dysfunction, the underlying mechanisms of DIPG radioresistance needs further studies that could eventually offer new opportunities to revert this phenotype in DIPG cells.

Acknowledgments

DC, JG and MAD acknowledge financial support from Société Française de Lutte contre les Cancers et les leucémies de l'Enfant, Fédérations Enfants & Santé, INCa (Grant PLBIO-14-253) and charites The DIPG Collaborative, and L'Etoile de Martin. CW was supported by a fellowship from "Course of Excellence in Oncology – Fondation Philanthropia" and CSE by a fellowship from National Council for Scientific and Technological Development (CNPq)/ Program "Science without borders" in Brasil.

The authors are grateful to the Necker hospital tumor and DNA banks and the Necker operating room nurses/assistants for their technical assistance, to L. Lacroix and P. Saulnier from the Translational Research Platform of Gustave Roussy, Y. Lecluse and P. Rameau from the PFIC core cytometric platform of Gustave Roussy.

Conflict of Interest

The authors declare no conflict of interest.

References

1. Louis DN, Perry A, Reifenberger G, von Deimling A, Figarella-Branger D, Cavenee WK, et al. The 2016 World Health Organization Classification of Tumors of the Central Nervous System: a summary. Acta Neuropathol. 2016;131:803–20.

2. Coutel Y. [Infiltrating glioblastoma of the brain stem in an 8-year-old child; normalization of the pneumoencephalogram after radiotherapy]. Rev Otoneuroophtalmol. 1959;31:119–23.

3. Cohen KJ, Jabado N, Grill J. Diffuse intrinsic pontine gliomas-current management and new biologic insights. Is there a glimmer of hope? Neuro-oncology. 2017;

4. Warren KE. Diffuse intrinsic pontine glioma: poised for progress. Front Oncol [Internet]. 2012 [cited 2016 Feb 17];2. Available from: http://www.ncbi.nlm.nih.gov/pmc/articles/PMC3531714/

5. Hargrave D, Bartels U, Bouffet E. Diffuse brainstem glioma in children: critical review of clinical trials. The Lancet Oncology. 2006;7:241–8.

6. Warren KE, Killian K, Suuriniemi M, Wang Y, Quezado M, Meltzer PS. Genomic aberrations in pediatric diffuse intrinsic pontine gliomas. Neuro Oncol. 2012;14:326–32.

7. Veringa SJE, Biesmans D, van Vuurden DG, Jansen MHA, Wedekind LE, Horsman I, et al. In vitro drug response and efflux transporters associated with drug resistance in pediatric high grade glioma and diffuse intrinsic pontine glioma. PLoS ONE. 2013;8:e61512.

8. Grasso CS, Tang Y, Truffaux N, Berlow NE, Liu L, Debily M-A, et al. Functionally defined therapeutic targets in diffuse intrinsic pontine glioma. Nat Med.

2015;21:555–9.

9. Wu G, Broniscer A, McEachron TA, Lu C, Paugh BS, Becksfort J, et al. Somatic histone H3 alterations in pediatric diffuse intrinsic pontine gliomas and non-brainstem glioblastomas. Nat Genet. 2012;44:251–3.

10. Schwartzentruber J, Korshunov A, Liu X-Y, Jones DTW, Pfaff E, Jacob K, et al. Driver mutations in histone H3.3 and chromatin remodelling genes in paediatric glioblastoma. Nature. 2012;482:226–31.

11. Castel D, Philippe C, Calmon R, Le Dret L, Truffaux N, Boddaert N, et al. Histone H3F3A and HIST1H3B K27M mutations define two subgroups of diffuse intrinsic pontine gliomas with different prognosis and phenotypes. Acta Neuropathol. 2015;130:815–27.

12. Castel D, Grill J, Debily M-A. Histone H3 genotyping refines clinico-radiological diagnostic and prognostic criteria in DIPG. Acta Neuropathol. 2016;131:795–6.

13. Puget S, Philippe C, Bax DA, Job B, Varlet P, Junier M-P, et al. Mesenchymal Transition and PDGFRA Amplification/Mutation Are Key Distinct Oncogenic Events in Pediatric Diffuse Intrinsic Pontine Gliomas. PLoS ONE. 2012;7:e30313.

14. Grill J, Puget S, Andreiuolo F, Philippe C, MacConaill L. Critical oncogenic mutations in newly diagnosed pediatric diffuse intrinsic pontine glioma. Pediatric Blood & Cancer. 2012;58:489–91.

15. Taylor KR, Mackay A, Truffaux N, Butterfield YS, Morozova O, Philippe C, et al. Recurrent activating ACVR1 mutations in diffuse intrinsic pontine glioma. Nat Genet. 2014;46:457–61.

16. Fontebasso AM, Papillon-Cavanagh S, Schwartzentruber J, Nikbakht H, Gerges N, Fiset P-O, et al. Recurrent somatic mutations in ACVR1 in pediatric

midline high-grade astrocytoma. Nat Genet. 2014;46:462–6.

17. Wu G, Diaz AK, Paugh BS, Rankin SL, Ju B, Li Y, et al. The genomic landscape of diffuse intrinsic pontine glioma and pediatric non-brainstem high-grade glioma. Nat Genet. 2014;46:444–50.

18. Buczkowicz P, Hoeman C, Rakopoulos P, Pajovic S, Letourneau L, Dzamba M, et al. Genomic analysis of diffuse intrinsic pontine gliomas identifies three molecular subgroups and recurrent activating ACVR1 mutations. Nat Genet. 2014;46:451–6.

19. Plessier A, Le Dret L, Varlet P, Beccaria K, Lacombe J, Mériaux S, et al. New in vivo avatars of diffuse intrinsic pontine gliomas (DIPG) from stereotactic biopsies performed at diagnosis. Oncotarget. 2017;8:52543–59.

20. O'Rahilly R, Müller F, Hutchins GM, Moore GW. Computer ranking of the sequence of appearance of 73 features of the brain and related structures in staged human embryos during the sixth week of development. Am J Anat. 1987;180:69–86.

21. Buch K, Peters T, Nawroth T, Sänger M, Schmidberger H, Langguth P. Determination of cell survival after irradiation via clonogenic assay versus multiple MTT Assay--a comparative study. Radiat Oncol. 2012;7:1.

22. Barde I, Salmon P, Trono D. Production and Titration of Lentiviral Vectors. Current Protocols in Neuroscience [Internet]. John Wiley & Sons, Inc.; 2001 [cited 2015 Jul 23]. Available from: http://onlinelibrary.wiley.com.gate1.inist.fr/doi/10.1002/0471142301.ns0421s53/abstract

23. Truffaux N, Philippe C, Paulsson J, Andreiuolo F, Guerrini-Rousseau L, Cornilleau G, et al. Preclinical evaluation of dasatinib alone and in combination with

cabozantinib for the treatment of diffuse intrinsic pontine glioma. Neuro-oncology. 2015;17:953–64.

24. Gröbner SN, Worst BC, Weischenfeldt J, Buchhalter I, Kleinheinz K, Rudneva VA, et al. The landscape of genomic alterations across childhood cancers. Nature. 2018;555:321–7.

25. Mackay A, Burford A, Carvalho D, Izquierdo E, Fazal-Salom J, Taylor KR, et al. Integrated Molecular Meta-Analysis of 1,000 Pediatric High-Grade and Diffuse Intrinsic Pontine Glioma. Cancer Cell. 2017;32:520-537.e5.

26. Dong C, Yuan Z, Li Q, Wang Y. The clinicopathological and prognostic significance of TP53 alteration in K27M mutated gliomas: an individual-participant data meta-analysis. Neurol Sci. 2018;39:1191–201.

27. Kleiblova P, Shaltiel IA, Benada J, Ševčík J, Pecháčková S, Pohlreich P, et al. Gain-of-function mutations of PPM1D/Wip1 impair the p53-dependent G1 checkpoint. J Cell Biol. 2013;201:511–21.

28. Zhang L, Chen LH, Wan H, Yang R, Wang Z, Feng J, et al. Exome sequencing identifies somatic gain-of-function *PPM1D* mutations in brainstem gliomas. Nature Genetics. 2014;46:726–30.

29. Loughery J, Cox M, Smith LM, Meek DW. Critical role for p53-serine 15 phosphorylation in stimulating transactivation at p53-responsive promoters. Nucleic Acids Res. 2014;42:7666–80.

30. Miyahara H, Yadavilli S, Natsumeda M, Rubens JA, Rodgers L, Kambhampati M, et al. The dual mTOR kinase inhibitor TAK228 inhibits tumorigenicity and enhances radiosensitization in diffuse intrinsic pontine glioma. Cancer Lett. 2017;400:110–6.

31. Varlet P, Debily M-A, Teuff GL, Tauziede-Espariat A, Pages M, Andreiuolo F,

et al. DIPG-20. PRE-RANDOMISATION CENTRAL REVIEW AND REAL-TIME BIOMARKERS SCREENING IN THE MULTICENTRE BIOLOGICAL MEDICINE FOR DIPG ERADICATION (BIOMEDE) TRIAL: LESSONS LEARNT FROM THE FIRST 120 BIOPSIES. Neuro-Oncology. 2018;20:i52–3.

32. Filbin MG, Tirosh I, Hovestadt V, Shaw ML, Escalante LE, Mathewson ND, et al. Developmental and oncogenic programs in H3K27M gliomas dissected by single-cell RNA-seq. Science. 2018;360:331–5.

Tables

Table 1: Univariate and multivariate analysis of survival using a Cox model

Factors	N	Univariate			Multivariate		
		HR	95% CI	*p*	HR	95% CI	*p*
Age at diagnosis	79	1.031	0.9677-1.099	0.345			
Sex	79	0.9052	0.5744-1.427	0.668			
Principal mutations							
H3F3A	77	1.702	1.06-2.732	0.0276 *	0.8907	0.4010-1.979	0.7763
HIST1HB3	78	0.5304	0.3211-0.876	0.0133 *	0.6797	0.2505-1.844	0.4484
TP53	77	2.391	1.475-3.876	0.000403 ***	2.1384	1.1670-3.919	0.0139 *
ACVR1	68	0.5521	0.3196-0.9536	0.0331 *	1.0351	0.4339-2.469	0.9381
PPM1D	71	1.547	0.6957-3.441	0.284			

A

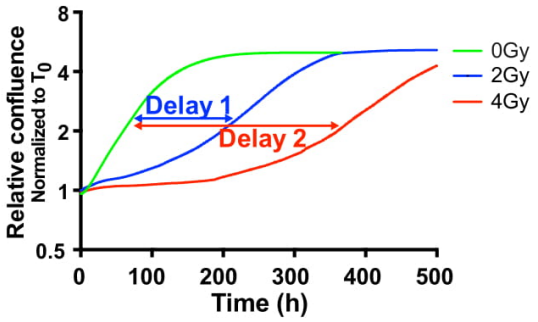

$$Survival = 2^{-\frac{t_{delay}}{t_{doubling\ time}}}$$

B

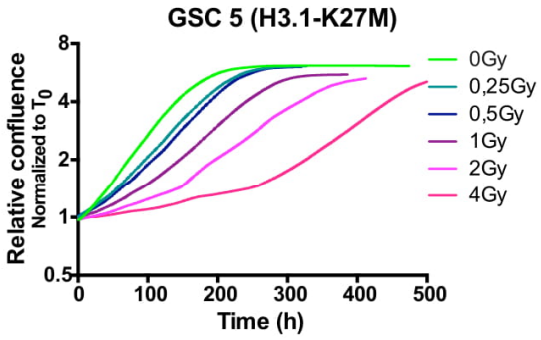

C

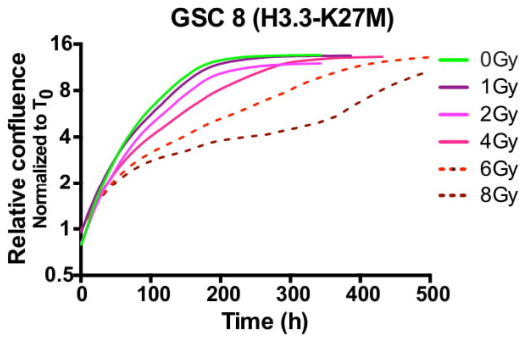

D

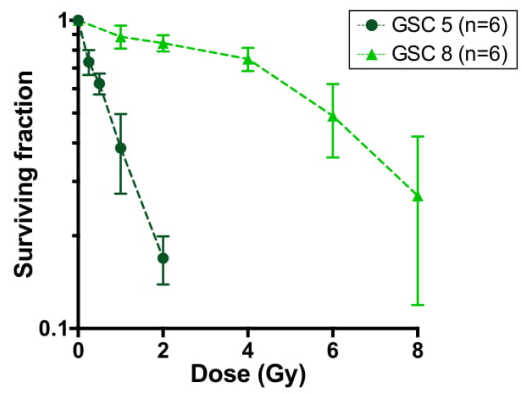

E

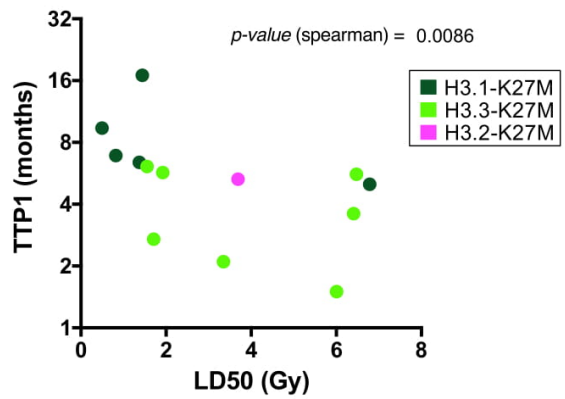

Figure legends

Figure 1. *In vitro* GSC response to radiotherapy correlate with the heterogeneous patient clinical response.

A-B) Proliferation assay post-irradiation was performed on GSC harbouring either H3.1- (GSC5) (**A**), or H3.3-K27M (GSC8) **(B)** alteration. Escalation dose ranging from 0 to 4Gy or from 0 to 8Gy were tested in GSC5 and GSC 8, respectively, and was applied as one unique dose at T=0h. Curves represent the relative confluence mean of four wells. C) Six independent assays were performed and used to compute the survival fraction and determined the radiation dose response Average surviving fractions are represented with standard deviation (SD). **D**) Plot representing time to progression (TTP1, time between the 1st day of radiotherapy and first relapse) in patients according to the *in vitro* LD50 of the corresponding GSC. E) Patients presenting the shorter TTP1 are correlated with a corresponding GSC associated with a high *in vitro* radioresistance (r = -0,7088).

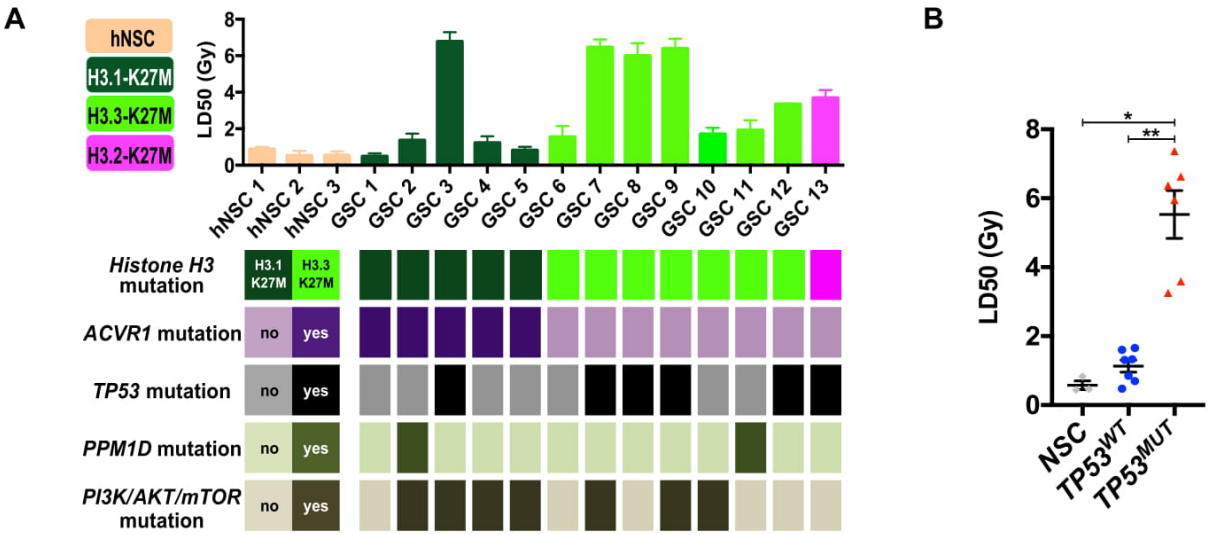
A
hNSC
H3.1-K27M
H3.3-K27M
H3.2-K27M
LD50 (Gy)
0
2
4
6
8
hNSC 1
hNSC 2
hNSC 3
GSC 1
GSC 2
GSC 3
GSC 4
GSC 5
GSC 6
GSC 7
GSC 8
GSC 9
GSC 10
GSC 11
GSC 12
GSC 13
Histone H3 mutation
H3.1 K27M
H3.3 K27M
ACVR1 mutation
no
yes
TP53 mutation
no
yes
PPM1D mutation
no
yes
PI3K/AKT/mTOR mutation
no
yes
B
LD50 (Gy)
0
2
4
6
8
*
**
NSC
TP53WT
TP53MUT

Figure 2. Correlation of the mutational landscape of DIPG cellular models to radiosensitivity.

A) Average LD50 determined *in vitro* from at least 3 independent assays (Error bars indicate SD). B) Genomic alterations of GSC in histone H3, *ACVR1*, *PPM1D*, *TP53* as well as components of the PI3K/AKT/mTOR pathway are indicated.

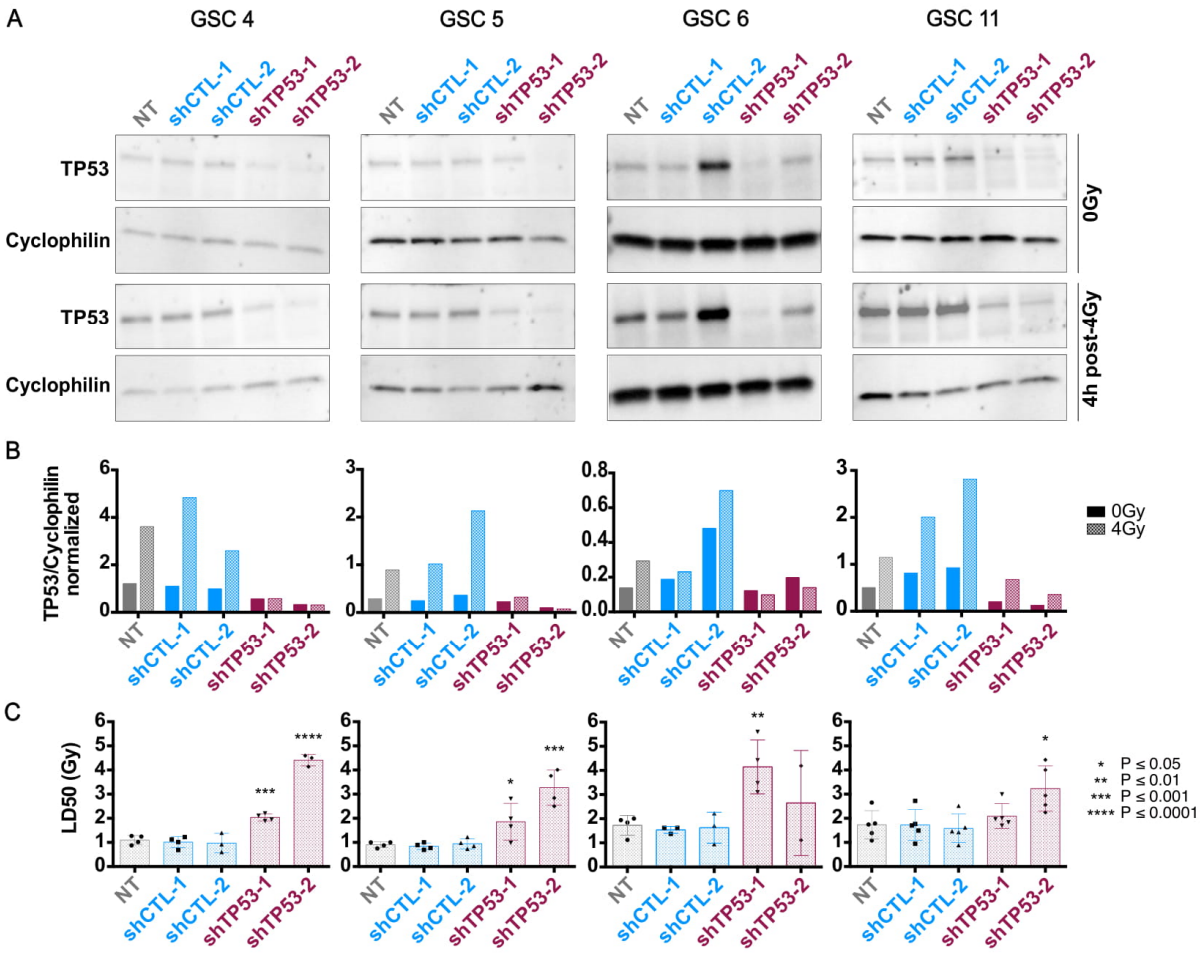
A
GSC 4
GSC 5
GSC 6
GSC 11
NT
shCTL-1
shCTL-2
shTP53-1
shTP53-2
TP53
Cyclophilin
0Gy
4h post-4Gy
B
TP53/Cyclophilin normalized
0Gy
4Gy
C
LD50 (Gy)
* P ≤ 0.05
** P ≤ 0.01
*** P ≤ 0.001
**** P ≤ 0.0001

Figure 3. Increase of *in vitro* radioresistance of TP53-WT GSC after *TP53* knockdown.

(**A**) Western blot analysis of GSC transduced with shRNA targeting *TP53* (shTP53-1, shTP53-2) or negative control shRNA (shCTL-1, shCTL-2) or non-transduced (NT) without or 4h after a 4Gy irradiation. Relative TP53 protein levels standardized by Cyclophilin as loading control. (**B**) Densimetric quantification of western blot presented in A. TP53 protein level was normalized to cyclophilin expression. (**C**) The LD50 was determined by proliferation assay in NT and transduced cells with shCTRL and two different shTP53. Bar graphs represent the mean with SD in separate experiments. ns, not significant; *, $P \leq 0.05$; **, $P \leq 0.01$; ***, $P \leq 0.001$; ****, $P \leq 0.0001$.

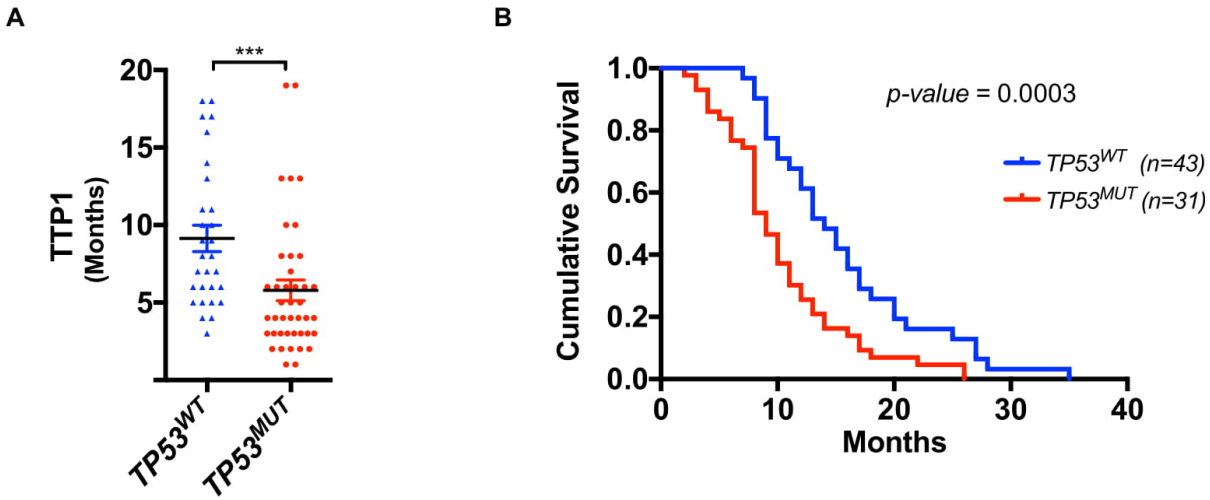
A
***
TTP1 (Months)
20
15
10
5
TP53WT
TP53MUT
B
Cumulative Survival
1.0
0.8
0.6
0.4
0.2
0.0
0
10
20
30
40
Months
p-value = 0.0003
TP53WT (n=43)
TP53MUT (n=31)

Figure 4. TP53 mutations are associated with shorter effect or RT and worse prognosis in DIPG patients.

A) Time to progression was stratified according to *TP53* mutational status, n=29 $TP53^{WT}$ and n=42 $TP53^{MUT}$ (Mann-Whitney, *** $P \leq 0.001$). B) Overall survival of n=43 $TP53^{WT}$ and n=31 $TP53^{MUT}$ DIPG patients was plotted according to time (months)(p=0.0003, logrank test).

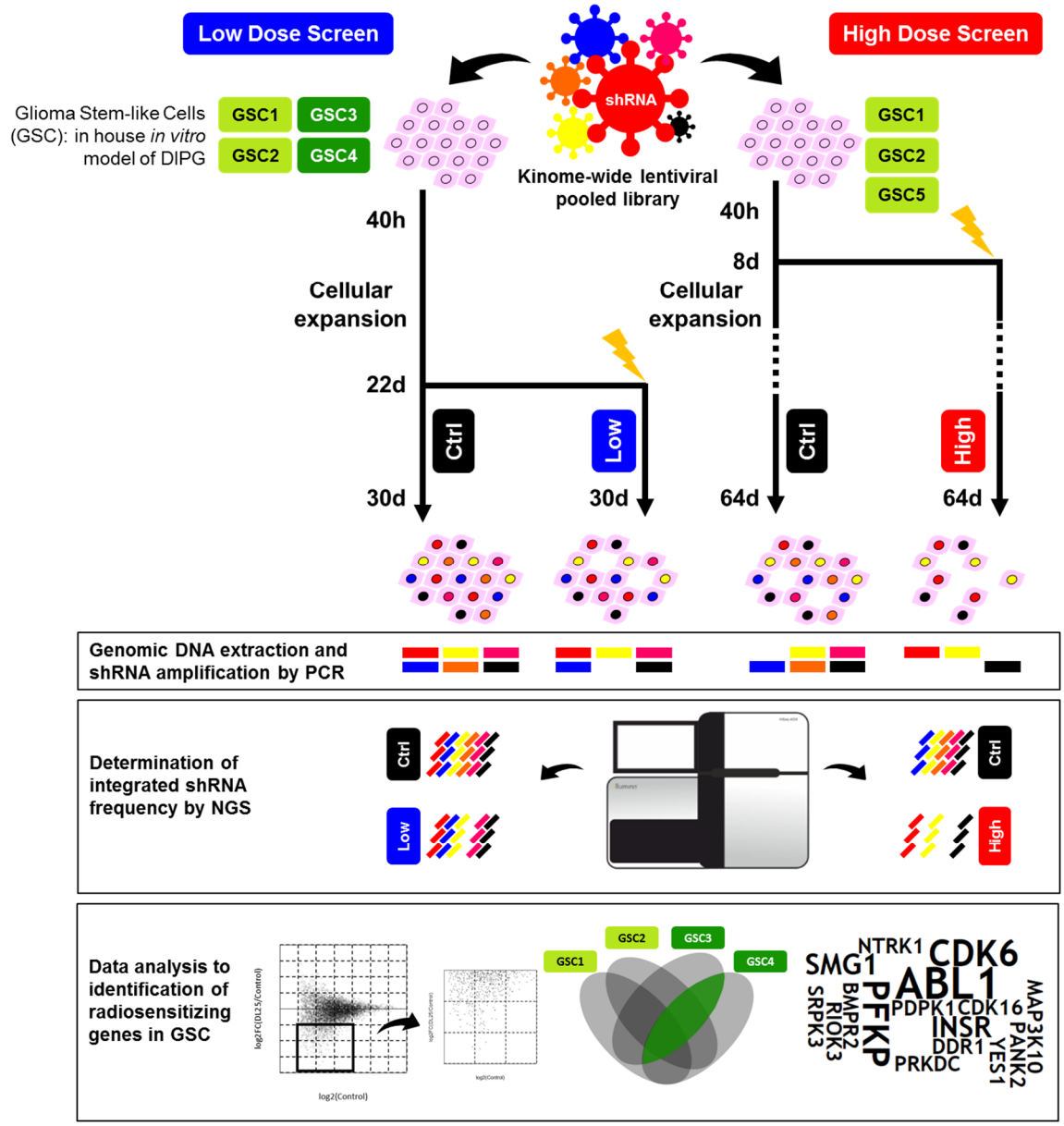

Figure 1. RNA interference screening of genes sensitizing DIPG to radiation. *In vitro* synthetic lethality screening strategy targeting the whole kinome in combination with radiation.

PROJECT III. Identification of genes sensitizing the cells to radiotherapy

Radiotherapy remains the only validated treatment, although only bringing a transient symptom relief followed by a constant subsequent progression within a variable delay. A heterogeneous response to radiotherapy at diagnosis in DIPG patients was identified depending on the type of mutated histone H3 previously of the initiation of my thesis. Consequently, we planned to investigate the genes that can sensitize DIPG to radiotherapy, by conducting an RNAi kinome-wide screen (**Figure 1**). This screen was realised in parallel of the survival screen, so one unique screen was launched in the four H3K27M DIPG cells and each GSC sample was divided in two distinct arms 15 days after transduction. We choose to conduct the screen using an irradiation dose that allows to inhibit 25% of cellular growth (LD75), in order to have the ability to observe synergic effects of radiation and the gene knockdown by RNA interference. We looked for shRNAs depleted between irradiated and non-irradiated cells at 30 days post-transduction in order to identify only shRNAs sensitizing cells to radiation but not survival genes, which would be the case if we had decided to compare irradiated cells at 30 days to the reference timepoint at 40h post transduction.

1. MATERIAL AND METHODS

1.1. Glioma stem-like cell (GSC) culture

Human Glioma Stem Cell (GSC) models were developed in the laboratory, as previously described in Plessier and coll (Plessier et al. 2017). We used five GSC models harboring either H3.3-K27M (n=3, GSC1, GSC2 & GSC5) or H3.1-K27M mutations (n=2, GSC3 and GSC4). The cells were grown in Neurocult^{TM} medium supplemented with heparin (2 µg/mL, Stemcell Technologies), EGF/FGF (20ng/mL, Miltenyi) and PDGF (10 ng/mL, Miltenyi) at 37°C and 5% CO2 on laminin-coated flask (1µg/µL, Sigma-Aldrich). Culture medium was renewed every 2-3 days. Passage was performed when cells reached 70-80% of confluence by dissociation using accutase® (ThermoFisher Scientific).

1.2. *In vitro* by proliferation assay

Cells were plated at 10.000-20.000 cells/cm2 (n=3) in 96 well-plates and exposed to different doses of radiation ranging from 0.25 to 8 Gray (Gy) with the irradiator XRAD 320 (Precision X-Ray) 24h after plating. Phase contrast images of cells were taken every 24h using a 10X objective using videomicroscopy (Incucyte® ZOOM) during at least 10 days. The percentage of image area occupied by cells was measured thanks to CellPlayer Analysis software for image segmentation (Essen Bioscience).

1.3. Kinome-wide shRNA screen

The first “low dose” screen was performed as previously described in the

article I. At day 22, the cells were submitted to X-ray ionizing radiation in the XRad 320 biological irradiation (0.941 Gy/min ± 5%) at LD75. The cells were amplified and maintained 8 additional days in culture, then the cells were harvested and gDNA extracted. For the “high dose” screen, H3.3-K27M were submitted to LD75 seven days after transduction and the cells were amplified during a total of 64 days before gDNA extraction.

1.4. Library production and sequencing

Library production and pooled screening deconvolution were performed as described in the article I. We computed the log2fold-change of normalized frequency of irradiated cells *versus* normalized frequency of untreated cells for each shRNA, in order to assess the difference in construct abundance between treated and untreated samples. Similar multi-level selection criteria than those used in Article I was applied for a candidate gene identification: (i) selection of shRNAs with more than 50 reads for raw data of untreated cells; (ii) selection of shRNAs with a fold-change decrease equal or superior to 2 comparing irradiated and untreated cells and (iii) selection of candidate genes with multiple (at least 2-3) shRNAs depleted following irradiation.

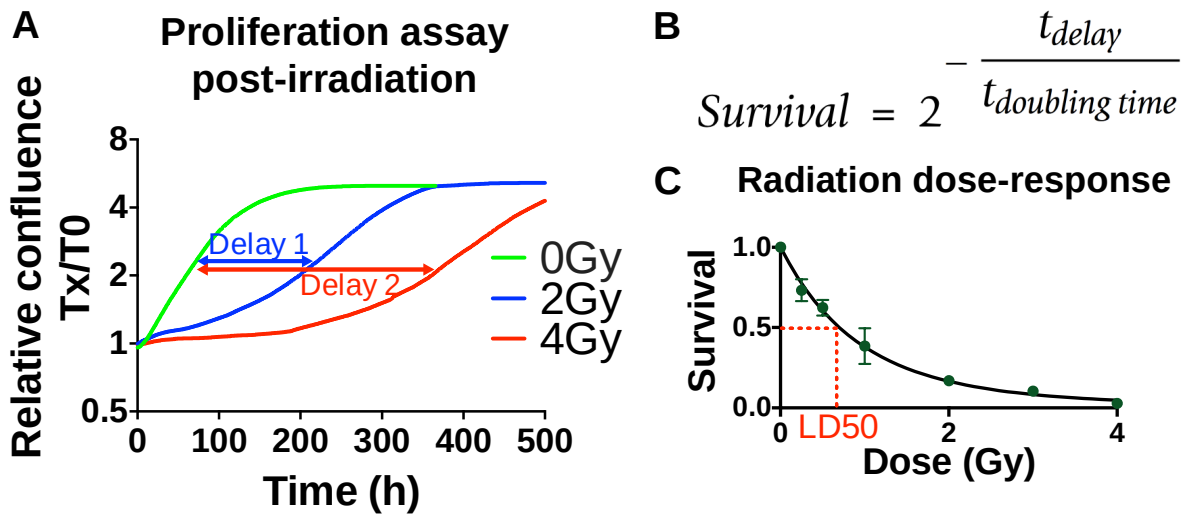

Figure 2. Determination of radiation dose-response. Proliferation assay via videomicroscopy (Incucyte® ZOOM) allowed to determine **(A)** the delay in cellular proliferation over the time. **(B)** Together with the doubling time, this allows the determination of the survival fraction and the calculation of **(C)** the lethal dose that inhibits the cellular growth at different proportions. In this screen, we were interested on the LD75, that allows the inhibition in 25% of cellular growth (adapted from Buch et al. 2012).

2. Results

2.1. Determination of LD25 radiation dose of GSC cells

The impact of irradiation on cell growth was evaluated by comparing the proliferation curves of different doses of radiation to the reference untreated sample (**Figure 2A**). The proliferation assay allowed to determine the delay in cell growth over time for the different doses of radiation (*data not showed*). The doubling time is computed using the increase of the occupied surface by cells over the time (**Figure 2B**). This allowed the calculation of the survival fraction (**Figure 2C)** and the determination of the lethal dose that allows to inhibit 50% of cellular growth (LD50). In this screen we were particularly interested in identifying the LD75, in order to observe synergic effects of radiation and the gene knockdown by RNAi. The two H3.1-K27M GSC cells give similar survival curves and allowed to define a LD75 of 0.25 Gy (*data not showed*). The three H3.3-K27M GSC cell survival curves are very close to each other reflecting the homogeneity between the GSC of this subgroup of DIPG tumours. The data allowed us to define the LD75 of 2 Gy for H3.3-K27M models (*data not showed*).

2.2. Relevance of the screen

Analysis of the sequencing data shown a good representativity and correlation of the shRNA library in samples at the initial timepoint at 40 hours (average correlation, $r2 = 0.97 \pm 0.019$), indicating that there is no bias in the transduction among the models *(data not showed*). No overall alteration of the number of shRNAs was observed in the untreated samples at 30 days with the identification of 85.47 ±0.02% of the kinome-wide library. As expected, only few

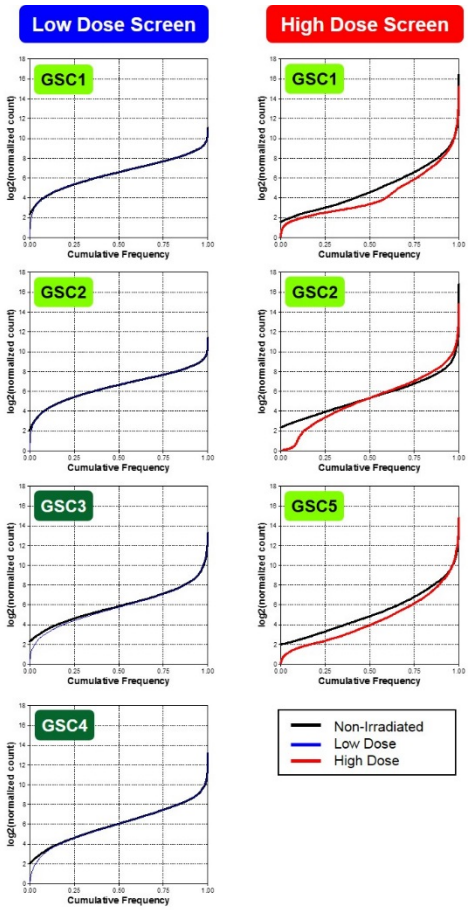

Figure 3. Representation of the kinome-wide shRNA library before and after irradiation. Cumulative frequency of shRNAs in the untreated and irradiated samples are presented Shift in the curve of irradiated cells represents the significant depletion in a subset of shRNAs (Wilcoxon rank sum test, ***p < 0.0001 for all DIPG models).

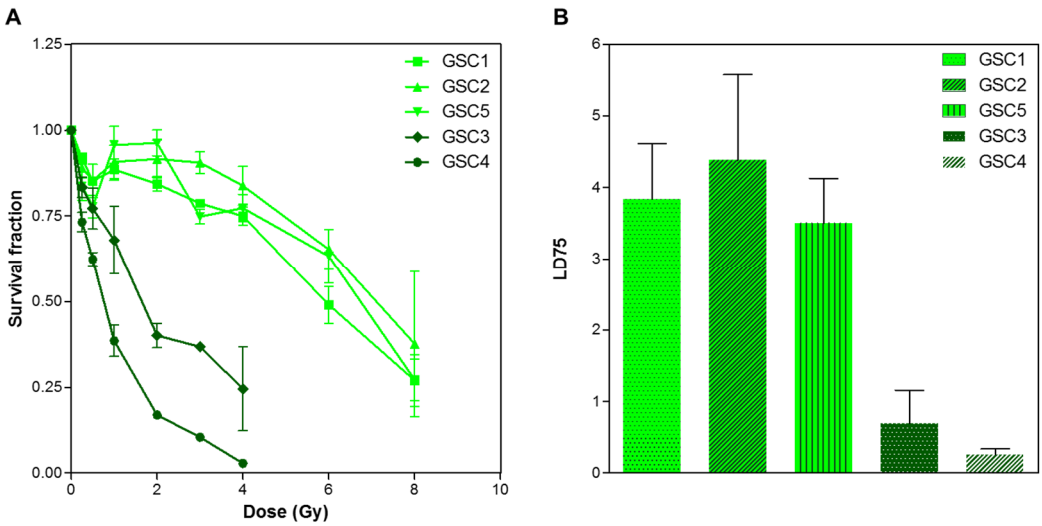

Figure 4. Determination of the LD75. The survival fraction **(A)** and the lethal dose **(B)** that allows to inhibit 25% of the cellular growth (LD75) was determined by analysis of proliferation assay at distinct dose of radiation for the 5 GSC models (n=3).

shRNAs present significant frequency changes after irradiation enrichment or depletion, respectively in 2.92% and 4.29% of the shRNA constructs. In comparison to the survival screen, the shRNAs distributions are tighter and centered on log2FC equal to zero, which indicates that in the low dose screen there were less shRNAs that can sensitize the cells to radiation (article I). We observed a significant depletion in a subset of shRNA frequency that impair cell growth in the presence of radiation only in the H3.1-K27M models in the low dose screen (Wilcoxon rank sum test, ***p < 0.0001) (**Figure 3**) as the curve of irradiated and untreated samples for H3.3-K27M GSC are almost fully overlapped. These results confirm the higher radioresistance of H3.3-K27M GSC models that we showed in the work presented in the article II. The first screen was named “low dose”, since posterior analysis have shown that 2 Gy corresponds to an inhibition of 15% of cellular growth, instead of 25%. Consequently, we decided to perform in H3.3-K27M models a second screen – named “high dose” but at a dose of irradiation, *i.e.* 4Gy that we have shown to correspond to the mean LD75 (3.9 ±0.44, (**Figure 4**) for the three tested models.

2.3. Low dose radiation and kinome-wide screen

2.3.1. Radioresistance influence in hit identification

As in the survival screen, several filters were applied to select the candidate genes, especially the shRNA presenting a log2fold-change of at least -1 and -3 in low-dose and high dose screen respectively in more than 2 models, as well as the genes with a shRNA redundancy higher than 2-3. In the low-dose screen a wide heterogeneity was observed among the GSC models the number of candidate genes ranging from 3 to 134 for GSC1 and GSC3 respectively (**Figure 5A**). The

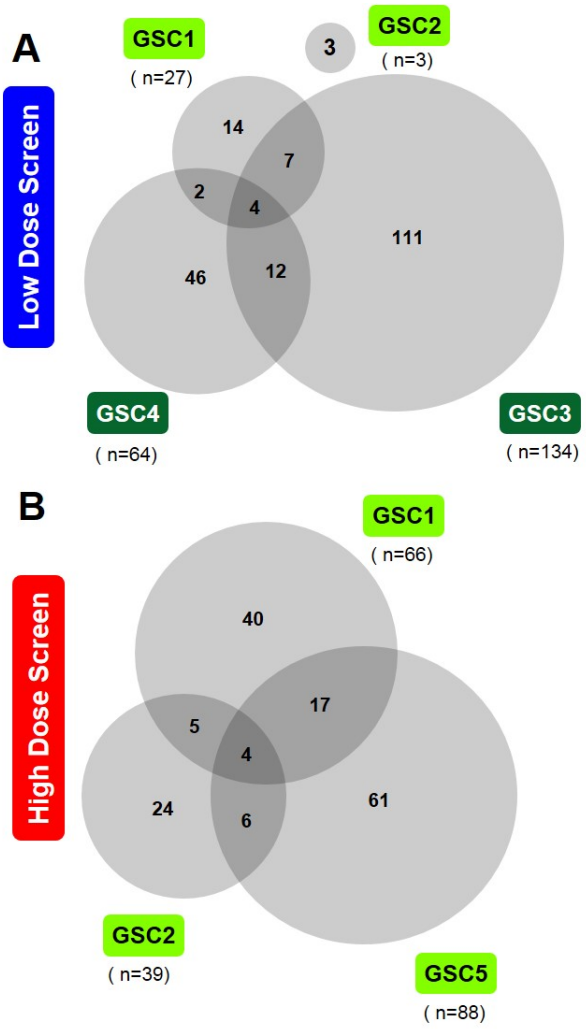

Figure 5. Gene hits selection. A. Overlapping of the gene hits selected as underrepresented in control cells in comparison with irradiated cells at low dose 30 days after of transduction in each H3-K27M cellular models. Only few genes were identified in H3.3-K27M models and none is shared between the 2 models, while for H3.1-K27M models there are 16 genes that are shared between the 2 models. **B. Gene hits distribution in the high dose screen.** There are more of genes shared by at least 2 H3.3-K27M models (n = 32).

number of candidates by model was smaller for H3.3-K27M cells reflecting their radioresistance. Anyway, an important difference was also observed between the 2 H3.1-K27M GSC as 2 time-more candidates were selected in GSC3 *versus* GSC4 and 82% of candidate are exclusive to this GSC3. This result can reflect the significant difference of LD75 identified *a posteriori* of launching the screen as LD75 is 2 to 3 time more elevated in GSC3 than GSC4 (**Figure 4B**).

We then compared the gene candidates among the models to identified genes whose extinction sensitize cells to irradiation, either in one of the main DIPG subgroups or in all the models, excluding GSC2 as none of 3 genes (*BLK*, *FASTK* and *HUNK*) identified in these cells where identified in another one. GSC2 have been proved once again to not be the most adapted model to the radiation screen, due to its intrinsic radioresistance (**Figure 5A**). Among the three genes identified exclusively in GSC2: *FASTK* is a FAS-activated serine / threonine kinase that encodes a antiapoptotic protein and seems to be deregulated in astrocytoma development (Zhi et al. 2013). *BLK* is a proto-oncogene from the Src family that usually is deregulated in gliomas; and *HUNK* is an effector of AKT prosurvival signalling by suppressing *c-MYC* expression. Four genes were identified as sensitizing 3 of 4 GSCs to irradiation, *CDK6*, *INSR*, *PRKDC* and *YES1*. *CDK6* and *INSR* have been previously identified in the survival screen (article I) as implicated in cell survival for the same models, without an effect in GSC2. Moreover, RNAi and pharmacological inhibition of *CDK6* have been shown to decrease cell proliferation and sensitize cells to ionizing radiation in medulloblastoma. *YES1* has also been identified in the all 3 H3.3-K27M models of the high dose screen. *INSR* and *YES1* have been associated with survival and proliferation in GBM though AKT/mTOR pathways. Interestingly, the identification of PRKDC in both H3.1-K27M and H3.3-

K27M models corresponds to a positive control of our irradiation screen, since this protein has a known key role in cell cycle arrest and DNA repair.

2.3.2. Identification of genes increasing radiosensitivity of H3.1-K27M

Additionally, a detailed analysis of the radiation distributions show that more genes are able to increase the radiosensitivity of H3.1-K27M models, when knocked down, reflecting the more important radioresistance observed in our H3.3-K27M models. A total of 19% and 9.5% were identified respectively in GSC3 and GSC4 and a total of 16 target genes were found as impairing similarly cell survival in conjunction with radiation in the 2 H3.1-K27M.

Among the genes identified as impairing H3.1-K27M (L12), we identified genes previously reported to be involved especially in DDR and radioresistance (*i.e. ABL1*, *DDR1* and *SMG1)*. Moreover, genes that are related to proliferation (*i.e. BMPR2*, *CDK16*, *MAP3K10*, *PKPK1* and *PFKP*) in adult glioma and other cell lines, were also identified (Hover et al. 2016; Ćwiek et al. 2014; K. H. Kim et al. 2013; Lee et al. 2017). We compared those genes with the results of the survival screen and we have seen that *ABL1* genes was already identified in the survival screen (article I). *DDR1* was not considered exclusive to H3.1-K27M due to its identification in the high dose screen.

We have identified the neurotrophic tyrosine kinase receptor type 1 (*NTRK1*, encoding TrkA) as a candidate target gene exclusively in the H3.1-K27M models. *NTRK* gene fusions leading to constitutively or overexpressed chimeric kinase have been reported in paediatric non-brainstem tumours and are emerging as new targets with drugs already available. In adult GBM, RNA-seq analysis in a cohort of 162

patients have shown that despite the low expression of *NTRK1* wild-type transcript, fusion transcripts are highly expressed (J. Kim et al. 2014). The 3' exons of *NTRK1* are found fused to 5′ exons of the gene neurofascin (*NFASC*) or brevican (*BCAN*) that two genes that are highly expressed in neuronal tissues, (J. Kim et al. 2014; Cook et al. 2017). The expression of these fusions proteins increases cell proliferation *in vitro* and tumour formation in *in vivo* mice models, suggesting their role in GBM initiation or maintenance. Moreover, *NTRK1-BCAN* fusion generated using CRISPR-Cas9-based gene editing in NSCs also drives tumorigenesis (Cook et al. 2017). Wu and coll. have reported recurrent fusions involving *NTRK1*, *NTRK2* and *NTRK3* in 40% of non-brainstem (NBS) HGG and 4% of H3.3-K27M DIPG patients (Wu et al. 2014). In our DIPG cohort this gene is weakly expressed and no NTRK1 fusion was identified in the analysis by RNA-seq of 80 patients of our DIPG cohort. Although the use of specific inhibitors has been suggested in several cancers (Dai et al. 2018), for DIPG patients there is no solid evidence of the benefit of targeting this gene as potential therapeutic targets. Moreover, for the moment, no relation between NTRK fusions and radiosensitivity.

We have interestingly identified the cyclin-dependent kinase CDK16 (PCTK1) as a candidate target gene exclusively in the H3.1-K27M models. This gene has been previously identified in an RNAi screen in c-Myc-overexpressing medulloblastoma. They were able to confirm though RNAi and pharmacological inhibition that this kinase impairs cellular proliferation and tumour growth through the activation of AKT/mTOR pathway (Ćwiek et al. 2014). A recent study in lung cancer, have shown that CDK16 negatively regulates p53 stability in p53-WT controlling its transcriptional activity. Moreover, CDK16 knockdown increases radiosensitivity in lung cells (Xie et al. 2018). In contrast to H3.3-K27M models,

H3.1-K27M are not associated with *TP53* alterations, which could explain the identification of this gene exclusively in this subgroup. Further analysis are required to determine the role of CDK16 in H3.1-K27M radiosensitivity and the potential use of this gene as a therapeutical target.

Functional annotations of target genes that 16 genes identified in both H3.1-K27M models, together with H3.3-K27M GSC1, using the kinome-wide library as reference have shown a significant enrichment of genes involved in cell development (p-value = 2.62 e-02, *DPK1, ABL1, NTRK1, BMPR2, CDK16, DDR1, PANK2*). Several of these genes are expressed in neurons, as indicated by a significant enrichment of the cellular component “neuronal cell body” (p-value = 1.1 e-02, *PDPK1, ABL1, NTRK1, BMPR2*).

2.3.3. Identification of genes increasing radiosensitivity of H3.3-K27M

In the low dose screen, as mentioned previously only few genes increase the radiosensitivity of H3.3-K27M models when inhibited at LD75, respectively 4% and 0.45% of the kinome-wide library, reflecting the intrinsic radioresistance of H3.3-K27M (**Figure 5A**). None of the genes was shared by the 2 H3.3-K27M models in this experimental condition.

We performed a screen exclusively in H3.3-K27M models in order to determine genes that can sensitize these radioresistant cells to the radiotherapy, due to (i) the few target genes identified in the previous screen, (ii) the absence of common genes among the 2 H3.3-K27M models and (iii) in an attempt to identify a therapeutic target to associate with radiation in this radioresistant subgroup of DIPG. For that, we changed some parameters in the experimental design: (i) we increase

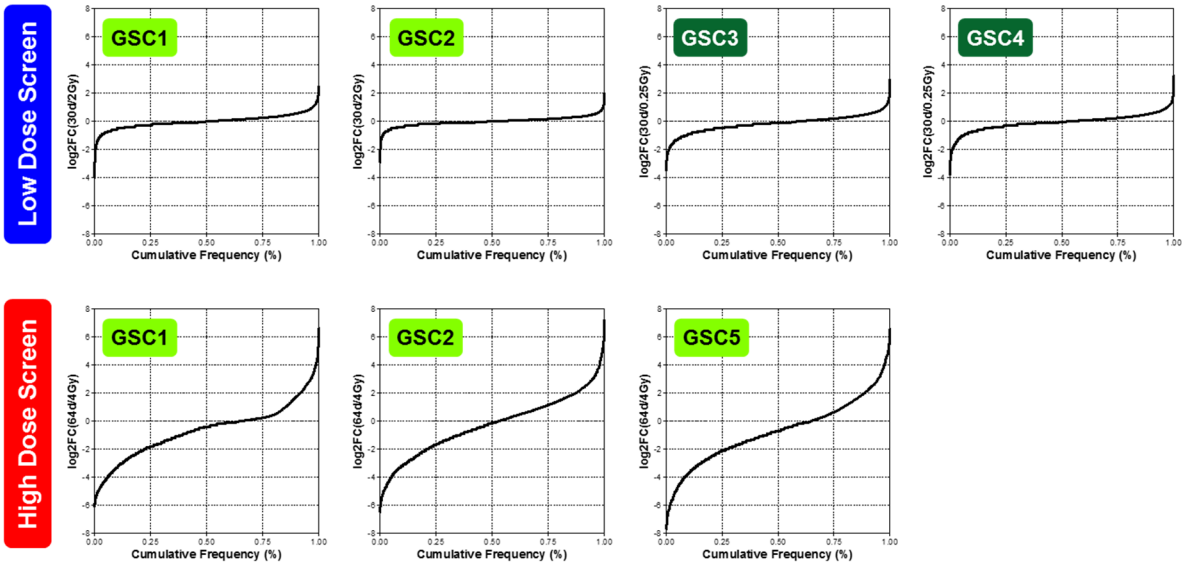

Figure 6. Distribution of shRNA modulation between non-irradiated and irradiated cells. Cumulative frequency of the log2 fold change shows that for the low dose screen, more shRNAs are modulated to H3.1-K27M models than H3.3. Regarding the high dose screen, there is an important modulation when compared to the previous screen.

by twice the dose of radiation, since posterior results have shown that the 2 Gy was not effectively the LD75 as previously identified. We also change the (ii) time of treatment conducted 7 days after transduction instead of 22. Finally, (iii) we extend the time of cell growth after transduction to 64 days in this second screening as the doubling time of GSC was precisely defined after launching the screen and found to be lower than expected. A longer time of cell expansion after transduction ensure to be able to measure more important differences of frequencies and thus in log2FC. We considered that a longer duration could capture the effects over time of catastrophic disasters due to the combination of gene knockdown and radiation, that we certainly did not identified in the first screen. The comparison of the untreated samples of low and high dose showed that there is a deletion in a subset of shRNAs over time. As expected, in this second screen more elevated fold-changes were obtained, as shown by the cumulative frequencies (**Figure 6**).

Regarding the log2FC of irradiated *versus* untreated samples we have shown that only 1.45 to 6.9% of the shRNAs increase radiosensitivity in the low dose screen, while in the high dose screen these shRNAs range from 36.36 to 45.46%. This augmentation of the proportion of shRNAs increased or decreased can be considered as an evidence that the observed effect is due to a factual effect of the shRNA knock-down and not due to false-positive effects. As consequence, we applied more stringent criteria of selection as follow in addition to the first filter of the survival screen (article I): (i) a log2FC of irradiated sample *versus* non irradiated inferior to -3 and (ii) a redundancy, *i.e.* the number of distinct shRNAs per gene depleted, equal or superior to 3. A total of 32 genes were identified in at least 2 H3.3-K27M models (**Figure 5B**). As expected, we retrieved the 3 common genes between the low dose and the high dose screen (**Figure 7**): *CDK6, INSR* and *YES1*

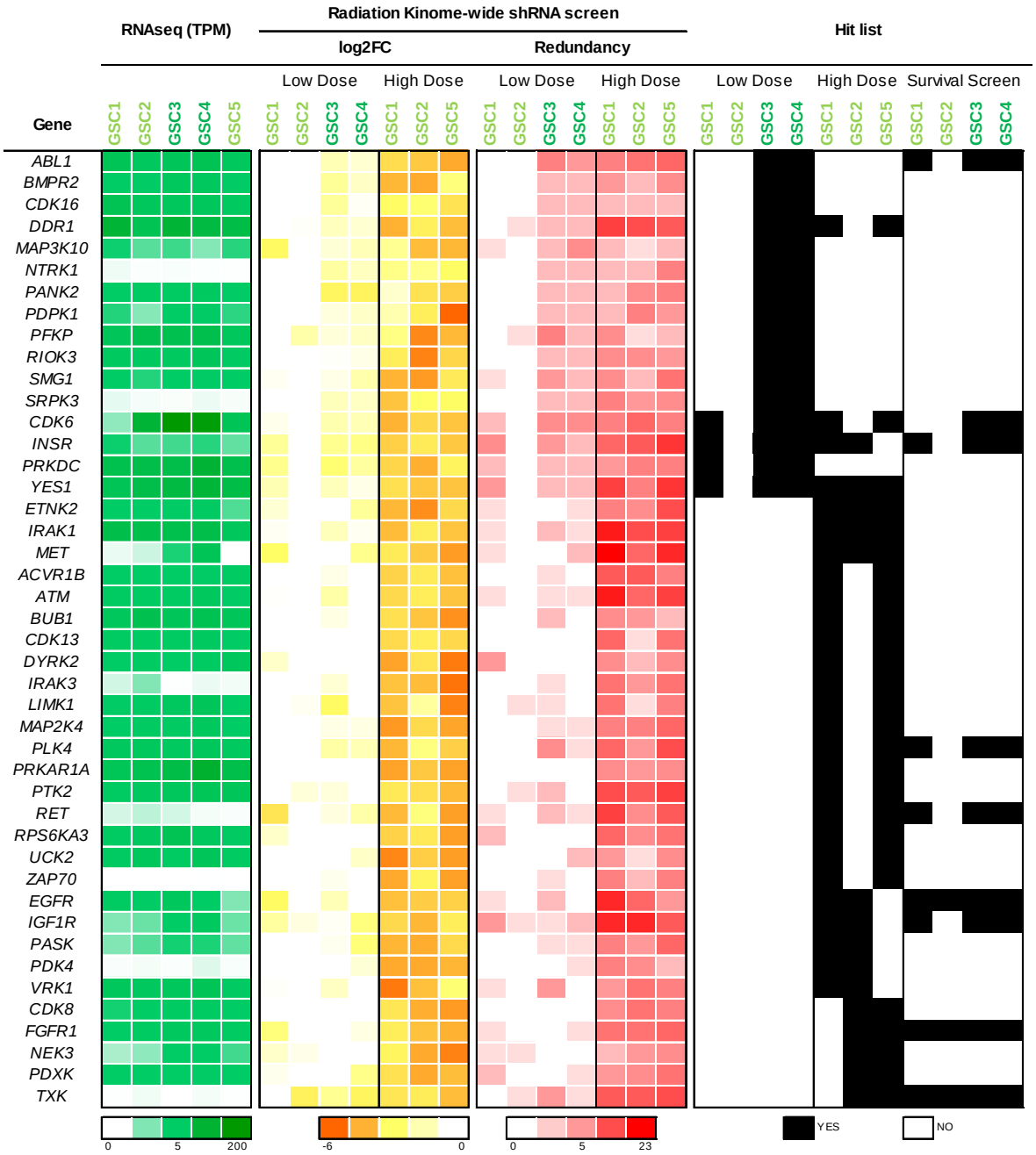

Figure 7. Gene hits selection. Heatmap representing the RNA-seq gene expression level (tpm), the average modulation of shRNA frequency after 30 days (low dose) or 64 days (high dose) of outgrowth for the shRNA that passed the selection criteria as well as the shRNA redundancy for the 44 genes identified in at least 2 distinct DIPG models. The genes identified in the survival screen are also presented.

by these cells, increasing radiosensitivity. *IRAK1* is an interleukin-1 receptor-associated kinase 1, associated with NF-kB pathway. Surprisingly, this gene was identified in the high dose screen. This gene has been associated with activation of TLR signalling followed by low dose (0.05 Gy) radiation, while high doses (1 Gy) of radiation has been shown to induce p53 activation. Further analysis have to be perform in order to clarify the mechanisms behind DDR activation in DIPG to better understand of the pathways involved in radioresistance.

Identified in both radiation screen, *YES1* could also be considered a relevant hit identified in this screen (**Figure 7**). YES1 is responsible by the phosphorylation of YAP1 leading to activation of apoptotic pathway. In adult gliomas, the *YAP1* expression have been associated with high infiltrative and aggressive gliomas, such as astrocytomas and oligodendrogliomas (Orr et al. 2011). In our DIPG models, *YAP1* seems to be more expressed than in the control NSC. In GBM, *YAP1* have been demonstrated to promote cellular growth *in vitro*. Due to the implication of YAP1 in glioma tumorigenesis and the regulatory effect of YES1, this could be a potential therapeutic target in association to radiation therapy in both H3.3-K27M and H3.1-K27M models.

In gliomas, *ABL1* (**Figure 7**) has been mechanistically linked to DDR via histone modification in adults GBM through the action of TIE2 (Hossain et al. 2016). TIE2 is a tyrosine kinase receptor (TKR) that phosphorylates the tyrosine 51 of the histone H4 (H4Y51)(Cheung et al. 2005), which in turn leads to the recruitment of ABL1 involved in the NHEJ repair pathway (Hossain et al. 2017). The knockdown of *ABL1* using either siRNA or pharmacologic inhibitor decreased NHEJ cellular activity after ionizing radiation (Hossain et al. 2016) and was suggested to be a

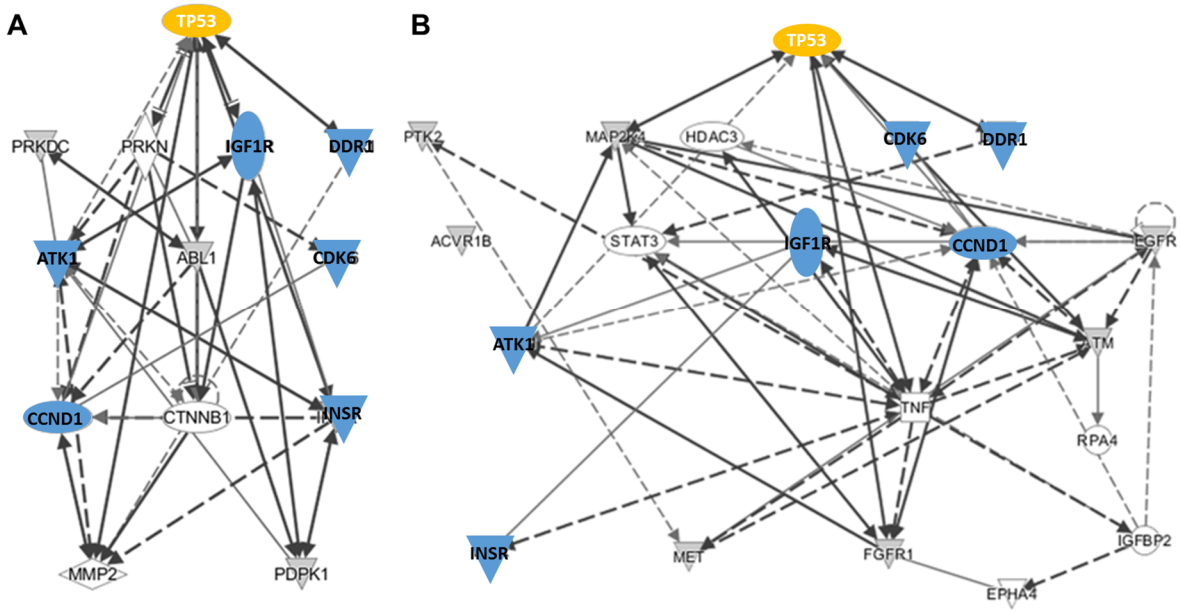

Figure 8. Ingenuity pathway analysis of the (A) H3.1-K27M and (B) H3.3-K27M lists. When regarding all the 16 genes in common to H3.1-K27M models and the genes in common to at least 2 H3.3-K27M model, there is overlap of genes related to TP53 pathway.

strategy to overcome radiation resistance in adult GBM. It could be interesting to test this inhibitor in DIPG cells, since ABL1 was identified in both high dose screen and survival screen (article I).

Our candidate gene from the survival screen *VRK3* (article I) was not found depleted in irradiated *versus* untreated cells. However, interestingly another member of the same family *VRK1* (**Figure 7**) was identified as sensitizing the cells to radiation in two of the three cell lines of the high dose screen. It could be interesting to evaluate the role of *VRK1* in our models and verify similarities with our candidate gene *VRK3*.

Pathway analysis using Ingenuity Pathway Analysis (IPA) shown the presence of several genes related to cell cycle, cell death and survival in the genes of H3.1-K27M, while for H3.3-K27M we have additionally involvement of genes in nervous system development, DNA replication, recombination and repair. We can also highlight the presence of several genes related to the TP53 pathway that are in common to H3.1- and H3.3-K27M gene lists (**Figure 8**). Although complementary analysis must be performed, this screen starts to shed light into the molecular pathways involved in DIPG radioresistance and the identification of new adjuvants to radiotherapy.

Discussion and Perspectives

DISCUSSION AND PERSPECTIVES

In the first part of the project, we performed a synthetic lethality screen using RNAi in DIPG, the first reported in this disease and more generally in paediatric HGG. Our objectives were both to identify genes whose extinction impair cell survival to increase the knowledge on the underlying mechanisms of DIPG oncogenesis and identify oncogenic and non-oncogenic addictions in K27M mutated cells as a basis for new treatments. The screen was performed using an interfering RNA library targeting the human kinome, as kinases are often deregulated in cancer and kinase inhibitors are considered as a major class of anti-cancer therapeutics. The heterogeneous mutational landscape of DIPG was taken into account by the selection of 4 archetypical DIPG GSCs models harbouring either H3.1-K27M (n=2) and H3.3-K27M (n=2) mutations, respectively associated with *ACVR1* and *TP53* alterations.

Many parameters were settled before the launch of the screen to ensure the robustness of the results based on similar negative selection screens conducted in other cell types, in particular as this project started at a time when our GSC models were still under characterization. First, we optimized the transduction and titration protocols as there is an important variability among GSCs in particular between H3.1- and H3.3-mutated cells, the former being more easily transduced. Indeed, we planned to transduce the cells at low multiplicity of infection (MOI), *i.e.* 0.3 in order to ensure the presence of only a single shRNA *per* cell. Moreover, the number of transduced cells was chosen to reach a representativity of 600, meaning that each construct would be introduced in 600 distinct cells. At this M.O.I. only 3% of the cells are predicted to contain more than one shRNA thus avoiding to identify a depletion

of a particular shRNA resulting from the interaction between 2 distinct constructs within a particular cell. We then determined the lethal dose (LD100) of puromycin in our non-transduced DIPG cells, in order to select only the cells that integrated the lentiviral constructs into their genomes, representing around 25% at MOI 0.3. The sensibility to this antibiotic was similar for all GSCs, *i.e.* 0,222 µg/mL.

We decided to use NSC as control cells to select essential genes in DIPG without any deleterious effect in normal cells in order to validate their potential interest as therapeutic targets. Actually, NSC appear to be the more relevant control cells to use as they are cultured in the same experimental conditions than GSC to avoid any experimental bias in our analysis, and because they share some phenotypic features with GSC, especially their stemness properties. The only NSCs available at that time were normal human NSCs deriving from hindbrain (NSC1), mid-forebrain (NSC2) and spinal cord area of the human central nervous system that were acquired commercially at passages ranging from 22 to 32. The cells needed to be significantly amplified as fifteen million cells were required to launch the screen while maintaining the representativity of 600. Unfortunately, we observed that we were not able to amplify those cells for more than six consecutive passages before observing cellular senescence, meaning that we had only a window of three passages to amplify and launch the screen. Indeed, we needed that the cells are still dividing after transduction to be able to observe a potential phenotype of proliferation arrest for essential genes. Consequently, the screen was conducted with control cells relatively close to senescence which is of course not optimal, in particular as we are looking for gene required for cell expansion. Later on, we got access to normal human embryos from which we derived NSC which present a greater ability to divide as we did not observe any signs of senescence or reduction

of doubling time until 10 passages. These NSC cells appear as control cells and were used for further validation of candidate target genes as the primary screen was already performed.

One of the major limitations of the shRNA pooled library used in our project was the absence of internal negative controls. The negative controls allow the measurement of the impact on cells of transduction and/or RNA interference with the particular lentiviral construct used. More importantly, they are useful to analyze the overall distributions of log2FC of shRNA frequency and normalize if needed, as they should be around 0. Because of the lack of negative controls in the library, we used core essential genes that have been identified previously through similar approaches in adult GBM, as well as other types of cancer, as our positive controls.

We have identified seven essential genes in common to all models, whatever the heterogeneity among the models. One of them, *EGFR* was overexpressed in around 40% of DIPG and a specific inhibitor is currently under scrutiny in the BIOMEDE clinical trial (NCT02233049). Five of them were directly or indirectly linked to the PI3K/AKT pathway, frequently altered in DIPG and targeted by another drug evaluated in BIOMEDE. These results show for the first time the feasibility of RNAi screens in DIPG models and indicate the relevance of hit identification.

Anyway, we observed a heterogeneity among the models as fewer modulations of log2FC were globally obtained with GSC2 *versus* the other cells. Interestingly, this model was derived from a patient that had a severe and rapid disease progression and the corresponding orthotropic xenografts murine models present a rapid development, compared to others *in vivo* models. Thus, the selection of this model was not the best choice for the screen due to its particularities that do not reflect the majority of DIPG patients.

Moreover, negative dropout screens usually used a cellular expansion of about 10 to 15 days after transduction to identify the shRNAs associated with a significant depletion across time. This value is defined according to the doubling time of the cellular models, usually close to 24h for the majority of the published screens. In these models, we can expect an important difference in fold-change after 15 days of expansion. When we launched the screen, we already knew that GSC do not proliferate quickly, without a precise estimation of their growth rate, as the model were still in development. After starting the screen, their doubling time was determined precisely, and found to be 2 times or more long than the cellular models usually used in such screen. Consequently, we should have maintained cells in culture for more than 22 days to be able to easily select candidate constructs associated with an important modulation of their frequency. For this reason, we then conducted *a posteriori* a second screen in H3.3 with a cellular expansion during 64 days. In this second screen, we identified as expected greater fold-changes than the previous one. It would have been better to perform the initial screen in these conditions, but almost impossible because of the proximity to NSC senescence.

The selection of genes affecting cellular growth in 3 out of 4 models allowed the identification of 41 genes after applying our selection criteria filtering. Several genes have already been identified by similar approach in adult GBM, such as *AURKB*, *PLK1*, *FGFR1*, *CDK6* and *EGFR*. We decided to focus on genes that are not currently evaluated in clinical trials and that have not been previously associated to DIPG, as we want to explore new therapeutic alternatives far from the pathways already targeted by drugs in current or past clinical trial. Indeed, for example PTEN/PI3K/AKT pathway is a central pathway in cells and the targeting of pathway with such essential role and without any recurrent mutation driving the oncogenesis

observed in patients can lead to failure in therapeutic evaluation, and can have deleterious effect of surrounding normal cells *in vivo*.

We selected *VRK3* as a potential target hit for further analysis. We have successfully confirmed that *VRK3* knockdown lead to important consequences in cell growth arrest and drastic morphological changes. However, the impact of *VRK3* knockdown remains elusive in particular in the DIPG context. In the next months we need to confirm the negative impact of VRK3 KD on DIPG cell behavior *in vivo*. Indeed, we used GSC in the screen as the cancer stem cell population existing in the tumour is considered a reservoir of progenitors less differentiated at the origin of tumour growth and the phenomenon of treatment resistance. Nevertheless, we want to confirm that the gene extinction has the ability to affect the totality of the tumour and not exclusively GSCs. We will transduce GSC cells with an integrative lentiviral vector allowing an inducible expression of *VRK3* targeting shRNA and expressing Firefly luciferase that can be detected *in vivo* by bioluminescence. We will then inject these cells in the pons of immunocompromised mice. The presence of bioluminescence will allow to follow tumor growth before the induction of *VRK3* KD and evaluate the resultant tumor regression in comparison to control mice. If we confirm *in vivo* that *VRK3* KD can impair DIPG tumour progression, we will then extend the study to other DMG K27M-mutated, including thalamic tumours, to evaluate if VRK3 can be an effective target of all the tumours harbouring a K27M alteration.

Although *VRK3* seemed to be a relevant target, there is, which do not allow the direct clinical transfer of this result. Consequently, we should limited knowledge of its functions and pathway involvement and an absence of specific VRK3 inhibitors in the near future identify exhaustively the pathways directly impacted by its

inhibition in DIPG cells in order to try to find a way to mimic its repression in cells. As *VRK3* KD was shown to induce a sustained phospho-ERK expression in neurons (Kang and Kim 2006) that can conduct to induced cell death, we will evaluated ERK inhibitors to mimic this effect of *VRK3* repression even if preliminary results obtained in GSC2 do not confirm this effect in DIPG.

To identify the pathways altered subsequently to *VRK3* inhibition, we plan to use two distinct strategies in parallel. First, a phospho-RTK assay will be conducted before and after *VRK3* KD to measure the phosphorylation level of 375 distinct proteins involved in several pathways with array containing 1318 antibodies. The phospho-kinase assay experiment was already optimized and we hope that in the next months it will highlight altered signalling pathways. Second, we plan to be more exhaustive and get an unbiased view on the molecular impact of *VRK3* repression and also better define its exact role in DIPG by performing transcriptomic analysis by RNA-seq. Since drugs targeting *VRK3* are not readily available, the identification of genes affected by *VRK3* knockdown may allow us to define exhaustively the signaling pathways affected for which drug inhibitors may already available and by this way identify drugs that could mimic *VRK3* extinction. The effect of such drugs would be then evaluated first *in vitro* and subsequently *in vivo* in our DIPG xenograft models to consider a rapid transfer of new therapeutics into the clinic.

The second objective of the project was to increase our knowledge on the underlying mechanisms of DIPG oncogenesis. In particular we could initially expect to identify differences between H3.1-K27M and H3.3-K27M oncogenic programs as the lab previously shown important differences especially in gene expression profiles with H3.3-mutated tumours associated with an oligodendrocytic/proneural signature, while H3.1-mutated tumours present a more astrocytic signature. We did

not find specificity of each subgroup when regarding the kinome-wide screen.

We preferred to start with a restricted screen using a small library targeting only the human kinome to confirm the feasibility of such screen in our models before to conduct a larger one. Anyway, to really conduct an exhaustive search without any *a priori* on gene function of all the DIPG vulnerabilities we should conduct a genome-wide screen. This larger library would be more pertinent to understand DIPG oncogenesis and will help us identify exhaustively, without any *a priori* on their function, the key molecular pathways that DIPG rely on for cell growth and survival. Furthermore, the feedback of the kinome-wide screen helped us to refine our experimental design for the genome-wide screening that will be conducted in the future, taking benefit of all the experimental conditions that were already well defined.

In parallel, since radiotherapy is the mainstay of DIPG treatment, and since we have previously shown a differential response to radiotherapy regarding the histone H3 mutational status, H3.1-K27M patients responding better H3.3-K27M ones, we wanted to identify the molecular determinants of the response to radiation. We evaluated the response to radiotherapy in 13 DIPG *in vitro* models and showed that the heterogeneous response observed in the patients was recapitulated in our *in vitro* models. The comparison of their mutational landscape to their radiosensitivity showed that the main driver of the DIPG radioresistance was the mutation of *TP53* and not the type of histone H3 mutated which explained the radioresistance despite its association with response to radiotherapy and survival. Now we showed that this link was due to the strong association of the TP53 genotype with the type of histone H3 mutated. Yet, only a slight difference was observed between control NSC and H3-K27M/*TP53*^{WT} tumors. Unfortunately, we cannot really confirm this observation as only few DIPG patients without K27M

mutation are available. The results indicated that *TP53* deficiency could serve as a biomarker of radioresistance in DIPG, and this could sustain a potential new patient stratification. Additionally, in the future we will need to explain the underlying mechanisms involved in DIPG radioresistance – beyond the loss of *TP53*. We decided to use a negative selection screen similar to the strategy used in article I to probe if we could identify genes whose extinction increase sensitization to IR. Such candidate genes would be interesting targets to be used in conjunction with radiotherapy in DIPG patients. The screen was performed using the same parameters previously described in the article, with irradiation of the cells several days after transduction at LD75. Interestingly the number of hits identified was more important in the H3.1 K27M mutated tumours which are the most radiosensitive. We have identified 12 target genes into this subgroup, common to both tested models. No common hit was shared by the two H3.3-K27M, resulting in part from GSC2 which was less prone to shRNA depletion as already discussed. More importantly, follow up experiments including an extended range of dose used to determine survival fractions showed that our estimation of LD75 was wrong, under-evaluated around 2 fold. Thus, the screen was performed at LD closed to 85, instead of 75, explaining why only few hits were identified in this low-dose screen conducted in H3.3-mutated cells. Consequently, a second “high-dose” screen was performed in H3.3-K27M cells using an increased dose of irradiation (closer to real LD75), and also an extended time of cell expansion before deconvolution by NGS.

Three targets were found to be depleted in both DIPG subgroups following irradiation (in both low and high dose screens), *i.e.* CDK6, *INSR* and *YES1*. *INSR* was also identified in the survival screen in 3/4 GSCs cells. On the other hand, *CDK6* was found as impairing cell survival of H3.1 mutated cells only.

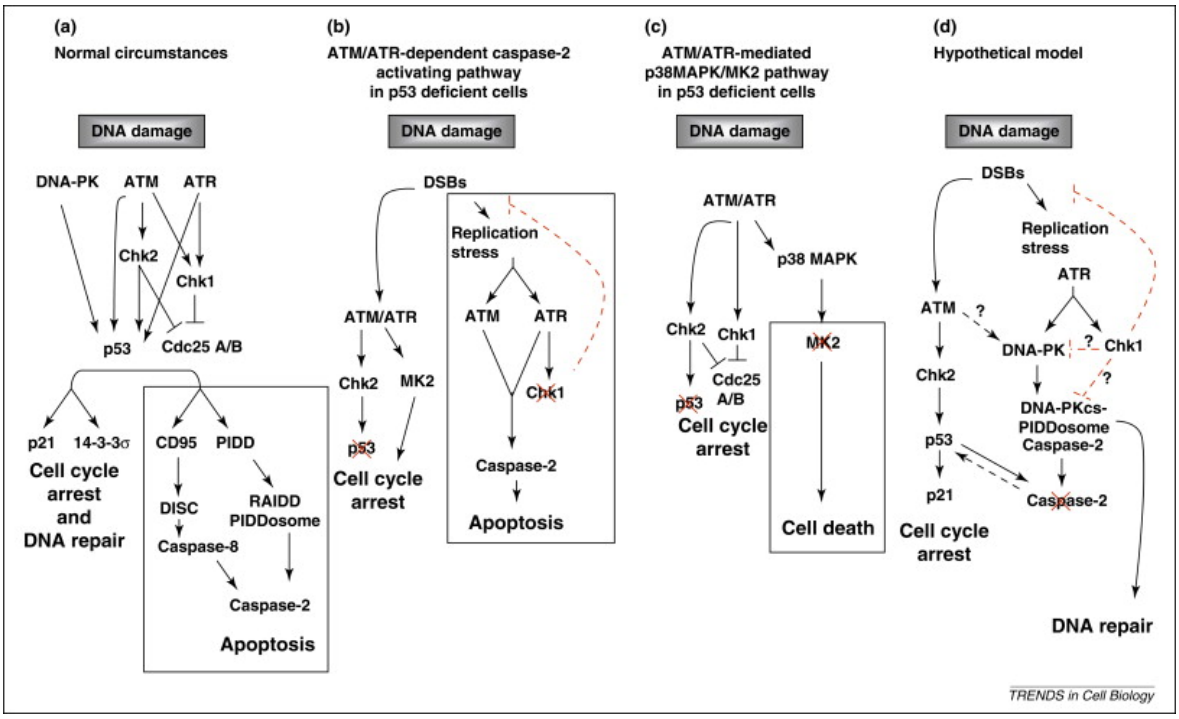

Figure 1. DDR in *TP53*-proficient and –deficient cells. ATM, ATR and DNA-PK are the major genes involved in DDR in normal circumstances, while in *TP53*-deficient cells alternative pathways can take place using mainly CHK1 instead of CHK2 (Vakifahmetoglu-Norberg and Zhivotovsky 2010).

We expected to encounter differences between H3.1-K27M and H3.3-K27M models, as the laboratory previously showed important differences in response to RT in patients. Accordingly, ten targets genes were found to sensitize only H3.1-K27M cells to irradiation and not H3.3-K27M cells even when subjected to high doses, the majority already involved in proliferation in adult gliomas and other cells lines (*BMPR2, CDK16, MAP3K10, PDPK1* and *PFKP).*

In the high-dose screen, 28 candidate genes sensitizing specifically H3.3-K27M cells to irradiation were identified in at least 2 of the 3 GSC tested. In particular, *ETNK2*, *IRAK1* and *MET* were found in all 3 GSCs, and thus constitute the best candidates to be evaluated in the radioresistant H3.3-K27M cells. In particular, MET inhibitor will be interesting to evaluate in DIPG as they have shown to overcome radioresistance of adult GBM GSC (De Bacco et al. 2016). In contrast, we did not identify *PLK1* identified in a similar screen in adult GBM looking for radiosensitizing gene (Tandle et al. 2013b). It is interesting to note that VRK1 was identified in 2 of the 3 H3.3-K27M models, whereas VRK3 was not found to sensitize cells to radiation.

Two major genes, *ATM* and *ATR*, are involved in DNA damage repair of DSB resulting from irradiation. Both lead to TP53 activation. Interestingly *ATM* was identified as a candidate target in 2 of the 3 H3.3 mutated GSCs. We identified *EGFR* in high dose H3.3 screen and it was identified by others using an isogenic pair of cell lines with and without TP53 deficiency (L. Xie et al. 2012). The ingenuity pathway analysis of gene hits specific of H3.1 and H3.3-K27M showed that many of them in each subgroup are linked directly and indirectly to TP53 (**Project III - Figure 8**).

In the article II, we have shown that *TP53* is the major driver of DIPG

radioresistance. It has been previously shown that *TP53* deficient cells activates p38MAPK/MK2 pathway downstream to ATM and ATR, due to the impaired TP53 activity. The p38 pathway usually acts in response to several stress signals and in the *TP53*-deficient context it is considered an alternative DDR pathway (**Figure 1**) (Reinhardt et al. 2007; Satsuka, Mehta, and Laimins 2015). Moreover, DDR in *TP53*-deficient context seems to depend on CHK1 rather than CHK2 to ensure cell survival (**Figure 1**). Consequently, it can explain the identification of *CHK1* as an essential gene in H3.3-K27M models. Indeed, it has been shown in several cancers that to bypass deficiencies in DDR pathway (such as *TP53*) and maintain genomic stability, the cells use alternative pathways to manage internal and external damages and thus create a dependence on these pathways. The knockdown of *CHK1* seems to act in this dependence and could be a potential target to be tested in combination with radiation therapy. It will be interesting to test CHK1 inhibitor in the future.

The identification of targets specifically in H3.1-K27M that were not depleted even in the high dose H3.3-K27M screen, as well as the difference in radiosensitivity highlighted in Article II raises the question of the radiotherapy treatment in DIPG patients. The current protocols of treatment do not take into account the *TP53* genomic alteration of these patients and this study indicates that distinct protocols for $TP53^{WTT}$ and $TP53^{MUT}$ could be considered.

More globally, all our work presented in this thesis clearly highlights TP53 as playing a central role in DIPG, in the two subgroups presenting or not *TP53* alteration. Indeed, a significant part of DIPG essential genes are linked to TP53 as well as many of the targets identified as radiosensitizing.

References

REFERENCES

Abbotts, Rachel, and David M. Wilson. 2017. “Coordination of DNA Single Strand Break Repair.” *Free Radical Biology and Medicine*, Oxidative DNA Damage & Repair, 107 (June): 228–44. https://doi.org/10.1016/j.freeradbiomed.2016.11.039.

Albright, A. L., R. J. Packer, R. Zimmerman, L. B. Rorke, J. Boyett, and G. D. Hammond. 1993. “Magnetic Resonance Scans Should Replace Biopsies for the Diagnosis of Diffuse Brain Stem Gliomas: A Report from the Children’s Cancer Group.” *Neurosurgery* 33 (6): 1026-1029; discussion 1029-1030.

Allen, Jeffrey, Joao Siffert, Bernadine Donahue, Anita Nirenberg, Regina Jakacki, Patricia Robertson, Robert DaRosso, Louisa Thoron, Mark Rosovsky, and Richard Pinto. 1999. “A Phase I/II Study of Carboplatin Combined with Hyperfractionated Radiotherapy for Brainstem Gliomas.” *Cancer* 86 (6): 1064–69. https://doi.org/10.1002/(SICI)1097-0142(19990915)86:6<1064::AID-CNCR24>3.0.CO;2-1.

Avondoglio, Dane, Tamalee Scott, Whoon Kil, Mary Sproull, Philip J Tofilon, and Kevin Camphausen. 2009. “High Throughput Evaluation of Gamma-H2AX.” *Radiation Oncology* 4 (1): 31. https://doi.org/10.1186/1748-717X-4-31.

Bailey, S., A. Howman, K. Wheatley, D. Wherton, N. Boota, B. Pizer, D. Fisher, et al. 2013. “Diffuse Intrinsic Pontine Glioma Treated with Prolonged Temozolomide and Radiotherapy – Results of a United Kingdom Phase II Trial (CNS 2007 04).” *European Journal of Cancer* 49 (18): 3856–62. https://doi.org/10.1016/j.ejca.2013.08.006.

Bao, Shideng, Qiulian Wu, Roger E. McLendon, Yueling Hao, Qing Shi, Anita B. Hjelmeland, Mark W. Dewhirst, Darell D. Bigner, and Jeremy N. Rich. 2006. “Glioma Stem Cells Promote Radioresistance by Preferential Activation of the DNA Damage Response.” *Nature* 444 (7120): 756–60. https://doi.org/10.1038/nature05236.

Barde, Isabelle, Patrick Salmon, and Didier Trono. 2001. “Production and Titration of Lentiviral Vectors.” In *Current Protocols in Neuroscience*. John Wiley & Sons, Inc. http://onlinelibrary.wiley.com.gate1.inist.fr/doi/10.1002/0471142301.ns0421s53/abstract.

Barrangou, Rodolphe, Christophe Fremaux, Hélène Deveau, Melissa Richards, Patrick Boyaval, Sylvain Moineau, Dennis A. Romero, and Philippe Horvath. 2007. “CRISPR Provides Acquired Resistance against Viruses in Prokaryotes.” *Science (New York, N.Y.)* 315 (5819): 1709–12. https://doi.org/10.1126/science.1138140.

Bartkova, J., P. Hamerlik, M.-T. Stockhausen, J. Ehrmann, A. Hlobilkova, H. Laursen, O. Kalita, et al. 2010. “Replication Stress and Oxidative Damage Contribute to Aberrant Constitutive Activation of DNA Damage Signalling in Human Gliomas.” *Oncogene* 29 (36): 5095–5102. https://doi.org/10.1038/onc.2010.249.

Baskar, Rajamanickam, Kuo Ann Lee, Richard Yeo, and Kheng-Wei Yeoh. 2012. “Cancer and Radiation Therapy: Current Advances and Future Directions.” *International Journal of Medical Sciences* 9 (3): 193–99. https://doi.org/10.7150/ijms.3635.

Bassett, Danielle S., and Michael S. Gazzaniga. 2011. “Understanding Complexity

in the Human Brain." *Trends in Cognitive Sciences* 15 (5): 200–209. https://doi.org/10.1016/j.tics.2011.03.006.

Baumann, Michael, Mechthild Krause, Jens Overgaard, Jürgen Debus, Søren M. Bentzen, Juliane Daartz, Christian Richter, Daniel Zips, and Thomas Bortfeld. 2016. "Radiation Oncology in the Era of Precision Medicine." *Nature Reviews Cancer* 16 (4): 234–49. https://doi.org/10.1038/nrc.2016.18.

Bax, Dorine A., Alan Mackay, Suzanne E. Little, Diana Carvalho, Marta Viana-Pereira, Narinder Tamber, Anita E. Grigoriadis, et al. 2010. "A Distinct Spectrum of Copy Number Aberrations in Pediatric High-Grade Gliomas." *Clinical Cancer Research* 16 (13): 3368–77. https://doi.org/10.1158/1078-0432.CCR-10-0438.

Bedard, Philippe L., Aaron R. Hansen, Mark J. Ratain, and Lillian L. Siu. 2013. "Tumour Heterogeneity in the Clinic." *Nature* 501 (7467): 355–64. https://doi.org/10.1038/nature12627.

Bellon, Sophie, Didier Gasparutto, Christine Saint-Pierre, and Jean Cadet. 2006. "Guanine-Thymine Intrastrand Cross-Linked Lesion Containing Oligonucleotides: From Chemical Synthesis to in Vitro Enzymatic Replication." *Organic & Biomolecular Chemistry* 4 (20): 3831–37. https://doi.org/10.1039/b609460k.

Bender, Sebastian, Yujie Tang, Anders M Lindroth, Volker Hovestadt, David T W Jones, Marcel Kool, Marc Zapatka, et al. 2013. "Reduced H3K27me3 and DNA Hypomethylation Are Major Drivers of Gene Expression in K27M Mutant Pediatric High-Grade Gliomas." *Cancer Cell* 24 (5): 660–72. https://doi.org/10.1016/j.ccr.2013.10.006.

Bi, Xin. 2015. "Mechanism of DNA Damage Tolerance." *World Journal of Biological Chemistry* 6 (3): 48–56. https://doi.org/10.4331/wjbc.v6.i3.48.

Biddlestone-Thorpe, Laura, Muhammad Sajjad, Elizabeth Rosenberg, Jason M. Beckta, Nicholas C. K. Valerie, Mary Tokarz, Bret R. Adams, et al. 2013. "ATM Kinase Inhibition Preferentially Sensitizes p53-Mutant Glioma to Ionizing Radiation." *Clinical Cancer Research: An Official Journal of the American Association for Cancer Research* 19 (12): 3189–3200. https://doi.org/10.1158/1078-0432.CCR-12-3408.

Bieging, Kathryn T., Stephano Spano Mello, and Laura D. Attardi. 2014. "Unravelling Mechanisms of p53-Mediated Tumour Suppression." *Nature Reviews Cancer* 14 (5): 359–70. https://doi.org/10.1038/nrc3711.

Birmingham, Amanda, Laura M. Selfors, Thorsten Forster, David Wrobel, Caleb J. Kennedy, Emma Shanks, Javier Santoyo-Lopez, et al. 2009. "Statistical Methods for Analysis of High-Throughput RNA Interference Screens." *Nature Methods* 6 (8): 569–75. https://doi.org/10.1038/nmeth.1351.

Blackford, Andrew N., and Stephen P. Jackson. 2017. "ATM, ATR, and DNA-PK: The Trinity at the Heart of the DNA Damage Response." *Molecular Cell* 66 (6): 801–17. https://doi.org/10.1016/j.molcel.2017.05.015.

Boettcher, Michael, and Michael T. McManus. 2015. "Choosing the Right Tool for the Job: RNAi, TALEN, or CRISPR." *Molecular Cell* 58 (4): 575–85. https://doi.org/10.1016/j.molcel.2015.04.028.

Bolus, Norman E. 2017. "Basic Review of Radiation Biology and Terminology." *Journal of Nuclear Medicine Technology* 45 (4): 259–64. https://doi.org/10.2967/jnmt.117.195230.

Bonner, William M., Christophe E. Redon, Jennifer S. Dickey, Asako J. Nakamura,

Olga A. Sedelnikova, Stéphanie Solier, and Yves Pommier. 2008. “γH2AX and Cancer.” *Nature Reviews Cancer* 8 (12): 957–67. https://doi.org/10.1038/nrc2523.

Branzei, Dana, and Marco Foiani. 2008. “Regulation of DNA Repair throughout the Cell Cycle.” *Nature Reviews Molecular Cell Biology* 9 (4): 297–308. https://doi.org/10.1038/nrm2351.

Brummelkamp, T. R., K. Berns, E. M. Hijmans, J. Mullenders, A. Fabius, M. Heimerikx, A. Velds, et al. 2004. “Functional Identification of Cancer-Relevant Genes through Large-Scale RNA Interference Screens in Mammalian Cells.” *Cold Spring Harbor Symposia on Quantitative Biology* 69 (January): 439–46. https://doi.org/10.1101/sqb.2004.69.439.

Buch, Karl, Tanja Peters, Thomas Nawroth, Markus Sänger, Heinz Schmidberger, and Peter Langguth. 2012. “Determination of Cell Survival after Irradiation via Clonogenic Assay versus Multiple MTT Assay--a Comparative Study.” *Radiation Oncology (London, England)* 7: 1. https://doi.org/10.1186/1748-717X-7-1.

Buczkowics, Pawel, Christine Hoeman, Patricia Rakopoulos, Sanja Pajovic, Louis Letourneau, Misko Dzamba, Andrew Morrison, Peter Lewis, Eric Bouffet, and Ute Bartels. 2013. “Genomic Analysis of Diffuse Intrinsic Pontine Gliomas Identifies Three Molecular Subgroups and Recurrent Activating ACVR1 Mutations : Nature Genetics : Nature Publishing Group.” *Nature Genetics* 46 (April): 451–56. https://doi.org/10.1038/ng.2936.

Buczkowicz, Pawel, Ute Bartels, Eric Bouffet, Oren Becher, and Cynthia Hawkins. 2014. “Histopathological Spectrum of Paediatric Diffuse Intrinsic Pontine Glioma: Diagnostic and Therapeutic Implications.” *Acta Neuropathologica* 128 (4): 573–81. https://doi.org/10.1007/s00401-014-1319-6.

Buczkowicz, Pawel, and Cynthia Hawkins. 2015. “Pathology, Molecular Genetics, and Epigenetics of Diffuse Intrinsic Pontine Glioma.” *Frontiers in Oncology* 5: 147. https://doi.org/10.3389/fonc.2015.00147.

Buczkowicz, Pawel, Christine Hoeman, Patricia Rakopoulos, Sanja Pajovic, Louis Letourneau, Misko Dzamba, Andrew Morrison, et al. 2014. “Genomic Analysis of Diffuse Intrinsic Pontine Gliomas Identifies Three Molecular Subgroups and Recurrent Activating ACVR1 Mutations.” *Nature Genetics* 46 (5): 451–56. https://doi.org/10.1038/ng.2936.

Butowski, Nicholas A. 2015. “Epidemiology and Diagnosis of Brain Tumors.” *Continuum: Lifelong Learning in Neurology* 21 (2, Neuro–oncology): 301–13. https://doi.org/10.1212/01.CON.0000464171.50638.fa.

Bystron, Irina, Colin Blakemore, and Pasko Rakic. 2008. “Development of the Human Cerebral Cortex: Boulder Committee Revisited.” *Nature Reviews Neuroscience* 9 (2): 110–22. https://doi.org/10.1038/nrn2252.

Cadet, Jean, Thierry Douki, and Jean-Luc Ravanat. 2010. “Oxidatively Generated Base Damage to Cellular DNA.” *Free Radical Biology and Medicine* 49 (1): 9–21. https://doi.org/10.1016/j.freeradbiomed.2010.03.025.

Cadet, Jean, and J. Richard Wagner. 2013. “DNA Base Damage by Reactive Oxygen Species, Oxidizing Agents, and UV Radiation.” *Cold Spring Harbor Perspectives in Biology* 5 (2). https://doi.org/10.1101/cshperspect.a012559.

Cadet, Jean, J. Richard Wagner, Vladimir Shafirovich, and Nicholas E. Geacintov. 2014. “One-Electron Oxidation Reactions of Purine and Pyrimidine Bases in Cellular DNA.” *International Journal of Radiation Biology* 90 (6): 423–32.

https://doi.org/10.3109/09553002.2013.877176.
Caër, Le, and Sophie. 2011. “Water Radiolysis: Influence of Oxide Surfaces on H2 Production under Ionizing Radiation.” *Water* 3 (1): 235–53. https://doi.org/10.3390/w3010235.
Carrassa, Laura, and Giovanna Damia. 2017. “DNA Damage Response Inhibitors: Mechanisms and Potential Applications in Cancer Therapy.” *Cancer Treatment Reviews* 60 (November): 139–51. https://doi.org/10.1016/j.ctrv.2017.08.013.
Carruthers, Ross, Shafiq U. Ahmed, Karen Strathdee, Natividad Gomez-Roman, Evelyn Amoah-Buahin, Colin Watts, and Anthony J. Chalmers. 2015. “Abrogation of Radioresistance in Glioblastoma Stem-like Cells by Inhibition of ATM Kinase.” *Molecular Oncology* 9 (1): 192–203. https://doi.org/10.1016/j.molonc.2014.08.003.
Carthew, Richard W., and Erik J. Sontheimer. 2009. “Origins and Mechanisms of miRNAs and siRNAs.” *Cell* 136 (4): 642–55. https://doi.org/10.1016/j.cell.2009.01.035.
Cartmill, M., and J. Punt. 1999. “Diffuse Brain Stem Glioma. A Review of Stereotactic Biopsies.” *Child’s Nervous System: ChNS: Official Journal of the International Society for Pediatric Neurosurgery* 15 (5): 235–237; discussion 238.
Castel, David, Jacques Grill, and Marie-Anne Debily. 2016. “Histone H3 Genotyping Refines Clinico-Radiological Diagnostic and Prognostic Criteria in DIPG.” *Acta Neuropathologica* 131 (5): 795–96. https://doi.org/10.1007/s00401-016-1568-7.
Castel, David, Cathy Philippe, Raphaël Calmon, Ludivine Le Dret, Nathalène Truffaux, Nathalie Boddaert, Mélanie Pagès, et al. 2015a. “Histone H3F3A and HIST1H3B K27M Mutations Define Two Subgroups of Diffuse Intrinsic Pontine Gliomas with Different Prognosis and Phenotypes.” *Acta Neuropathologica* 130 (6): 815–27. https://doi.org/10.1007/s00401-015-1478-0.
———. 2015b. “Histone H3F3A and HIST1H3B K27M Mutations Define Two Subgroups of Diffuse Intrinsic Pontine Gliomas with Different Prognosis and Phenotypes.” *Acta Neuropathologica*, September. https://doi.org/10.1007/s00401-015-1478-0.
Cerniglia, George J., Jayashree Karar, Sonia Tyagi, Melpo Christofidou-Solomidou, Ramesh Rengan, Constantinos Koumenis, and Amit Maity. 2012. “Inhibition of Autophagy as a Strategy to Augment Radiosensitization by the Dual Phosphatidylinositol 3-Kinase/Mammalian Target of Rapamycin Inhibitor NVP-BEZ235.” *Molecular Pharmacology* 82 (6): 1230–40. https://doi.org/10.1124/mol.112.080408.
Chalhoub, Nader, and Suzanne J. Baker. 2009. “PTEN and the PI3-Kinase Pathway in Cancer.” *Annual Review of Pathology* 4: 127–50. https://doi.org/10.1146/annurev.pathol.4.110807.092311.
Chan, Kui Ming, Jing Han, Dong Fang, Haiyun Gan, and Zhiguo Zhang. 2013. “A Lesson Learned from the H3.3K27M Mutation Found in Pediatric Glioma: A New Approach to the Study of the Function of Histone Modifications in Vivo?” *Cell Cycle* 12 (16): 2546–52. https://doi.org/10.4161/cc.25625.
Chang, Jeffrey T., and Joseph R. Nevins. 2006. “GATHER: A Systems Approach to Interpreting Genomic Signatures.” *Bioinformatics (Oxford, England)* 22 (23):

2926–33. https://doi.org/10.1093/bioinformatics/btl483.

Chapman, Elisabeth J., and James C. Carrington. 2007. “Specialization and Evolution of Endogenous Small RNA Pathways.” *Nature Reviews. Genetics* 8 (11): 884–96. https://doi.org/10.1038/nrg2179.

Chen, Helen H. W., Macus Tien Kuo, Helen H. W. Chen, and Macus Tien Kuo. 2017. “Improving Radiotherapy in Cancer Treatment: Promises and Challenges.” *Oncotarget* 8 (37): 62742–58. https://doi.org/10.18632/oncotarget.18409.

Chen, Jian, Yanjiao Li, Tzong-Shiue Yu, Renée M. McKay, Dennis K. Burns, Steven G. Kernie, and Luis F. Parada. 2012. “A Restricted Cell Population Propagates Glioblastoma Growth after Chemotherapy.” *Nature* 488 (7412): 522–26. https://doi.org/10.1038/nature11287.

Chen, Jun-Rui, Yu Yao, Hong-Zhi Xu, and Zhi-Yong Qin. 2016. “Isocitrate Dehydrogenase (IDH)1/2 Mutations as Prognostic Markers in Patients With Glioblastomas.” *Medicine* 95 (9). https://doi.org/10.1097/MD.0000000000002583.

Chen, Wei, Yu-Wei Zhang, Yang Li, Jian-Wen Zhang, Tong Zhang, Bin-Sheng Fu, Qi Zhang, and Nan Jiang. 2016. “Constitutive Expression of Wnt/B‐catenin Target Genes Promotes Proliferation and Invasion of Liver Cancer Stem Cells.” *Molecular Medicine Reports* 13 (4): 3466–74. https://doi.org/10.3892/mmr.2016.4986.

Cheng, Peng, Emma Phillips, Sung-Hak Kim, David Taylor, Thomas Hielscher, Laura Puccio, Anita B. Hjelmeland, Peter Lichter, Ichiro Nakano, and Violaine Goidts. 2015a. “Kinome-Wide shRNA Screen Identifies the Receptor Tyrosine Kinase AXL as a Key Regulator for Mesenchymal Glioblastoma Stem-like Cells.” *Stem Cell Reports* 4 (5): 899–913. https://doi.org/10.1016/j.stemcr.2015.03.005.

———. 2015b. “Kinome-Wide shRNA Screen Identifies the Receptor Tyrosine Kinase AXL as a Key Regulator for Mesenchymal Glioblastoma Stem-like Cells.” *Stem Cell Reports* 4 (5): 899–913. https://doi.org/10.1016/j.stemcr.2015.03.005.

Cheung, Wang L., Fiona B. Turner, Thanuja Krishnamoorthy, Branden Wolner, Sung-Hee Ahn, Melissa Foley, Jean A. Dorsey, Craig L. Peterson, Shelley L. Berger, and C. David Allis. 2005. “Phosphorylation of Histone H4 Serine 1 during DNA Damage Requires Casein Kinase II in S. Cerevisiae.” *Current Biology: CB* 15 (7): 656–60. https://doi.org/10.1016/j.cub.2005.02.049.

Cho, Kwang-Jae, Eun-Ji Park, Min-Sik Kim, and Young-Hoon Joo. 2017. “Characterization of FaDu-R, a Radioresistant Head and Neck Cancer Cell Line, and Cancer Stem Cells.” *Auris, Nasus, Larynx*, August. https://doi.org/10.1016/j.anl.2017.07.011.

Chornenkyy, Yevgen, Sameer Agnihotri, Man Yu, Pawel Buczkowicz, Patricia Rakopoulos, Brian Golbourn, Livia Garzia, et al. 2015. “Poly-ADP-Ribose Polymerase as a Therapeutic Target in Pediatric Diffuse Intrinsic Pontine Glioma and Pediatric High-Grade Astrocytoma.” *Molecular Cancer Therapeutics* 14 (11): 2560–68. https://doi.org/10.1158/1535-7163.MCT-15-0282.

Cohen, Adam, Sheri Holmen, and Howard Colman. 2013. “IDH1 and IDH2 Mutations in Gliomas.” *Current Neurology and Neuroscience Reports* 13 (5): 345. https://doi.org/10.1007/s11910-013-0345-4.

Cohen, Kenneth J., Richard L. Heideman, Tianni Zhou, Emiko J. Holmes, Robert S.

Lavey, Eric Bouffet, and Ian F. Pollack. 2011. “Temozolomide in the Treatment of Children with Newly Diagnosed Diffuse Intrinsic Pontine Gliomas: A Report from the Children’s Oncology Group.” *Neuro-Oncology* 13 (4): 410–16. https://doi.org/10.1093/neuonc/noq205.

Cohen, Kenneth J., Nada Jabado, and Jacques Grill. 2017a. “Diffuse Intrinsic Pontine Gliomas-Current Management and New Biologic Insights. Is There a Glimmer of Hope?” *Neuro-Oncology*, March. https://doi.org/10.1093/neuonc/nox021.

———. 2017b. “Diffuse Intrinsic Pontine Gliomas—current Management and New Biologic Insights. Is There a Glimmer of Hope?” *Neuro-Oncology* 19 (8): 1025–34. https://doi.org/10.1093/neuonc/nox021.

Conti, Luciano, Steven M Pollard, Thorsten Gorba, Erika Reitano, Mauro Toselli, Gerardo Biella, Yirui Sun, et al. 2005. “Niche-Independent Symmetrical Self-Renewal of a Mammalian Tissue Stem Cell.” *PLoS Biology* 3 (9). https://doi.org/10.1371/journal.pbio.0030283.

Cook, John A., David Gius, David A. Wink, Murali C. Krishna, Angelo Russo, and James B. Mitchell. 2004. “Oxidative Stress, Redox, and the Tumor Microenvironment.” *Seminars in Radiation Oncology* 14 (3): 259–66. https://doi.org/10.1016/j.semradonc.2004.04.001.

Cook, Peter J., Rozario Thomas, Ram Kannan, Esther Sanchez de Leon, Alexander Drilon, Marc K. Rosenblum, Maurizio Scaltriti, Robert Benezra, and Andrea Ventura. 2017. “Somatic Chromosomal Engineering Identifies BCAN-NTRK1 as a Potent Glioma Driver and Therapeutic Target.” *Nature Communications* 8 (July). https://doi.org/10.1038/ncomms15987.

Coutel, Y. 1959. “[Infiltrating glioblastoma of the brain stem in an 8-year-old child; normalization of the pneumoencephalogram after radiotherapy].” *Revue D’oto-Neuro-Ophtalmologie* 31: 119–23.

Ćwiek, Paulina, Zaira Leni, Fabiana Salm, Valeriya Dimitrova, Beata Styp-Rekowska, Gianpaolo Chiriano, Michael Carroll, et al. 2014. “RNA Interference Screening Identifies a Novel Role for PCTK1/CDK16 in Medulloblastoma with c-Myc Amplification.” *Oncotarget* 6 (1): 116–29.

Dai, Xiaofeng, Rutaganda Theobard, Hongye Cheng, Mengtao Xing, and Jianying Zhang. 2018. “Fusion Genes: A Promising Tool Combating against Cancer.” *Biochimica et Biophysica Acta (BBA) - Reviews on Cancer* 1869 (2): 149–60. https://doi.org/10.1016/j.bbcan.2017.12.003.

Danussi, Carla, Promita Bose, Prasanna T. Parthasarathy, Pedro C. Silberman, John S. Van Arnam, Mark Vitucci, Oliver Y. Tang, et al. 2018. “Atrx Inactivation Drives Disease-Defining Phenotypes in Glioma Cells of Origin through Global Epigenomic Remodeling.” *Nature Communications* 9 (1): 1057. https://doi.org/10.1038/s41467-018-03476-6.

Darnell, Diana, and Scott F. Gilbert. 2017. “Neuroembryology.” *Wiley Interdisciplinary Reviews. Developmental Biology* 6 (1). https://doi.org/10.1002/wdev.215.

De Bacco, Francesca, Antonio D’Ambrosio, Elena Casanova, Francesca Orzan, Roberta Neggia, Raffaella Albano, Federica Verginelli, et al. 2016. “MET Inhibition Overcomes Radiation Resistance of Glioblastoma Stem-like Cells.” *EMBO Molecular Medicine* 8 (5): 550–68. https://doi.org/10.15252/emmm.201505890.

D’Errico, Mariarosaria, Barbara Pascucci, Egidio Iorio, Bennett Van Houten, and

Eugenia Dogliotti. 2013. “The Role of CSA and CSB Protein in the Oxidative Stress Response.” *Mechanisms of Ageing and Development*, Special Issue on the segmental progeria Cockayne syndrome, 134 (5): 261–69. https://doi.org/10.1016/j.mad.2013.03.006.

Di Stefano, Anna Luisa, Alessandra Fucci, Veronique Frattini, Marianne Labussiere, Karima Mokhtari, Pietro Zoppoli, Yannick Marie, et al. 2015. “Detection, Characterization, and Inhibition of FGFR-TACC Fusions in IDH Wild-Type Glioma.” *Clinical Cancer Research: An Official Journal of the American Association for Cancer Research* 21 (14): 3307–17. https://doi.org/10.1158/1078-0432.CCR-14-2199.

Diehl, Paul, Donato Tedesco, and Alex Chenchik. 2014. “Use of RNAi Screens to Uncover Resistance Mechanisms in Cancer Cells and Identify Synthetic Lethal Interactions.” *Drug Discovery Today. Technologies* 11 (March): 1–116. https://doi.org/10.1016/j.ddtec.2013.12.002.

Diehn, Maximilian, Robert W. Cho, Neethan A. Lobo, Tomer Kalisky, Mary Jo Dorie, Angela N. Kulp, Dalong Qian, et al. 2009. “Association of Reactive Oxygen Species Levels and Radioresistance in Cancer Stem Cells.” *Nature* 458 (7239): 780–83. https://doi.org/10.1038/nature07733.

Dimou, Leda, and Magdalena Götz. 2014. “Glial Cells as Progenitors and Stem Cells: New Roles in the Healthy and Diseased Brain.” *Physiological Reviews* 94 (3): 709–37. https://doi.org/10.1152/physrev.00036.2013.

Ding, Yu, Christopher G. Hubert, Jacob Herman, Philip Corrin, Chad M. Toledo, Kyobi Skutt-Kakaria, Julio Vazquez, et al. 2013. “Cancer-Specific Requirement for BUB1B/BUBR1 in Human Brain Tumor Isolates and Genetically Transformed Cells.” *Cancer Discovery* 3 (2): 198–211. https://doi.org/10.1158/2159-8290.CD-12-0353.

Dong, Chengya, Zhengrong Yuan, Qi Li, and Yajie Wang. 2018. “The Clinicopathological and Prognostic Significance of TP53 Alteration in K27M Mutated Gliomas: An Individual-Participant Data Meta-Analysis.” *Neurological Sciences* 39 (7): 1191–1201. https://doi.org/10.1007/s10072-018-3407-1.

Douki, Thierry, Jean-Luc Ravanat, Dimitar Angelov, J. Richard Wagner, and Jean Cadet. 2004. “Effects of Duplex Stability on Charge-Transfer Efficiency within DNA.” In *Long-Range Charge Transfer in DNA I*, 1–25. Topics in Current Chemistry. Springer, Berlin, Heidelberg. https://doi.org/10.1007/b94409.

Du, Zhanhui, Xiuxiang Song, Fangfang Yan, Jingjing Wang, Yuxia Zhao, and Shangming Liu. 2018. “Genome-Wide Transcriptional Analysis of BRD4-Regulated Genes and Pathways in Human Glioma U251 Cells.” *International Journal of Oncology*, March. https://doi.org/10.3892/ijo.2018.4324.

Elbashir, S. M., J. Harborth, W. Lendeckel, A. Yalcin, K. Weber, and T. Tuschl. 2001. “Duplexes of 21-Nucleotide RNAs Mediate RNA Interference in Cultured Mammalian Cells.” *Nature* 411 (6836): 494–98. https://doi.org/10.1038/35078107.

Enns, L., A. Rasouli-Nia, M. Hendzel, B. Marples, and M. Weinfeld. 2015. “Association of ATM Activation and DNA Repair with Induced Radioresistance after Low-Dose Irradiation.” *Radiation Protection Dosimetry* 166 (1–4): 131–36. https://doi.org/10.1093/rpd/ncv203.

Evers, Bastiaan, Katarzyna Jastrzebski, Jeroen P. M. Heijmans, Wipawadee Grernrum, Roderick L. Beijersbergen, and Rene Bernards. 2016. “CRISPR

Knockout Screening Outperforms shRNA and CRISPRi in Identifying Essential Genes." *Nature Biotechnology* 34 (6): 631–33. https://doi.org/10.1038/nbt.3536.

Falck, Jacob, Julia Coates, and Stephen P. Jackson. 2005. "Conserved Modes of Recruitment of ATM, ATR and DNA-PKcs to Sites of DNA Damage." *Nature* 434 (7033): 605–11. https://doi.org/10.1038/nature03442.

Fan, Xing, William Matsui, Leila Khaki, Duncan Stearns, Jiong Chun, Yue-Ming Li, and Charles G. Eberhart. 2006. "Notch Pathway Inhibition Depletes Stem-like Cells and Blocks Engraftment in Embryonal Brain Tumors." *Cancer Research* 66 (15): 7445–52. https://doi.org/10.1158/0008-5472.CAN-06-0858.

Farhan, Mohd, Haitao Wang, Uma Gaur, Peter J. Little, Jiangping Xu, and Wenhua Zheng. 2017. "FOXO Signaling Pathways as Therapeutic Targets in Cancer." *International Journal of Biological Sciences* 13 (7): 815–27. https://doi.org/10.7150/ijbs.20052.

Fedorov, Oleg, Brian Marsden, Vanda Pogacic, Peter Rellos, Susanne Müller, Alex N. Bullock, Juerg Schwaller, Michael Sundström, and Stefan Knapp. 2007. "A Systematic Interaction Map of Validated Kinase Inhibitors with Ser/Thr Kinases." *Proceedings of the National Academy of Sciences of the United States of America* 104 (51): 20523–28. https://doi.org/10.1073/pnas.0708800104.

Fei, Peiwen, and Wafik S. El-Deiry. 2003. "P53 and Radiation Responses." *Oncogene* 22 (37): 5774–83. https://doi.org/10.1038/sj.onc.1206677.

Filbin, Mariella G., Itay Tirosh, Volker Hovestadt, McKenzie L. Shaw, Leah E. Escalante, Nathan D. Mathewson, Cyril Neftel, et al. 2018. "Developmental and Oncogenic Programs in H3K27M Gliomas Dissected by Single-Cell RNA-Seq." *Science (New York, N.Y.)* 360 (6386): 331–35. https://doi.org/10.1126/science.aao4750.

Fineran, Peter C., and Emmanuelle Charpentier. 2012. "Memory of Viral Infections by CRISPR-Cas Adaptive Immune Systems: Acquisition of New Information." *Virology* 434 (2): 202–9. https://doi.org/10.1016/j.virol.2012.10.003.

Fire, Andrew, SiQun Xu, Mary K. Montgomery, Steven A. Kostas, Samuel E. Driver, and Craig C. Mello. 1998. "Potent and Specific Genetic Interference by Double-Stranded RNA in *Caenorhabditis Elegans*." *Nature* 391 (6669): 806–11. https://doi.org/10.1038/35888.

Foiani M., Lucca C., and Ferrari E. 2010. "A Lethal Combination for Cancer Cells: Synthetic Lethality Screenings for Drug Discovery." *European Journal of Cancer* 46 (16): 2889–95. https://doi.org/10.1016/j.ejca.2010.07.031.

Fontebasso, Adam M., Simon Papillon-Cavanagh, Jeremy Schwartzentruber, Hamid Nikbakht, Noha Gerges, Pierre-Olivier Fiset, Denise Bechet, et al. 2014. "Recurrent Somatic Mutations in ACVR1 in Pediatric Midline High-Grade Astrocytoma." *Nature Genetics* 46 (5): 462–66. https://doi.org/10.1038/ng.2950.

Gage, Fred H. 2000. "Mammalian Neural Stem Cells." *Science* 287 (5457): 1433–38. https://doi.org/10.1126/science.287.5457.1433.

Gao, Shan, Chen Yang, Shan Jiang, Xiao-Ning Xu, Xin Lu, You-Wen He, Annie Cheung, and Hui Wang. 2014. "Applications of RNA Interference High-Throughput Screening Technology in Cancer Biology and Virology." *Protein & Cell* 5 (11): 805–15. https://doi.org/10.1007/s13238-014-0076-6.

Garcia, Benjamin A., Sandra B. Hake, Robert L. Diaz, Monika Kauer, Stephanie A. Morris, Judith Recht, Jeffrey Shabanowitz, et al. 2007. “Organismal Differences in Post-Translational Modifications in Histones H3 and H4.” *The Journal of Biological Chemistry* 282 (10): 7641–55. https://doi.org/10.1074/jbc.M607900200.

Gargiulo, Gaetano, Matteo Cesaroni, Michela Serresi, Nienke de Vries, Danielle Hulsman, Sophia W. Bruggeman, Cesare Lancini, and Maarten van Lohuizen. 2013. “In Vivo RNAi Screen for BMI1 Targets Identifies TGF-β/BMP-ER Stress Pathways as Key Regulators of Neural- and Malignant Glioma-Stem Cell Homeostasis.” *Cancer Cell* 23 (5): 660–76. https://doi.org/10.1016/j.ccr.2013.03.030.

Geoerger, Birgit, Darren Hargrave, Fabienne Thomas, Anna Ndiaye, Didier Frappaz, Felipe Andreiuolo, Pascale Varlet, et al. 2011. “Innovative Therapies for Children with Cancer Pediatric Phase I Study of Erlotinib in Brainstem Glioma and Relapsing/Refractory Brain Tumors.” *Neuro-Oncology* 13 (1): 109–18. https://doi.org/10.1093/neuonc/noq141.

Gilbert, Luke A., Max A. Horlbeck, Britt Adamson, Jacqueline E. Villalta, Yuwen Chen, Evan H. Whitehead, Carla Guimaraes, et al. 2014. “Genome-Scale CRISPR-Mediated Control of Gene Repression and Activation.” *Cell* 159 (3): 647–61. https://doi.org/10.1016/j.cell.2014.09.029.

Gilbert, Scott F. 2000. *Developmental Biology*. 6th ed. Sinauer Associates.

Ginhoux, Florent, Shawn Lim, Guillaume Hoeffel, Donovan Low, and Tara Huber. 2013. “Origin and Differentiation of Microglia.” *Frontiers in Cellular Neuroscience* 7. https://doi.org/10.3389/fncel.2013.00045.

Goidts, V., J. Bageritz, L. Puccio, S. Nakata, M. Zapatka, S. Barbus, G. Toedt, et al. 2012. “RNAi Screening in Glioma Stem-like Cells Identifies PFKFB4 as a Key Molecule Important for Cancer Cell Survival.” *Oncogene* 31 (27): 3235–43. https://doi.org/10.1038/onc.2011.490.

Goldberg, Aaron D., Laura A. Banaszynski, Kyung-Min Noh, Peter W. Lewis, Simon J. Elsaesser, Sonja Stadler, Scott Dewell, et al. 2010. “Distinct Factors Control Histone Variant H3.3 Localization at Specific Genomic Regions.” *Cell* 140 (5): 678–91. https://doi.org/10.1016/j.cell.2010.01.003.

Goodwin, Jonathan F., and Karen E. Knudsen. 2014. “Beyond DNA Repair: DNA-PK Function in Cancer.” *Cancer Discovery* 4 (10): 1126–39. https://doi.org/10.1158/2159-8290.CD-14-0358.

Goto, Yoko, Sho Koyasu, Minoru Kobayashi, and Hiroshi Harada. 2017. “The Emerging Roles of the Ubiquitination/Deubiquitination System in Tumor Radioresistance Regarding DNA Damage Responses, Cell Cycle Regulation, Hypoxic Responses, and Antioxidant Properties: Insight into the Development of Novel Radiosensitizing Strategies.” *Mutation Research/Fundamental and Molecular Mechanisms of Mutagenesis* 803–805 (October): 76–81. https://doi.org/10.1016/j.mrfmmm.2017.07.007.

“GPP Web Portal - Protocols.” n.d. Accessed June 26, 2017. http://portals.broadinstitute.org/gpp/public/resources/protocols.

Grasso, Catherine S., Yujie Tang, Nathalene Truffaux, Noah E. Berlow, Lining Liu, Marie-Anne Debily, Michael J. Quist, et al. 2015a. “Functionally Defined Therapeutic Targets in Diffuse Intrinsic Pontine Glioma.” *Nature Medicine* 21 (6): 555–59. https://doi.org/10.1038/nm.3855.

———. 2015b. “Functionally Defined Therapeutic Targets in Diffuse Intrinsic

Pontine Glioma." *Nature Medicine* 21 (6): 555–59. https://doi.org/10.1038/nm.3855.

Graves, Paul, and Yan Zeng. 2012. "Biogenesis of Mammalian MicroRNAs: A Global View." *Genomics, Proteomics & Bioinformatics* 10 (5): 239–45. https://doi.org/10.1016/j.gpb.2012.06.004.

Grill, Jacques, Stephanie Puget, Felipe Andreiuolo, Cathy Philippe, and Laura MacConaill. 2012. "Critical Oncogenic Mutations in Newly Diagnosed Pediatric Diffuse Intrinsic Pontine Glioma." *Pediatric Blood & Cancer* 58 (4): 489–91. https://doi.org/10.1002/pbc.24060.

Grill, Jacques, Stephanie Puget, Felipe Andreiuolo, Cathy Philippe, Laura MacConaill, and Mark W. Kieran. 2012. "Critical Oncogenic Mutations in Newly Diagnosed Pediatric Diffuse Intrinsic Pontine Glioma." *Pediatric Blood & Cancer* 58 (4): 489–91. https://doi.org/10.1002/pbc.24060.

Gröbner, Susanne N., Barbara C. Worst, Joachim Weischenfeldt, Ivo Buchhalter, Kortine Kleinheinz, Vasilisa A. Rudneva, Pascal D. Johann, et al. 2018. "The Landscape of Genomic Alterations across Childhood Cancers." *Nature* 555 (7696): 321–27. https://doi.org/10.1038/nature25480.

Guo, S., and K. J. Kemphues. 1995. "Par-1, a Gene Required for Establishing Polarity in C. Elegans Embryos, Encodes a Putative Ser/Thr Kinase That Is Asymmetrically Distributed." *Cell* 81 (4): 611–20.

Ha, Minju, and V. Narry Kim. 2014. "Regulation of microRNA Biogenesis." *Nature Reviews Molecular Cell Biology* 15 (8): 509–24. https://doi.org/10.1038/nrm3838.

Halliday, John, Karim Helmy, Siobhan S. Pattwell, Kenneth L. Pitter, Quincey LaPlant, Tatsuya Ozawa, and Eric C. Holland. 2014. "In Vivo Radiation Response of Proneural Glioma Characterized by Protective p53 Transcriptional Program and Proneural-Mesenchymal Shift." *Proceedings of the National Academy of Sciences of the United States of America* 111 (14): 5248–53. https://doi.org/10.1073/pnas.1321014111.

Han, Xuetao, Xiaoying Xue, Huandi Zhou, Ge Zhang, Xuetao Han, Xiaoying Xue, Huandi Zhou, and Ge Zhang. 2017. "A Molecular View of the Radioresistance of Gliomas." *Oncotarget* 8 (59): 100931–41. https://doi.org/10.18632/oncotarget.21753.

Hargrave, Darren, Ute Bartels, and Eric Bouffet. 2006a. "Diffuse Brainstem Glioma in Children: Critical Review of Clinical Trials." *The Lancet Oncology* 7 (3): 241–48. https://doi.org/10.1016/S1470-2045(06)70615-5.

———. 2006b. "Diffuse Brainstem Glioma in Children: Critical Review of Clinical Trials." *The Lancet Oncology* 7 (3): 241–48. https://doi.org/10.1016/S1470-2045(06)70615-5.

Harris, Peter S., Sujatha Venkataraman, Irina Alimova, Diane K. Birks, Andrew M. Donson, Jeffrey Knipstein, Adrian Dubuc, et al. 2012. "Polo-like Kinase 1 (PLK1) Inhibition Suppresses Cell Growth and Enhances Radiation Sensitivity in Medulloblastoma Cells." *BMC Cancer* 12 (March): 80. https://doi.org/10.1186/1471-2407-12-80.

Harrison, Charlotte. 2012. "RNA Interference: Reducing off-Target Effects of shRNA." Research Highlights. Nature Reviews Drug Discovery. December 31, 2012. https://doi.org/10.1038/nrd3933.

Hart, Traver, Kevin R. Brown, Fabrice Sircoulomb, Robert Rottapel, and Jason Moffat. 2014a. "Measuring Error Rates in Genomic Perturbation Screens:

Gold Standards for Human Functional Genomics." *Molecular Systems Biology* 10 (7): 733. https://doi.org/10.15252/msb.20145216.

———. 2014b. "Measuring Error Rates in Genomic Perturbation Screens: Gold Standards for Human Functional Genomics." *Molecular Systems Biology* 10 (July): 733.

Hart, Traver, Amy Hin Yan Tong, Katie Chan, Jolanda Van Leeuwen, Ashwin Seetharaman, Michael Aregger, Megha Chandrashekhar, et al. 2017. "Evaluation and Design of Genome-Wide CRISPR/SpCas9 Knockout Screens." *G3 (Bethesda, Md.)* 7 (8): 2719–27. https://doi.org/10.1534/g3.117.041277.

Hashimoto, Hiroshi, Asami Hishiki, Kodai Hara, and Sotaro Kikuchi. 2017. "Structural Basis for the Molecular Interactions in DNA Damage Tolerances." *Biophysics and Physicobiology* 14 (December): 199–205. https://doi.org/10.2142/biophysico.14.0_199.

He, Lin, and Gregory J. Hannon. 2004. "MicroRNAs: Small RNAs with a Big Role in Gene Regulation." *Nature Reviews Genetics* 5 (7): 522–31. https://doi.org/10.1038/nrg1379.

Hennika, Tammy, Guo Hu, Nagore G. Olaciregui, Kelly L. Barton, Anahid Ehteda, Arjanna Chitranjan, Cecilia Chang, et al. 2017. "Pre-Clinical Study of Panobinostat in Xenograft and Genetically Engineered Murine Diffuse Intrinsic Pontine Glioma Models." *PLoS ONE* 12 (1). https://doi.org/10.1371/journal.pone.0169485.

Higgins, Geoff S, Remko Prevo, Yin-Fai Lee, Thomas Helleday, Ruth J Muschel, Steve Taylor, Michio Yoshimura, Ian D Hickson, Eric J Bernhard, and W Gillies McKenna. 2010. "A siRNA Screen of Genes Involved in DNA Repair Identifies Tumour Specific Radiosensitisation by POLQ Knockdown." *Cancer Research* 70 (7): 2984–93. https://doi.org/10.1158/0008-5472.CAN-09-4040.

Hilton, Isaac B., Anthony M. D'Ippolito, Christopher M. Vockley, Pratiksha I. Thakore, Gregory E. Crawford, Timothy E. Reddy, and Charles A. Gersbach. 2015. "Epigenome Editing by a CRISPR-Cas9-Based Acetyltransferase Activates Genes from Promoters and Enhancers." *Nature Biotechnology* 33 (5): 510–17. https://doi.org/10.1038/nbt.3199.

Horvath, Philippe, and Rodolphe Barrangou. 2010. "CRISPR/Cas, the Immune System of Bacteria and Archaea." *Science (New York, N.Y.)* 327 (5962): 167–70. https://doi.org/10.1126/science.1179555.

Hossain, Mohammad B., Rehnuma Shifat, David G. Johnson, Mark T. Bedford, Konrad R. Gabrusiewicz, Nahir Cortes-Santiago, Xuemei Luo, et al. 2016. "TIE2-Mediated Tyrosine Phosphorylation of H4 Regulates DNA Damage Response by Recruiting ABL1." *Science Advances* 2 (4). https://doi.org/10.1126/sciadv.1501290.

Hossain, Mohammad B., Rehnuma Shifat, Jingyi Li, Xuemei Luo, Kenneth R. Hess, Yisel Rivera-Molina, Francisco Puerta Martinez, et al. 2017. "TIE2 Associates with Caveolae and Regulates Caveolin-1 To Promote Their Nuclear Translocation." *Molecular and Cellular Biology* 37 (21). https://doi.org/10.1128/MCB.00142-17.

Housden, Benjamin E., and Norbert Perrimon. 2016. "Comparing CRISPR and RNAi-Based Screening Technologies." *Nature Biotechnology* 34 (6): 621–23. https://doi.org/10.1038/nbt.3599.

Hover, Laura D., Philip Owens, Alexander L. Munden, Jialiang Wang, Lola B.

Chambless, Corey R. Hopkins, Charles C. Hong, Harold L. Moses, and Ty W. Abel. 2016. “Bone Morphogenetic Protein Signaling Promotes Tumorigenesis in a Murine Model of High-Grade Glioma.” *Neuro-Oncology* 18 (7): 928–38. https://doi.org/10.1093/neuonc/nov310.

Hu, Mingjun, Jieli Du, Lihong Cui, Tingqin Huang, Xiaoye Guo, Yonglin Zhao, Xudong Ma, et al. 2016. “IL-10 and PRKDC Polymorphisms Are Associated with Glioma Patient Survival.” *Oncotarget* 7 (49): 80680–87. https://doi.org/10.18632/oncotarget.13028.

Hu, Nan, Rachel Richards, and Randy Jensen. 2016. “Role of Chromosomal 1p/19q Co-Deletion on the Prognosis of Oligodendrogliomas: A Systematic Review and Meta-Analysis.” *Interdisciplinary Neurosurgery* 5 (September): 58–63. https://doi.org/10.1016/j.inat.2016.06.008.

Hubert, Christopher G., Robert K. Bradley, Yu Ding, Chad M. Toledo, Jacob Herman, Kyobi Skutt-Kakaria, Emily J. Girard, et al. 2013. “Genome-Wide RNAi Screens in Human Brain Tumor Isolates Reveal a Novel Viability Requirement for PHF5A.” *Genes & Development* 27 (9): 1032–45. https://doi.org/10.1101/gad.212548.112.

Hummel, Trent R., Ralph Salloum, Rachid Drissi, Shiva Kumar, Matthew Sobo, Stewart Goldman, Ahna Pai, et al. 2016. “A Pilot Study of Bevacizumab-Based Therapy in Patients with Newly Diagnosed High-Grade Gliomas and Diffuse Intrinsic Pontine Gliomas.” *Journal of Neuro-Oncology* 127 (1): 53–61. https://doi.org/10.1007/s11060-015-2008-6.

Hustedt, Nicole, and Daniel Durocher. 2017. “The Control of DNA Repair by the Cell Cycle.” *Nature Cell Biology* 19 (1): 1–9. https://doi.org/10.1038/ncb3452.

INCa. 2018. “Les Cancers En France - Édition 2017.” 2018. http://www.e-cancer.fr/ressources/cancers_en_france/.

Jackson, Aimee L., and Peter S. Linsley. 2010. “Recognizing and Avoiding siRNA off-Target Effects for Target Identification and Therapeutic Application.” *Nature Reviews Drug Discovery* 9 (1): 57–67. https://doi.org/10.1038/nrd3010.

Jaffray, David A., and Mary K. Gospodarowicz. 2015. “Radiation Therapy for Cancer.” In *Cancer: Disease Control Priorities, Third Edition (Volume 3)*, edited by Hellen Gelband, Prabhat Jha, Rengaswamy Sankaranarayanan, and Susan Horton. Washington (DC): The International Bank for Reconstruction and Development / The World Bank. http://www.ncbi.nlm.nih.gov/books/NBK343621/.

Jang, Chuan-Wei, Yoichiro Shibata, Joshua Starmer, Della Yee, and Terry Magnuson. 2015. “Histone H3.3 Maintains Genome Integrity during Mammalian Development.” *Genes & Development* 29 (13): 1377–92. https://doi.org/10.1101/gad.264150.115.

Jansen, M.H.A., D.G. van Vuurden, W.P. Vandertop, and G.J.L. Kaspers. 2012. “Diffuse Intrinsic Pontine Gliomas: A Systematic Update on Clinical Trials and Biology.” *Cancer Treatment Reviews* 38 (1): 27–35. https://doi.org/10.1016/j.ctrv.2011.06.007.

Janssens, Geert O., Lorenza Gandola, Stephanie Bolle, Henry Mandeville, Monica Ramos-Albiac, Karen van Beek, Helen Benghiat, et al. 2017. “Survival Benefit for Patients with Diffuse Intrinsic Pontine Glioma (DIPG) Undergoing Re-Irradiation at First Progression: A Matched-Cohort Analysis on Behalf of the SIOP-E-HGG/DIPG Working Group.” *European Journal of Cancer* 73

(March): 38–47. https://doi.org/10.1016/j.ejca.2016.12.007.

Janssens, Geert O., Marc H. Jansen, Selmer J. Lauwers, Peter J. Nowak, Foppe R. Oldenburger, Eric Bouffet, Frank Saran, et al. 2013. “Hypofractionation vs Conventional Radiation Therapy for Newly Diagnosed Diffuse Intrinsic Pontine Glioma: A Matched-Cohort Analysis.” *International Journal of Radiation Oncology, Biology, Physics* 85 (2): 315–20. https://doi.org/10.1016/j.ijrobp.2012.04.006.

Jeibmann, Astrid, and Werner Paulus. 2009. “Drosophila Melanogaster as a Model Organism of Brain Diseases.” *International Journal of Molecular Sciences* 10 (2): 407–40. https://doi.org/10.3390/ijms10020407.

Jennings, Mark T., Richard Sposto, James M. Boyett, L. Gilbert Vezina, Emi Holmes, Mitchell S. Berger, Carol S. Bruggers, et al. 2002. “Preradiation Chemotherapy in Primary High-Risk Brainstem Tumors: Phase II Study CCG-9941 of the Children’s Cancer Group.” *Journal of Clinical Oncology: Official Journal of the American Society of Clinical Oncology* 20 (16): 3431–37. https://doi.org/10.1200/JCO.2002.04.109.

Jenuwein, Thomas, and C. David Allis. 2001. “Translating the Histone Code.” *Science* 293 (5532): 1074–80. https://doi.org/10.1126/science.1063127.

Jiang, Yong, Haizheng Hong, Huachuan Cao, and Yinsheng Wang. 2007. “In Vivo Formation and in Vitro Replication of a Guanine-Thymine Intrastrand Cross-Link Lesion.” *Biochemistry* 46 (44): 12757–63. https://doi.org/10.1021/bi7012195.

Joerger, Andreas C., and Alan R. Fersht. 2016. “The p53 Pathway: Origins, Inactivation in Cancer, and Emerging Therapeutic Approaches.” *Annual Review of Biochemistry* 85 (1): 375–404. https://doi.org/10.1146/annurev-biochem-060815-014710.

Johnson, Kimberly J., Jennifer Cullen, Jill S. Barnholtz-Sloan, Quinn T. Ostrom, Chelsea E. Langer, Michelle C. Turner, Roberta McKean-Cowdin, et al. 2014. “Childhood Brain Tumor Epidemiology: A Brain Tumor Epidemiology Consortium Review.” *Cancer Epidemiology, Biomarkers & Prevention : A Publication of the American Association for Cancer Research, Cosponsored by the American Society of Preventive Oncology* 23 (12): 2716–36. https://doi.org/10.1158/1055-9965.EPI-14-0207.

Johnstone, Ricky W. 2002. “Histone-Deacetylase Inhibitors: Novel Drugs for the Treatment of Cancer.” *Nature Reviews Drug Discovery* 1 (4): 287–99. https://doi.org/10.1038/nrd772.

Jones, Chris, and Suzanne J. Baker. 2014. “Unique Genetic and Epigenetic Mechanisms Driving Paediatric Diffuse High-Grade Glioma.” *Nat Rev Cancer*, September. http://dx.doi.org/10.1038/nrc3811.

Kahn, Michael. 2015. “Wnt Signaling in Stem Cells and Tumor Stem Cells.” *Seminars in Reproductive Medicine* 33 (5): 317–25. https://doi.org/10.1055/s-0035-1558404.

Kampmann, Martin, Michael C. Bassik, and Jonathan S. Weissman. 2014. “Functional Genomics Platform for Pooled Screening and Mammalian Genetic Interaction Maps.” *Nature Protocols* 9 (8): 1825–47. https://doi.org/10.1038/nprot.2014.103.

Kampmann, Martin, Max A. Horlbeck, Yuwen Chen, Jordan C. Tsai, Michael C. Bassik, Luke A. Gilbert, Jacqueline E. Villalta, et al. 2015. “Next-Generation Libraries for Robust RNA Interference-Based Genome-Wide Screens.”

Proceedings of the National Academy of Sciences of the United States of America 112 (26): E3384-3391. https://doi.org/10.1073/pnas.1508821112.

Kang, Myung-Su, Tae-Yong Choi, Hye Guk Ryu, Dohyun Lee, Seung-Hyun Lee, Se-Young Choi, and Kyong-Tai Kim. 2017. “Autism-like Behavior Caused by Deletion of Vaccinia-Related Kinase 3 Is Improved by TrkB Stimulation.” *The Journal of Experimental Medicine* 214 (10): 2947–66. https://doi.org/10.1084/jem.20160974.

Kang, Tae-Hong, and Kyong-Tai Kim. 2006. “Negative Regulation of ERK Activity by VRK3-Mediated Activation of VHR Phosphatase.” *Nature Cell Biology* 8 (8): 863. https://doi.org/10.1038/ncb1447.

Kao, Gary D., Zibin Jiang, Anne Marie Fernandes, Anjali K. Gupta, and Amit Maity. 2007. “Inhibition of Phosphatidylinositol-3-OH Kinase/Akt Signaling Impairs DNA Repair in Glioblastoma Cells Following Ionizing Radiation.” *The Journal of Biological Chemistry* 282 (29): 21206–12. https://doi.org/10.1074/jbc.M703042200.

Kastan, Michael B., and Jiri Bartek. 2004. “Cell-Cycle Checkpoints and Cancer.” Special Features. Nature. November 17, 2004. https://doi.org/10.1038/nature03097.

Katagiri, Takenobu. 2012. “Recent Topics in Fibrodysplasia Ossificans Progressiva.” *Journal of Oral Biosciences* 54 (3): 119–23. https://doi.org/10.1016/j.job.2012.03.004.

Kelley, Kevin, Jonathan Knisely, Marc Symons, and Rosamaria Ruggieri. 2016. “Radioresistance of Brain Tumors.” *Cancers* 8 (4). https://doi.org/10.3390/cancers8040042.

Keunen, Kristin, Serena J. Counsell, and Manon J. N. L. Benders. 2017. “The Emergence of Functional Architecture during Early Brain Development.” *NeuroImage*, Functional Architecture of the Brain, 160 (October): 2–14. https://doi.org/10.1016/j.neuroimage.2017.01.047.

Khuong-Quang, Dong-Anh, Pawel Buczkowicz, Patricia Rakopoulos, Xiao-Yang Liu, Adam M. Fontebasso, Eric Bouffet, Ute Bartels, et al. 2012. “K27M Mutation in Histone H3.3 Defines Clinically and Biologically Distinct Subgroups of Pediatric Diffuse Intrinsic Pontine Gliomas.” *Acta Neuropathologica* 124 (3): 439–47. https://doi.org/10.1007/s00401-012-0998-0.

Kim, Jinkuk, Yeri Lee, Hee-Jin Cho, Young-Eun Lee, Jaeyeol An, Gye-Hyun Cho, Young-Hyeh Ko, Kyeung Min Joo, and Do-Hyun Nam. 2014. “NTRK1 Fusion in Glioblastoma Multiforme.” *PLoS ONE* 9 (3). https://doi.org/10.1371/journal.pone.0091940.

Kim, Kang Ho, Ho Jun Seol, Eun Hee Kim, Jinguen Rheey, Hyun Jin Jin, Yeri Lee, Kyeung Min Joo, Jeongwu Lee, and Do-Hyun Nam. 2013. “Wnt/β-Catenin Signaling Is a Key Downstream Mediator of MET Signaling in Glioblastoma Stem Cells.” *Neuro-Oncology* 15 (2): 161–71. https://doi.org/10.1093/neuonc/nos299.

Kim, Taik H., Hong W. Chin, Susan Pollan, Joseph H. Hazel, and John H. Webster. 1980. “Radiotherapy of Primary Brain Stem Tumors.” *International Journal of Radiation Oncology*Biology*Physics* 6 (1): 51–57. https://doi.org/10.1016/0360-3016(80)90203-5.

Kim, Yonghyun, Kang Ho Kim, Jeena Lee, Young-Ae Lee, Misuk Kim, Se Jeong Lee, Kernyu Park, et al. 2012. “Wnt Activation Is Implicated in Glioblastoma Radioresistance.” *Laboratory Investigation; a Journal of Technical Methods*

and Pathology 92 (3): 466–73. https://doi.org/10.1038/labinvest.2011.161.

Kleiblova, Petra, Indra A. Shaltiel, Jan Benada, Jan Ševčík, Soňa Pecháčková, Petr Pohlreich, Emile E. Voest, et al. 2013. "Gain-of-Function Mutations of PPM1D/Wip1 Impair the p53-Dependent G1 Checkpoint." *The Journal of Cell Biology* 201 (4): 511–21. https://doi.org/10.1083/jcb.201210031.

Kleihues, P., P. C. Burger, and B. W. Scheithauer. 1993. "The New WHO Classification of Brain Tumours." *Brain Pathology (Zurich, Switzerland)* 3 (3): 255–68.

Kleihues, Paul, David N. Louis, Bernd W. Scheithauer, Lucy B. Rorke, Guido Reifenberger, Peter C. Burger, and Webster K. Cavenee. 2002. "The WHO Classification of Tumors of the Nervous System." *Journal of Neuropathology and Experimental Neurology* 61 (3): 215-225; discussion 226-229.

Komori, Takashi. 2017. "The 2016 WHO Classification of Tumours of the Central Nervous System: The Major Points of Revision." *Neurologia Medico-Chirurgica* 57 (7): 301–11. https://doi.org/10.2176/nmc.ra.2017-0010.

Konermann, Silvana, Mark D. Brigham, Alexandro E. Trevino, Julia Joung, Omar O. Abudayyeh, Clea Barcena, Patrick D. Hsu, et al. 2015. "Genome-Scale Transcriptional Activation by an Engineered CRISPR-Cas9 Complex." *Nature* 517 (7536): 583–88. https://doi.org/10.1038/nature14136.

Korones, David N., Paul G. Fisher, Cynthia Kretschmar, Tianni Zhou, Zhengjia Chen, James Kepner, and Carolyn Freeman. 2008. "Treatment of Children with Diffuse Intrinsic Brain Stem Glioma with Radiotherapy, Vincristine and Oral VP-16: A Children's Oncology Group Phase II Study." *Pediatric Blood & Cancer* 50 (2): 227–30. https://doi.org/10.1002/pbc.21154.

Korshunov, Andrey, Regina Sycheva, and Andrey Golanov. 2005. "The Prognostic Relevance of Molecular Alterations in Glioblastomas for Patients Age < 50 Years." *Cancer* 104 (4): 825–32. https://doi.org/10.1002/cncr.21221.

Korur, Serdar, Roland M. Huber, Balasubramanian Sivasankaran, Michael Petrich, Pier Morin, Brian A. Hemmings, Adrian Merlo, and Maria Maddalena Lino. 2009. "GSK3beta Regulates Differentiation and Growth Arrest in Glioblastoma." *PloS One* 4 (10): e7443. https://doi.org/10.1371/journal.pone.0007443.

Koschmann, Carl, Anda-Alexandra Calinescu, Felipe J. Nunez, Alan Mackay, Janet Fazal-Salom, Daniel Thomas, Flor Mendez, et al. 2016. "ATRX Loss Promotes Tumor Growth and Impairs Non-Homologous End Joining DNA Repair in Glioma." *Science Translational Medicine* 8 (328): 328ra28. https://doi.org/10.1126/scitranslmed.aac8228.

Kostović, Ivica, and Nataša Jovanov-Milošević. 2006. "The Development of Cerebral Connections during the First 20–45 Weeks' Gestation." *Seminars in Fetal and Neonatal Medicine* 11 (6): 415–22. https://doi.org/10.1016/j.siny.2006.07.001.

Kotliarova, Svetlana, Sandra Pastorino, Lara C. Kovell, Yuri Kotliarov, Hua Song, Wei Zhang, Rolanda Bailey, et al. 2008. "Glycogen Synthase Kinase-3 Inhibition Induces Glioma Cell Death through c-MYC, Nuclear Factor-kappaB, and Glucose Regulation." *Cancer Research* 68 (16): 6643–51. https://doi.org/10.1158/0008-5472.CAN-08-0850.

Kouzarides, Tony. 2007. "Chromatin Modifications and Their Function." *Cell* 128 (4): 693–705. https://doi.org/10.1016/j.cell.2007.02.005.

Kreso, Antonija, and John E. Dick. 2014. "Evolution of the Cancer Stem Cell Model."

Cell Stem Cell 14 (3): 275–91. https://doi.org/10.1016/j.stem.2014.02.006.

Kriegstein, Arnold, and Arturo Alvarez-Buylla. 2009. “The Glial Nature of Embryonic and Adult Neural Stem Cells.” *Annual Review of Neuroscience* 32: 149–84. https://doi.org/10.1146/annurev.neuro.051508.135600.

Krokan, Hans E., and Magnar Bjørås. 2013. “Base Excision Repair.” *Cold Spring Harbor Perspectives in Biology* 5 (4). https://doi.org/10.1101/cshperspect.a012583.

Kulkarni, Shreya, Surbhi Goel-Bhattacharya, Sejuti Sengupta, and Brent H. Cochran. 2018a. “A Large-Scale RNAi Screen Identifies SGK1 as a Key Survival Kinase for GBM Stem Cells.” *Molecular Cancer Research: MCR* 16 (1): 103–14. https://doi.org/10.1158/1541-7786.MCR-17-0146.

———. 2018b. “A Large-Scale RNAi Screen Identifies SGK1 as a Key Survival Kinase for GBM Stem Cells.” *Molecular Cancer Research* 16 (1): 103–14. https://doi.org/10.1158/1541-7786.MCR-17-0146.

Kunkel, Thomas A., and Dorothy A. Erie. 2005. “Dna Mismatch Repair.” *Annual Review of Biochemistry* 74 (1): 681–710. https://doi.org/10.1146/annurev.biochem.74.082803.133243.

Kwon, Deborah Y., Ying-Tao Zhao, Janine M. Lamonica, and Zhaolan Zhou. 2017. “Locus-Specific Histone Deacetylation Using a Synthetic CRISPR-Cas9-Based HDAC.” *Nature Communications* 8 (May): 15315. https://doi.org/10.1038/ncomms15315.

Lam, Jenny K W, Michael Y T Chow, Yu Zhang, and Susan W S Leung. 2015. “siRNA Versus miRNA as Therapeutics for Gene Silencing.” *Molecular Therapy. Nucleic Acids* 4 (9): e252. https://doi.org/10.1038/mtna.2015.23.

Langerak, Petra, and Paul Russell. 2011. “Regulatory Networks Integrating Cell Cycle Control with DNA Damage Checkpoints and Double-Strand Break Repair.” *Phil. Trans. R. Soc. B* 366 (1584): 3562–71. https://doi.org/10.1098/rstb.2011.0070.

Langhans, Julia, Lukas Schneele, Nancy Trenkler, Hélène Bandemer, Lisa Nonnenmacher, Georg Karpel-Massler, Markus D. Siegelin, et al. 2017. “The Effects of PI3K-Mediated Signalling on Glioblastoma Cell Behaviour.” *Oncogenesis* 6 (11): 398. https://doi.org/10.1038/s41389-017-0004-8.

Lans, Hannes, Jurgen A. Marteijn, and Wim Vermeulen. 2012. “ATP-Dependent Chromatin Remodeling in the DNA-Damage Response.” *Epigenetics & Chromatin* 5 (January): 4. https://doi.org/10.1186/1756-8935-5-4.

Lapin, Danielle H., Maria Tsoli, and David S. Ziegler. 2017. “Genomic Insights into Diffuse Intrinsic Pontine Glioma.” *Frontiers in Oncology* 7 (March). https://doi.org/10.3389/fonc.2017.00057.

Lee, Chang-Lung, Jordan M. Blum, and David G. Kirsch. 2013. “Role of p53 in Regulating Tissue Response to Radiation by Mechanisms Independent of Apoptosis.” *Translational Cancer Research* 2 (5): 412–21.

Lee, Chrissie Y., Ronald L. Johnson, Jennifer Wichterman-Kouznetsova, Rajarshi Guha, Marc Ferrer, Pinar Tuzmen, Scott E. Martin, Wenge Zhu, and Melvin L. DePamphilis. 2012. “High-Throughput Screening for Genes That Prevent Excess DNA Replication in Human Cells and for Molecules That Inhibit Them.” *Methods (San Diego, Calif.)* 57 (2): 234–48. https://doi.org/10.1016/j.ymeth.2012.03.031.

Lee, Fransiska. 1975. “Radiation of Infratentorial and Supratentorial Brain-Stem Tumors.” *Journal of Neurosurgery* 43 (1): 65–68.

https://doi.org/10.3171/jns.1975.43.1.0065.

Lee, Jia-Cheng, Keh-Shih Chuang, Yi-Wei Chen, Fang-Yuh Hsu, Fong-In Chou, Sang-Hue Yen, and Yuan-Hung Wu. 2017. “Preliminary Dosimetric Study on Feasibility of Multi-Beam Boron Neutron Capture Therapy in Patients with Diffuse Intrinsic Pontine Glioma without Craniotomy.” *PLoS ONE* 12 (6). https://doi.org/10.1371/journal.pone.0180461.

Lee, Jong-Ho, Rui Liu, Jing Li, Chuanbao Zhang, Yugang Wang, Qingsong Cai, Xu Qian, et al. 2017. “Stabilization of Phosphofructokinase 1 Platelet Isoform by AKT Promotes Tumorigenesis.” *Nature Communications* 8 (1): 949. https://doi.org/10.1038/s41467-017-00906-9.

Lee, Namgyu, Dae-Kyum Kim, Seung Hyun Han, Hye Guk Ryu, Sung Jin Park, Kyong-Tai Kim, and Kwan Yong Choi. 2017. “Comparative Interactomes of VRK1 and VRK3 with Their Distinct Roles in the Cell Cycle of Liver Cancer.” *Molecules and Cells* 40 (9): 621–31. https://doi.org/10.14348/molcells.2017.0108.

Lee, Yann, Adrienne C. Scheck, Timothy F. Cloughesy, Albert Lai, Jun Dong, Haumith K. Farooqi, Linda M. Liau, Steve Horvath, Paul S. Mischel, and Stanley F. Nelson. 2008. “Gene Expression Analysis of Glioblastomas Identifies the Major Molecular Basis for the Prognostic Benefit of Younger Age.” *BMC Medical Genomics* 1 (October): 52. https://doi.org/10.1186/1755-8794-1-52.

Lemmon, Mark A., and Joseph Schlessinger. 2010. “Cell Signaling by Receptor-Tyrosine Kinases.” *Cell* 141 (7): 1117–34. https://doi.org/10.1016/j.cell.2010.06.011.

Lerner, Robin G., Stefan Grossauer, Banafsheh Kadkhodaei, Ian Meyers, Maxim Sidorov, Katharina Koeck, Rintaro Hashizume, et al. 2015. “Targeting a Plk1-Controlled Polarity Checkpoint in Therapy-Resistant Glioblastoma-Propagating Cells.” *Cancer Research* 75 (24): 5355–66. https://doi.org/10.1158/0008-5472.CAN-14-3689.

Lessing, Derek, and Nancy M. Bonini. 2009. “Maintaining the Brain: Insight into Human Neurodegeneration From Drosophila Mutants.” *Nature Reviews. Genetics* 10 (6): 359. https://doi.org/10.1038/nrg2563.

Lewis, Peter W., Manuel M. Müller, Matthew S. Koletsky, Francisco Cordero, Shu Lin, Laura A. Banaszynski, Benjamin A. Garcia, Tom W. Muir, Oren J. Becher, and C. David Allis. 2013. “Inhibition of PRC2 Activity by a Gain-of-Function H3 Mutation Found in Pediatric Glioblastoma.” *Science* 340 (6134): 857–61. https://doi.org/10.1126/science.1232245.

Li, Guo-Min. 2008. “Mechanisms and Functions of DNA Mismatch Repair.” *Cell Research* 18 (1): 85–98. https://doi.org/10.1038/cr.2007.115.

Li, Hui-Fang, Jung-Sik Kim, and Todd Waldman. 2009. “Radiation-Induced Akt Activation Modulates Radioresistance in Human Glioblastoma Cells.” *Radiation Oncology (London, England)* 4 (October): 43. https://doi.org/10.1186/1748-717X-4-43.

Littman, Philip, Patricia Jarrett, Larissa T. Bilaniuk, Lucy B. Rorke, Robert A. Zimmerman, Derek A. Bruce, Steven C. Carabell, and Luis Schut. 1980. “Pediatric Brain Stem Gliomas.” *Cancer* 45 (11): 2787–92. https://doi.org/10.1002/1097-0142(19800601)45:11<2787::AID-CNCR2820451113>3.0.CO;2-V.

Liu, Ta-Jen, Dimpy Koul, Tiffany LaFortune, Ningyi Tiao, Rui Jun Shen, Sauveur-

Michel Maira, Carlos Garcia-Echevrria, and W. K. Alfred Yung. 2009. “NVP-BEZ235, a Novel Dual Phosphatidylinositol 3-Kinase/Mammalian Target of Rapamycin Inhibitor, Elicits Multifaceted Antitumor Activities in Human Gliomas.” *Molecular Cancer Therapeutics* 8 (8): 2204–10. https://doi.org/10.1158/1535-7163.MCT-09-0160.

Liu, Zhixian, Qingrong Sun, and Xiaosheng Wang. 2016. “PLK1, A Potential Target for Cancer Therapy.” *Translational Oncology* 10 (1): 22–32. https://doi.org/10.1016/j.tranon.2016.10.003.

Livak, K. J., and T. D. Schmittgen. 2001. “Analysis of Relative Gene Expression Data Using Real-Time Quantitative PCR and the 2(-Delta Delta C(T)) Method.” *Methods (San Diego, Calif.)* 25 (4): 402–8. https://doi.org/10.1006/meth.2001.1262.

Lobon-Iglesias, M. J., G. Giraud, D. Castel, C. Philippe, M. A. Debily, C. Briandet, F. Fouyssac, et al. 2018. “Diffuse Intrinsic Pontine Gliomas (DIPG) at Recurrence: Is There a Window to Test New Therapies in Some Patients?” *Journal of Neuro-Oncology* 137 (1): 111–18. https://doi.org/10.1007/s11060-017-2702-7.

Lomonaco, Stephanie L., Susan Finniss, Cunli Xiang, Ana Decarvalho, Felix Umansky, Steven N. Kalkanis, Tom Mikkelsen, and Chaya Brodie. 2009. “The Induction of Autophagy by Gamma-Radiation Contributes to the Radioresistance of Glioma Stem Cells.” *International Journal of Cancer* 125 (3): 717–22. https://doi.org/10.1002/ijc.24402.

Lord, Christopher J., and Alan Ashworth. 2012. “The DNA Damage Response and Cancer Therapy.” *Nature* 481 (7381): 287–94. https://doi.org/10.1038/nature10760.

Loughery, Jayne, Miranda Cox, Linda M. Smith, and David W. Meek. 2014. “Critical Role for p53-Serine 15 Phosphorylation in Stimulating Transactivation at p53-Responsive Promoters.” *Nucleic Acids Research* 42 (12): 7666–80. https://doi.org/10.1093/nar/gku501.

Louis, David N., Hiroko Ohgaki, Otmar D. Wiestler, Webster K. Cavenee, Peter C. Burger, Anne Jouvet, Bernd W. Scheithauer, and Paul Kleihues. 2007. “The 2007 WHO Classification of Tumours of the Central Nervous System.” *Acta Neuropathologica* 114 (2): 97–109. https://doi.org/10.1007/s00401-007-0243-4.

Louis, David N., Arie Perry, Guido Reifenberger, Andreas von Deimling, Dominique Figarella-Branger, Webster K. Cavenee, Hiroko Ohgaki, Otmar D. Wiestler, Paul Kleihues, and David W. Ellison. 2016. “The 2016 World Health Organization Classification of Tumors of the Central Nervous System: A Summary.” *Acta Neuropathologica* 131 (6): 803–20. https://doi.org/10.1007/s00401-016-1545-1.

Louvi, Angeliki, and Spyros Artavanis-Tsakonas. 2006. “Notch Signalling in Vertebrate Neural Development.” *Nature Reviews. Neuroscience* 7 (2): 93–102. https://doi.org/10.1038/nrn1847.

Ludwig, Kirsten, and Harley I. Kornblum. 2017. “Molecular Markers in Glioma.” *Journal of Neuro-Oncology* 134 (3): 505–12. https://doi.org/10.1007/s11060-017-2379-y.

Lund, E., and J. E. Dahlberg. 2006. “Substrate Selectivity of Exportin 5 and Dicer in the Biogenesis of microRNAs.” *Cold Spring Harbor Symposia on Quantitative Biology* 71: 59–66. https://doi.org/10.1101/sqb.2006.71.050.

Mackay, Alan, Anna Burford, Diana Carvalho, Elisa Izquierdo, Janat Fazal-Salom, Kathryn R. Taylor, Lynn Bjerke, et al. 2017a. “Integrated Molecular Meta-Analysis of 1,000 Pediatric High-Grade and Diffuse Intrinsic Pontine Glioma.” *Cancer Cell* 32 (4): 520–537.e5. https://doi.org/10.1016/j.ccell.2017.08.017.

———. 2017b. “Integrated Molecular Meta-Analysis of 1,000 Pediatric High-Grade and Diffuse Intrinsic Pontine Glioma.” *Cancer Cell* 32 (4): 520–537.e5. https://doi.org/10.1016/j.ccell.2017.08.017.

Madugundu, Guru S., Jean Cadet, and J. Richard Wagner. 2014. “Hydroxyl-Radical-Induced Oxidation of 5-Methylcytosine in Isolated and Cellular DNA.” *Nucleic Acids Research* 42 (11): 7450–60. https://doi.org/10.1093/nar/gku334.

Malik, Arif, Misbah Sultana, Aamer Qazi, Mahmood Husain Qazi, Gulshan Parveen, Sulayman Waquar, Abdul Basit Ashraf, and Mahmood Rasool. 2016. “Role of Natural Radiosensitizers and Cancer Cell Radioresistance: An Update.” Research article. Analytical Cellular Pathology. 2016. https://doi.org/10.1155/2016/6146595.

Mandell, Lynda R, Richard Kadota, Carolyn Freeman, Edwin C Douglass, James Fontanesi, Michael E Cohen, Edward Kovnar, et al. 1999. “There Is No Role for Hyperfractionated Radiotherapy in the Management of Children with Newly Diagnosed Diffuse Intrinsic Brainstem Tumors: Results of a Pediatric Oncology Group Phase III Trial Comparing Conventional vs. Hyperfractionated Radiotherapy.” *International Journal of Radiation Oncology*Biology*Physics* 43 (5): 959–64. https://doi.org/10.1016/S0360-3016(98)00501-X.

Mantamadiotis, Theo. 2017. “Towards Targeting PI3K-Dependent Regulation of Gene Expression in Brain Cancer.” *Cancers* 9 (6). https://doi.org/10.3390/cancers9060060.

Margueron, Raphaël, and Danny Reinberg. 2011. “The Polycomb Complex PRC2 and Its Mark in Life.” *Nature* 469 (7330): 343–49. https://doi.org/10.1038/nature09784.

Martin, Alberto, and Matthew D. Scharff. 2002. “AID and Mismatch Repair in Antibody Diversification.” *Nature Reviews Immunology* 2 (8): 605–14. https://doi.org/10.1038/nri858.

Martynoga, Ben, Daniela Drechsel, and François Guillemot. 2012. “Molecular Control of Neurogenesis: A View from the Mammalian Cerebral Cortex.” *Cold Spring Harbor Perspectives in Biology* 4 (10): a008359. https://doi.org/10.1101/cshperspect.a008359.

Marzluff, William F., Preetam Gongidi, Keith R. Woods, Jianping Jin, and Lois J. Maltais. 2002. “The Human and Mouse Replication-Dependent Histone Genes.” *Genomics* 80 (5): 487–98.

Massimino, Maura, Veronica Biassoni, Rosalba Miceli, Elisabetta Schiavello, Monika Warmuth-Metz, Piergiorgio Modena, Michela Casanova, et al. 2014. “Results of Nimotuzumab and Vinorelbine, Radiation and Re-Irradiation for Diffuse Pontine Glioma in Childhood.” *Journal of Neuro-Oncology* 118 (2): 305–12. https://doi.org/10.1007/s11060-014-1428-z.

McLachlan, Neil M., and Sarah J. Wilson. 2017. “The Contribution of Brainstem and Cerebellar Pathways to Auditory Recognition.” *Frontiers in Psychology* 8. https://doi.org/10.3389/fpsyg.2017.00265.

Mehta, Monal, Atif Khan, Shabbar Danish, Bruce G. Haffty, and Hatem E. Sabaawy. 2015. “Radiosensitization of Primary Human Glioblastoma Stem-like Cells

with Low-Dose AKT Inhibition." *Molecular Cancer Therapeutics* 14 (5): 1171–80. https://doi.org/10.1158/1535-7163.MCT-14-0708.

Metzlaff, M, M O'Dell, P. D Cluster, and R. B Flavell. 1997. "RNA-Mediated RNA Degradation and Chalcone Synthase A Silencing in Petunia." *Cell* 88 (6): 845–54. https://doi.org/10.1016/S0092-8674(00)81930-3.

Misuraca, Katherine L., Guo Hu, Kelly L. Barton, Alexander Chung, and Oren J. Becher. 2016. "A Novel Mouse Model of Diffuse Intrinsic Pontine Glioma Initiated in Pax3-Expressing Cells." *Neoplasia (New York, N.Y.)* 18 (1): 60–70. https://doi.org/10.1016/j.neo.2015.12.002.

Miyahara, Hiroaki, Sridevi Yadavilli, Manabu Natsumeda, Jeffrey A. Rubens, Louis Rodgers, Madhuri Kambhampati, Isabella C. Taylor, et al. 2017a. "The Dual mTOR Kinase Inhibitor TAK228 Inhibits Tumorigenicity and Enhances Radiosensitization in Diffuse Intrinsic Pontine Glioma." *Cancer Letters* 400: 110–16. https://doi.org/10.1016/j.canlet.2017.04.019.

———. 2017b. "The Dual mTOR Kinase Inhibitor TAK228 Inhibits Tumorigenicity and Enhances Radiosensitization in Diffuse Intrinsic Pontine Glioma." *Cancer Letters* 400 (August): 110–16. https://doi.org/10.1016/j.canlet.2017.04.019.

Mizutani, Ken-ichi, Keejung Yoon, Louis Dang, Akinori Tokunaga, and Nicholas Gaiano. 2007. "Differential Notch Signalling Distinguishes Neural Stem Cells from Intermediate Progenitors." *Nature* 449 (7160): 351–55. https://doi.org/10.1038/nature06090.

Moffat, Jason, and David M. Sabatini. 2006. "Building Mammalian Signalling Pathways with RNAi Screens." *Nature Reviews Molecular Cell Biology* 7 (3): 177–87. https://doi.org/10.1038/nrm1860.

Mohr, Stephanie E., and Norbert Perrimon. 2013. "RNAi Screening: New Approaches, Understandings, and Organisms." *Wiley Interdisciplinary Reviews: RNA* 3 (2): 145–58. https://doi.org/10.1002/wrna.110.

Mohr, Stephanie E., Jennifer A. Smith, Caroline E. Shamu, Ralph A. Neumüller, and Norbert Perrimon. 2014. "RNAi Screening Comes of Age: Improved Techniques and Complementary Approaches." *Nature Reviews. Molecular Cell Biology* 15 (9): 591–600. https://doi.org/10.1038/nrm3860.

Molnár, Zoltán, and Gavin Clowry. 2012. "Cerebral Cortical Development in Rodents and Primates." *Progress in Brain Research* 195: 45–70. https://doi.org/10.1016/B978-0-444-53860-4.00003-9.

Morgens, David W., Richard M. Deans, Amy Li, and Michael C. Bassik. 2016. "Systematic Comparison of CRISPR/Cas9 and RNAi Screens for Essential Genes." *Nature Biotechnology* 34 (6): 634–36. https://doi.org/10.1038/nbt.3567.

Morris, Saint-Aaron L., and Suyun Huang. 2016. "Crosstalk of the Wnt/β-Catenin Pathway with Other Pathways in Cancer Cells." *Genes & Diseases* 3 (1): 41–47. https://doi.org/10.1016/j.gendis.2015.12.003.

Moscoso, Gonzalo. 2009. "Early Embryonic Development of the Brain." In *Fetal and Neonatal Neurology and Neurosurgery*, 4th edition, 960. Atlanta, GA: Levene, M.I. & Chervenak, F.A. http://docplayer.net/4544085-Early-embryonic-development-of-the-brain-gonzalo-moscoso.html.

Nager, Mireia, Deepshikha Bhardwaj, Carles Cantí, Loreta Medina, Pere Nogués, and Judit Herreros. 2012. "β-Catenin Signalling in Glioblastoma Multiforme and Glioma-Initiating Cells." *Chemotherapy Research and Practice* 2012.

https://doi.org/10.1155/2012/192362.

Nandakumar, Pravanya, Alireza Mansouri, and Sunit Das. 2017. “The Role of ATRX in Glioma Biology.” *Frontiers in Oncology* 7 (September). https://doi.org/10.3389/fonc.2017.00236.

Napoli, C, C Lemieux, and R Jorgensen. 1990. “Introduction of a Chimeric Chalcone Synthase Gene into Petunia Results in Reversible Co-Suppression of Homologous Genes in Trans.” *The Plant Cell* 2 (4): 279–89.

Negretti, Laura, Karim Bouchireb, Christine Levy-Piedbois, Jean Louis Habrand, Frederic Dhermain, Chantal Kalifa, Jacques Grill, and Christelle Dufour. 2011. “Hypofractionated Radiotherapy in the Treatment of Diffuse Intrinsic Pontine Glioma in Children: A Single Institution’s Experience.” *Journal of Neuro-Oncology* 104 (3): 773–77. https://doi.org/10.1007/s11060-011-0542-4.

Ohgaki, Hiroko, and Paul Kleihues. 2007. “Genetic Pathways to Primary and Secondary Glioblastoma.” *The American Journal of Pathology* 170 (5): 1445–53. https://doi.org/10.2353/ajpath.2007.070011.

Olson, James. 2018. “Identification of Small Molecule Inhibitors of PHF5A for Glioblastoma.” *Grantome*. http://grantome.com/grant/NIH/R01-CA193841-01.

O’Neil, Nigel J., Melanie L. Bailey, and Philip Hieter. 2017. “Synthetic Lethality and Cancer.” *Nature Reviews Genetics* advance online publication (June). https://doi.org/10.1038/nrg.2017.47.

O’Rahilly, R., F. Müller, G. M. Hutchins, and G. W. Moore. 1987. “Computer Ranking of the Sequence of Appearance of 73 Features of the Brain and Related Structures in Staged Human Embryos during the Sixth Week of Development.” *The American Journal of Anatomy* 180 (1): 69–86. https://doi.org/10.1002/aja.1001800106.

Orr, Brent A., Haibo Bai, Yazmin Odia, Deepali Jain, Robert A. Anders, and Charles G. Eberhart. 2011. “Yes-Associated Protein 1 Is Widely Expressed in Human Brain Tumors and Promotes Glioblastoma Growth.” *Journal of Neuropathology and Experimental Neurology* 70 (7): 568–77. https://doi.org/10.1097/NEN.0b013e31821ff8d8.

Packer, Roger J., Mark Krailo, Minesh Mehta, Katherine Warren, Jeffrey Allen, Regina Jakacki, Judith G. Villablanca, Akiko Chiba, and Gregory Reaman. 2005. “Phase 1 Study of Concurrent RMP-7 and Carboplatin with Radiotherapy for Children with Newly Diagnosed Brainstem Gliomas.” *Cancer* 104 (6): 1281–87. https://doi.org/10.1002/cncr.21301.

Paddison, Patrick J., Amy A. Caudy, Emily Bernstein, Gregory J. Hannon, and Douglas S. Conklin. 2002. “Short Hairpin RNAs (shRNAs) Induce Sequence-Specific Silencing in Mammalian Cells.” *Genes & Development* 16 (8): 948–58. https://doi.org/10.1101/gad.981002.

Paddison, Patrick J., Jose M. Silva, Douglas S. Conklin, Mike Schlabach, Mamie Li, Shola Aruleba, Vivekanand Balija, et al. 2004. “A Resource for Large-Scale RNA-Interference-Based Screens in Mammals.” *Nature* 428 (6981): 427–31. https://doi.org/10.1038/nature02370.

Patel, Kunal S., Bob S. Carter, and Clark C. Chen. 2018. “Role of Biopsies in the Management of Intracranial Gliomas.” *Progress in Neurological Surgery* 30: 232–43. https://doi.org/10.1159/000464439.

Paugh, Barbara S., Alberto Broniscer, Chunxu Qu, Claudia P. Miller, Junyuan Zhang, Ruth G. Tatevossian, James M. Olson, et al. 2011. “Genome-Wide Analyses

Identify Recurrent Amplifications of Receptor Tyrosine Kinases and Cell-Cycle Regulatory Genes in Diffuse Intrinsic Pontine Glioma." *Journal of Clinical Oncology* 29 (30): 3999–4006. https://doi.org/10.1200/JCO.2011.35.5677.

Paugh, Barbara S, Chunxu Qu, Chris Jones, Zhaoli Liu, Martyna Adamowicz-Brice, Junyuan Zhang, Dorine A Bax, et al. 2010. "Integrated Molecular Genetic Profiling of Pediatric High-Grade Gliomas Reveals Key Differences With the Adult Disease." *Journal of Clinical Oncology* 28 (18): 3061–68. https://doi.org/10.1200/JCO.2009.26.7252.

Paugh, Barbara S., Xiaoyan Zhu, Chunxu Qu, Raelene Endersby, Alexander K. Diaz, Junyuan Zhang, Dorine A. Bax, et al. 2013. "Novel Oncogenic PDGFRA Mutations in Pediatric High-Grade Gliomas." *Cancer Research* 73 (20): 6219–29. https://doi.org/10.1158/0008-5472.CAN-13-1491.

Paull, Tanya T. 2015. "Mechanisms of ATM Activation." *Annual Review of Biochemistry* 84 (1): 711–38. https://doi.org/10.1146/annurev-biochem-060614-034335.

Pecot, Chad V., George A. Calin, Robert L. Coleman, Gabriel Lopez-Berestein, and Anil K. Sood. 2011. "RNA Interference in the Clinic: Challenges and Future Directions." *Nature Reviews Cancer* 11 (1): 59–67. https://doi.org/10.1038/nrc2966.

Petri, Sebastian, and Gunter Meister. 2013. "siRNA Design Principles and off-Target Effects." *Methods in Molecular Biology (Clifton, N.J.)* 986: 59–71. https://doi.org/10.1007/978-1-62703-311-4_4.

Piatek, Monica J., and Andreas Werner. 2014. "Endogenous siRNAs: Regulators of Internal Affairs." *Biochemical Society Transactions* 42 (4): 1174–79. https://doi.org/10.1042/BST20140068.

Plessier, Alexandre, Ludivine Le Dret, Pascale Varlet, Kévin Beccaria, Joëlle Lacombe, Sébastien Mériaux, Françoise Geffroy, et al. 2017. "New in Vivo Avatars of Diffuse Intrinsic Pontine Gliomas (DIPG) from Stereotactic Biopsies Performed at Diagnosis." *Oncotarget*, February. https://doi.org/10.18632/oncotarget.15002.

Plessier, Alexandre, Ludivine Le Dret, Pascale Varlet, Kévin Beccaria, Joëlle Lacombe, Sébastien Mériaux, Françoise Geffroy, et al. 2017. "New in Vivo Avatars of Diffuse Intrinsic Pontine Gliomas (DIPG) from Stereotactic Biopsies Performed at Diagnosis." *Oncotarget* 8 (32): 52543–59. https://doi.org/10.18632/oncotarget.15002.

Pollack, Ian F., Ronald L. Hamilton, C. David James, Sydney D. Finkelstein, Judith Burnham, Allan J. Yates, Emiko J. Holmes, Tianni Zhou, Jonathan L. Finlay, and Children's Oncology Group. 2006. "Rarity of PTEN Deletions and EGFR Amplification in Malignant Gliomas of Childhood: Results from the Children's Cancer Group 945 Cohort." *Journal of Neurosurgery* 105 (5 Suppl): 418–24. https://doi.org/10.3171/ped.2006.105.5.418.

Pollack, Ian F., Ronald L. Hamilton, Robert W. Sobol, Marina N. Nikiforova, Maureen A. Lyons-Weiler, William A. LaFramboise, Peter C. Burger, et al. 2011. "IDH1 Mutations Are Common in Malignant Gliomas Arising in Adolescents: A Report from the Children's Oncology Group." *Child's Nervous System : ChNS : Official Journal of the International Society for Pediatric Neurosurgery* 27 (1): 87–94. https://doi.org/10.1007/s00381-010-1264-1.

Pollack, Ian F., Clinton F. Stewart, Mehmet Kocak, Tina Young Poussaint, Alberto

Broniscer, Anu Banerjee, James G. Douglas, Larry E. Kun, James M. Boyett, and J. Russell Geyer. 2011. “A Phase II Study of Gefitinib and Irradiation in Children with Newly Diagnosed Brainstem Gliomas: A Report from the Pediatric Brain Tumor Consortium.” *Neuro-Oncology* 13 (3): 290–97. https://doi.org/10.1093/neuonc/noq199.

Polleux, F., and William Snider. 2010. “Initiating and Growing an Axon.” *Cold Spring Harbor Perspectives in Biology* 2 (4). https://doi.org/10.1101/cshperspect.a001925.

Porkholm, Mikaela, Leena Valanne, Tuula Lönnqvist, Stefan Holm, Birgitta Lannering, Pekka Riikonen, Dorota Wojcik, et al. 2014. “Radiation Therapy and Concurrent Topotecan Followed by Maintenance Triple Anti-Angiogenic Therapy with Thalidomide, Etoposide, and Celecoxib for Pediatric Diffuse Intrinsic Pontine Glioma.” *Pediatric Blood & Cancer* 61 (9): 1603–9. https://doi.org/10.1002/pbc.25045.

Pouget, J.-P., S. Frelon, J.-L. Ravanat, I. Testard, F. Odin, and J. Cadet. 2002. “Formation of Modified DNA Bases in Cells Exposed Either to Gamma Radiation or to High-LET Particles.” *Radiation Research* 157 (5): 589–95.

Puget, Stephanie, Kevin Beccaria, Thomas Blauwblomme, Thomas Roujeau, Syril James, Jacques Grill, Michel Zerah, Pascale Varlet, and Christian Sainte-Rose. 2015a. “Biopsy in a Series of 130 Pediatric Diffuse Intrinsic Pontine Gliomas.” *Child’s Nervous System* 31 (10): 1773–80. https://doi.org/10.1007/s00381-015-2832-1.

———. 2015b. “Biopsy in a Series of 130 Pediatric Diffuse Intrinsic Pontine Gliomas.” *Child’s Nervous System* 31 (10): 1773–80. https://doi.org/10.1007/s00381-015-2832-1.

Puget, Stephanie, Cathy Philippe, Dorine A. Bax, Bastien Job, Pascale Varlet, Marie-Pierre Junier, Felipe Andreiuolo, et al. 2012a. “Mesenchymal Transition and PDGFRA Amplification/Mutation Are Key Distinct Oncogenic Events in Pediatric Diffuse Intrinsic Pontine Gliomas.” *PLoS ONE* 7 (2): e30313. https://doi.org/10.1371/journal.pone.0030313.

———. 2012b. “Mesenchymal Transition and PDGFRA Amplification/Mutation Are Key Distinct Oncogenic Events in Pediatric Diffuse Intrinsic Pontine Gliomas.” *PLoS ONE* 7 (2): e30313. https://doi.org/10.1371/journal.pone.0030313.

Qi, Xiangrong Sharon, Frank Pajonk, Susan McCloskey, Daniel A. Low, Patrick Kupelian, Michael Steinberg, and Ke Sheng. 2017. “Radioresistance of the Breast Tumor Is Highly Correlated to Its Level of Cancer Stem Cell and Its Clinical Implication for Breast Irradiation.” *Radiotherapy and Oncology: Journal of the European Society for Therapeutic Radiology and Oncology* 124 (3): 455–61. https://doi.org/10.1016/j.radonc.2017.08.019.

Qian, Xueming, Qin Shen, Susan K. Goderie, Wenlei He, Alexandra Capela, Andrew A. Davis, and Sally Temple. 2000. “Timing of CNS Cell Generation: A Programmed Sequence of Neuron and Glial Cell Production from Isolated Murine Cortical Stem Cells.” *Neuron* 28 (1): 69–80. https://doi.org/10.1016/S0896-6273(00)00086-6.

Rajagopal, Nisha, Sharanya Srinivasan, Kameron Kooshesh, Yuchun Guo, Matthew D. Edwards, Budhaditya Banerjee, Tahin Syed, Bart J. M. Emons, David K. Gifford, and Richard I. Sherwood. 2016. “High-Throughput Mapping of Regulatory DNA.” *Nature Biotechnology* 34 (2): 167–74. https://doi.org/10.1038/nbt.3468.

Regad, Tarik. 2015. “Targeting RTK Signaling Pathways in Cancer.” *Cancers* 7 (3): 1758–84. https://doi.org/10.3390/cancers7030860.

Reid, Paul Ambrose, Puthenparampil Wilson, Yanrui Li, Loredana Gabriela Marcu, and Eva Bezak. 2017. “Current Understanding of Cancer Stem Cells: Review of Their Radiobiology and Role in Head and Neck Cancers.” *Head & Neck* 39 (9): 1920–32. https://doi.org/10.1002/hed.24848.

Reinhardt, H. Christian, Aaron S. Aslanian, Jacqueline A. Lees, and Michael B. Yaffe. 2007. “p53-Deficient Cells Rely on ATM- and ATR-Mediated Checkpoint Signaling through the p38MAPK/MK2 Pathway for Survival after DNA Damage.” *Cancer Cell* 11 (2): 175–89. https://doi.org/10.1016/j.ccr.2006.11.024.

Reynolds, Pamela, Stanley W. Botchway, Anthony W. Parker, and Peter O’Neill. 2013. “Spatiotemporal Dynamics of DNA Repair Proteins Following Laser Microbeam Induced DNA Damage – When Is a DSB Not a DSB?” *Mutation Research* 756 (1–2): 14–20. https://doi.org/10.1016/j.mrgentox.2013.05.006.

Rock, K, O Mcardle, P Forde, M Dunne, D Fitzpatrick, B O’Neill, and C Faul. 2012. “A Clinical Review of Treatment Outcomes in Glioblastoma Multiforme—the Validation in a Non-Trial Population of the Results of a Randomised Phase III Clinical Trial: Has a More Radical Approach Improved Survival?” *The British Journal of Radiology* 85 (1017): e729–33. https://doi.org/10.1259/bjr/83796755.

Ropolo, Monica, Antonio Daga, Fabrizio Griffero, Mara Foresta, Gianluigi Casartelli, Annalisa Zunino, Alessandro Poggi, et al. 2009. “Comparative Analysis of DNA Repair in Stem and Nonstem Glioma Cell Cultures.” *Molecular Cancer Research* 7 (3): 383–92. https://doi.org/10.1158/1541-7786.MCR-08-0409.

Rossi, Marco, Letizia Magnoni, Clelia Miracco, Elisa Mori, Piero Tosi, Luigi Pirtoli, Paolo Tini, Giuseppe Oliveri, Elena Cosci, and Annette Bakker. 2011. “β-Catenin and Gli1 Are Prognostic Markers in Glioblastoma.” *Cancer Biology & Therapy* 11 (8): 753–61.

Roujeau, Thomas, Guilherme Machado, Matthew R. Garnett, Catherine Miquel, Stephanie Puget, Birgit Geoerger, Jacques Grill, et al. 2007. “Stereotactic Biopsy of Diffuse Pontine Lesions in Children.” *Journal of Neurosurgery* 107 (1 Suppl): 1–4. https://doi.org/10.3171/PED-07/07/001.

Rouleau, Michèle, Anand Patel, Michael J. Hendzel, Scott H. Kaufmann, and Guy G. Poirier. 2010. “PARP Inhibition: PARP1 and beyond.” *Nature Reviews Cancer* 10 (4): 293–301. https://doi.org/10.1038/nrc2812.

Rowitch, David H., and Arnold R. Kriegstein. 2010. “Developmental Genetics of Vertebrate Glial–cell Specification.” *Nature* 468 (7321): 214–22. https://doi.org/10.1038/nature09611.

Rzymski, T., P. Grzmil, A. Meinhardt, S. Wolf, and P. Burfeind. 2008. “PHF5A Represents a Bridge Protein between Splicing Proteins and ATP-Dependent Helicases and Is Differentially Expressed during Mouse Spermatogenesis.” *Cytogenetic and Genome Research* 121 (3–4): 232–44. https://doi.org/10.1159/000138890.

Sa, Jason K., Yeup Yoon, Misuk Kim, Yeonghwan Kim, Hee Jin Cho, Jin-Ku Lee, Gi-Soo Kim, et al. 2015. “In Vivo RNAi Screen Identifies NLK as a Negative Regulator of Mesenchymal Activity in Glioblastoma.” *Oncotarget* 6 (24): 20145–59. https://doi.org/10.18632/oncotarget.3980.

Sacco, Roberto, Emanuele Cacci, and Gaia Novarino. 2018. “Neural Stem Cells in

Neuropsychiatric Disorders." *Current Opinion in Neurobiology*, Neurobiology of Disease, 48 (February): 131–38. https://doi.org/10.1016/j.conb.2017.12.005.

Sander, Jeffry D., and J. Keith Joung. 2014. "CRISPR-Cas Systems for Editing, Regulating and Targeting Genomes." *Nature Biotechnology* 32 (4): 347–55. https://doi.org/10.1038/nbt.2842.

Satsuka, Ayano, Kavi Mehta, and Laimonis Laimins. 2015. "p38MAPK and MK2 Pathways Are Important for the Differentiation-Dependent Human Papillomavirus Life Cycle." *Journal of Virology* 89 (3): 1919–24. https://doi.org/10.1128/JVI.02712-14.

Schaefer, Christiane, Nikhil Mallela, Jochen Seggewiß, Birgit Lechtape, Heymut Omran, Uta Dirksen, Eberhard Korsching, and Jenny Potratz. 2018. "Target Discovery Screens Using Pooled shRNA Libraries and next-Generation Sequencing: A Model Workflow and Analytical Algorithm." *PLOS ONE* 13 (1): e0191570. https://doi.org/10.1371/journal.pone.0191570.

Schultz, Nikolaus, Dina R Marenstein, Dino A De Angelis, Wei-Qing Wang, Sven Nelander, Anders Jacobsen, Debora S Marks, Joan Massagué, and Chris Sander. 2011. "Off-Target Effects Dominate a Large-Scale RNAi Screen for Modulators of the TGF-β Pathway and Reveal microRNA Regulation of TGFBR2." *Silence* 2 (March): 3. https://doi.org/10.1186/1758-907X-2-3.

Schwartzentruber, Jeremy, Andrey Korshunov, Xiao-Yang Liu, David T. W. Jones, Elke Pfaff, Karine Jacob, Dominik Sturm, et al. 2012a. "Driver Mutations in Histone H3.3 and Chromatin Remodelling Genes in Paediatric Glioblastoma." *Nature* 482 (7384): 226–31. https://doi.org/10.1038/nature10833.

———. 2012b. "Driver Mutations in Histone H3.3 and Chromatin Remodelling Genes in Paediatric Glioblastoma." *Nature* 482 (7384): 226–31. https://doi.org/10.1038/nature10833.

Semple, Bridgette D., Klas Blomgren, Kayleen Gimlin, Donna M. Ferriero, and Linda J. Noble-Haeusslein. 2013. "Brain Development in Rodents and Humans: Identifying Benchmarks of Maturation and Vulnerability to Injury across Species." *Progress in Neurobiology* 0: 1–16. https://doi.org/10.1016/j.pneurobio.2013.04.001.

Shabalina, Svetlana A., and Eugene V. Koonin. 2008. "Origins and Evolution of Eukaryotic RNA Interference." *Trends in Ecology & Evolution* 23 (10): 578–87. https://doi.org/10.1016/j.tree.2008.06.005.

Shalem, Ophir, Neville E. Sanjana, Ella Hartenian, Xi Shi, David A. Scott, Tarjei Mikkelson, Dirk Heckl, et al. 2014. "Genome-Scale CRISPR-Cas9 Knockout Screening in Human Cells." *Science (New York, N.Y.)* 343 (6166): 84–87. https://doi.org/10.1126/science.1247005.

Sharma, Sonia, and Anjana Rao. 2009. "RNAi Screening: Tips and Techniques." *Nature Immunology* 10 (8): 799–804. https://doi.org/10.1038/ni0809-799.

Shriver, Marey, Saravanakumar Marimuthu, Colin Paul, Janelle Geist, Tessa Seale, Konstantinos Konstantopoulos, and Aikaterini Kontrogianni-Konstantopoulos. 2016. "Giant Obscurins Regulate the PI3K Cascade in Breast Epithelial Cells via Direct Binding to the PI3K/p85 Regulatory Subunit." *Oncotarget* 7 (29): 45414–28. https://doi.org/10.18632/oncotarget.9985.

Signore, M., F. Pelacchi, S. di Martino, D. Runci, M. Biffoni, S. Giannetti, L. Morgante, et al. 2014. "Combined PDK1 and CHK1 Inhibition Is Required to Kill Glioblastoma Stem-like Cells in Vitro and in Vivo." *Cell Death & Disease* 5

(May): e1223. https://doi.org/10.1038/cddis.2014.188.

Sims, David, Ana M Mendes-Pereira, Jessica Frankum, Darren Burgess, Maria-Antonietta Cerone, Cristina Lombardelli, Costas Mitsopoulos, et al. 2011. “High-Throughput RNA Interference Screening Using Pooled shRNA Libraries and next Generation Sequencing.” *Genome Biology* 12 (10): R104. https://doi.org/10.1186/gb-2011-12-10-r104.

Singleton, Katherine R., Keith T. Earley, and Lynn E. Heasley. 2017. “Analysis of Drug Resistance Using Kinome-Wide Functional Screens.” In *Kinase Signaling Networks*, 163–77. Methods in Molecular Biology. Humana Press, New York, NY. https://doi.org/10.1007/978-1-4939-7154-1_11.

Sirbu, Bianca M., and David Cortez. 2013. “DNA Damage Response: Three Levels of DNA Repair Regulation.” *Cold Spring Harbor Perspectives in Biology* 5 (8). https://doi.org/10.1101/cshperspect.a012724.

Smith, Joanne, Lye Mun Tho, Naihan Xu, and David A. Gillespie. 2010. “The ATM-Chk2 and ATR-Chk1 Pathways in DNA Damage Signaling and Cancer.” *Advances in Cancer Research* 108: 73–112. https://doi.org/10.1016/B978-0-12-380888-2.00003-0.

Smyth, L. M., P. a. W. Rogers, J. C. Crosbie, and J. F. Donoghue. 2017. “Characterization of Diffuse Intrinsic Pontine Glioma Radiosensitivity Using Synchrotron Microbeam Radiotherapy and Conventional Radiation Therapy In Vitro.” *Radiation Research* 189 (2): 146–55. https://doi.org/10.1667/RR4633.1.

Song, Gin-Ah, Hyun-Jung Kim, Kyung-Mi Woo, Jeong-Hwa Baek, Gwan-Shik Kim, Jin-Young Choi, and Hyun-Mo Ryoo. 2010. “Molecular Consequences of the ACVR1(R206H) Mutation of Fibrodysplasia Ossificans Progressiva.” *The Journal of Biological Chemistry* 285 (29): 22542–53. https://doi.org/10.1074/jbc.M109.094557.

Song, Haengjin, Wanil Kim, Sung-Hoon Kim, and Kyong-Tai Kim. 2016. “VRK3-Mediated Nuclear Localization of HSP70 Prevents Glutamate Excitotoxicity-Induced Apoptosis and Aβ Accumulation via Enhancement of ERK Phosphatase VHR Activity.” *Scientific Reports* 6 (1). https://doi.org/10.1038/srep38452.

Sonoda, Eiichiro, Helfrid Hochegger, Alihossein Saberi, Yoshihito Taniguchi, and Shunichi Takeda. 2006. “Differential Usage of Non-Homologous End-Joining and Homologous Recombination in Double Strand Break Repair.” *DNA Repair* 5 (9–10): 1021–29. https://doi.org/10.1016/j.dnarep.2006.05.022.

Sorrells, Shawn F., Mercedes F. Paredes, Arantxa Cebrian-Silla, Kadellyn Sandoval, Dashi Qi, Kevin W. Kelley, David James, et al. 2018. “Human Hippocampal Neurogenesis Drops Sharply in Children to Undetectable Levels in Adults.” *Nature* 555 (7696): 377–81. https://doi.org/10.1038/nature25975.

Sousa e Melo, Felipe de, and Louis Vermeulen. 2016. “Wnt Signaling in Cancer Stem Cell Biology.” *Cancers* 8 (7). https://doi.org/10.3390/cancers8070060.

Steck, J., and W. A. Friedman. 1995. “Stereotactic Biopsy of Brainstem Mass Lesions.” *Surgical Neurology* 43 (6): 563-567; discussion 567-568.

Stiles, Joan, and Terry L. Jernigan. 2010. “The Basics of Brain Development.” *Neuropsychology Review* 20 (4): 327–48. https://doi.org/10.1007/s11065-010-9148-4.

Strong, Michael J., Juanita Garces, Juan Carlos Vera, Mansour Mathkour, Noah Emerson, and Marcus L. Ware. 2015. “Brain Tumors: Epidemiology and

Current Trends in Treatment." *Journal of Tumour Research & Reports* 1 (1). https://doi.org/10.4172/2475-3203.1000102.

Sturm, Dominik, Hendrik Witt, Volker Hovestadt, Dong-Anh Khuong-Quang, David T.W. Jones, Carolin Konermann, Elke Pfaff, et al. 2012. "Hotspot Mutations in H3F3A and IDH1 Define Distinct Epigenetic and Biological Subgroups of Glioblastoma." *Cancer Cell* 22 (4): 425–37. https://doi.org/10.1016/j.ccr.2012.08.024.

Sudbery, Ian, Anton J Enright, Andrew G Fraser, and Ian Dunham. 2010. "Systematic Analysis of off-Target Effects in an RNAi Screen Reveals microRNAs Affecting Sensitivity to TRAIL-Induced Apoptosis." *BMC Genomics* 11 (March): 175. https://doi.org/10.1186/1471-2164-11-175.

Szenker, Emmanuelle, Dominique Ray-Gallet, and Geneviève Almouzni. 2011. "The Double Face of the Histone Variant H3.3." *Cell Research* 21 (3): 421–34. https://doi.org/10.1038/cr.2011.14.

Talarico, Cristina, Vincenzo Dattilo, Lucia D'Antona, Agnese Barone, Nicola Amodio, Stefania Belviso, Francesca Musumeci, et al. 2016. "SI113, a SGK1 Inhibitor, Potentiates the Effects of Radiotherapy, Modulates the Response to Oxidative Stress and Induces Cytotoxic Autophagy in Human Glioblastoma Multiforme Cells." *Oncotarget* 7 (13): 15868–84. https://doi.org/10.18632/oncotarget.7520.

Talbert, Paul B., and Steven Henikoff. 2017. "Histone Variants on the Move: Substrates for Chromatin Dynamics." *Nature Reviews Molecular Cell Biology* 18 (2): 115–26. https://doi.org/10.1038/nrm.2016.148.

Tandle, Anita T., Tamalee Kramp, Whoon J Kil, Aditya Halthore, Kristen Gehlhaus, Uma Shankavaram, Philip J. Tofilon, Natasha J. Caplen, and Kevin Camphausen. 2013a. "Inhibition of PLK1 in Glioblastoma Multiforme Induces Mitotic Catastrophe and Enhances Radiosensitization." *European Journal of Cancer (Oxford, England : 1990)* 49 (14): 3020–28. https://doi.org/10.1016/j.ejca.2013.05.013.

Tandle, Anita T., Tamalee Kramp, Whoon J. Kil, Aditya Halthore, Kristen Gehlhaus, Uma Shankavaram, Philip J. Tofilon, Natasha J. Caplen, and Kevin Camphausen. 2013b. "Inhibition of Polo-like Kinase 1 in Glioblastoma Multiforme Induces Mitotic Catastrophe and Enhances Radiosensitisation." *European Journal of Cancer (Oxford, England: 1990)* 49 (14): 3020–28. https://doi.org/10.1016/j.ejca.2013.05.013.

Tang, Yanyan, Wenwu He, Yunfei Wei, Zhanli Qu, Jinming Zeng, and Chao Qin. 2013. "Screening Key Genes and Pathways in Glioma Based on Gene Set Enrichment Analysis and Meta-Analysis." *Journal of Molecular Neuroscience: MN* 50 (2): 324–32. https://doi.org/10.1007/s12031-013-9981-z.

Tang, Zefang, Chenwei Li, Boxi Kang, Ge Gao, Cheng Li, and Zemin Zhang. 2017. "GEPIA: A Web Server for Cancer and Normal Gene Expression Profiling and Interactive Analyses." *Nucleic Acids Research* 45 (W1): W98–102. https://doi.org/10.1093/nar/gkx247.

Taylor, Isabella C., Marianne Hütt-Cabezas, William D. Brandt, Madhuri Kambhampati, Javad Nazarian, Howard T. Chang, Katherine E. Warren, Charles G. Eberhart, and Eric H. Raabe. 2015. "Disrupting NOTCH Slows Diffuse Intrinsic Pontine Glioma Growth, Enhances Radiation Sensitivity, and Shows Combinatorial Efficacy With Bromodomain Inhibition." *Journal of Neuropathology & Experimental Neurology* 74 (8): 778–90.

https://doi.org/10.1097/NEN.0000000000000216.

Taylor, K R, Alan Mackay, Nathalene Truffaux, Yaron S Butterfield, Olena Morozova, Cathy Philippe, David Castel, et al. 2014. “Recurrent Activating ACVR1 Mutations in Diffuse Intrinsic Pontine Glioma.” *Nat Genet* 46 (5): 457–61.

Taylor, Kathryn R, Alan Mackay, Nathalène Truffaux, Yaron S Butterfield, Olena Morozova, Cathy Philippe, David Castel, et al. 2014. “Recurrent Activating ACVR1 Mutations in Diffuse Intrinsic Pontine Glioma.” *Nature Genetics* 46 (5): 457–61. https://doi.org/10.1038/ng.2925.

Temple, Sally. 2001. “The Development of Neural Stem Cells.” Special Features. Nature. November 1, 2001. https://doi.org/10.1038/35102174.

Teng, Yang D., Filipe N. C. Santos, Peter M. Black, Deniz Konya, Kook In Park, Richard L. Sidman, and Evan Y. Snyder. 2008. “18 - Neural Stem Cells.” In *Principles of Regenerative Medicine*, edited by Anthony Atala, Robert Lanza, James A. Thomson, and Robert M. Nerem, 300–317. San Diego: Academic Press. https://doi.org/10.1016/B978-012369410-2.50020-6.

Thompson, Jordan M., Quy H. Nguyen, Manpreet Singh, and Olga V. Razorenova. 2015. “Approaches to Identifying Synthetic Lethal Interactions in Cancer.” *The Yale Journal of Biology and Medicine* 88 (2): 145–55.

Todorova, Pavlina Krasimirova, Bipasha Mukherjee, and Sandeep Burma. 2017. “MET Signaling Promotes DNA Repair and Radiation Resistance in Glioblastoma Stem-like Cells.” *Annals of Translational Medicine* 5 (3). https://doi.org/10.21037/atm.2017.01.67.

Truffaux, Nathalène, Cathy Philippe, Janna Paulsson, Felipe Andreiuolo, Léa Guerrini-Rousseau, Gaétan Cornilleau, Ludivine Le Dret, et al. 2015. “Preclinical Evaluation of Dasatinib Alone and in Combination with Cabozantinib for the Treatment of Diffuse Intrinsic Pontine Glioma.” *Neuro-Oncology* 17 (7): 953–64. https://doi.org/10.1093/neuonc/nou330.

Urbán, Noelia, and François Guillemot. 2014. “Neurogenesis in the Embryonic and Adult Brain: Same Regulators, Different Roles.” *Frontiers in Cellular Neuroscience* 8 (November). https://doi.org/10.3389/fncel.2014.00396.

Vanan, Magimairajan Issai, and David D. Eisenstat. 2015. “DIPG in Children – What Can We Learn from the Past?” *Frontiers in Oncology* 5 (October). https://doi.org/10.3389/fonc.2015.00237.

Vanhecke, Dominique, and Michal Janitz. 2005. “Functional Genomics Using High-Throughput RNA Interference.” *Drug Discovery Today* 10 (3): 205–12. https://doi.org/10.1016/S1359-6446(04)03352-5.

Varlet, Pascale, Marie-Anne Debily, Gwenael Le Teuff, Arnault Tauziede-Espariat, Mélanie Pages, Felipe Andreiuolo, Emanuele Lechapt-Zalcman, et al. 2018a. “DIPG-20. PRE-RANDOMISATION CENTRAL REVIEW AND REAL-TIME BIOMARKERS SCREENING IN THE MULTICENTRE BIOLOGICAL MEDICINE FOR DIPG ERADICATION (BIOMEDE) TRIAL: LESSONS LEARNT FROM THE FIRST 120 BIOPSIES.” *Neuro-Oncology* 20 (suppl_2): i52–53. https://doi.org/10.1093/neuonc/noy059.113.

———. 2018b. “DIPG-20. PRE-RANDOMISATION CENTRAL REVIEW AND REAL-TIME BIOMARKERS SCREENING IN THE MULTICENTRE BIOLOGICAL MEDICINE FOR DIPG ERADICATION (BIOMEDE) TRIAL: LESSONS LEARNT FROM THE FIRST 120 BIOPSIES.” *Neuro-Oncology* 20 (suppl_2): i52–53. https://doi.org/10.1093/neuonc/noy059.113.

Veldhuijzen van Zanten, Sophie E. M., Joshua Baugh, Brooklyn Chaney, Dennis De

Jongh, Esther Sanchez Aliaga, Frederik Barkhof, Johan Noltes, et al. 2017. “Development of the SIOPE DIPG Network, Registry and Imaging Repository: A Collaborative Effort to Optimize Research into a Rare and Lethal Disease.” *Journal of Neuro-Oncology* 132 (2): 255–66. https://doi.org/10.1007/s11060-016-2363-y.

Venneti, Sriram, Mihir T. Garimella, Lisa M. Sullivan, Daniel Martinez, Jason T. Huse, Adriana Heguy, Mariarita Santi, Craig B. Thompson, and Alexander R. Judkins. 2013. “Evaluation of Histone 3 Lysine 27 Trimethylation (H3K27me3) and Enhancer of Zest 2 (EZH2) in Pediatric Glial and Glioneuronal Tumors Shows Decreased H3K27me3 in H3F3A K27M Mutant Glioblastomas.” *Brain Pathology* 23 (5): 558–64. https://doi.org/10.1111/bpa.12042.

Verdone, Loredana, Micaela Caserta, and Ernesto Di Mauro. 2005. “Role of Histone Acetylation in the Control of Gene Expression.” *Biochemistry and Cell Biology = Biochimie Et Biologie Cellulaire* 83 (3): 344–53. https://doi.org/10.1139/o05-041.

Verhaak, Roel G.W., Katherine A. Hoadley, Elizabeth Purdom, Victoria Wang, Yuan Qi, Matthew D. Wilkerson, C. Ryan Miller, et al. 2010. “An Integrated Genomic Analysis Identifies Clinically Relevant Subtypes of Glioblastoma Characterized by Abnormalities in PDGFRA, IDH1, EGFR and NF1.” *Cancer Cell* 17 (1): 98. https://doi.org/10.1016/j.ccr.2009.12.020.

Veringa, Susanna J. E., Dennis Biesmans, Dannis G. van Vuurden, Marc H. A. Jansen, Laurine E. Wedekind, Ilona Horsman, Pieter Wesseling, et al. 2013. “In Vitro Drug Response and Efflux Transporters Associated with Drug Resistance in Pediatric High Grade Glioma and Diffuse Intrinsic Pontine Glioma.” *PloS One* 8 (4): e61512. https://doi.org/10.1371/journal.pone.0061512.

Vojta, Aleksandar, Paula Dobrinić, Vanja Tadić, Luka Bočkor, Petra Korać, Boris Julg, Marija Klasić, and Vlatka Zoldoš. 2016. “Repurposing the CRISPR-Cas9 System for Targeted DNA Methylation.” *Nucleic Acids Research* 44 (12): 5615–28. https://doi.org/10.1093/nar/gkw159.

Wang, Hao, Xiaoyu Mu, Hua He, and Xiao-Dong Zhang. 2018. “Cancer Radiosensitizers.” *Trends in Pharmacological Sciences* 39 (1): 24–48. https://doi.org/10.1016/j.tips.2017.11.003.

Wang, Jialiang, Timothy P. Wakeman, Justin D. Lathia, Anita B. Hjelmeland, Xiao-Fan Wang, Rebekah R. White, Jeremy N. Rich, and Bruce A. Sullenger. 2010. “Notch Promotes Radioresistance of Glioma Stem Cells.” *STEM CELLS* 28 (1): 17–28. https://doi.org/10.1002/stem.261.

Wang, Tim, Jenny J. Wei, David M. Sabatini, and Eric S. Lander. 2014. “Genetic Screens in Human Cells Using the CRISPR/Cas9 System.” *Science (New York, N.Y.)* 343 (6166): 80–84. https://doi.org/10.1126/science.1246981.

Wang, Wen-juan, Lin-mei Long, Neng Yang, Qing-qing Zhang, Wen-jun Ji, Jiang-hu Zhao, Zheng-hong Qin, Zhong Wang, Gang Chen, and Zhong-qin Liang. 2013. “NVP-BEZ235, a Novel Dual PI3K/mTOR Inhibitor, Enhances the Radiosensitivity of Human Glioma Stem Cells in Vitro.” *Acta Pharmacologica Sinica* 34 (5): 681–90. https://doi.org/10.1038/aps.2013.22.

Wang, Yanling, Haineng Xu, Tianrun Liu, Menggui Huang, Param-Puneet Butter, Chunsheng Li, Lin Zhang, et al. 2018. “Temporal DNA-PK Activation Drives Genomic Instability and Therapy Resistance in Glioma Stem Cells.” *JCI Insight* 3 (3). https://doi.org/10.1172/jci.insight.98096.

Warren, Katherine E. 2012. “Diffuse Intrinsic Pontine Glioma: Poised for Progress.” *Frontiers in Oncology* 2 (December). https://doi.org/10.3389/fonc.2012.00205.

Warren, Katherine E., Keith Killian, Miia Suuriniemi, Yonghong Wang, Martha Quezado, and Paul S. Meltzer. 2012. “Genomic Aberrations in Pediatric Diffuse Intrinsic Pontine Gliomas.” *Neuro-Oncology* 14 (3): 326–32. https://doi.org/10.1093/neuonc/nor190.

Webb, S. J., C. S. Monk, and C. A. Nelson. 2001. “Mechanisms of Postnatal Neurobiological Development: Implications for Human Development.” *Developmental Neuropsychology* 19 (2): 147–71. https://doi.org/10.1207/S15326942DN1902_2.

Wen, Patrick Y., and Santosh Kesari. 2008. “Malignant Gliomas in Adults | NEJM.” 2008. https://www-nejm-org.insb.bib.cnrs.fr/doi/full/10.1056/NEJMra0708126.

Wiedenheft, Blake, Samuel H. Sternberg, and Jennifer A. Doudna. 2012. “RNA-Guided Genetic Silencing Systems in Bacteria and Archaea.” *Nature* 482 (7385): 331–38. https://doi.org/10.1038/nature10886.

Wilson, Ross C., and Jennifer A. Doudna. 2013. “Molecular Mechanisms of RNA Interference.” *Annual Review of Biophysics* 42: 217–39. https://doi.org/10.1146/annurev-biophys-083012-130404.

Wolff, Johannes E., Michael E. Rytting, Tribhawan S. Vats, Peter E. Zage, Joann L. Ater, Shiao Woo, John Kuttesch, Leena Ketonen, and Anita Mahajan. 2012. “Treatment of Recurrent Diffuse Intrinsic Pontine Glioma: The MD Anderson Cancer Center Experience.” *Journal of Neuro-Oncology* 106 (2): 391–97. https://doi.org/10.1007/s11060-011-0677-3.

Wu, Gang, Alberto Broniscer, Troy A McEachron, Charles Lu, Barbara S Paugh, Jared Becksfort, Chunxu Qu, et al. 2012a. “Somatic Histone H3 Alterations in Pediatric Diffuse Intrinsic Pontine Gliomas and Non-Brainstem Glioblastomas.” *Nature Genetics* 44 (3): 251–53. https://doi.org/10.1038/ng.1102.

———. 2012b. “Somatic Histone H3 Alterations in Pediatric Diffuse Intrinsic Pontine Gliomas and Non-Brainstem Glioblastomas.” *Nature Genetics* 44 (3): 251–53. https://doi.org/10.1038/ng.1102.

Wu, Gang, Alexander K Diaz, Barbara S Paugh, Sherri L Rankin, Bensheng Ju, Yongjin Li, Xiaoyan Zhu, Chunxu Qu, Xiang Chen, Junyuan Zhang, John Easton, Michael Edmonson, Xiaotu Ma, Charles Lu, Panduka Nagahawatte, Erin Hedlund, Michael Rusch, Stanley Pounds, Tong Lin, Arzu Onar-Thomas, Robert Huether, Richard Kriwacki, Matthew Parker, Pankaj Gupta, Jared Becksfort, Lei Wei, Heather L Mulder, Kristy Boggs, Bhavin Vadodaria, Donald Yergeau, Jake C Russell, Kerri Ochoa, Robert S Fulton, Lucinda L Fulton, Chris Jones, Frederick A Boop, Alberto Broniscer, Cynthia Wetmore, Amar Gajjar, Li Ding, Elaine R Mardis, Richard K Wilson, Michael R Taylor, James R Downing, David W Ellison, Jinghui Zhang, and Suzanne J Baker. 2014. “The Genomic Landscape of Diffuse Intrinsic Pontine Glioma and Pediatric Non-Brainstem High-Grade Glioma.” *Nature Genetics* 46 (5): 444–50. https://doi.org/10.1038/ng.2938.

Wu, Gang, Alexander K. Diaz, Barbara S. Paugh, Sherri L. Rankin, Bensheng Ju, Yongjin Li, Xiaoyan Zhu, Chunxu Qu, Xiang Chen, Junyuan Zhang, John Easton, Michael Edmonson, Xiaotu Ma, Charles Lu, Panduka Nagahawatte,

Erin Hedlund, Michael Rusch, Stanley Pounds, Tong Lin, Arzu Onar-Thomas, Robert Huether, Richard Kriwacki, Matthew Parker, Pankaj Gupta, Jared Becksfort, Lei Wei, Heather L. Mulder, Kristy Boggs, Bhavin Vadodaria, Donald Yergeau, Jake C. Russell, Kerri Ochoa, Robert S. Fulton, Lucinda L. Fulton, Chris Jones, Frederick A. Boop, Alberto Broniscer, Cynthia Wetmore, Amar Gajjar, Li Ding, Elaine R. Mardis, Richard K. Wilson, Michael R. Taylor, James R. Downing, David W. Ellison, Jinghui Zhang, Suzanne J. Baker, et al. 2014. “The Genomic Landscape of Diffuse Intrinsic Pontine Glioma and Pediatric Non-Brainstem High-Grade Glioma.” *Nature Genetics* 46 (5): 444–50. https://doi.org/10.1038/ng.2938.

Wu, Jun, Guozheng Lai, Feng Wan, Zhengzheng Xiao, Lingcheng Zeng, Xiongwei Wang, Fei Ye, and Ting Lei. 2012. “Knockdown of Checkpoint Kinase 1 Is Associated with the Increased Radiosensitivity of Glioblastoma Stem-Like Cells.” *The Tohoku Journal of Experimental Medicine* 226 (4): 267–74. https://doi.org/10.1620/tjem.226.267.

Wurdak, Heiko, Shoutian Zhu, Angelica Romero, Mihaela Lorger, James Watson, Chih-Yuan Chiang, Jay Zhang, et al. 2010. “An RNAi Screen Identifies TRRAP as a Regulator of Brain Tumor-Initiating Cell Differentiation.” *Cell Stem Cell* 6 (1): 37–47. https://doi.org/10.1016/j.stem.2009.11.002.

Xie, Jie, Yan Li, Ke Jiang, Kaishun Hu, Sheng Zhang, Xiaorong Dong, Xiaofang Dai, et al. 2018. “CDK16 Phosphorylates and Degrades p53 to Promote Radioresistance and Predicts Prognosis in Lung Cancer.” *Theranostics* 8 (3): 650–62. https://doi.org/10.7150/thno.21963.

Xie, Li, Claude Gazin, Sung Mi Park, Lihua J. Zhu, Marie-anne Debily, Ellen L. W. Kittler, Maria L. Zapp, et al. 2012. “A Synthetic Interaction Screen Identifies Factors Selectively Required for Proliferation and TERT Transcription in p53-Deficient Human Cancer Cells.” *PLoS Genetics* 8 (12): e1003151. https://doi.org/10.1371/journal.pgen.1003151.

Xie, Shi-Yang, Guang Li, Chong Han, Yang-Yang Yu, and Nan Li. 2017. “RKIP Reduction Enhances Radioresistance by Activating the Shh Signaling Pathway in Non-Small-Cell Lung Cancer.” *OncoTargets and Therapy* 10: 5605–19. https://doi.org/10.2147/OTT.S149200.

Xu, Yan-Ming, Ji-Ying Du, and Andy T. Y. Lau. 2014. “Posttranslational Modifications of Human Histone H3: An Update.” *PROTEOMICS* 14 (17–18): 2047–60. https://doi.org/10.1002/pmic.201300435.

Yang, Hui, Dan Ye, Kun-Liang Guan, and Yue Xiong. 2012. “IDH1 and IDH2 Mutations in Tumorigenesis: Mechanistic Insights and Clinical Perspectives.” *Clinical Cancer Research : An Official Journal of the American Association for Cancer Research* 18 (20): 5562–71. https://doi.org/10.1158/1078-0432.CCR-12-1773.

Yang, Jian, Jing Fan, Ying Li, Fuhai Li, Peikai Chen, Yubo Fan, Xiaofeng Xia, and Stephen T. Wong. 2013. “Genome-Wide RNAi Screening Identifies Genes Inhibiting the Migration of Glioblastoma Cells.” *PloS One* 8 (4): e61915. https://doi.org/10.1371/journal.pone.0061915.

Yoshihara, Minako, Li Jiang, Shinya Akatsuka, Mikita Suyama, and Shinya Toyokuni. 2014. “Genome-Wide Profiling of 8-Oxoguanine Reveals Its Association with Spatial Positioning in Nucleus.” *DNA Research* 21 (6): 603–12. https://doi.org/10.1093/dnares/dsu023.

Yu, Ruby, Gloria Jih, Nahid Iglesias, and Danesh Moazed. 2014. “Determinants of

Heterochromatic siRNA Biogenesis and Function." *Molecular Cell* 53 (2): 262–76. https://doi.org/10.1016/j.molcel.2013.11.014.

Zaghloul, Mohamed S., Eman Eldebawy, Soha Ahmed, Amr G. Mousa, Amr Amin, Amal Refaat, Iman Zaky, Nada Elkhateeb, and Mohamed Sabry. 2014. "Hypofractionated Conformal Radiotherapy for Pediatric Diffuse Intrinsic Pontine Glioma (DIPG): A Randomized Controlled Trial." *Radiotherapy and Oncology* 111 (1): 35–40. https://doi.org/10.1016/j.radonc.2014.01.013.

Zaky, Wafik, Michael Wellner, Robert J. Brown, Stefan Blüml, Jonathan L. Finlay, and Girish Dhall. 2013. "Treatment of Children with Diffuse Intrinsic Pontine Gliomas with Chemoradiotherapy Followed by a Combination of Temozolomide, Irinotecan, and Bevacizumab." *Pediatric Hematology and Oncology* 30 (7): 623–32. https://doi.org/10.3109/08880018.2013.829895.

Zarghooni, Maryam, Ute Bartels, Eric Lee, Pawel Buczkowicz, Andrew Morrison, Annie Huang, Eric Bouffet, and Cynthia Hawkins. 2010a. "Whole-Genome Profiling of Pediatric Diffuse Intrinsic Pontine Gliomas Highlights Platelet-Derived Growth Factor Receptor α and Poly (ADP-Ribose) Polymerase As Potential Therapeutic Targets." *Journal of Clinical Oncology* 28 (8): 1337–44. https://doi.org/10.1200/JCO.2009.25.5463.

———. 2010b. "Whole-Genome Profiling of Pediatric Diffuse Intrinsic Pontine Gliomas Highlights Platelet-Derived Growth Factor Receptor α and Poly (ADP-Ribose) Polymerase As Potential Therapeutic Targets." *Journal of Clinical Oncology* 28 (8): 1337–44. https://doi.org/10.1200/JCO.2009.25.5463.

Zeman, Michelle K., and Karlene A. Cimprich. 2014. "Causes and Consequences of Replication Stress." *Nature Cell Biology* 16 (1): 2–9. https://doi.org/10.1038/ncb2897.

Zhang, Junxia, Kai Huang, Zhendong Shi, Jian Zou, Yingyi Wang, Zhifan Jia, Anling Zhang, et al. 2011. "High β-Catenin/Tcf-4 Activity Confers Glioma Progression via Direct Regulation of AKT2 Gene Expression." *Neuro-Oncology* 13 (6): 600–609. https://doi.org/10.1093/neuonc/nor034.

Zhang, Liwei, Lee H. Chen, Hong Wan, Rui Yang, Zhaohui Wang, Jie Feng, Shaohua Yang, et al. 2014a. "Exome Sequencing Identifies Somatic Gain-of-Function PPM1D Mutations in Brainstem Gliomas." *Nature Genetics* 46 (7): 726–30. https://doi.org/10.1038/ng.2995.

———. 2014b. "Exome Sequencing Identifies Somatic Gain-of-Function *PPM1D* Mutations in Brainstem Gliomas." *Nature Genetics* 46 (7): 726–30. https://doi.org/10.1038/ng.2995.

Zhang, Xiaohua, Tao Chen, Jiannan Zhang, Qin Mao, Shanquan Li, Wenhao Xiong, Yongming Qiu, Qiuling Xie, and Jianwei Ge. 2012. "Notch1 Promotes Glioma Cell Migration and Invasion by Stimulating β-Catenin and NF-κB Signaling via AKT Activation." *Cancer Science* 103 (2): 181–90. https://doi.org/10.1111/j.1349-7006.2011.02154.x.

Zhang, Xiaohua Douglas. 2010. "An Effective Method for Controlling False Discovery and False Nondiscovery Rates in Genome-Scale RNAi Screens." *Journal of Biomolecular Screening* 15 (9): 1116–22. https://doi.org/10.1177/1087057110381783.

Zhang, Xiaohua Douglas, Pei Fen Kuan, Marc Ferrer, Xiaohua Shu, Yingxue C. Liu, Adam T. Gates, Priya Kunapuli, et al. 2008. "Hit Selection with False Discovery Rate Control in Genome-Scale RNAi Screens." *Nucleic Acids*

Research 36 (14): 4667–79. https://doi.org/10.1093/nar/gkn435.

Zheng, Hongwu, Haoqiang Ying, Ruprecht Wiedemeyer, Haiyan Yan, Steven N. Quayle, Elena V. Ivanova, Ji-Hye Paik, et al. 2010. “PLAGL2 Regulates Wnt Signaling to Impede Differentiation in Neural Stem Cells and Gliomas.” *Cancer Cell* 17 (5): 497–509. https://doi.org/10.1016/j.ccr.2010.03.020.

Zheng, Liwei, and Marc M. Greenberg. 2017. “DNA Damage Emanating From a Neutral Purine Radical Reveals the Sequence Dependent Convergence of the Direct and Indirect Effects of γ-Radiolysis.” *Journal of the American Chemical Society* 139 (49): 17751–54. https://doi.org/10.1021/jacs.7b10942.

Zhi, Feng, Guangxin Zhou, Naiyuan Shao, Xiwei Xia, Yimin Shi, Qiang Wang, Yi Zhang, et al. 2013. “miR-106a-5p Inhibits the Proliferation and Migration of Astrocytoma Cells and Promotes Apoptosis by Targeting FASTK.” *PLOS ONE* 8 (8): e72390. https://doi.org/10.1371/journal.pone.0072390.

Zhong, Qian, Zhi-Hua Liu, Zhi-Rui Lin, Ze-Dong Hu, Li Yuan, Yan-Min Liu, Ai-Jun Zhou, et al. 2018. “TheRARS-MAD1L1Fusion Gene Induces Cancer Stem Cell-like Properties and Therapeutic Resistance in Nasopharyngeal Carcinoma.” *Clinical Cancer Research: An Official Journal of the American Association for Cancer Research* 24 (3): 659–73. https://doi.org/10.1158/1078-0432.CCR-17-0352.

Zhou, Wei, Mao Sun, Guang-Hui Li, Yong-Zhong Wu, Ying Wang, Fu Jin, Yun-Yun Zhang, Li Yang, and Dong-Lin Wang. 2013. “Activation of the Phosphorylation of ATM Contributes to Radioresistance of Glioma Stem Cells.” *Oncology Reports* 30 (4): 1793–1801. https://doi.org/10.3892/or.2013.2614.

Zhou, Yi, Ji-Hoon Lee, Wenxia Jiang, Jennie L. Crowe, Shan Zha, and Tanya T. Paull. 2017. “Regulation of the DNA Damage Response by DNA-PKcs Inhibitory Phosphorylation of ATM.” *Molecular Cell* 65 (1): 91–104. https://doi.org/10.1016/j.molcel.2016.11.004.

Zhuang, Wenzhuo, Zhenghong Qin, and Zhongqin Liang. 2009. “The Role of Autophagy in Sensitizing Malignant Glioma Cells to Radiation Therapy.” *Acta Biochimica Et Biophysica Sinica* 41 (5): 341–51.

Zmarzły, Nikola, Emilia Wojdas, Aleksandra Skubis, Bartosz Sikora, and Urszula Mazurek. 2017. “DNA Methylation: Gene Expression Regulation.” *Folia Biologica et Oecologica* 12 (1): 1–10. https://doi.org/10.1515/fobio-2016-0001.

Zülch, K. J. 1978. “Principles of the New WHO Classification of Brain Tumors.” In *Head Injuries. Tumors of the Cerebellar Region*, 279–84. Advances in Neurosurgery. Springer, Berlin, Heidelberg. https://doi.org/10.1007/978-3-642-67028-2_56.

université PARIS-SACLAY | ÉCOLE DOCTORALE Cancérologie, biologie, médecine, santé (CBMS)

Caractérisation moléculaire des gliomes malins pédiatriques du tronc cérébral (DIPG) et identification de nouvelles stratégies thérapeutiques par un crible ARN interférant de létalité synthétique

Mots clés : DIPG, crible d'ARN interférence, létalité synthétique, Histone H3-K27M, radioresistance

Résumé : Les DIPG représentent les tumeurs cérébrales pédiatriques les plus sévères. Aucun progrès dans leur prise en charge n'a été accompli au cours des 50 dernières années et la radiothérapie ne demeure que transitoirement efficace. Récemment, une mutation somatique de l'histone H3 (K27M) spécifique des DIPG a été trouvée chez environ 95% des patients. Elle est aujourd'hui considérée comme l'événement oncogénique initiateur de ces tumeurs. Deux sous-groupes majeurs de patients présentant des programmes oncogéniques et une réponse à la radiothérapie distincts peuvent être définis en fonction du gène dans lequel l'altération survient, codant les variantes protéiques H3.1 ou H3.3. Nous avons réalisé deux cribles de létalité synthétique par ARN interférence ciblant le kinome humain afin d'identifier d'une part les gènes nécessaires à la survie des DIPG et d'autre part les gènes dont l'inhibition sensibilise ces tumeurs à la radiothérapie. Le double objectif de ce projet était de mieux comprendre la biologie sous-jacente à l'oncogenèse des DIPG et de découvrir de nouvelles cibles thérapeutiques.
Nous avons mis en évidence 41 gènes requis pour la survie des DIPG sans effet délétère majeur sur des cellules contrôles normales. Parmi eux, nous avons identifié *VRK3* codant une serine thréonine kinase dont les fonctions restent peu décrites à ce jour et qui n'avait jamais été associée préalablement à l'oncogenèse de DIPG. Nous avons pu confirmer par la suite que son inhibition conduit à un arrêt total de la prolifération des cellules de DIPG associé à d'importants changements morphologiques, plus particulièrement dans les tumeurs mutées pour H3.3-K27M. VRK3 constitue par conséquent une nouvelle cible thérapeutique prometteuse dans cette pathologie à l'issue fatale pour la totalité des patients.
En parallèle, un crible de survie similaire a été réalisé en conjonction avec l'irradiation des cellules. Très peu d'ARN interférents ont permis de sensibiliser les cellules H3.3-K27M à la radiothérapie contrairement aux cellules H3.1-K27M. Ce travail nous a permis de mettre en évidence une différence significative de radiosensibilité des modèles vitro de DMG en fonction du sous-groupe de tumeurs considéré, H3.1- ou H3.3-K27M muté, conformément à la survie des patients observée suite à la radiothérapie. Ces résultats inédits laissent entrevoir des perspectives d'amélioration du traitement de référence des patients atteints de DIPG actuellement identique quelle que soit leur génotype.

Molecular characterization of paediatric brainstem gliomas (DIPG) and identification of new therapeutic targets using gene extinction strategies

Keywords : DIPG, high throughput screening, shRNA, synthetic lethality, kinome-wide, radiation

Abstract: DIPG is one of the most severe paediatric brain tumours. No progress has been made in their management over the past 50 years and radiotherapy remains only transiently effective. Recently, a specific somatic mutation in the histone H3 (K27M) has been found in approximately 95% of DIPG patients and can be considered as the oncogenic driver of these tumours. Two major subgroup of patients with distinct oncogenic program and response to radiotherapy can be defined according to the gene in which the alteration occurs, encoding the H3.1 or H3.3 protein variants. We performed two synthetic lethality screens by RNA interference targeting the human kinome in order to identify the genes responsible for DIPG cell survival, as well as those sensitizing tumour cells to radiotherapy after inhibition. The dual purpose of this project was to better understand the biology underlying oncogenesis of DIPGs and to discover new therapeutic targets.
We identified 41 genes required for DIPG cell survival with no major deleterious effect on normal control cells. Among them, we identified *VRK3*, a serine threonine kinase never involved in DIPG oncogenesis with functions remaining poorly described to date. We have shown that its inhibition leads to a complete arrest of DIPG cell proliferation and is additionnaly associated with important morphological changes, more particularly in H3.3-K27M mutated tumours. VRK3 is therefore a promising new therapeutic target for all patients in this fatal pathology.
In parallel, a similar survival screen was performed in conjunction to cell radiation and very few interfering RNAs enhance H3.3-K27M cell radiosensitivity, in contrast to H3.1-K27M cells. These data highlighted a significant difference in radiosensitivity of the DMG in vitro models in H3.1- versus H3.3-K27M mutated tumours, in a concordant way with patient survival following radiotherapy. These unprecedented results suggest new opportunities for improving the current treatment of DIPG patients regardless of their genotype.